Perineuronal nets in recovery after acute spinal cord injury

Sîan Frances Irvine

PhD thesis

Submitted in accordance with the requirements for a degree of Doctor in Philosophy

University of Leeds

Biomedical Sciences

September 2019

Intellectual property rights

Declaration

The candidate confirms that the work submitted is her own, except where work which has formed part of jointly authored publications has been included. The contribution of the candidate and the other authors to this work has been explicitly indicated below. The candidate confirms that appropriate credit has been given within the thesis where reference has been made to the work of others.

Chapter 3 is based on work published in a jointly authored manuscript:

Irvine SF, Kwok JCF. *Perineuronal Nets in Spinal Motoneurones: Chondroitin Sulphate Proteoglycan around Alpha Motoneurones*. International Journal of Molecular Sciences. 2018; 19(4):1172.

Chapter 3: Jessica Kwok and Sîan F Irvine conceived and designed the experiments; Sîan F Irvine performed all experiments and analysed the data; Jessica Kwok contributed reagents/materials/analysis tools.

Chapters 4 and 5 are based on *in vivo* animal work. This research has been carried out by a team which has included primarily myself and Sylvain Gigout with help from Philippa Warren or Janice Ng for PNN consolidation experiments. My own contributions, fully and explicitly indicated in the thesis, have been:

Chapter 4: All behavioural work, analyses and administration of treatments were performed by Sîan Irvine with exception of primary hindlimb horizontal ladder scoring and von Frey assay for PNN consolidation studies. Subsequent analyses for these were completed by Sîan Irvine.

Chapter 5: All surgeries, electrophysiological experiments, histology, imaging and analyses were designed and performed by Sîan Irvine. Cleared samples were imaged as a service by Faculty of Biomedical Sciences (FBS) Bioimaging facility (Dr Ruth Hughes).

The other members of the group and their contributions have been as follows: Behavioural work, care and administration of treatments were carried out by the team detailed above but mainly with Sylvain Gigout. Philippa Warren performed behavioural analyses of horizontal ladder, von Frey assay and scoring for open field assessment for the PNN consolidation detailed in Chapter 4.

The design of all experiments has been developed by Sîan Irvine with supervision by Jessica Kwok, contributions from the team as detailed above and with cooperation from Central Biomedical Services at the University of Leeds.

The small molecule perineuronal net inhibitor (PNNi) was acquired by Dr Jessica Kwok for use in this project.

This work was financed by grants from the Wings for Life Foundation and The University of Leeds 110 Years Scholarship. The author declares no competing financial interests.

Acknowledgements

First and foremost, thanks go to my supervisor Dr Jessica Kwok. Thank you for the opportunity to work with you and for all of the support and advice throughout the entirety of my PhD. Thank you for believing in me and for showing me there is always another way. This experience has allowed me to grow so much.

To the diligent Dr Sylvain Gigout, keep being you. Without your teamwork, in sickness and in health, this project would not be what it is.

To all of the in vivo *and SCI crew, especially Dr Roger Kissane and Dr Pip Warren, for providing all the craic! Thanks for the fun musical surgery sessions and for all the support and guidance, no matter the time of day. I have learnt so much from you. To Natalie, Nicole and Dr 'V' Lall for the pizza and coffee dates and always being able to find time for a chat, a giggle and a breath of fresh air. Thanks to the Kwok lab members past and present (including Katie, Lynda, Ashleigh, Luke, Stuart, Janice, Sylvain and James) for your light and positive energy.*

Thank you to Dr Samit Chakrabarty and Dr Ronaldo Ichiyama, you both helped spark an interest in motor control without which I wouldn't be here today. Thanks to all the staff in the CBS, (Lan, Neil, Pam, Stan, Mel, Scott and David) you and Khawar helped to make this project possible.

Thanks to all my friends in Leeds, home and otherwise for all the support and fun times, including some of the lovely ladies in my life (Kat, Sophie, Anna and of course Christian). To Cat Dunn as my unofficial social secretary and to Simon for our planty chats and for just being you.

To my family, thank you for putting up with me and all the sacrifices I have made for this project. Know that I miss and love you all and I give so much credit to you for all

the values that have gotten me here today. You taught me to see the positive and to keep everything in perspective.

Finally, to my Dr Pierce Mullen for his unwavering love and support through the highs and the downright lows. Thanks for being my partner in crime. Together we have gotten through not one but two PhD experiences and I cannot wait for life together on the other side.

Abstract

To promote recovery after spinal cord injury (SCI), treatments aim to enhance regeneration of severed axons and the plasticity of surviving circuitry. Perineuronal nets (PNNs) are specialised extracellular matrix structures surrounding neuronal sub-populations throughout the central nervous system, implicated in the termination of developmental plasticity. Removal of PNNs via chondroitinase ABC injection (ChABC) successfully enhances plasticity and thus functional recovery after SCI. Firstly, we reveal that alpha motoneurones are highly associated with PNNs (~90%), suggesting that modifications of synaptic inputs to this population may contribute to the above-mentioned functional motor recovery. ChABC has proven beneficial to recovery alongside other treatments including rehabilitation, however, poses significant hurdles in its translation to human application. This study investigates the efficacy of a licensed non-invasive drug, PNN inhibitor (PNNi) to remove PNNs to enhance recovery after acute SCI. Adult female Lister Hooded rats received a moderate T9 contusion and acute treatment of PNNi/vehicle, with/without combination of delayed rehabilitative treadmill training. Functional recovery was assessed using sensory and locomotor behavioural tests. Systemic PNNi partially removed PNNs, predominantly from the spinal cord, inducing structural and functional plasticity in distinct regional and uninjured tissues. Chronic PNNi conferred hyper-plasticity that hampered functional hindlimb sensorimotor recovery. However, after a small forelimb deficit with SCI, systemic plasticity enhancement induced forelimb changes that were comparable to uninjured controls but not significantly different from injured control forelimb performance. Shaping and controlling plasticity with rehabilitation and limiting duration of PNN removal showed trends of permitting further hindlimb motor recovery than spontaneously reacquired, indicating a requirement for stabilisation of new synapses by PNN reformation and refinement to functional

connections by experience-driven plasticity. Our data suggests that whilst PNNi induces plasticity, further refinement of the PNNi treatment regime is necessary to provide optimal levels and shaping of plasticity for the best functional outcomes.

Table of Contents

Table of Figures

Table of Tables

List of abbreviations

5-HT	5-hydroxytryptamine/serotonin
ACAN	Aggrecan core protein
AMPA	α-amino-3-hydroxy-5-methyl-4-isoxazolepropionic acid
AP	Anteroposterior
ASIA	American Spinal Injury Association
BBB	Basso, Beattie and Bresnahan (open field hindlimb locomotor score)
BCAN	Brevican core protein
BDA	Biotin dextran amine
BDNF	Brain-derived neurotrophic factor
BSCB	Blood spinal cord barrier
Bral2	Brain-specific link protein 2/HAPLN4
Ca^{2+}	Calcium ions
ChAT	Choline acetyltransferase
ChABC	Chondroitinase ABC
CNS	Central nervous system
CNTN-1	Contactin-1
CS	Chondroitin sulphate
CSPGs	Chondroitin sulphate proteoglycans

CST	Corticospinal tract
CTB	Cholera toxin subunit B
CRTL1	Cartilage link protein 1/HAPLN1
Cx	Contusion
DPI	Days post injury
ECM	Extracellular matrix
EGF	Endothelial growth factor
F	Facial
Fe^{3+}	Iron ions
FL	Forelimb
GAD65/67	Glutamic acid decarboxylase isoforms 65 and 67
GABA	Gamma-aminobutyric acid
GAG	Glycosaminoglycan
GalNAc	N-acetylgalactosamine
GFAP	Glial fibrillary acidic protein
Gs	Gastrocnemius
HA	Hyaluronic acid/ hyaluronan
HAPLN	Hyaluronan and proteoglycan binding link protein
HAS	Hyaluronan synthase
HL	Hindlimb

HMW	High molecular weight
HYAL	Hyaluronidase
ICMS	Intracortical microstimulation
IHC	Immunohistochemistry
IFNγ	Interferon gamma
IL	Interleukin
i.m.	intramuscular
i.p.	intraperitoneal
JAK	Janus kinase
Kdyn	Kilodyne
LAR	Leukocyte common antigen-related phosphatase
LSM	Laser scanning microscope
M1	Primary motor cortex
M1	Classically activated macrophages
M2	Alternatively-activated or wound healing macrophages
MAG	Myelin-associated glycoprotein
Mn	Motoneurone
ML	Mediolateral
MMP	Matrix metalloproteinase
mTOR	Mechanistic/mammalian target of rapamycin

Na^+	Sodium ions
NeuN	Neuron-specific nuclear protein
NCAN	Neurocan core protein
NDS	Normal donkey serum
NG2	Neuron-glial antigen 2
NgR	Nogo receptor
NMDA	N-methyl-D-aspartate
Nogo	Neurite outgrowth inhibitor
OCT	Optimum cutting temperature medium
OMgp	Oligodendrocyte myelin glycoprotein
PB	Phosphate buffer
PBS	Phosphate buffer saline
PBST	Phosphate buffer saline with Triton-X100
PFA	Paraformaldehyde
PTEN	Phosphatase and Tenisin homolog
PTPRZ	Phosphacan/ protein tyrosine phosphatase receptor zeta
PTPσ	Protein tyrosine phosphatase receptor
PNNi	Small molecule perineuronal net inhibitor
PNNs	Perineuronal nets
PV	Parvalbumin

ROCK	Rho-associated protein kinase
ROS	Reactive oxygen species
RT	Room temperature
s/c	subcutaneous
SCI	Spinal cord injury
SD	Standard deviation
SEM	Standard error of the mean
Sema	Semaphorin
SOCS3	Suppressor of cytokine signalling-3
STAT3	Signal Transducer And Activator Of Transcription 3
T	Training
TA	Tibia anterior
TBS	Tris buffer saline
TGFβ	Tumour growth factor beta
TNF	Tumour necrosis factor
VCAN	Versican core protein
VEGF	Vascular endothelial growth factor
VGLUT2	Vesicular glutamate transporter 2
VH	Ventral horn
Bio-WFA	Biotin-conjugated *Wisteria floribunda* agglutinin

WFA *Wisteria floribunda* agglutinin

WPI Weeks post injury

Chapter 1: General Introduction

1.1: Spinal cord injury

Spinal cord injury (SCI) is a devastating condition for which there is currently no cure. Injury to the spinal cord disrupts sensory, motor and autonomic control, leading to loss of functions, paralysis, intense pain and progressive neurodegeneration.

The most frequent causes of SCI are blunt or penetrating trauma as a result of motor vehicle collisions (39.5 %) or falls (38.8 %) (Singh *et al.* 2014; Kumar *et al.* 2018). Recent global epidemiology reports estimate that for every million people, there are 105 new cases of traumatic SCI every year (Kumar *et al.* 2018). In developing and low-income countries, SCI presents with high mortality (Lee *et al.* 2014; Kumar *et al.* 2018). Whereas, in high-income countries, medical advancements have significantly improved survival rates. However, the subsequent growing pool of patients living with chronic SCI consequently results in high financial and physical expenses to both the individuals and society (Ackery, Tator and Krassioukov 2004; Middleton *et al.* 2012; Krueger *et al.* 2013; Lee *et al.* 2014; Hachem, Ahuja and Fehlings 2017).

Over the past few decades, as societal demographic has shifted, this has been reflected in the changing SCI patient profile. Due to an aging population, the average age of incidence has increased, resulting in a greater number of falls and whilst still most prevalent in men, the SCI incidence for women has also increased (Bárbara-Bataller *et al.* 2018). Given the prospect that the population of patients living with SCI is only going to continue to grow, this emphasises the need for new therapies to improve SCI recovery.

The spinal cord is both the major conduit for the transmission of motor and sensory information between the brain and the periphery, as well as a neural centre for the coordination and articulation of many reflexes and central pattern generators. Therefore, injury to the cord disrupts these processes, with the immediate severing of axons commonly resulting in the permanent loss of both sensory and motor

capabilities, including autonomic functions such as bladder control, below the level of injury. SCI is a heterogeneous disease which can be classified into four different anatomical wounds (Hulsebosch 2002; Bunge *et al.* 1993; Bunge, Puckett and Hiester 1997). (1) Full or complete transection is diagnosed with the total absence of any sensation or motor control in the sacral regions of the cord (Waters, Adkins and Yakura 1991; Maynard *et al.* 1997; Kirshblum *et al.* 2011). (2) Lacerations or cuts are often caused by sharp bone fragments that partially sever the cord (Alizadeh, Dyck and Karimi-Abdolrezaee 2019). While complete SCI makes up approximately 50 % of injuries, full severing of the cord rarely occurs (Tator and Fehlings 1991). The rest of the injury types describe incomplete injuries, where even minimal bridging of the cord above and below the injury remains. (3) Contusive impact with or without persistent compression, is the most common injury type, frequently occurring with fracture-dislocation of vertebrae after blunt force trauma and is easily replicated in animal models (Dumont *et al.* 2001; Choo *et al.* 2009; Scheff and Roberts 2009; Cheriyan *et al.* 2014). The cord is bruised but not severed, leaving the dura intact and results in the formation of a cyst or cavity. A non-traumatic injury usually presents as a slow and building compression of the spinal cord within the vertebral column (Schmidt and Markovchick 1992). Finally (4), a solid cord injury, is the least common and presents with normal appearance of the spinal cord but contains a cavity (Bunge *et al.* 1993; Bunge, Puckett and Hiester 1997; Hulsebosch 2002).

Diagnosis of remaining function and extent of injury is essential to developing treatment and rehabilitative plans. Many scales exist to measure specific functions after SCI, as well as assessing general functional motor and sensory capabilities, for example, the Functional Independence Measure (FIM), Spinal Cord Independence Measure (SCIM I and II), Walking Index for SCI II (WISCI II) (Catz *et al.* 1997; Hall *et al.* 1999; Dittuno and Ditunno 2001; Ditunno *et al.* 2000; Catz *et al.* 2002a). However, these do not address the level or severity of the physical injury. Clinically, the physical

severity and level of injury is classified using the American Spinal Injury Association (ASIA) Impairment scale (Table 1.1), a modification of the previously used Frankel scale (Frankel *et al.* 1969; Maynard *et al.* 1997; Kirshblum *et al.* 2011). Motor and sensory function is determined by examining the dermatomes (C2 – S5) and myotomes (C5 – T1, L2 – S1). Based on these measurements, patients are ranked in a five point scale describing severity and completeness of injury, as complete (ASIA-A), sensory only (ASIA-B), motor control with no practical application (ASIA-C), motor useful (ASIA-D), or no neurological deficit/complete recovery (ASIA-E), as described in Table 1.1. ASIA assessment is internationally recognised and is routinely used as part of diagnosis at 72 hrs post-injury (Brown *et al.* 1991), as well as a measure for recovery or changes in function over time.

Table 1.1: International Spinal Cord Society Neurological Scale/American Spinal Injury Association (ASIA) Impairment scale, revised in 2011 (Kirshblum *et al.* 2011)

ASIA Impairment Scale		
A	Complete	No motor or sensory function is preserved in the sacral segments S4–S5
B	Incomplete	Sensory but not motor function is preserved below the neurological level and includes the sacral segments S4–S5
C	Incomplete	Motor function is preserved below the neurological level, and more than half of key muscles below the neurological level have a muscle grade less than 3
D	Incomplete	Motor function is preserved below the neurological level, and at least half of key muscles below the neurological level have a muscle grade of 3 or more
E	Incomplete	Motor and sensory functions are normal

ASIA assessment and the time when they are first carried out can be used as a predictor for clinical prognosis and life expectancy (Middleton *et al.* 2012). Incompleteness of injury (ASIA-B and -C) when first assigned indicated a greater chance of functional recovery (20 – 50 % for ASIA-B, > 50 % for ASIA-C), with little

to no chance of spontaneous recovery for complete SCI (ASIA-A) patients observed with following ASIA assessments within the first year (Catz *et al.* 2002b; Scivoletto, Morganti and Molinari 2004; Burns *et al.* 2012). However, establishing a general test for indicating functional prognosis is difficult due to variabilities between individual cases due to differences to age, gender, weight, etcetera.

Much research has been performed seeking to improve various aspects of functionality to SCI patients, but what do patients want? Qualitative surveys illustrated that the top priorities included bowel/bladder, sexual function and trunk stability, regardless of level of injury (Simpson et al., 2012; Anderson, 2004; Ditunno, P.L. et al., 2008). Interestingly, paraplegic and tetraplegic patients ranked walking movement and arm/hand function, respectively, as higher priorities than normal sensation and chronic pain (Anderson, 2004).

1.2: SCI: obstacles to recovery

The pathophysiology after primary mechanical injury to the spinal cord has been extensively studied by scientists hoping to uncover pharmacological targets to promote recovery after SCI, particularly *in vivo*, where rats in particular show a marked similarity to the human pathology of SCI (Metz *et al.* 2000; Scheff *et al.* 2003). The primary injury severs axons resulting in immediate interruption of signalling and loss of functions. Within minutes of the initial trauma, a cascade of intrinsic and extrinsic secondary mechanisms is induced (Kaplan, Ong Tone and Fournier 2015). These mechanisms persist and progressively foster degeneration and inflammation through the acute, sub-acute and chronic phases of SCI. Long-term prognosis is closely correlated to the severity of the primary injury and progression of the secondary injury, discussed below.

1.2.1: Inflammatory damage and cell death

The primary mechanical injury causes severe vascular and cellular damage to the injury epicentre, also known as the 'core', in the grey and white matter of the spinal cord (Tator and Fehlings 1991). Destruction of the intramedullary microvasculature and blood spinal cord barrier (BSCB) induces haemorrhage and ischaemia that spreads rapidly and exponentially from the core (Bilgen *et al.* 2000; Ackery, Tator and Krassioukov 2004; Maikos and Shreiber 2007; Khaing *et al.* 2018). The resultant local cell death and hypoxia to tissues leads to formation of reactive oxygen species (ROS) which yields more damage. Acute inflammation is triggered by the release of cytokines by damaged or necrotic cells as well as from the blood and is an important and beneficial response by the immune system to injury (Rock and Kono 2008; Stammers, Liu and Kwon 2012). The inflammatory response is progressive; first recruiting residual astrocytes and microglia in the central nervous system (CNS) alongside infiltration by blood-borne neutrophils, then lymphocytes in response to

further cytokine production, such as interleukin-1 (IL-1) by activated glial cells (Gendelman 2002). T-lymphocyte-mediated phagocytosis and B-lymphocyte antibody production contribute to an immune response that exacerbates tissue degeneration and produces further inflammation (Hayes *et al.* 2002; Ankeny *et al.* 2006). Reactive astrocytes do, however, exert inhibitory effects to recovery, for example, with the production of matrix metalloproteinases (MMP), including MMP-9, which increases vascular permeability, therefore further activating the immune response with detrimental effects to functional recovery (Noble *et al.* 2002; Hansen *et al.* 2013).

Table 1.2: Classification of macrophages, modified from (Zhou, He and Ren 2014).

Tumour necrosis factor-α (TNFα); interferon-γ (IFNγ); interleukin-1β (IL-1β); nitric oxide (NO)

		M2		
Classification	**M1**	**M2a**	**M2b**	**M2c**
Phenotypes	Classical / pro-inflammatory activation	Alternative activation, anti-inflammatory	Deactivation / wound healing	Repair and remodelling of damaged tissues
Cytokines / chemokines	TNFα, IFNγ, IL-1β, IL-6, IL-12, IL-23, NO	IL-4, IL-13	IL-10, TGFβ	IL-10

Inflammation is a complex mechanism that at first is beneficial and neuroprotective and suggested to be part of an endogenous strategy for neuronal regeneration within the CNS (Donnelly and Popovich 2008). Within the first week post-injury (WPI), a delicate balance of both pro-inflammatory cytokines, such as IL-12, tumour necrosis factor (TNF) and interferon-gamma (IFNγ), and anti-inflammatory cytokines, including IL-10, tumour growth factor beta (TGFβ) and nerve growth factor (NGF), are produced by astrocytes and microglia as they clear debris local to the injury (McTigue *et al.* 2000; Longbrake *et al.* 2007; Genovese *et al.* 2009; Kigerl *et al.* 2009; Zhou, He and Ren 2014). These cytokines cause a series of changes to monocytes or microglia to

form classically activated (M1) macrophages or pro-inflammatory macrophages or alternatively-activated (M2) macrophages which are associated with anti-inflammation and wound healing (Table 1.2). Many studies have manipulated the inflammatory response in order to improve recovery to varying success. For example, promoting the M1 pro-inflammatory response at 1 day post-injury (DPI) aggravated the injury, increasing tissue loss compared to 4 DPI (Klusman and Schwab 1997). This suggests that neuroprotective autoimmunity is highly regulated and emphasises the need for establishing optimal time points for developing therapies. Approximately 1 WPI, a changing microenvironment, including build-up of myelin debris, drives a switch of activated macrophages exclusively to the M1 pro-inflammatory (Table 1.2), which can last months to years (Pruss *et al.* 2011; Wang *et al.* 2015c). This chronic inflammation is characteristic to the progression of the secondary injury and contributes to continuing death of tissue surrounding the core or 'penumbral' tissue (Nesic *et al.* 2001; Jackson *et al.* 2005).

Alongside a progressively dysfunctional inflammatory response, acute cellular damage results in the release of powerful neurotransmitters, particularly glutamate, into the extracellular space causing excitotoxicity (Dumont *et al.* 2001). This high concentration of glutamate leads to over-activation of glutamate receptors, such as N-methyl-D-aspartate (NMDA), α-amino-3-hydroxy-5-methyl-4-isoxazolepropionic acid (AMPA) and kainite receptors, inducing a flooding influx of Na^+ and Ca^{2+} to neurones and glial cells (Szydlowska and Tymianski 2010). Overload of Ca^{2+} activates a vast cascade of intracellular processes, resulting in activation of apoptotic pathways mainly in local neurones and oligodendrocytes (Springer, Azbill and Knapp 1999; Tantral *et al.* 2004; Szydlowska and Tymianski 2010). In addition, Ca^{2+} dysregulation damages mitochondria, generating ROS and therefore causing oxidative damage (Dumont *et al.* 2001). ROS while transient cause lipid peroxidation of fatty acids leading to lysis of plasma membranes and ultimately necrosis (Xu *et al.*

2005). Both excitotoxicity and lipid peroxidation induce ionic imbalance where consequent rising intracellular Na^+ concentrations promote swelling and oedema (Bilgen *et al.* 2000), resulting in further ischaemia and hypoxic cell death.

Oligodendrocytes and neurones are particularly vulnerable to glutamate excitotoxicity, leading to apoptotic death *en masse* local to the core and penumbral tissue (Matute *et al.* 2002; Szydlowska and Tymianski 2010). The demyelination and loss of neurones from the injury site results in a sudden blockade of transmission between the brain and the spinal cord (James *et al.* 2011; Oyinbo 2011). Ongoing necrosis of neurones and glial cells occurs from the acute to sub-acute stages of injury, including progressive Wallerian degeneration of severed axons affecting all areas of the cord above the lesion (Becerra *et al.* 1995).

1.2.2: Barriers to regeneration

Despite the secondary damage to the spinal cord after injury, the CNS does attempt to recover with some spontaneous sprouting, particularly in rodent models, but ultimately fails, resulting in lost functions (Filli *et al.* 2014; Siegel *et al.* 2015). The peripheral nervous system, unlike the CNS, has much better success at regeneration (Broude *et al.* 1997). It was suggested that this is due to the intrinsic ability of peripheral neurones. However, CNS neurones are able to grow with success in peripheral grafts but peripheral nerves were unable to regenerate in injured CNS tissue (Richardson, McGuinness and Aguayo 1980; David and Aguayo 1981). This indicated that the peripheral nervous system has an environment more conducive to endogenous reparative and regenerative processes, whilst the extracellular environment in the CNS is inhibitory to these attempts, similar to what Ramón y Cajal proposed many years ago (y Cajal 1991). However, by increasing the intrinsic growth state, peripheral neurones were able to overcome the inhibitory extracellular environment in the injured CNS and grow through the spinal lesion (Neumann and

Woolf 1999), suggesting that manipulation of intrinsic properties after injury could promote central regeneration. Therefore, both intrinsic and extrinsic mechanisms inhibitory to regeneration and plasticity could be targeted to promote better functional recovery after SCI in the adult.

1.2.2.1: Intrinsic inhibition of regeneration

The intrinsic ability of a neurone to regenerate is dependent on the intracellular signalling pathways associated with axonal growth that are activated in response to injury. Many of these pathways are also activated during development but in axotomised central neurones contribute to the failure of axonal sprouting. While not as well investigated as extrinsic targets for regeneration, researchers have begun to make headway in the manipulation of downstream pathways promoting or preventing growth and repair to promote functional recovery.

Some of the pathways involved in inhibition of regeneration have been investigated. These include the inactivation of mammalian/mechanistic target of rapamycin (mTOR) pathway (Park *et al.* 2008; Liu *et al.* 2010; Geoffroy *et al.* 2016), and activation of the Rho-associated protein kinase (ROCK) pathway after injury (Conrad *et al.* 2005). Modulation of the mTOR pathways, by viral deletion of the tumour suppressor gene, Phosphatase and Tenisin homolog (PTEN), a negative regulator of mTOR, has been demonstrated to activate axonal regeneration in multiple models of CNS injury, including optic nerve crush (Park *et al.* 2008). This has also been demonstrated to result in functional recovery, such as restoration of diaphragm function (Urban *et al.* 2019b), and after thoracic hemisection induced long distance regeneration of corticospinal tract (CST) neurones, including significant distances past the lesion site (Liu *et al.* 2010).

The Rho/ROCK pathway, as discussed later, is activated by the binding of many extracellular inhibitory molecules, such as neurite outgrowth inhibitor (Nogo) and various chondroitin sulphate proteoglycans (CSPGs) to various receptors (Koprivica

et al. 2005; Montani *et al.* 2009; Fisher *et al.* 2011; Dickendesher *et al.* 2012; Pendleton *et al.* 2013). Co-deletion of PTEN and Nogo in a dorsal hemisection model combines intrinsic and extrinsic mechanisms to harness both the mTOR and Rho/ROCK pathways (Geoffroy *et al.* 2015). With double deletion, CST sprouting was robust, however, was similar to PTEN deletion alone, but was able to sprout for longer distances (Geoffroy *et al.* 2015). PTEN has also been co-deleted with the suppressor of cytokine signalling-3 (SOCS3) gene, a negative regulator of the Janus kinase (JAK)/ signal transducers and activators of transcription (STAT) pathway, with robustly synergistic effects of axonal regeneration after optic nerve crush (Sun *et al.* 2011). The same SOCS3/PTEN co-deletion was also able to promote vigorous and additive effects to CST sprouting after unilateral pyramidotomy, to a degree that was capable of reducing motor impairments in a skilled walking task (Jin *et al.* 2015). The studies discussed here represent a growing trend in developing future therapies to combine methods to overcome intrinsic and extrinsic inhibition to regeneration to promote recovery after SCI.

1.2.2.2: Extrinsic inhibition of regeneration

Many extrinsic mechanisms that are inhibitory to regeneration have been extensively studied and include the glial scar as well as the changing biochemical composition of the extracellular environment after CNS injury.

1.2.2.2.1: The glial scar

A key characteristic of SCI is the rapid formation of a glial scar around the injury epicentre in the central spinal cord surrounded by anatomically conserved white matter. Within the first few hours post-injury, a heterogeneous population of glial cells, composed mainly of newly proliferated reactive astrocytes, as well as activated microglia and neuron-glial antigen 2 (NG2)-positive glia, begins to form a dense mesh-like barrier around the lesion core, eventually delineating a fluid-filled cavity (Silver and Miller 2004; Wanner *et al.* 2013; Adams and Gallo 2018). Deposition of

the scar is primarily directed by glial cells in contusion (Cx)-like injuries, whereas in lacerations or penetrating injury that disrupt the meninges, fibroblast migration to the core is increased (Silver and Miller 2004). The formation of a glial scar is beneficial to repair, as acute to sub-acute viral ablation of reactive astrocytes (Faulkner *et al.* 2004), as well as disruption of formation mediated by astrocyte-selective STAT3 deletion (Herrmann *et al.* 2008; Wanner *et al.* 2013) was detrimental to functional recovery and increased demyelination and neuronal death. These findings suggest a role for glial scar formation in the restriction of the inflammatory response and preservation of tissue. These protective influences include a role in reconstructing the BSCB by gradually reducing the BSCB permeability up to 56 DPI (Cohen *et al.* 2009). The glial scar matures in approximately 4 weeks in the rat (Hu *et al.* 2010; Huang *et al.* 2014), with the clearing of cellular debris by microglia/macrophages to leave the scar, which can last for years after injury.

It is well established that the glial scar is initially protective in the acute stages of SCI, preventing the spread of further damage. However, the effect of the chronic presence of the glial scar on regeneration is controversial. A leading claim is that the chronic glial scar becomes an obstacle to regeneration, acting not only as a physical barrier against spontaneous axonal sprouting into the lesion site but contributing to the inhibitory shift in the biochemical environment to regeneration (Silver and Miller 2004; Wanner *et al.* 2013). Whilst others contend that removal of the chronic glial scar does not promote regeneration (Anderson *et al.* 2016).

The accumulation and persistence of a number of extracellular inhibitory molecules after injury are thought to prevent regeneration, including myelin-associated growth inhibitors, such as Nogo-A (Wang *et al.* 2015a), as well as various neuronal repulsive guidance molecules, such as semaphorins (Sema) (Pasterkamp *et al.* 1999; Soderblom *et al.* 2013) and CSPGs, as discussed below.

1.2.2.2.2: Myelin-associated inhibitory factors

After SCI, the extensive destruction of myelin releases inhibitory factors into the extracellular space. Several myelin-associated inhibitory factors have been identified and of these Nogo has been the most extensively researched. Its most inhibitory isoform, Nogo-A, is released by oligodendrocytes and myelin into the extracellular space following SCI and binds to its receptors, notably including the Nogo-66 receptor 1 (NgR1) (Schwab 2010). NgR1 is also activated by other myelin-associated growth inhibitors like myelin-associated glycoprotein (MAG) and oligodendrocyte myelin glycoprotein (OMgp) (Wang *et al.* 2002) and induces collapse of growth cones and other neurite inhibition through downstream signalling of the Rho/ROCK pathway (Montani *et al.* 2009). In support of this, neutralisation of Nogo-A using antibodies, such as 11C7 and IN-1, or pharmacological blockade of Rho/ROCK signalling has been demonstrated to enhance regenerative growth and sprouting resulting in functional recovery after SCI (Liebscher *et al.* 2005; Freund *et al.* 2006; Mullner *et al.* 2008). These notably have included treatment of SCI in macaque monkeys with the anti-Nogo 11C7 antibody via intrathecal infusion via osmotic mini pumps (Freund *et al.* 2009; Freund *et al.* 2007). Due to these positive results, a human anti-Nogo antibody (ATI 355) has been developed for translation to the clinic, in collaboration with Novartis. Completion of a Phase I (NCT00406016) clinical trial for this antibody in 2011 (Zorner and Schwab 2010; Kucher *et al.* 2018) revealed that this was well tolerated and the long anticipated multinational Phase II clinical trials (Germany: NCT03935321; Switzerland: EudraCT #2016-001227-31) for acute cervical SCI have begun in 2019 and are estimated for completion in 2023.

An alternative solution is the use of a soluble NgR decoy receptor, NgR(310)ecto-Fc (Nogo Trap/ AXER-204; developed by ReNetX Bio, Inc., formerly Axerion Therapeutics, Inc.), that neutralises all three of the myelin-associated inhibitory factors: Nogo, MAG, and OMgp, and was effective in improving functional locomotor

skills, even after chronic SCI (Wang *et al.* 2011b; Wang *et al.* 2014). A Phase Ib–IIa clinical trial for the fusion protein AXER-204 to treat chronic SCI is currently recruiting in the USA (NCT03989440). Whilst these Nogo interventions are currently some of the closest treatments developed for SCI to actual clinical use, both rely on invasive means of delivery.

1.2.2.2.3: Axonal guidance molecules

Sema, also called collapsins, are repulsive axonal guidance molecules important in development that mediate their guidance through the collapse of growth cones (Luo, Raible and Raper 1993). Oligodendrocytes express various membrane-associated Semas, such as Sema4D and Sema5A, which are upregulated after CNS injury (Moreau-Fauvarque *et al.* 2003; Goldberg *et al.* 2004). Following traumatic lesions, infiltration of fibroblasts and activation of glial cells is responsible for secretion of Sema3 local to the injury core after SCI (Pasterkamp *et al.* 1999; Soderblom *et al.* 2013) where it plays a role in the inhibition of revascularisation, remyelination and axonal regeneration through signalling of a variety of receptors (Mecollari, Nieuwenhuis and Verhaagen 2014). Sema3 repulses sprouting axons of descending pathways, such as the CST, that express Sema3-sensitive receptors as they attempt to penetrate the lesion site (De Winter *et al.* 2002), limiting regeneration. This was partially overcome by selective Sema3A inhibition via osmotic mini pump delivery with regeneration of serotonergic/5-hydroxytryptamine (5-HT)-positive but not CST fibres (Kaneko *et al.* 2006). Inhibition of Sema3A (Kaneko *et al.* 2006) but not Sema3 receptors (Mire *et al.* 2008) was able to enhance axonal regeneration due to competition of Sema3 receptors with growth factors, such as VEGF and TGFβ (Mecollari, Nieuwenhuis and Verhaagen 2014).

1.2.2.2.4: CSPGs and glycosaminoglycans

Like Sema, CSPGs are a family of repulsive guidance molecules that are important during development (Kwok *et al.* 2011; Siebert and Osterhout 2011). CSPGs are key components of the extracellular matrix (ECM) and there many different types that are expressed at various time points throughout development, including CNS specific CSPGs, such as neurocan (NCAN) and brevican (BCAN) (Herndon and Lander 1990; Oohira *et al.* 1994; Yamada *et al.* 1994). Post-injury, CSPGs are secreted into the ECM by reactive astrocytes in response to the rise in pro-inflammatory cytokines and are generally considered to be inhibitory to regeneration (Lemons, Howland and Anderson 1999; Silver and Miller 2004). Various CSPGs, including phosphacan (PTPRZ) and some lectican members, BCAN, NCAN and versican (VCAN), are differentially regulated and released both locally and distant from the lesion core in animal models (Jones, Margolis and Tuszynski 2003; Tang, Davies and Davies 2003; Massey *et al.* 2008) and the injured human spinal cord (Buss *et al.* 2009; Andrews *et al.* 2012), suggesting functional variability. Enzymatic degradation of CSPGs using the bacterial enzyme chondroitinase ABC (ChABC) or blockade of CSPG signalling has been extensively demonstrated to improve functional and anatomical recovery after CNS injury (Moon *et al.* 2001; Bradbury *et al.* 2002; Massey *et al.* 2006; Massey *et al.* 2008; Carter, McMahon and Bradbury 2011; Zhao *et al.* 2013; Lang *et al.* 2015; Warren *et al.* 2018).

Other glycans such as hyaluronan (HA) also change in response to injury. HA is one of the main components of the ECM and the varying molecular weights that it can be found as, are known to influence the biophysical properties of tissues (Cyphert, Trempus and Garantziotis 2015). Native high molecular weight (HMW) HA is degraded after neuro-inflammation by the activity of ROS (Šoltés *et al.* 2006), or by enzymatic degradation by upregulated endogenous hyaluronidase-4 (Tachi *et al.* 2015) and HMW levels rebound to higher than normal levels within 4 WPI (Struve *et*

al. 2005). The size of HA chains appears to play a modulatory role in inflammation and astrocyte proliferation where low molecular weight or fragmented HA initially aids glial scar formation by inducing astrogliosis as well as CSPG secretion (Khaing *et al.* 2011; Cyphert, Trempus and Garantziotis 2015). Whereas, the delayed increase in HMW HA diminishes the release of pro-inflammatory cytokines and is inhibitory to angiogenesis (Struve *et al.* 2005; Khaing *et al.* 2011; Austin, Gilchrist and Fehlings 2012; Cyphert, Trempus and Garantziotis 2015). Investigation into HA fragments revealed that hyaluronan tetrasaccharide (HA4) promotes functional recovery when applied to SCI lesion with osmotic mini pump delivery (Wakao *et al.* 2011). The mechanism for this is linked to induced expression of brain-derived neurotrophic factor (BDNF) and vascular endothelial growth factor (VEGF) and anti-apoptotic factors, therefore conferring neuroprotection against excitotoxicity and enhancing CST regenerative sprouting (Wakao *et al.* 2011; Wang *et al.* 2012; Wang *et al.* 2015b).

1.3: Perineuronal nets: the plasticity modulator

Whilst CSPGs are found loose in the ECM in normal and pathological CNS, they are also major constituents of a more compact and specialised ECM structure found around subsets of neurones, known as perineuronal nets (PNNs) (Kwok *et al.* 2011) (later described in detail in section 1.3.1: Structure of PNNs). Despite being discovered in 1893 by Golgi (Celio *et al.* 1998), it is only in the last two decades or so that mounting evidence has revealed the role of PNNs as key modulators of plasticity in the developing and pathological CNS (Wang and Fawcett 2012). The following section will explore the structure and formation of PNNs and how to manipulate novel targets to better control plasticity.

1.3.1: Structure of PNNs

PNNs are pericellular aggregated ECM structures that surround neuronal subpopulations throughout the CNS – mainly parvalbumin (PV)-positive GABAergic interneurons (Brauer *et al.* 1993; Härtig, Brauer and Brückner 1992; Yamada, Ohgomori and Jinno 2015). PNNs are composed of a compact arrangement of a variety of proteoglycans and glycoproteins. All PNN-positive neurones possess membrane-bound enzymes called hyaluronan synthase (HAS) on their cell surface that produce chains of the ubiquitous glycosaminoglycan (GAG) HA and anchor them to the cell surface (Figure 1.1A) (Kwok, Carulli and Fawcett 2010; Giamanco and Matthews 2012). Greater structural variation may also be provided by the binding of HA chains to CD44 receptors on the cell surface (Toole 2004). However, as CD44 is not found on the neuronal surface, it is likely that HAS is the main anchor for PNN tethering (Galtrey *et al.* 2008). HAS forms HA from disaccharide repeating subunits of glucuronic acid (GlcA) and N-acetyl D-glucosamine (GlcNAc), bound together by alternating β1,3 and β1,4 glycosidic bonds (Figure 1.1C) (Kwok, Carulli and Fawcett 2010; Giamanco and Matthews 2012). Other PNN components include some of the

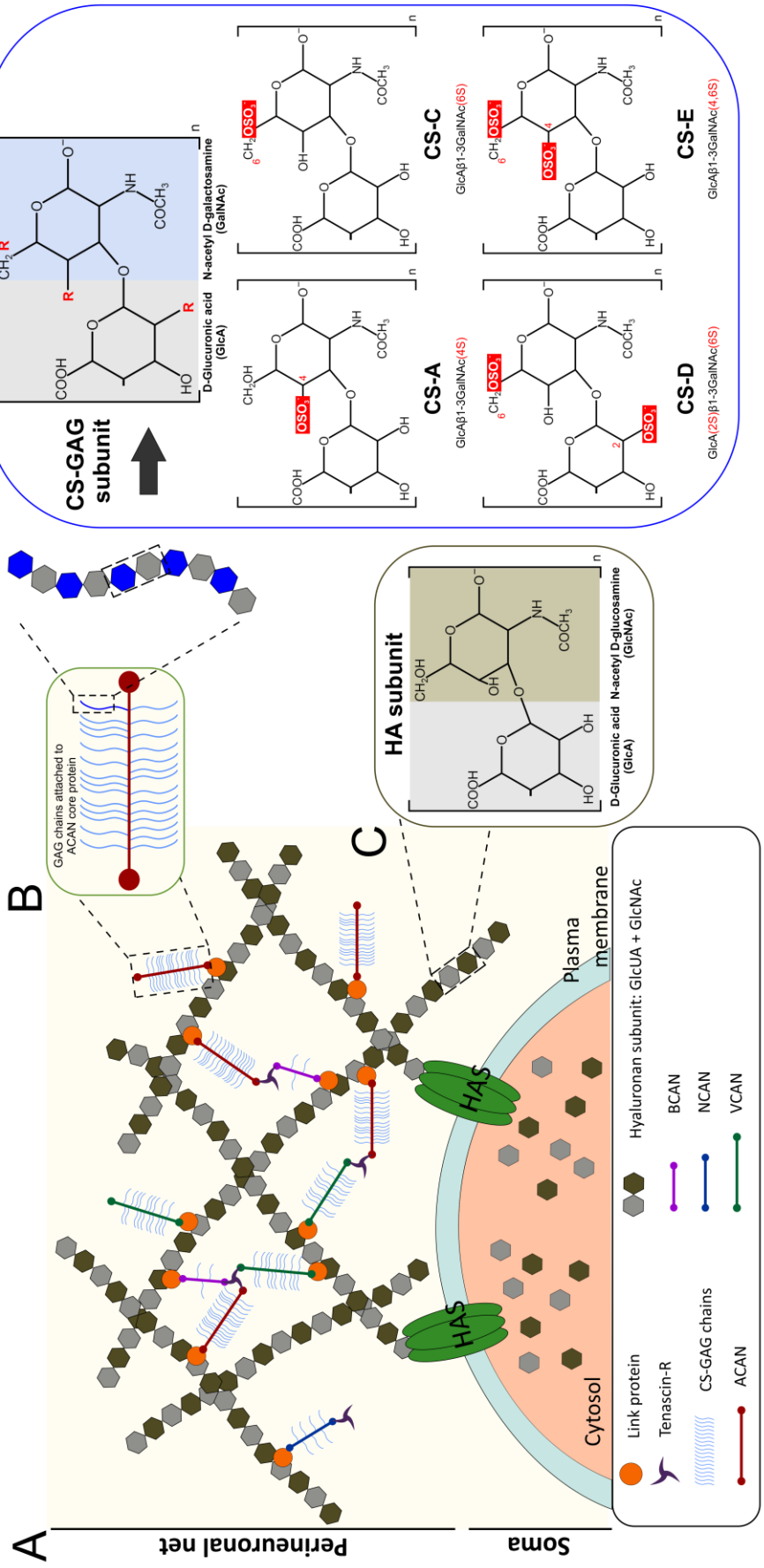

Figure 1.1: Structure of perineuronal nets (PNNs) and their glycosaminoglycan (GAG) components.

A) Aggregated structure of PNNs, modified from (Kwok *et al.* 2011). Hyaluronan (HA) is extruded from the surface of some cells from a plasma membrane enzyme called hyaluronan synthase (HAS). HA forms a backbone upon which various chondroitin sulphate proteoglycans (CSPGs), including aggrecan (ACAN), brevican (BCAN), neurocan (NCAN) and versican (VCAN), bind via a link protein. The PNN structure is further aggregated into a mesh by tenascin-R. **B)** CSPGs are composed of a core protein with chondroitin sulphate glycosaminoglycans (CS-GAGs) attached. These are made up of disaccharide subunits that are often sulphated, as illustrated by the R positions. R denotes a position where the hydroxide (OH) group can be replaced by sulphation (OSO_3^-). The following sulphated CS-GAG subunit isoforms can be used in any combination to form CS-GAG chains, conferring further heterogeneity. **C)** HA is a non-sulphated GAG, composed of a repeating disaccharide, with glucuronic acid (GlcA), like CS-GAGs, and N-acetyl D-glucosamine (GlcNAc).

CSPG family, particularly the lecticans and PTPRZ, which bind via a link domain upon the dense pericellular HA scaffold (Figure 1.1A) (Yamaguchi 2000; Kwok, Carulli and Fawcett 2010; Giamanco and Matthews 2012). The CSPG/HA binding is stabilised by the interaction of HA and proteoglycan binding link proteins (HAPLN), including cartilage link protein 1 (CRTL1/HAPLN1) and brain-specific link protein 2 (Bral2/HAPLN4) (Oohashi *et al.* 2002; Spicer, Joo and Bowling 2003; Kwok, Carulli and Fawcett 2010). Although all HAPLNs will bind to all lecticans, they bind with different affinities. CRTL1 is thought to bind strongly to the CSPGs aggrecan (ACAN) and NCAN (Asher *et al.* 1995), whilst Bral2 has been shown to bind BCAN, and Bral1 (HAPLN2) to VCAN in the nodes of Ranvier (Oohashi *et al.* 2002; Bekku *et al.* 2003). The tertiary mesh structure is further aggregated by tenascin-binding domains on the lectican core protein to which the trimeric tenascin-R (Tn-R) adheres up to three CSPGs together (Aspberg, Binkert and Ruoslahti 1995; Deepa *et al.* 2006; Kwok *et al.* 2011; Giamanco and Matthews 2012; Morawski *et al.* 2014). Both Tn-R and CRTL1 are indispensable for the stabilisation and compact architecture of PNNs (Carulli *et al.* 2010; Morawski *et al.* 2014).

While many of the PNN components, including the HAS enzymes are found in a number of isoforms (Kwok *et al.* 2011), the variety of lecticans are thought to provide much of the heterogeneity of PNNs (Yamaguchi 2000). CSPGs are composed of a core protein, which differentiates the various CSPGs from one another, with varying numbers of CS-GAG chains attached to a serine residue via tetrasaccharide linkage (Figure 1.1A, C) (Yamaguchi 2000). The CS-GAG chains are unbranched polymers composed of repeating subunits of glucuronic acid (GlcA) and N-acetyl D-galactosamine (GalNAc), attached by alternating β1,3 and β1,4 glycosidic bonds (Figure 1.1B) (Kwok *et al.* 2011). CS-GAG disaccharide subunits are more often than not modified by chondroitin sulfotransferase (CSST) enzymes (Carulli *et al.* 2010). The four most common sulphations are illustrated in Figure 1.1B. CS-A and CS-C are

both monosulphated on the fourth position and sixth position of the GalNAc, respectively (Figure 1.1B), and sulphation ratio of each are differentially predominant with development (Carulli *et al.* 2010) and after injury (Yi *et al.* 2012). Each sugar is monosulphated in CS-D, with the second position on GlcA and the sixth on GalNAc, whereas CS-E is has a disulphated GalNAc in positions 4 and 6 (Figure 1.1B). Although disulphated CS-GAGs are present in low quantity in the CNS, CS-D and CS-E are found much more abundantly in PNNs than in the diffuse ECM (Deepa *et al.* 2006). CS-GAGs can have any combination of these sulphations along its length and the pattern of sulphation can influence the binding of molecules. For example, the CS-E moiety has been demonstrated to selectively bind Sema3A, the repulsive guidance molecule (Dick *et al.* 2013; Vo *et al.* 2013), as well as the transcription factor, orthodendicle homeobox 2 (Otx2) (Sugiyama *et al.* 2008; Beurdeley *et al.* 2012), suggesting the ability to sequester inhibitory molecules within the PNN. CS-E also appears to sequester growth factors, such as BDNF (Gama *et al.* 2006) and nerve growth factor (NGF) (Rogers *et al.* 2011). It has been proposed that the binding of various growth factors to CSPGs in PNNs may prevent growth factors from interacting with their natural receptor (Miller and Hsieh-Wilson 2015) thus preventing growth promoting events, such as sprouting. However, the mechanism of inhibition of axonal growth and aberrant synaptic connections by other PNN components has yet to be studied and is a key concept to understanding the role of PNNs in restriction of plasticity.

The sulphation pattern of these CS-GAG chains provides a further degree of heterogeneity (Gama *et al.* 2006; Kitagawa 2014). With such a wide variety of possible components available, it is therefore no surprise that the expression and the molecular selection of glycoproteins and proteoglycans composing the PNN varies between CNS regions (Dauth *et al.* 2016; Mueller *et al.* 2016). It is thought that the heterogeneity of PNNs contributes to the dynamic properties of these structures.

1.3.2: PNNs: Formation and function of PNNs

PNNs are widely distributed throughout the CNS and are implicated in the pathologies of various neurological disorders, including Alzheimer's disease, epilepsy and schizophrenia are thought to implicate PNNs (Suttkus *et al.* 2014a; Pantazopoulos and Berretta 2016; McRae and Porter 2012; Cabungcal *et al.* 2013), as well as in recovery from traumatic CNS injuries, such as SCI (García-Alías *et al.* 2009; Wang *et al.* 2011a). Much of this can be attributed to their role in the restriction of plasticity, which they mediate through the stabilisation of synaptic connections made to their resident cell in the holes of the their net-like structure (Tsien 2013). The accumulation of highly inhibitory molecules, such as CSPGs and sequestered Sema3A bound to CS-E residues, confers protection against the formation of aberrant connections (de Winter *et al.* 2016). PNNs are also thought to act as a cation reservoir, for the fast buffering of ions required for synaptic function, due to the intense negative charge from the high concentration of anionic GAG chains from aggregated CSPGs and HA (Hartig *et al.* 1999; Morawski *et al.* 2015). This may confer neuroprotective effects against oxidative stress induced by Fe^{3+} or by ROS (Morawski *et al.* 2004; Cabungcal *et al.* 2013; Suttkus *et al.* 2014a) and glutamate-induced excitotoxicity (Okamoto, Mori and Endo 1994).

The formation of PNNs coincides with the closure of sensory critical periods (Carulli *et al.* 2010) and is hypothesised to be critical in the termination of developmental plasticity (Pizzorusso *et al.* 2002). The critical period can be defined as a period during an animal's lifespan devoted to the precise shaping of neural connections driven by sensory experience and is therefore highly malleable, with damage or disuse leading to lasting impairment in the normal development and function (Berardi, Pizzorusso and Maffei 2000). Sensory deprivation during the critical period by dark rearing, whisker trimming or absence of song exposure in birds delayed the formation of PNNs in the associated neural centre, resulting in the persistence of plasticity into adulthood

(Pizzorusso *et al.* 2002; McRae *et al.* 2007; Balmer *et al.* 2009; Carulli *et al.* 2010). In particular, during dark rearing experiments, obstruction of visual cues from one eye during the sensory critical period for the visual cortex resulted in the formation of experience-driven connections favouring the unobstructed eye, giving monocular dominance (Pizzorusso *et al.* 2002). Conversely, due to the stabilisation of 'normal' connections with the closure of the critical period, monocular dominance did not occur in adult animals subjected to the same conditions (Pizzorusso *et al.* 2002). In summary, during development, axons project in selective pathways to their appropriate destination, directed by extracellular guidance cues – some of which have already been discussed above (section 1.2.2.2: Extrinsic inhibition of regeneration). This is followed by a "waiting period", during which the dendritic morphology forms before the axons terminate on their specific targets. Subsequently, the elimination of inappropriate synapses and dendrites occurs, with refinement to functional synapses. Maturation of the neural circuitry occurs with development of the PNN matrix architecture around subpopulations of neurones throughout the CNS to provide consolidation of the newly established connections. The persistence of PNNs into adulthood is therefore thought to mediate restriction of plasticity. In the cervical spinal cord, the closure of the critical period and formation of PNNs occurs around postnatal day 14 in the rat, but takes four to five years in humans (Kwok *et al.* 2011).

The bacterial enzyme ChABC selectively degrades the CS-GAG side chains from the CSPG core proteins and HA, in both the neural ECM and PNNs (Crespo *et al.* 2007; Galtrey *et al.* 2007; Lin *et al.* 2008). ChABC has been utilised in multiple models in the brain to remove PNNs in order to restore plasticity, including the erasure of fear memories (Hylin *et al.* 2013), restoration of ocular dominance to the non-deprived eye after dark rearing (Pizzorusso *et al.* 2002) and compensation following incorrect repair of a peripheral nerve injury (Galtrey *et al.* 2007). CRTL1, as discussed above, is a key PNN cross linker molecule and its upregulation is essential to trigger the formation

of PNNs (Carulli *et al.* 2010). Therefore, when adult CNS-specific CRTL1 knockout (KO) mice were dark reared, the development of PNNs was attenuated (Carulli *et al.* 2010), similar to the effect of ChABC injection. This resulted in the persistence of ocular dominance plasticity in these adult CRTL1 KO mice that allowed compensatory innervation for the dark rearing to the ipsilateral visual cortex (Carulli *et al.* 2010). This provided key evidence that the removal of PNNs by ChABC, but not degradation of CSPGs, mediated the enhancement of ocular dominance plasticity and that the structural integrity of PNNs is essential to its ability to limit plastic changes to the circuitry (Pizzorusso *et al.* 2002; Carulli *et al.* 2010).

Interestingly, better functional outcomes to severe CNS injury are seen in children (Wang *et al.* 2004), suggesting that while plasticity is heightened, due to development, there is a greater capacity for compensatory central reorganisation. Adjunct to this, the restriction of central plasticity, via intrinsic and extrinsic mechanisms (discussed in section 1.2.2: Barriers to regeneration above) including the formation of PNNs, may also contribute to the failure of spontaneous recovery in injured adults (Filli *et al.* 2014). Models of reactivation of plasticity by removal of PNNs are not limited to developmental studies in the brain, and the use of ChABC to enhance functional recovery has been extensively investigated in CNS injury models (Moon *et al.* 2001; Bradbury *et al.* 2002; García-Alías *et al.* 2009; Zhao *et al.* 2011) (further explored below in section 1.4.1: Removal of PNNs).

Complimentary to this, PNN removal and the consequent enhancement of central plasticity has also been demonstrated to compensate for deficits in function in a peripheral nerve injury model (Galtrey *et al.* 2007). When ChABC was administered to the corresponding level of innervation in the spinal cord, rather than the peripheral lesion site, the increase in plasticity induced functional recovery even after incorrect nerve repair (Galtrey *et al.* 2007). When the mechanism behind the functional recovery was further investigated, it was found that the intrathecal ChABC treatment

produced the sprouting of new intraspinal connections, increasing the spinal excitability and synaptic efficiency (Bosch *et al.* 2012). It was revealed that polysynaptic and not monosynaptic reflexes were sensitive to reorganisation in a window of central plasticity after injury (Bosch *et al.* 2012). It was noted that "recovery" of functions did not appear to return connectivity to that of intact or naïve animals but created new and alternative pathways. Deletion of Tn-R also attenuated formation of PNNs but less severely than CRTL1 KO (Brückner *et al.* 2000; Carulli *et al.* 2010). In a model of peripheral injury where the facial nerve was axotomised, Tn-R KO mice showed recovery of whisker function (Brückner *et al.* 2000; Guntinas-Lichius *et al.* 2005), providing evidence that the structural integrity of PNNs mediates the central plasticity after peripheral nerve injury. Similarly, injection of ChABC into the cervical spinal cord after unilateral brain lesion, induced plastic changes to uninjured spinal circuitry, including contralateral CST sprouting that was able to overcome functional forelimb (FL) deficits (Soleman *et al.* 2012). These studies highlight a similar compensatory response induced by removal of PNNs in uninjured CNS tissue after remote neural injury and illustrate that recovery induced by ChABC is not exclusively a result of regeneration.

1.4: Controlling plasticity through modulation of PNNs

Despite a myriad of targets within the complex secondary biochemical injury mechanism, current treatment options for acute SCI are limited to pain and symptomatic management, except for intravenous methylprednisolone therapy. Methylprednisolone use is controversial and aims to target secondary mechanisms of injury such as macrophage infiltration. However, methylprednisolone appears to only show minor benefit at the risk of adverse pulmonary and gastrointestinal effects (Botelho *et al.* 2009; Evaniew *et al.* 2015).

Future treatments need to harness plasticity and/or regeneration in order to overcome loss of functions after SCI. As explored above, PNNs are key plasticity regulators which contain a whole host of targets, many of which are glycans. These present new challenges to drug discovery and add to the struggle to find clinically effective therapeutics due to the heterogeneity of SCI. PNNs can be removed to reopen the window of plasticity (see section 1.3: Perineuronal nets: the plasticity modulator) through either degradation of existing PNNs or through interference with the formation or turnover of the PNNs. However, modulation of sulphation and the receptors that PNN components activate in order to mediate their inhibitory effects also represent possible avenues to harness the plasticity mediated by PNNs. The following will review the methods of modulating the inhibitory properties of PNNs to promote recovery after SCI.

1.4.1: Removal of PNNs

The most common methods for PNN removal harness enzymatic degradation of the constituent glycans in PNNs, particularly using the bacterial enzymes ChABC and hyaluronidase. Of these, ChABC has been extensively used as an experimental tool to re-induce plasticity (see section 1.3.2: PNNs: Formation and function of PNNs) via

the dual action of removing both CS-GAG chains and HA (Figure 1.1B-C) (Prabhakar *et al.* 2005; Crespo *et al.* 2007). This thesis will explore an alternative method of removing PNNs by interrupting the turnover of PNNs using a novel small molecule PNN inhibitor (PNNi), the effects of which are discussed in Chapters 4-6. The following will therefore concentrate on the preceding body of research removing PNNs enzymatically to promote recovery after SCI.

1.4.1.1: ChABC

Utilising ChABC treatment for SCI causes widespread ECM changes including at the glial scar and to the biophysical properties of PNNs, particularly with lentiviral delivery (Bartus *et al.* 2014; Milbreta *et al.* 2014). ChABC was first demonstrated to show regeneration after traumatic brain injury (Moon *et al.* 2001) and swiftly applied to SCI with functional regeneration of descending CST neurones after a cervical crush injury (Bradbury *et al.* 2002). Following studies have since demonstrated anatomical recovery of CST, rubrospinal and other spinal neuronal populations, as well as functional recovery in various SCI models (Barritt *et al.* 2006; Tester and Howland 2008; García-Alías *et al.* 2009; Alilain *et al.* 2011; Carter, McMahon and Bradbury 2011; García-Alías *et al.* 2015; James *et al.* 2015). ChABC is most beneficial after more incomplete injuries with the remnants forming a neural bridge rostral and caudal to the injury site through which regeneration and/or plasticity of spared neurones can occur (Iseda *et al.* 2008; Bai *et al.* 2010; Harris *et al.* 2010; Cheng *et al.* 2015). Importantly, whilst ChABC-mediated recovery has been documented in acute SCI studies, it has also been observed in chronic SCI models (García-Alías *et al.* 2009; Carter, McMahon and Bradbury 2011; Wang *et al.* 2011a; Shinozaki *et al.* 2016; Warren *et al.* 2018; Warren and Alilain 2019), greatly extending the impact on SCI patients this strategy could potentially provide. The most extreme example of this, demonstrated robust restoration of diaphragm function with ChABC administration up

to one and a half years after an injury than induced complete hemi-diaphragm paralysis (Warren *et al.* 2018).

It is thought that recovery after dissolving inhibitory PNN components is mediated by a combination of plasticity of intraspinal circuits along with regenerative sprouting and rearrangement of severed and spared fibres (Barritt *et al.* 2006). Release of neurotrophic factors, such as BDNF (Gama *et al.* 2006) and nerve growth factor (NGF) (Rogers *et al.* 2011), and developmental guidance cues sequestered by CS-GAG chains (Celio and Blumcke 1994; Dick *et al.* 2013) may contribute to the regenerative sprouting associated with ChABC administration. Additionally, ChABC confers neuroprotection, reducing inflammation and oxidative stress, and promoting the survival of neurones after injury through several signalling cascades (Carter *et al.* 2008; Akbari *et al.* 2017; Bartus *et al.* 2014). Delayed yet vigorous revascularisation of the lesion site was also observed with acute ChABC treatment (Bartus *et al.* 2014; Milbreta *et al.* 2014). These mechanisms suggest that optimal treatment is in acute or sub-acute stages of the injury, promoting reoxygenation and survival of tissue and minimising continued secondary injury mechanisms. However, whilst anatomical recovery can be induced in many models, this is not always adequate for functional recovery and can be both dose and injection site dependent. Whilst intrathecal administration to the lesion site has frequently been demonstrated to induce functional recovery in both complete transection and Cx injury models (Bradbury *et al.* 2002; Cheng *et al.* 2015), other locations can prove less than optimal. For example, attempts to enhance plasticity of severed CST neurones with intracortical ChABC delivery after a thoracic SCI, produced transient motor impairments that correlated with the transient cortical PNN digestion and blocked cervical CST sprouting (Orlando and Raineteau 2015). Whereas with injection of ChABC rostral or caudal to a cervical injury site induced anatomical recovery, including 5-HT-positive fibres, but not functional recovery (Tom *et al.* 2009). Even with lesion injections,

functional and anatomical recovery appears to be dose dependent, indicating that a larger spread of digestion correlates with recovery. Little to no sprouting occurred with low doses after complete transection, whereas both increased sprouting and functional recovery was observed with high dose bacterial ChABC (Cheng *et al.* 2015). Lentiviral gene delivery to overcome thermal instability issues also induces more potent and widespread ChABC digestion due to sustained delivery, with enhanced functional recovery (Bartus *et al.* 2014).

1.4.1.1.1: ChABC and rehabilitation

Whilst ChABC is a promising therapy in its ability to open a window of plasticity, the long distance regeneration is limited and the functional improvements observed in many studies, while significant, are modest, particularly without sustained ChABC delivery (Caggiano *et al.* 2005; Iseda *et al.* 2008; García-Alías *et al.* 2009; Harris *et al.* 2010). Investigations into combination therapies remain the most clinically desirable. As rehabilitation remains one of the major therapies available for SCI patients, importantly, combined ChABC and task-specific rehabilitative training provides an additive effect in enhancing the recovery of motor functions (García-Alías *et al.* 2009; Wang *et al.* 2011a; Shinozaki *et al.* 2016; Warren *et al.* 2018). In humans, the CST plays an important role in motor control, with direct corticomotor connections (Lemon *et al.* 1998). Whereas, in rodents, the CST primarily conveys skilled functions, such as reaching and grasping (Anderson, Gunawan and Steward 2007) while other general motor functions can be driven by alternative pathways, such as the rubrospinal or reticulospinal tract, after selective CST ablation (Whishaw *et al.* 1993; García-Alías *et al.* 2015). ChABC and task-specific rehabilitation showed a trend of increased CST sprouting in the digested area (García-Alías *et al.* 2009). In contrast, non-specific rehabilitation had a detrimental effect on the recovery of manual dexterity, compared to ChABC treatment alone, correlating with the reduced CST sprouting (García-Alías *et al.* 2009). Recent studies also suggest that combined task-

specific rehabilitation and caudal injection of ChABC, after selective CST and rubrospinal ablation, can induce partial recovery of skilled reaching via regeneration of spared reticulospinal tract neurones (García-Alías *et al.* 2015). These studies suggest that removal of PNNs by ChABC in combination with a short delay of task-specific rehabilitation (García-Alías *et al.* 2009; Krajacic *et al.* 2009; García-Alías *et al.* 2015) is optimal for functional recovery of skilled tasks, driving the refinement of appropriate connections and promoting practised behaviours. The mechanism of rehabilitation may also be through modulation of PNNs, as it has been shown that exercise can differentially mediate PNN expression, with increased expression in the spinal cord in both intact (Smith *et al.* 2015) and injured animals (Wang *et al.* 2011a). This is likely a mechanism by which to prevent the formation of inappropriate connections to spinal Mns. In the SCI rehabilitation model, the ChABC-induced degradation of PNNs and CSPGs attenuates the exercise-driven increase in PNN expression leading to functional improvements (Wang *et al.* 2011a; Smith *et al.* 2015).

1.4.1.1.2: Combination therapies

Whilst many therapies have been developed to overcome inhibitory mechanisms to central plasticity or regeneration, none of these has presented as a single ‘miracle cure’. Instead, it is likely that multiple mechanisms of promoting regeneration and plasticity are required to be harnessed. Notably, the plastic effects generated by ChABC are additive in combination with other treatments to enhance axonal regeneration such as anti-Nogo antibody (Zhao *et al.* 2013), various growth factors (Karimi-Abdolrezaee *et al.* 2010), neurotrophins (Massey *et al.* 2008; Lee, McKeon and Bellamkonda 2010; Kanno *et al.* 2014), as well as cell transplantation (Huang *et al.* 2010; Karimi-Abdolrezaee *et al.* 2010). However, the compatibility of many of these combinations have not yet been investigated with rehabilitative training. Unfortunately, in those that have, such as the combination of ChABC, growth factors and locomotor training, demonstrate that anatomical plasticity does not always

translate to behavioural improvements (Alluin *et al.* 2014). Yet still, there are many investigated combinations that show better recovery with each individual treatment than together, such alongside the enzyme, sialidase to reverse inhibitory MAG signalling (Mountney *et al.* 2013). It is generally thought that therapeutic combinations that are beneficial to recovery do so by harnessing different mechanisms to one another (Mountney *et al.* 2013).

1.4.1.1.3: Clinical application

ChABC has been an invaluably powerful experimental tool that has allowed the positive regenerative and plastic effects of removing PNNs to be demonstrated, as discussed above. However, ChABC is an invasive therapy that requires intrathecal injections to the lesion site and due to its thermal instability requires repeated injection (Chen, Li and Yuan 2015). To sustain the bioavailability of ChABC, researchers have developed thermostable ChABC (Lee, McKeon and Bellamkonda 2010; Hu *et al.* 2018) and a gene delivery system which induces the secretion of the enzyme by mammalian cells (Muir *et al.* 2010; Bartus *et al.* 2014). This gene therapy delivery has been utilised in much of the research above and the latest iteration has mostly controlled the timing of delivery using a doxycycline switch (Burnside *et al.* 2018), highlighting the desirable role of PNNs to consolidate new connections.

Despite its shortcomings, ChABC has completed phase III clinical trials (#NCT00634946) and is approved for use under the name Condoliase for intervertebral disc displacement in Japan (Chiba *et al.* 2018; Matsuyama *et al.* 2018) and currently undergoing Phase III clinical trials in the US (#NCT03607838). However, to date, ChABC has only undergone clinical trials for treatment of canine SCI, using the microtubule delivery of the thermostable version of the enzyme (Hu *et al.* 2018) and not yet in humans. Despite this, progressive functional improvements with delayed ChABC treatment have been observed after cervical hemisection in a recent primate model of SCI (Rosenzweig *et al.* 2019). However, despite the

relevancy here in modelling SCI in a spinal cord more like the human anatomy, the injury depicted here does not represent the common Cx injuries seen clinically. The lack of 5-HT-positive recovery observed in the primate model also highlights the limitations of what has been found in SCI rodent models.

In summary, ChABC has extensively demonstrated that removal of PNNs has an extremely viable therapeutic potential. Therefore, it would be beneficial to explore other pharmacological avenues that result in the removal of PNNs, including less invasive methods.

1.4.1.2: Other enzymatic methods of PNN removal

Whilst ChABC is the most investigated method of removing PNNs, other enzymes exist that degrade the proteoglycans and glycoproteins essential for PNN structural integrity. Five isoforms of hyaluronidase (HYAL) exist and whilst most degrade HA preferentially with partial CS-GAG digestion (Moon, Asher and Fawcett 2003), some are predominantly selective to CS-GAGs (Kaneiwa *et al.* 2010). Early studies in SCI models demonstrated no benefit to HA digestion (Guth *et al.* 1980; Magness *et al.* 1980) and after brain or optic nerve injury induced only short distance regeneration (Tona and Bignami 1993; Moon, Asher and Fawcett 2003). Only recently has HYAL4 been characterised to preferentially digest CS-GAGs over HA chains (Kaneiwa *et al.* 2010). HYAL4 is progressively upregulated transiently in response to acute injury, suggesting an endogenous attempt to remove inhibitory CSPGs (Tachi *et al.* 2015). Unlike exogenous application of ChABC which is of bacterial origin, promotion of endogenous expression of HYAL4 could be harnessed to promote recovery after SCI with reduced immunogenicity.

A disintegrin and metalloproteinase with thrombospondin motifs (ADAMTS) and MMPs are endogenous enzymes that remodel the ECM and are also thought to modulate PNNs through proteolytic digestion of various components, including the core protein of ACAN (Pizzi and Crowe 2007; Durigova *et al.* 2011; Bozzelli *et al.*

2018). Various MMPs are upregulated following SCI (de Castro *et al.* 2000) and have differential effects on the prospect of recovery, with many inducing detrimental effects on vascular permeability and exacerbating inflammatory processes (Noble *et al.* 2002). Inhibition of MMP-9, for example, whilst preventing its digestive effects on PNNs, is associated with improvement of motor functions and greater white matter sparing, suggesting that its elevation post-injury impairs the recovery process (Asahi *et al.* 2001; Hansen *et al.* 2013). MMP-2, on the other hand, appears to be associated with wound healing, and its KO elevated CSPG-mediated inhibition, reduced axonal regeneration and impaired motor recovery (Hsu *et al.* 2006). These results indicate that promotion of MMP-2 expression could be an avenue worth pursuing to enhance plasticity and regeneration.

ADAMTS family members, ADAMTS-1 and -4, are upregulated after stroke with TNF expression (Cross *et al.* 2006), indicating that they are likely to also be present following SCI. When ADAMTS4, also known as aggrecanase-1, was applied via osmotic mini pump to a thoracic Cx injury, axonal sprouting was detected and the same level of functional motor recovery was observed as with ChABC (Tauchi *et al.* 2012). This could represent an endogenous mammalian alternative to the bacterial enzyme ChABC. However, further research for other mechanistic effects, such as neuroprotection, is required.

1.4.2: Modulation of receptors

CSPGs represent the main inhibitory factors present in PNNs and in recent years the receptors through which they mediate their effects have been elucidated. CSPGs interact with a number of receptors, including the PTPσ receptor (Shen *et al.* 2009; Pendleton *et al.* 2013) and leukocyte common antigen-related (LAR) phosphatase (Fisher *et al.* 2011; Xu *et al.* 2015). It has been well established that molecules associated with the Rho/ROCK signalling pathway show prolonged upregulation of

expression, induced by CSPGS, post- injury, and that inhibition of this pathway induces neurite outgrowth (Borisoff *et al.* 2003; Monnier *et al.* 2003; Sivasankaran *et al.* 2004; Conrad *et al.* 2005; Wei *et al.* 2014). However, it was not until the discovery of these receptors that the mechanism of how they activated this inhibitory pathway was exposed (Fisher *et al.* 2011; Pendleton *et al.* 2013). Although PTPσ receptor is a CSPG receptor, binding with high affinity to CS-E and CS-D disaccharides (Dickendesher *et al.* 2012), PNN-associated neurones do not express PTPσ receptor in the normal uninjured CNS (Yi *et al.* 2014). Instead, LAR and PTPσ receptors are found in growth cones during development and are upregulated after SCI (Zhang *et al.* 1998; Lang *et al.* 2015). As they are present on CST and 5-HT fibres, deletion of these receptors, therefore, prevented growth cone collapse, allowing regeneration of these fibres and functional motor recovery (Thompson *et al.* 2003; Fry *et al.* 2010; Xu *et al.* 2015). Pharmacological blockade of PTPσ receptor signalling using local application of a peptide, such as intracellular sigma peptide (ISP), has also been demonstrated to promote functional recovery in multiple SCI models (Lang *et al.* 2015; Urban *et al.* 2019a). For example, in a hemisection respiratory SCI model, PTPσ inhibition induced robust recovery of diaphragm function (Urban *et al.* 2019a). This was mediated via sprouting of spared contralateral bulbospinal respiratory fibres to the ipsilateral phrenic motor pool which when the hemisection was relesioned did not compromise diaphragm recovery (Urban *et al.* 2019a). ISP modulation of the PTPσ receptor may also confer its enhancement of regeneration through secretion of the protease Cathepsin B and its PNN degradation abilities (Tran *et al.* 2018). CSPGs may also mediate their negative effect on SCI recovery through modulation of the inflammatory process via LAR and PTPσ receptor signalling, with inhibition using intracellular LAR peptide (ILP) and ISP, respectively, promoting the anti-inflammatory M2 macrophage activation (Dyck *et al.* 2018).

CSPGs also bind to other receptors that are associated with myelin-associated inhibitors, including the Nogo-66 receptors, NgR1 and 3 (Dickendesher *et al.* 2012), and the endothelial growth factor (EGF) receptor (Koprivica *et al.* 2005) are also activators of the Rho/ROCK pathway (Niederöst *et al.* 2002; Montani *et al.* 2009; Joset *et al.* 2010). CSPGs are the first ligand identified to bind to the NgR3 (Dickendesher *et al.* 2012). Deletion of the CSPG binding NgR isoforms 1 and 3, also enhanced regeneration after an optic nerve crush, additive to the regeneration seen with NgR1-selective KO (Dickendesher *et al.* 2012). Similarly, blockade of EGF receptors induces improvements in motor, sensory and bladder functions, likely a consequence of the increased tissue sparing observed (Koprivica *et al.* 2005; Erschbamer, Pernold and Olson 2007).

Additionally, sulphation-specific CSPG binding with the cell adhesion molecule, Contactin-1 (CNTN-1) has been observed, revealing a facilitatory role for CS-E in the stimulation of neurite outgrowth (Mikami, Yasunaga and Kitagawa 2009). Developmental studies show that the soluble form of the PTPRZ, also known as the CSPG phosphacan, forms a complex with CNTN-1 expressed on the surface of oligodendrocyte precursor cells, dependant on the PTPRZ ectodomain and implicates CSPG-CNTN-1 binding as a promyelinating factor (Lamprianou *et al.* 2011).

In summary, CSPGs activate a wide variety of receptors, many of which appear to converge through the Rho/ROCK pathway, as well as other individual signalling cascades to confer inhibition of regeneration (Ohtake *et al.* 2016). However, the discovery of CS-E and PTPRZ binding to CNTN-1 suggests that CSPGs may also promote regeneration and remyelination (Mikami, Yasunaga and Kitagawa 2009; Lamprianou *et al.* 2011). This highlights that whilst blockade of inhibitory CSPG receptors could prevent the collapse of growth cones and improve cell survival after CNS injury (Dergham *et al.* 2002), developing ligand-specific binding molecules for

facilitatory receptors, such as CNTN-1, could provide additional targets beneficial for recovery after SCI.

1.4.3: Modulation of sulphation

Whilst CSPGs have been the one of the main PNN targets used to enhance regeneration/plasticity, removal is not the only methods through which we can manipulate their inhibitory effects. The sulphation of the CS-GAG disaccharides influences both the binding properties and the more highly sulphated, the greater the negative charge of these chains.

The predominant CS sulphation in the CNS ECM changes from CS-6S (CS-C), during the end of the critical period, to CS-4S (CS-A), both within the ECM and newly formed PNNs, with development to adulthood (Figure 1.1B) (Kitagawa *et al.* 1997; Deepa *et al.* 2006; Carulli *et al.* 2010; Miyata *et al.* 2012). The regulation of this shift is independent of sensory-experience, unlike the upregulation of CTRL1 that triggers PNN formation (Carulli *et al.* 2010; Miyata *et al.* 2012). However, the shift in CS-4/6S ratio is associated with increased inhibition to neurite extension and, subsequent restriction of plasticity, even with the same CSPG core protein variants (Beller *et al.* 2013). The aging CNS appears to further increase CS-A, and decrease CS-C in PNNs, resulting in greater restriction of plasticity (Miyata and Kitagawa 2016; Foscarin *et al.* 2017).

Sulphation patterns are also implicated in the regulation of plasticity (Miyata *et al.* 2012). Sulphation of the fourth or sixth position of GalNAc in the CS-GAG disaccharide is mainly conveyed by the CSST enzymes, chondroitin 4-sulphotransferase-1 (C4ST-1) or chondroitin 6-sulphotransferase-1 (C6ST-1), respectively (Habuchi 2000). Overexpression of C6ST-1 in mice prevented the developmental CS4/6S shift but not the formation of PNNs, however, did confer the

persistence of plasticity (Miyata *et al.* 2012). Some of the PNNs formed were negative for the 'universal PNN marker' *Wisteria floribunda* agglutinin (WFA) and instead were enriched in a marker for CS-C, suggesting that WFA binding is sulphation-specific (Miyata *et al.* 2012). These CS-C rich PNNs appeared to form a loose net structure that did not bind tightly around the synaptic contacts of the PNN-positive cell (Miyata *et al.* 2012), indicating an impaired ability to stabilise synapses. The CS-GAG sulphation pattern therefore appears to be able to affect the structural integrity of PNNs and consequently the restriction of plasticity.

After CNS injury, this ratio of CS-sulphation shifts marginally. After cortical injury in rats, this shifted back towards that seen in development, with upregulation of CS-C, as the CS-6 sulphation of GalNAc is believed to be permissive to growth (Gilbert *et al.* 2005; Properzi *et al.* 2005), and that CS-A levels decreased (Gilbert *et al.* 2005). However, in the mouse, both after SCI (Wang *et al.* 2008) and cortical impact (Yi *et al.* 2012), increases in CS-A were observed. It is unclear whether these contrasting sulphation shifts post-injury are a result of different effects of CNS injury between rats and mice. CS-E has also been reported to increase following CNS injury (Gilbert *et al.* 2005). However, both C4ST-1 and CS6ST-1 expression in the mouse was upregulated (Sun *et al.* 2011)

Various reports suggest that CS-A and CS-E are inhibitory, with overexpression of C4ST resulting in inhibition of neurite outgrowth (Gilbert *et al.* 2005; Wang *et al.* 2008; Brown *et al.* 2012). Whereas, after CNS injury, C6ST-1 KO mice displayed reduced spontaneous regeneration, suggesting that CS-C has positive effects on plasticity and regeneration (Sun *et al.* 2011). CS-E inhibition, using an antibody, promoted growth through downregulation of PTPσ receptor activation, preventing growth cone collapse (Brown *et al.* 2012). It should be noted that only some CS-sulphation moieties bind to CSPG receptors, including CS-E (Dickendesher *et al.* 2012).

Arylsulphatase B (ARSB) is a human enzyme, present in the liver, kidneys and pancreas that can lysosomally remove CS-A moieties from the non-reducing end of CS-GAG chains. ARSB was able to promote the extension of neurites *in vitro* and *in vivo* after optic nerve crush without removing PNNs (Pearson *et al.* 2018). When applied to a mouse SCI model, ARSB was able to induce functional motor recovery comparable but slightly delayed in comparison to ChABC and promoted axonal regeneration (Yoo *et al.* 2013). It appeared that different axonal fibres had different sensitivities to CS-GAGs with greatest 5-HT growth with complete CS-GAG digestion using ChABC but greater tyrosine hydroxylase (TH) fibre growth after selective CS-A removal using ARSB (Yoo *et al.* 2013). As ARSB is chemically stable and optimally active in the acidic environment of the spinal cord, this offers a more immunogenetic, and already licenced, alternative to ChABC for the treatment of SCI.

The effect of studies modulating sulphation suggest that using treatments that can reduce CS-A expression while promoting CS-C could provide possibilities to promote plasticity without removal of PNNs.

1.5: Aims and objectives of thesis

1.5.1: Characterisation of PNNs in the spinal motor pools:

Many studies look to improve motor functions by removing PNNs to increase plasticity of spared spinal circuits. However, in the spinal cord many of the cells associated with PNNs have yet to be elucidated, including the contribution of PNNs to motoneuronal synaptic stability. It is the gold standard to use the lectin WFA to label PNNs as it is understood to bind to the GalNAc sugar residue in CS-GAG chains. However, recent studies report PNNs without WFA binding (Miyata *et al.* 2012; Ueno *et al.* 2017; Yamada and Jinno 2017).

The first experimental chapter (Chapter 3: Characterisation of perineuronal nets in the spinal motor pools), therefore, aims to further characterise PNNs in the spinal cord, using immunohistochemical methods (IHC), by:

a) investigating the association of motoneurones (Mns) with PNNs in the spinal cord, including with Mn subclasses

b) Identifying the best label for PNNs associated with spinal Mns

c) Investigating the heterogeneity of PNNs across the spinal motor pools

It is expected that, as Mns are the last endpoint of neural motor control, they will be highly associated with PNNs as a means of stabilising their synaptic contacts and that WFA will not label all PNNs associated with this population.

1.5.2: Promoting plasticity for recovery using perineuronal net inhibitor

ChABC has effectively demonstrated that removal of PNNs is a viable avenue for enhancing recovery for treatment of both acute and chronic SCI. Crucially, this method also shows potential in combination with other therapies, including task-

specific rehabilitation, as the future of clinical application requires the application of our most effective therapies to overcome the inhibitory mechanisms for optimal functional recovery.

This study looks to utilise a novel small molecule for non-invasive removal of PNNs in a clinically relevant Cx model of acute SCI. Perineuronal net inhibitor (PNNi) is a pharmacological molecule already licenced for treatment of a non-CNS-related disease and until patenting for CNS disorders will be referred to as PNNi throughout this thesis. As this is the first time PNNi will be used to remove PNNs in this pathology, Chapter 4: Enhancing functional recovery using novel non-invasive PNN inhibition, firstly aimed to characterise the functional baseline of acute PNNi administration in intact normal adult rats.

1.5.2.1: Investigating the functional motor and sensory effects of acute (10 days) systemic PNN removal to the uninjured animal

Due to the efficacy of ChABC with rehabilitation, the remainder of Chapter 4: Enhancing functional recovery using novel non-invasive PNN inhibition looked to provide a combinatorial approach to testing the efficacy of PNNi along with rehabilitation in maximising functional recovery, as assessed by motor and sensory behavioural tests. As PNNi is an oral compound, the duration of PNN removal could be controlled allowing for PNN consolidation after a window of plasticity.

1.5.2.2: Promoting plasticity for functional recovery after acute SCI using novel PNN inhibitor (PNNi)

a) Determine the efficacy of chronic PNNi in promoting functional recovery in combination with rehabilitation by accessing the recovery of HL locomotor activity and sensory function

b) Determine the effect of consolidation of PNNs on functional recovery after a sustained period of PNNi removal (8 weeks PNNi treatment) in combination with rehabilitation

It was expected that PNNi would be able to open a window of plasticity allowing for the rearrangement of spared neural circuitry that would be driven to form functional connections with application of rehabilitative treatment. As PNNs form to stabilise mature and functional activity, it was expected that a defined window of treatment would allow greater recovery, due to the stabilisation of new functional synapses, particularly with sustained rehabilitation to drive further activity-dependant plasticity.

1.5.3: Mechanisms of PNNi-mediated plasticity

The final experimental chapter, Chapter 5: The mechanistic changes induced by systemic PNNi inhibition, aims to elucidate some of the mechanisms through which the above treatment paradigms effect functional recovery, firstly:

1.5.3.1: Assessing the effect of chronic PNNi administration on PNNs in the cortex and spinal cord through expression of key PNN components

1.5.3.2: Determine the efficacy of PNNi in promoting regeneration and plasticity after acute SCI, by assessing:

i. Changes to the excitatory-inhibitory balance
ii. Functional cortical motor pathways
iii. Anterograde and retrograde neuronal tracing

It is expected, based on previous unpublished results from acute administration that PNNi will induce greater removal of PNNs in the spinal cord, rather than brain regions, leading to greater levels of plasticity in the spinal cord. Positive shifts in excitatory-

inhibitory balance are expected to occur with PNNi administration with refinement of this with rehabilitation.

Chapter 2: General Materials and Methods

2.1: Animals

Adult female Lister-hooded rats (200-250 g) were obtained from Charles River Laboratories (Canterbury, UK). Rats were housed in pairs in Central Biomedical Services (University of Leeds, UK) in a temperature-controlled environment in (20 ± 1 ^{o}C), with a 12 hr light/dark cycle (lights on at 07:00). Access to food and water was *ad libitum*. All procedures and experiments complied with the UK Animals (Scientific Procedures) Act 1986, following the 3R principles and the ARRIVE guidelines.

2.2: Histology

2.2.1: Tissue preparation

Animals were given an overdose of sodium pentobarbital (Pentoject; Henry Schein; 200 mg/kg; intraperitoneal (i.p.) injection) to deeply anaesthetise without halting cardiac function. A transcardial perfusion (Gage, Kipke and Shain 2012) was then performed using sodium phosphate buffer (PB; 0.12 M sodium phosphate monobasic; 0.1 M NaOH; pH 7.4) followed by 4 % paraformaldehyde (PFA; in PB; pH 7.4) for tissue fixation. The brain and spinal cord were dissected out, post-fixed in PFA (4 %; 4 ^{o}C) overnight and cryoprotected in 30 % sucrose solution (30 % v/w sucrose in PB; 4 ^{o}C) until tissue saturation. The left brain hemisphere and appropriate spinal cord segments were excised and frozen in optimum temperature medium (OCT; Leica FSC 22 Frozen Section Media; Leica Biosystems) before storage at -80 ^{o}C until sectioning. Sectioning of tissue was performed using a cryostat (Leica CM1850; Leica Biosystems) into 40 µm transverse sections for free-floating sections and 25 µm for on-slide preparations. Free-floating sections were serially collected into 48-well plates containing physiological buffer solution (PBS; 0.13 M sodium chloride, 0.7 M sodium phosphate dibasic, 0.003 M sodium phosphate monobasic; pH 7.4) to remove the OCT before being transferred to 30 % sucrose solution for storage at 4 ^{o}C.

Table 2.1: Immunohistochemical detection of extracellular matrix components and neuronal markers, including concentration (conc.) of antibody.

Detected component	Marker	Host	Antibody Conc.	Source	Characterisation
CSPGs					
Aggrecan (mouse ACAN core protein)	Anti-ACAN	Rabbit polyclonal IgG	500 µg/ml	Millipore #AB1031	WB[2] (Lendvai *et al.,* 2013 & Sutkus *et al.,* 2014)
Brevican (BCAN; mouse cell-line derived recombinant human Brevican)	Anti-BCAN	Sheep polyclonal IgG	1 mg/ml	R&D Systems #AF4009	WB[2] (R&D Systems data sheet)
Neurocan (NCAN; N-terminal epitope)	Anti-NCAN	Mouse monoclonal IgG	369 µg/ml	DSHB[1] #1F6	WB[2] (Asher *et al.,* 2000 & Deepa *et al.,* 2006)
Versican (VCAN; hyaluronate-binding region)	Anti-VCAN	Mouse monoclonal IgG	169 µg/ml	DSHB[1] #12C5	WB[2] (Asher *et al.,* 2002 & Deepa *et al.,* 2006)
Phosphacan (PTPRZ)	Anti-PTPRZ	Mouse monoclonal IgG	165 µg/ml	DSHB[1] #3F8	WB[2] (Deepa *et al.,* 2006 & Vitellaro-Zuccarello *et al.,* 2006)
Lectins					
N-acetylgalactosamine (GalNAc)	Wisteria floribunda agglutinin (WFA)	N/A	2 mg/ml	Sigma #L8258	Koppe *et al.,* 1996
N-acetylgalactosamine (GalNAc)	Biotinylated Wisteria floribunda agglutinin (WFA)	N/A	2 mg/ml	Sigma #L1766	Koppe *et al.,* 1996

Hyaluronan (HA)	Biotinylated Hyaluronan-binding protein (Bio-HABP)	N/A	250 µg/ml	AMSBio #AMS.HKD-B141	(Tengblad 1981)
Wisteria floribunda agglutinin (WFA)	Anti-WFA	Rabbit polyclonal IgG	2 mg/ml	LifeSciences BioScience #LS-C76865	-
Cell markers					
Choline acetyltransferase (ChAT)	Anti-ChAT	Goat polyclonal IgG	-	Millipore #AB144P	-
Glutamic acid decarboxylase isoforms 65 and 67 (GAD65/67)	Anti- GAD65 + GAD67 (GAD65/67)	Rabbit polyclonal IgG	-	Abcam #ab11070	-
Glial Fibrillary Acidic Protein (GFAP); clone N206A/8	Anti-GFAP	Mouse monoclonal IgG1	1 mg/ml	Neuromab #75-240	WB[2] (Neuromab data sheet)
Neuron-specific nuclear protein (NeuN)	Anti-NeuN	Mouse monoclonal IgG1	1 mg/ml	Millipore #MAB377	WB[2] (Jin *et al.*, 2003)
Neuron-specific nuclear protein (NeuN)	Anti-NeuN	Rabbit polyclonal IgG	-	Millipore #ABN78	-
Vesicular Glutamate Transporter (VGLUT2)	Anti-VGLUT2	Mouse monoclonal IgG1	1 mg/ml	Abcam #ab79157	-

[1] *DSHB, Developmental Studies Hybridoma Bank, University of Iowa, USA*. [2]*WB, Western blotting*

2.2.2: Immunohistochemical techniques

At room temperature (RT), sections were washed three times for 5 min each in Tris-buffered saline (TBS; 0.1 M Tris base, 0.15 M NaCl; pH 7.4) to remove sucrose residue. Tissue was then blocked in 0.3 % TBST (1x TBS solution and 0.3 % v/v Triton X-100) and 3 % normal donkey serum (NDS; v/v) for two hours. The sections were then transferred to co-incubate at 4 °C in blocking buffer (3 % NDS in 0.3 % TBST; pH 7.4) containing primary antibodies (Table 2.1).

Following primary antibody incubation, sections were then washed thrice using TBS (10 mins; RT). To visualise each primary antibody staining, the tissue was then co-incubated in darkness with the fluorescent-conjugated secondary antibodies (1:500; 2 hrs; RT; Table 2.2) against the species of the primary antibodies. Tissues were then washed three times in TBS (10 mins; RT) whilst protected from light. A final wash in Tris non-saline (TNS; 0.5 M Tris, pH 7.6) was given to reduce precipitation before air-drying. Tissues were mounted on Superfrost Plus slides, air-dried and coverslipped with the mounting medium FluorSave™ Reagent (EMD Millipore).

Table 2.2: Fluorescent-conjugated secondary antibodies (2 mg/ml) used for immuno-detection of primary antibodies.

Antibody	Host	Source
Alexa fluor 488	chicken anti-goat IgG	Invitrogen #A21467
Alexa fluor 488	goat anti-mouse IgG1	Invitrogen #A21121
Alexa fluor 488	*Streptavidin*-conjugated	Invitrogen #S32354
Alexa fluor 568	donkey anti-mouse IgG	Invitrogen #A31571
Alexa fluor 568	donkey anti-rabbit IgG	Invitrogen #A10042
Alexa fluor 568	donkey anti-sheep IgG	Invitrogen #A21099
Alexa fluor 568	*Streptavidin*-conjugated	Invitrogen #S11226
Alexa fluor 647	donkey anti-mouse IgG	Invitrogen #A31571
Alexa fluor 647	Donkey anti-rabbit IgG	Invitrogen #A31573
Alexa fluor 647	*Streptavidin*-conjugated	Invitrogen #S32357

Immunostaining was routinely carried out using tissue from different animals and differing spinal segments. The following describes specific immunohistochemical experiments and the antibodies used.

2.2.2.1: Characterisation of PNNs in the spinal motor pools

Immunohistochemical techniques were used to label for cells in the spinal cord containing choline acetyltransferase (ChAT; goat; Millipore; 1:500; 72 hrs; 4 ^{o}C) and the PNNs surrounding subsets of these cells were labelled by biotinylated *Wisteria floribunda* agglutinin (bio-WFA; Sigma; 1:300; 24 hrs; 4 ^{o}C) and CSPG components, including ACAN (rabbit; Millipore; 1:250; 24 hrs; 4 ^{o}C), BCAN (sheep; R&D Systems; 1:500; 24 hrs; 4 ^{o}C) and NCAN (mouse; DSHB; 1:100 ; 24 hrs; 4 ^{o}C; Table 2.1). ChAT was used for Mn identification (Phelps *et al.* 1984) whilst WFA is commonly used as a marker for PNNs (Pizzorusso *et al.* 2002; Giamanco, Morawski and Matthews 2010). The combinations carried out in this study used the formula: ChAT - Bio-WFA - CSPG marker using various antibodies from Table 2.1, including for the lecticans ACAN, BCAN, NCAN and VCAN (mouse; DSHB; 1:100; 24 hrs; 4 ^{o}C). To differentiate between alpha and gamma Mns (Smith *et al.* 2015; Friese *et al.* 2009), tissue was co-stained with anti-ChAT and anti-NeuN (mouse; Millipore; 1:500; 24 hrs; 4 ^{o}C). Ventral alpha Mns showed large cell bodies and were positive for both ChAT and NeuN reactivity, whereas gamma Mns were also contained in the ventral motor pools but were only ChAT-positive (Smith *et al.* 2015; Friese *et al.* 2009). Characterisation of PNNs in the motor pools was compared throughout the spinal levels using serially collected free-floating tissues from the C1-6, mid-thoracic and the L1-6 spinal cord.

2.2.2.2: Changes after chronic PNNi administration in SCI model

Animals were used in the following study (described in section 2.3: Acute contusive SCI, following termination of the paradigm illustrated in Figure 2.1A) to determine the effect of chronic administration of the novel small molecule PNN inhibitor (PNNi). Biotinylated hyaluronan binding protein (Bio-HABP; AMSBio; 1:300; 24 hrs), bio-WFA

and ACAN were used to label PNNs and the ECM in the brain and spinal cord sections (Table 2.1). For confirmation of PNN identification, PNN components were co-stained using anti-NeuN (either mouse or rabbit; Millipore; 1:500; 24 hrs). Changes to excitatory-inhibitory balance were labelled using antibodies for vesicular glutamate transporter 2 (VGLUT2: Abcam; 1:500; 24 hrs) and for both glutamic acid decarboxylase isoforms 65 and 67 (GAD65/67; Abcam; 1:500; 24 hrs; Table 2.1), respectively. Serially collected 25 µm slide-mounted transverse spinal cord slices collected from the T4-6 region and 40 µm brain free-floating slices were used.

2.2.3: Image acquisition and quantification techniques

The fluorophores used to label the brain and spinal cord sections were visualised using a Zeiss LSM 880 (upright) confocal microscope. All images were randomised and the treatment groups and/or level of the spinal cord were blinded to the analyser.

2.2.3.1: Characterisation of PNNs in the spinal motor pools

Images were taken as tile scans of the entire spinal cord transverse section at 20 x magnification (1.03 µs per pixel, averaging: 4*)*. ChAT-positive cells and co-localisation with WFA-positive PNNs and other CSPG-positive PNNs were counted using the Cell Counter plugin (Kurt de Vos; https://imagej.nih.gov/ij/plugins/cell-counter.html) in the software FIJI (Schindelin *et al.* 2012). Mns were identified by location within the ventral horn (VH) of ChAT-positive cellular staining. All ChAT-positive cells were individually counted and sequentially analysed for presence of PNN staining. PNNs were only counted around ChAT-positive neurones and was identified by the presence of intense staining as a bright ‘halo’ directly adjacent to the perimeter of ChAT-positive cells. PNN staining was labelled as either WFA-positive, positive for the appropriate CSPG stain or as WFA-positive CSPG-positive. For differentiation of alpha and gamma Mns, cells co-localising both ChAT and NeuN staining where taken

as alpha Mns whereas the absence of NeuN denoted gamma Mns (Friese *et al.* 2009; Mullen, Buck and Smith 1992).

2.2.3.2: Detecting changes to PNNs after PNNi administration

Images were taken as tile scans of the entire spinal cord transverse section or 2 x 4 tile scans of the cortex at 20 x magnification (1.03 µs per pixel, averaging: 4*)*. The intensity (mean gray value), area and integrated density were recorded using the software FIJI (Schindelin *et al.* 2012) for HABP, Bio-WFA and ACAN for the VHs of each spinal cord section images and for a 400 µm x 1500 µm area of the imaged cortex to assess the effect of PNNi administration on these CNS regions. In the VH, ACAN- and WFA-positive PNNs around NeuN-positive cells were sequentially counted using the Cell Counter plugin (Kurt de Vos; https://imagej.nih.gov/ij/plugins/cell-counter.html) in the software FIJI (Schindelin *et al.* 2012) and normalised per number of NeuN-positive cells per VH. Excitatory-inhibitory balance was also assessed using the same measures in these areas for GAD65/67 and VGLUT2. For all stains, the mean gray value for the corresponding secondary control sections were subtracted from each individual measure to account for non-specific background staining.

2.3: Acute contusive SCI

2.3.1: Laminectomy and Cx injury

Using isofluorane as an anaesthetic (5 % in O_2 for induction and 2 % in O_2 for the duration of the procedure), animals were shaved, sterilised and eye lubricant was applied. A skin incision was made in the midline of the back to expose vertebral segments T7-13. Muscles were reflected to perform a dorsal laminectomy at T8. At the point, the cord was covered with spongostan™ (Ethicon™ #MS0002) for protection, a single absorbable suture was given to reflected muscles and sham animals were sutured closed. For all other animals, vertebral levels T7 and T8 were stabilised whilst an Infinite Horizon impactor (Precision Systems and Instrumentation, LLC, Fairfax Station, VA) was used to provide a 200 kdyn Cx (moderate-severe) (Scheff *et al.* 2003) at the level of T9 at the site of the T8 dorsal laminectomy. Spinal cord injured animals were then closed as described above, but the skin was closed with Autoclips® (Stoelting Europe, Ireland). Following surgery, animals were housed individually for seven days to recover during a period of reduced mobility. Post-Cx, bladders were expressed twice daily until urinary reflexes recovered (approximately two to three weeks post-injury). Analgesia (Vetergesic Buprenorphine; 0.015 mg/kg; Henry Schein Animal Health, Dumfries, UK) and antibiotics (Baytril enrofloxacin; 2.5 mg/kg; Henry Schein Animal Heath, Dumfries, UK) were given via subcutaneous injection immediately post-surgery and for three days following surgery. Treatment with an opioid, such as buprenorphine, was used as an analgesic instead of non-steroidal anti-inflammatories, such as ibuprofen, due to the ability of the latter group to positively modulate recovery after SCI (Wang *et al.* 2009). Additional antibiotics and/or analgesia were given to prevent infections on an individual basis for up to a week. All animals were monitored daily until the end of the experiment.

2.3.2: Treatments

Following the surgical Cx injury or sham procedures described above, animals were randomly grouped according to treatment paradigm, detailed above in Table 2.3 (*n=18* per group for chronic PNNi treatment timeline, Figure 2.1A; *n=5* per group for PNNi and PNNi + T only, Figure 2.1B), to test the efficacy of the small molecule PNN inhibitor (PNNi) on enhancing recovery after SCI. Due to the importance of rehabilitation as a SCI therapy, PNNi and rehabilitative training combination groups were included to look for issues of compatibility. For the chronic PNNi paradigm (Figure 2.1A), group sizes were calculated to account for multiple endpoints where *n= 3* for biochemistry (not described in thesis), *n=5* for neuronal tracing (see section 2.3.5: Neuronal tracing below) and *n=5* for two different electrophysiology experiments (*in vivo* ICMS experiments only will be discussed in thesis, described below in section 2.3.6: Terminal *in vivo* electrophysiology: intracortical microstimulation).

Table 2.3: Following sham or mid-thoracic contusion (Cx) injury surgical procedures, rats were categorised into treatment groups.

Group	SCI/Lam	Treatment	Training
Sham	Lam	-	-
Sham + PNNi	Lam	PNNi	-
PNNi	Cx	PNNi	-
PNNi + T	Cx	PNNi	✓
Vehicle	Cx	Nutella (vehicle)	-
Vehicle + T	Cx	Nutella (vehicle)	✓

Lam, laminectomy only; PNNi, perineuronal net inhibitor (2 g/kg).

2.3.2.1: Pharmacological administrations

Pharmacological treatment commenced from the day of injury (PNNi; 2 g/kg from a stock solution of 0.2 g/ml). This dosage is higher than the licenced dose of PNNi for treatment of a non-CNS-related disease and was established using preliminary *in*

vitro experiments (unpublished). Oral administration was achieved by syringe-feeding (Atcha *et al.* 2010), twice daily (~ 9 AM and 5.30 PM) to complete the daily dose, as opposed to via gavage. Oral syringe feeding was selected and optimised following a pilot study investigating the method of administration. Due to the low solubility of PNNi, an oil-based carrier of chocolate and hazelnut spread and sunflower oil was prepared to improve the palatability during daily feeding. The vehicle was fed independently as a control at the same weight-matched volume (Vehicle groups). The low solubility of the PNNi solution prevented blinding of the pharmacological treatment as both treatments were clearly visually different.

As PNNi is an oral compound the length of administration can be controlled. Firstly, the drug was administered chronically from day of injury/surgery to the day of termination and *n=18* for each of the groups (Table 2.3), following the experimental paradigm outlined in Figure 2.1A (chronic PNNi paradigm). As this may not be the optimal therapeutic timeline for optimal recovery after SCI, a second timeline was carried out as described in Figure 2.1B, where drug administration was given from the day of injury for a period of 8 weeks after which PNNs would be allowed to reform (*n=5* per group; 8 week PNNi paradigm).

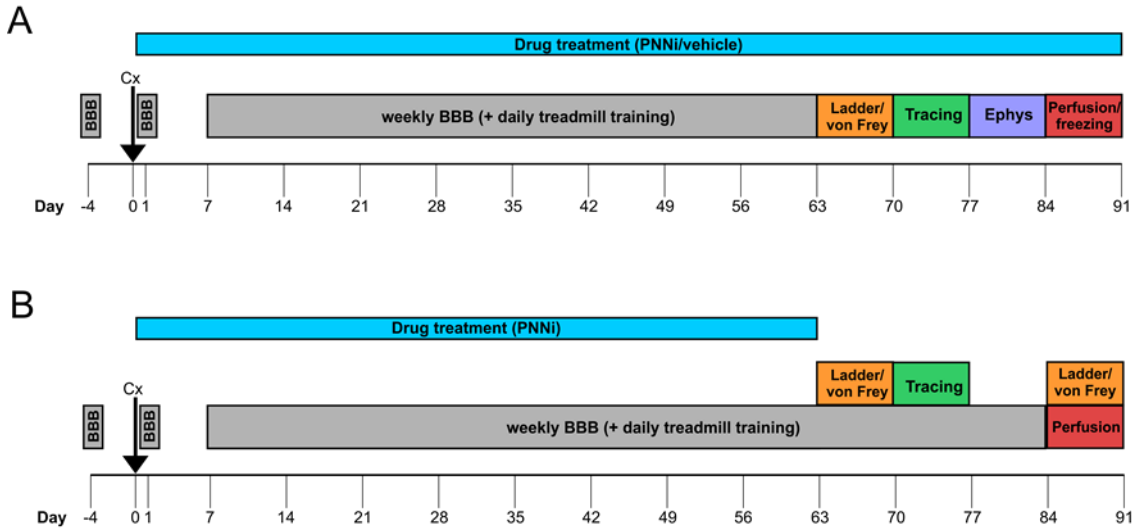

Figure 2.1: Timeline for pilot study showing the paradigms used to assess functional and anatomical recovery after mid-thoracic contusion (Cx) injury.

A) Primary timeline where PNNi or vehicle treatments were given from the day of injury to termination (chronic PNNi paradigm). All groups described in Table 2.3 followed this paradigm. **B)** Modified timeline where PNNi is given only from the day of injury for a period of 8 weeks to allow consolidation of PNNs before the completion of the paradigm (8 week PNNi paradigm).

2.3.2.2: Rehabilitation

Training was comprised of distributed practice interval treadmill training in the quadrupedal position to provide delayed task-specific rehabilitation (García-Alías *et al.* 2009; Heng and de Leon 2009; Shah *et al.* 2013; Battistuzzo *et al.* 2012). For all animals receiving rehabilitative training, the first session commenced 7 days post injury (DPI) following locomotor behavioural tests described below. To provide distributed practice, daily training consisted of 10 minutes on the treadmill, followed by a 10 minute break before a final 10 minute session on the treadmill (Marsh *et al.* 2011). Rats were trained five times a week at the maximal speed that they could maintain consecutive stepping for each 10-minute session on the treadmill. The training protocol lasted eight weeks when PNNi was given until termination (Figure 2.1A), however, where PNNi was given for eight weeks, rehabilitation was extended to give a total of twelve weeks training (Figure 2.1B).

2.3.3: Locomotor assessments

Behavioural and functional assessments of hindlimb (HL) function were assessed throughout the study (see Figure 2.1 for appropriate time points for chronic and 8 week PNNi timelines).

2.3.3.1: Basso, Beattie and Bresnahan HL locomotor open field test

HL locomotor ability was assessed at various time points throughout the acute SCI paradigm using the Basso, Beattie and Bresnahan (BBB) HL locomotor scale (Basso, Beattie and Bresnahan 1995). BBB testing was carried out using an open locomotor field (custom-built Perspex O-ring: diameter 80 cm, height 30 cm) were animals were placed for a duration of 4 minutes (Figure 2.2). Each BBB test was simultaneously assessed by two individuals (see Declaration above) to minimise subjective biases. The resulting scores were pooled and averaged for objectivity. BBB testing assesses HL motor function using a ranking scale from 0-21. Animals are ranked into three broad categories based on their BBB score (see Appendix 1: BBB HL locomotor scoring): the early phase (score of 0-7) presenting with little to no limb movement; the intermediate stage (score of 8-13) with bouts of uncoordinated stepping; and the late stage (score of 14-21) presenting with FL and HL coordination and stability (Basso, Beattie and Bresnahan 1995). Animals underwent a pre-injury BBB approximately 4 days before surgical procedures to provide a baseline. Following injury, BBBs were then carried out at 1 DPI to confirm injury and then weekly from 7 DPI. If animals also received rehabilitative training, BBBs were carried out beforehand. The final BBB assessment for the chronic PNNi paradigm (Figure 2.1A) was performed before beginning their other behavioural assessments at nine weeks post-injury, whereas for the 8 week PNNi paradigm (Figure 2.1B), BBB assessments continued until the week of termination.

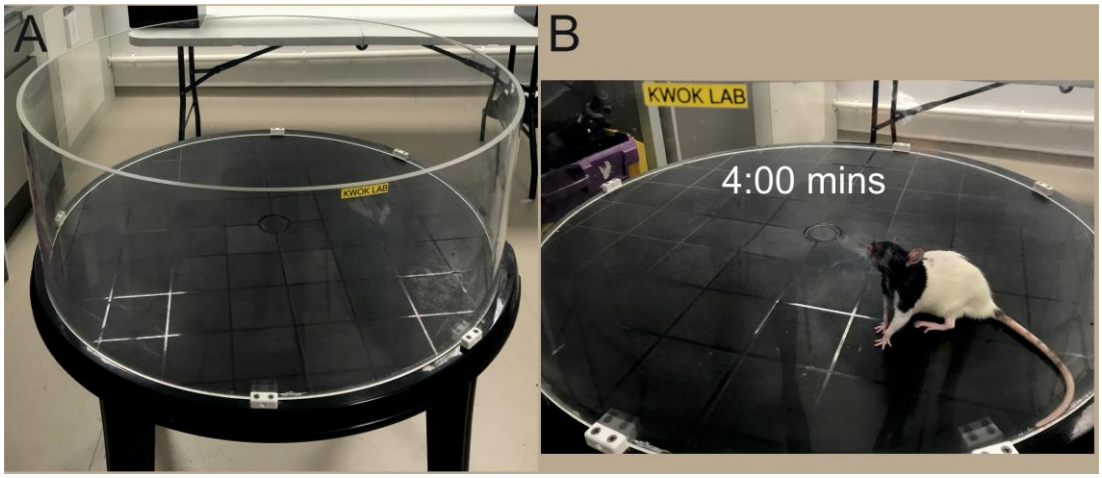

Figure 2.2: Basso, Beattie and Bresnahan (BBB) hindlimb (HL) locomotor open field test (Basso, Beattie and Bresnahan 1995).
A) Flat open field apparatus, approximately 1 m in diameter. **B)** Rats are placed in the open field apparatus for 4 minutes, weekly, to be assessed for HL locomotor performance.

2.3.3.2: Horizontal ladder

At 9 WPI, as well as at 12 WPI in the 8 week PNNi paradigm (Figure 2.1B), rats crossed a horizontal ladder with irregularly placed rungs (Figure 2.3) (Metz and Whishaw 2009) to assess changes to skilled walking between treatment groups. Rats were familiarised to the horizontal ladder in groups on a 'training' arrangement of rungs using a 'home' cage filled with sizzle nest and treats to train them to cross in one direction across the ladder (Figure 2.3A). A 'trial' configuration of rungs was established for testing ensuring that the test is novel after acclimatisation and kept consistent between all rats at the time point of nine WPI (Figure 2.3B). A separate test arrangement was produced for each time point assessed so that the test remained novel. Ladder walking was assessed at 12 WPI in the 8 week PNNi paradigm (Figure 2.1B) to investigate the changes in skilled motor functions after the end of PNNi administration. A minimum of five trials per animal were filmed using a camera (Canon Powershot SX720 HS; 1920 x 1080; 30 frames per second at 10x optical zoom; approximately 1.5 m away from Plexiglas walkway). Each trial was analysed frame by frame assessing each gait cycle for foot faults and paw placement

as described by Metz and Whishaw (Metz and Whishaw 2009). Animals were only assessed within the one metre test region of the ladder (illustrated by the orange tabs on the ladder, shown in Figure 2.3A). When analysed, trials were randomised and the analyser was blind to the treatment group.

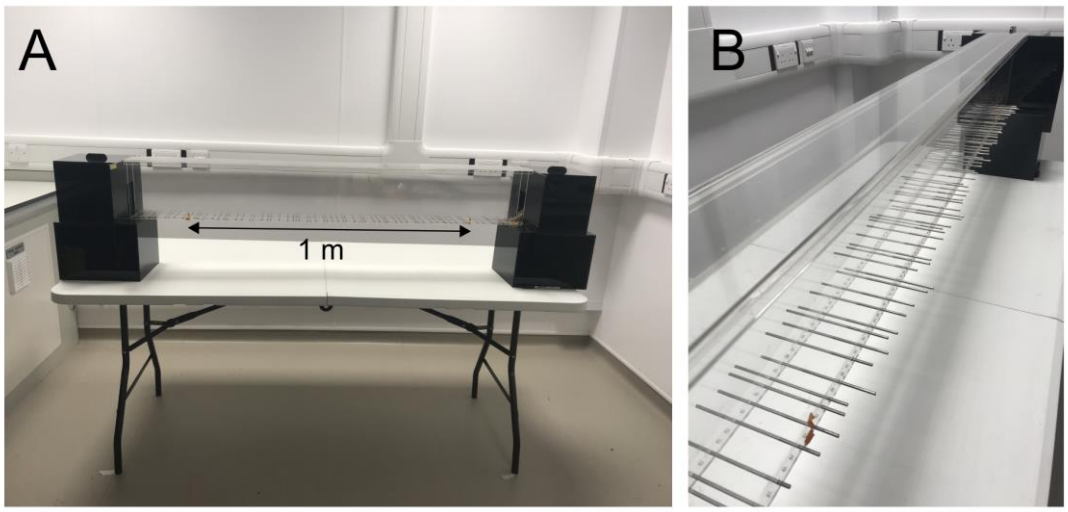

Figure 2.3: Horizontal ladder, modified from (Metz and Whishaw 2009). Animals cross the horizontal ladder from an empty box (left) to 'home' box (right) filled with nesting **(A)**. The irregular rung placement **(B)** tests fine motor skills and animals are only assessed for hindlimb or forelimb paw placement within the denoted (orange tabs) 1 metre segment **(A).**

2.3.4: Von Frey assay

Changes to HL sensory function were assessed using von Frey methodologies to look for hyperalgesia and neuropathic pain. Four animals at a time were acclimatised to Perspex cages with a wire mesh bottom (Complete Base assembly for plantar stimulation; Ugo Basile; Figure 2.4, A-B) for approximately fifteen to twenty minutes before the test began and until general movement and grooming activities stopped. Animals were alert and not drowsy. Von Frey filaments (Touch Test™ Sensory Evaluator Kit of 20; #39337500; Leica Biosystems, Milton Keynes, England; Figure 2.4C) were depressed through the mesh-bottomed cage against the more sensitive

plantar arch of the HL footpads where withdrawal of the limb was counted as a positive result. Flinching was also seen as a positive response whereas walking was an ambiguous response requiring retesting after an appropriate delay. The left hindpaw and right hindpaw of all animals were performed in series to provide a sufficient interval between stimuli. Sensory testing procedure and analysis was carried out as described by Chaplin et al. (1994) (Chaplan *et al.* 1994) using the Dixon up-down method (Dixon 1980) to determine the 50 % withdrawal threshold for each HL. Animals used in the chronic PNNi paradigm (*n=124*) were assessed at nine WPI and animals following the 8 week PNNi paradigm were assessed at both nine and twelve WPI (*n=5*) to assess recovery after Cx injury. A cohort of intact adult female rats (*n=11*) were also assessed before and after 10 days PNNi feeding. Animals from different treatment groups were routinely assessed simultaneously and randomly, maintaining partial blindness to the analyser.

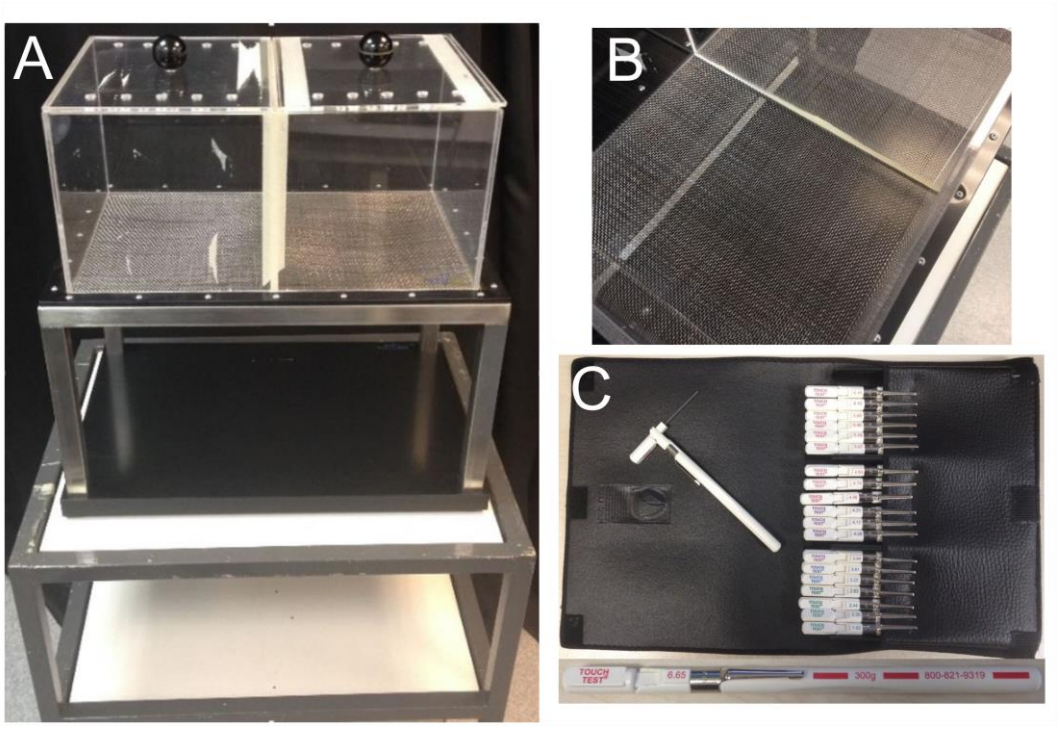

Figure 2.4: Apparatus for mechanical sensory assessment: the von Frey assay (Dixon 1980; Chaplan *et al.* 1994).

Animals were placed into the complete base assembly for plantar stimulation **(A)** with a wire mesh bottom **(B)** and acclimatised for approximately 20 minutes. Von Frey hairs of increasing logarithmic thickness **(C)** were pushed through the wire mesh bottom and perpendicularly depressed against the plantar surface of the left or right hindlimb, using the Dixon up-down method to determine the 50 % withdrawal threshold.

2.3.5: Neuronal tracing

Approximately 10 WPI, five animals from each group, described above in Table 2.3, received anterograde and retrograde neuronal tracing to label descending inputs to the spinal cord lesion site and to label HL Mns.

2.3.5.1: Surgical injection of retrograde and anterograde tracers

Animals were anaesthetised via inhalation of isofluorane (5 % in O_2 for induction and 2-2.5 % for the duration of surgical procedures) and placed on a homeostatic temperature control blanket (Harvard Apparatus Homoeothermic Monitoring System; Harvard Apparatus, Massachusetts, USA) for all procedures. The dorsal surface of the head and left HL were shaved and sterilised. A small incision in the skin was made between the tibialis anterior (TA) and the gastrocnemius (Gs) muscles of the left HL and blunt dissection was used to expose a small area of both muscles. Microinjections of the anterograde neuronal tracer cholera toxin subunit b (1 % CTB; Sigma; 10 µl per muscle; Figure 2.5B) were made using a 10 µl Hamilton syringe into the contralateral (left) TA and the Gs to label their Mns and Ia HL peripheral afferents. A maximum of 5 µl was injected per needle insertion and was injected and retracted slowly to minimise leakage and allow time for absorption.

Animals were then transferred to a stereotaxic frame to secure the head in place. After a midline incision was made to the top of the head, tissues were pushed back to reveal the landmarks of the skull. Bone wax was used to quell any bone bleeding. A unilateral 5 mm x 5 mm window was made immediately posterior to bregma and

lateral to midline on the right hemisphere (Figure 2.5A) using a small drill (Saeshin Dental STRONG 90 Micro motor with 102S Hand piece 35,000 RPM; Saeshin Precision Co., Daegu, Korea). Pressure injections of biotin dextran amine (BDA; 10 %; 10,000 MW, Invitrogen; 9 x 400 nl injections at depth of 1.5 mm; Figure 2.5B) into the HL motor cortex (Neafsey *et al.* 1986) on the right hemisphere using a glass micropipette (~ 10 µm tip) attached to a pneumatic PicoPump (#PV820; World Precision Instruments Ltd, Hertfordshire, UK; ~ 20 psi for a duration of 15 ms, nitrogen gas supply) to provide unilateral anterograde neuronal tracing of the CST. After completion of intracortical injections, the skull fragment was not replaced and instead the exposed craniotomy was protected with spongostan™ before the head was sutured closed.

Animals were anaesthetised for both retrograde and anterograde tracing procedures as a single surgery to minimise exposures to isofluorane and were kept for a minimum of two weeks post-tracing surgery before termination via transcardial perfusion (described above) to allow for BDA to reach the lesion site.

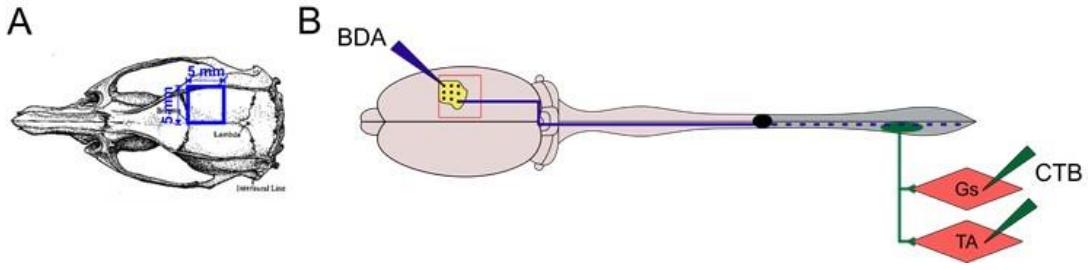

Figure 2.5: Injection of retrograde and anterograde neuronal tracers to label descending fibres and lumbar motor circuitry.

A craniotomy was performed to reveal the hindlimb (HL) motor cortex (A) where biotin dextran amine (BDA) was injected to anterogradely label corticospinal descending fibres (B). B) Cholera toxin subunit B (CTB) was injected into both the gastrocnemius (Gs) and tibialis anterior (TA) of the left HL to retrogradely label the innervating motoneurones.

2.3.5.2: Tissue clearing

The following tissue clearing protocol is modified from the iDISCO+ method (Renier *et al.* 2014). All incubations unless otherwise stated were carried out using a shaker at room temperature.

Using previously fixed tissue from neuronal traced rats (as detailed above in the section 2.3.5.1: Surgical injection of retrograde and anterograde tracers), a spinal cord segment (approximately 1 cm in length) containing the lesion site was dissected. The tissue was washed using PBS (2 x 30 mins) to remove the sucrose before pre-treatment with ethanol (EtOH). Three ascending concentration steps of EtOH were used (30 %, 50 %, 70 % EtOH/distilled H_2O; 3 hrs each), followed by an overnight incubation with 100 % EtOH. The tissue was further incubated with 100 % EtOH for 3 hrs before using a solution of 66 % dichloromethane (DCM)/33 % EtOH to delipidate the sample overnight. Rehydration with descending EtOH concentrations (70 %, 50 %, 30 % EtOH/dH_2O; 3 hrs each) was carried out, culminating in two 30-minute PBS washes.

Before beginning to immunostain the sample (see next section), a permeabilisation solution (0.2 % PBST/20 % dimethylsulfoxide (DMSO)/ 0.3 M glycine) was applied for 24 hrs, followed by a blocking solution (0.2 % PBST/10 % DMSO/6 % NDS/0.3 M glycine/10 µg/ml heparin) for 72 hrs. Three incubations were carried out: 1) WFA (non-biotinylated; 1:300; Sigma #L8258), 2) anti-WFA (rabbit; 1:500; Source BioScience LifeSciences #LS-C768650) alongside anti-GFAP (mouse; 1:500; Neuromab #75-240) and 3) corresponding secondary antibodies for visualisation, including *streptavidin*-conjugated Alexa Fluor 568 to visualise the neuronal tracer BDA (Table 2.2). Antibodies/lectin were added to a solution of 0.2 % PBST with 0.3 M glycine, 3 % NDS and 5 % DMSO and incubated for 72 hrs at 37 ^{o}C. Wash steps between incubations consisted of a total of six washes over 48 hrs using 0.2 % PBST.

Following immunolabelling of the sample, the tissue was dehydrated as before using ascending EtOH concentrations (30 %, 50 %, 70 % EtOH/dH_20; 3 hrs each), followed by an overnight 100 % EtOH incubation. Delipidation was carried out using first a 3-hr incubation in 66 % DCM/33 % EtOH and then two 30 minute incubations in 100 % DCM. The final refractive index matching of the tissue was carried out using incubation (no shaking) with dibenzyl ether (DBE), as illustrated in Figure 2.6. Tissue was stored in darkness in DBE at RT.

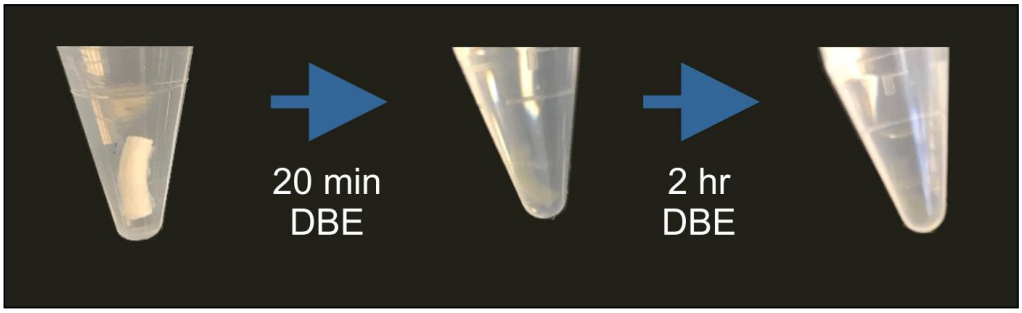

Figure 2.6: Refractive index matching of tissue using dibenzylether (DBE).

Tissue reached full transparency after approximately 2 hours.

2.3.5.3: Imaging and analysis

Imaging was performed using the FBS Bioimaging facility using the light sheet microscope (LaVision Ultramicroscope II; LaVision BioTec, Germany). The cleared spinal cord was mounted using Krazy glue® (Elmers Products, North Carolina, United States) as it was able to withstand the strong solvents used in this preparation. To image the cord was submerged in ethyl cinnamate (ECi) and imaged at 6.3 x zoom z-stacks with a step size of 5 µm. Images were 3D re-constructed using Imaris 9.2.6 (Bitplane AG, Switzerland).

2.3.6: Terminal *in vivo* electrophysiology: intracortical microstimulation

2.3.6.1: Surgical procedures

Approximately 11 weeks after injury/surgery animals (*n=5 per treatment group and n=5 intact rats*) underwent terminal electrophysiological procedures. Animals were anesthetised using an i.p. injection of ketamine/xylazine (Ketavet®, Henry Schein, 100 mg/kg; Rompun®, Henry Schein, 3.2 mg/kg). The throat and ventral surface of the head were shaved. Blunt dissection was used to expose the jugular vein and using micro scissors a small cut was made to cannulate the vessel for intravenous maintenance of anaesthesia. Test for the pinch withdrawal reflex was conducted approximately every 15-30 minutes to assess level of anaesthesia. Additionally, whisker twitching in the absence of stimulation indicated that an additional dose of anaesthesia was required. The rat was mounted in a stereotactic frame and the scalp was incised at the midline to expose the bony landmarks. A craniotomy was performed on the right hemisphere side exposing the entire motor cortex (approximately 5 mm posterior to 4 mm anterior and 5 mm lateral relative to bregma) using a dental drill (similar to described above). The dura was kept intact and warm saline (NaCl) was used to keep the brain moist. Xylazine was used only for induction of anaesthesia. Throughout the experiment, animals were kept on a homeostatic body-temperature control blanket and anaesthesia was maintained using ketamine (10-20 mg/kg) to preserve cortically evoked motor responses. Time taken from induction to the full exposure of the above described motor cortex area allowed for adequate reduction of the depressant effect of xylazine on cerebral cortex neurones to perform intracortical microstimulation (ICMS) (O'Regan 1989; Veilleux-Lemieux *et al.* 2012).

2.3.6.2: ICMS procedures

With the motor cortex of the right hemisphere exposed, ICMS was used to investigate functional reorganisation of the motor map. Using bregma as a cranial landmark, randomised electrode penetrations were made perpendicular to the pial surface (depth 1.3–1.7 mm) using a monopolar tungsten electrode (WE30030.5A5; Microprobes for Life Science, Maryland, USA). The exploration grid covered the entire area of the motor cortex using at least of 70 stimulation points with a minimum distance of 500 µm between points). Sites were randomly stimulated to minimise biasing from stimulation-evoked alterations to cortical representations (Nudo, Jenkins and Merzenich 1990; Brown and Sherrington 1912) or anaesthesia level. Mineral oil was used to keep the brain moist to prevent electrical conductance across the surface of the brain.

A stimulation train (0.2 ms pulses at 333 Hz for 40 ms, interval of 3 s between trains) was generated from Signal v6 via CED 1401 processor (Cambridge Electronic Design Ltd., Cambridge, England) to an isolated stimulator to regulate the amplitude of the stimulating current. Stimulation was considered successful if a motor response was evoked with a current <40 µA to prevent wide-spread cortical activation. For each positive stimulation site, the minimum current threshold for each evoked response was recorded alongside the side (contralateral/ipsilateral) and type of response (face/FL/HL) and the muscles stimulated. HL and FL movements were evoked almost exclusively on the contralateral side of the body. In situations when more than one type of movement was observed at a single stimulation site, the individual current activation thresholds were defined independently.

Virtual matrices were generated for each treatment group for both chronic PNNi and 8-week PNNi paradigms. A virtual matrix was generated for each movement type, for example, FL, HL and face, averaging the response of all animals in each treatment

group for all of the coordinates tested. Heat maps were generated using OriginPro 2019 (OriginLab, Northampton, MA) from these virtual matrices.

Following completion of the terminal electrophysiology protocol animals were terminated using the transcardial perfusion protocol as described above. The spinal cord tissue and the contralateral brain hemisphere from these animals was used to perform histological assessment, detailed in section 2.2.2.2: Changes after chronic PNNi administration in SCI model and Chapter 5: The mechanistic changes induced by systemic PNNi inhibition.

2.4: Experimental Design and Statistical Analysis

Data is presented as means ± standard deviation (SD) for all measured data and behavioural data is presented as means ± standard error of the mean (SEM). The significance threshold was defined as 0.05 and asterisks have been used to denote significance as *p<0.05, **p<0.01 and ***p<0.001. All data sets were analysed and graphed using OriginPro 2019 scientific graphing and data analysis software. Prior to statistical analysis, normality of data was determined using the Shapiro-Wilk test. Figures were produced and arranged using CorelDRAW 2018 Version 20.1.0.707 (Corel Corporation, Ottawa, Canada).

2.4.1: Characterisation of PNNs in the spinal motor pools

A minimum of three sections per spinal level (cervical, thoracic or lumbar) per animal (*n*=5) were stained and imaged, maintaining the same confocal microscopy settings per staining procedure. All counts per section were normalised by the number of ChAT-positive cells before averaging per animal. To test the influence of spinal cord level on PNN expression, results were pooled and analysed using one-way ANOVA, with Bonferroni correction for between groups multiple comparison.

2.4.2: Changes to PNNs and excitatory-inhibitory balance after chronic PNNi administration

Medial brain sections and spinal cord sections (T4-6) were stained from animals after the completion of the chronic PNNi paradigm (Figure 2.1A; *n=3 animals per group,* see Table 2.3). A minimum of four brain sections and five spinal cord sections (two VHs per section) per animal were stained and imaged with all confocal microscopy settings remaining constant throughout. For HABP staining, a minimum of ten spinal sections were analysed. Background subtractions were carried out, as described

above, by using the corresponding secondary control. These were then averaged per animal before being normalised by the Sham control group. To test the effect of each treatment/injury, results were pooled and grouped before being analysed using one-way ANOVA, with Bonferroni correction for between groups multiple comparison.

2.4.3: Cx impact

For the chronic PNNi paradigm (see Figure 2.1A) where treatments were given for the entirety of the study, Cx impact forces recorded from the Infinite Horizon impactor were compared between treatment groups using a one-way ANOVA with a post-hoc Bonferroni correction (*n=75*). For the 8 week PNNi paradigm (Figure 2.1B), where PNNi treatments were given for a limited time period so as to allow PNN consolidation, impact forces were compared using Student's t-test (*n=5 per group*).

2.4.4: Changes in weekly BBB hind limb locomotion over time

HL locomotor activity was assessed for each individual HL allowing for bilateralism of the injury to be assessed. The left and right HL scores were averaged to assess the overall HL locomotor deficit per animal (*n=124 for chronic PNNi paradigm and n=9 for 8 week PNNi paradigm*) for each time point. Results were pooled and grouped according to treatment and time point before they were analysed using a two-way mixed factorial ANOVA, with Bonferroni correction. BBB was analysed using ANOVA despite being ordinal data (Scheff, Saucier and Cain 2002).

2.4.5: Horizontal ladder

For each trial, steps were categorised as either a miss, slip or hit. The frequency of each of these stepping types was normalised by the number of steps taken. The

average score and the percentages for each stepping type for each trial were then averaged per animal before being pooled and grouped. For results from the chronic PNNi treatment paradigm, one-way ANOVA with Bonferroni correction was performed for each parameter. For 8 week PNNi paradigm data, Student's t-tests were applied for each parameter.

2.4.6: Sensory testing

The 50 % HL withdrawal response was calculated per HL and then averaged per animal. Data for weight at time of the test and for the HL withdrawal were grouped and pooled and for each parameter a one-way ANOVA was performed using the Bonferroni correction to determine differences between treatment groups.

2.4.7: Changes to functional cortical motor maps

Individual heat maps were generated for each movement and each animal (*n=36 per movement*) using OriginPro 2019 as above, creating an all or nothing representation (i.e. each site either tested negative or positive for each of the movement classes investigated). Using the software FIJI, the positive movement representations for each animal were drawn around and the area and centroid value were recorded. Area values were normalised to give the actual area in mm^2 by using a scale factor calculated from the grid on each map. Areas per animal were pooled and grouped for each movement and analysed using one-way ANOVA with a post-hoc Bonferroni correction.

Chapter 3: Characterisation of perineuronal nets in the spinal motor pools

The results in this chapter have been published in a jointly authored paper:

Irvine SF, Kwok JCF. *Perineuronal Nets in Spinal Motoneurones: Chondroitin Sulphate Proteoglycan around Alpha Motoneurones*. International Journal of Molecular Sciences. 2018; 19(4):1172.

Please find the manuscript attached in the appendix.

3.1: Introduction

PNNs are dense specialised ECM structures that surround neuronal subpopulations throughout the CNS. First described by Golgi as reticular structures in the late 1800s (Celio *et al.* 1998), PNNs have since been implicated in pathologies of various neurological disorders, including Alzheimer's disease, epilepsy and schizophrenia (McRae and Porter 2012; Cabungcal *et al.* 2013; Suttkus *et al.* 2014a; Pantazopoulos and Berretta 2016), as well as in traumatic CNS injuries, particularly SCI models (García-Alías *et al.* 2009; Wang *et al.* 2011a). A key role of PNNs is their involvement in the termination of developmental plasticity where they form an interdigitating mesh with mature somatic and dendritic contacts to confer synaptic stabilisation (Pizzorusso *et al.* 2002; Carulli *et al.* 2010; Tsien 2013).

PNNs are composed of a compact arrangement of a variety of neural ECM proteoglycans and proteins (Giamanco, Morawski and Matthews 2010; Kwok, Carulli and Fawcett 2010). These components primarily consist of CSPGs including the HA binding CSPGs called lecticans (4 members), bound upon a long HA backbone and stabilised by the HAPLNs (3 members) and Tn-R (Kwok *et al.* 2011). Upon this basic PNN structure, the binding of other CSPGs (such as PTPRZ) are thought to provide additional heterogeneity of PNNs (Yamaguchi 2000). CSPGs are composed of CS-GAG chains attached to a core protein which differentiates the various CSPGs from one another (Yamaguchi 2000). CS-GAGs confer a further vast degree of heterogeneity through variation of expression, chain length and sulphation patterns, even to the same core protein (Gama *et al.* 2006; Kitagawa 2014). However, exploration of the extent of this heterogeneity has so far been limited.

Although many studies have investigated the molecular heterogeneity of PNNs in distinct neuronal populations in regions of the brain (Carulli *et al.* 2006; Deepa *et al.* 2006; Fader *et al.* 2016; Yamada and Jinno 2017), much of the composition and associated populations in the spinal cord is relatively unknown. Similar to the brain

(Vitellaro-Zuccarello *et al.* 2007), in the spinal cord many of the known cells enwrapped by PNNs are fast-spiking inhibitory parvalbumin (PV)-positive interneurones (approximately half of PV+ positive neurones) (Brauer *et al.* 1993; Yamada, Ohgomori and Jinno 2015), and have also been associated with calbindin-positive Renshaw cells (Vitellaro-Zuccarello *et al.* 2007). However, in contrast to the brain, reports suggest that PNNs in the spinal cord also surround cells with large neuronal cell bodies, particularly within the VH likely representing Mns (Takahashi-Iwanaga, Murakami and Abe 1998; Bertolotto, Manzardo and Guglielmone 1996; Vitellaro-Zuccarello *et al.* 2007; Galtrey *et al.* 2008; Smith *et al.* 2015). Spinal Mns are vital and irreplaceable components in the processing of descending control and sensory feedback and are organised into anatomical motor pools according to their peripheral muscle targets. Mns are a heterogeneous population of neurones with the main subclasses, alpha and gamma Mns, innervating contractile extrafusal fibres and proprioceptive intrafusal fibres within the motor unit, respectively (Manuel and Zytnicki 2011).

Enzymatic removal of PNNs using ChABC after CNS injury has been shown in multiple models, predominately SCI, to reopen a window of plasticity to promote improvements in motor functions (Bradbury *et al.* 2002; García-Alías *et al.* 2009). Regeneration of descending tracts can contribute to this functional recovery (Barritt *et al.* 2006; Zhao *et al.* 2013), however the extent and mechanism of changes in local spinal circuitry attributing to this recovery remains unclear. Additionally, studies also implicate exercise and rehabilitative training to activity-dependant modulation of PNNs in the ventral motor pools (Wang *et al.* 2011a; Smith *et al.* 2015), suggesting a relationship between PNNs and Mns that is important for normal motor functions.

3.2: Aims

This study therefore aims to investigate the expression and molecular composition of PNNs in the spinal motor pools; the population of PNN-associated neurones in the spinal cord likely to be involved in functional motor recovery after SCI, and to identify the best PNN marker for this population.

Immunohistochemical staining was performed using antibodies against ChAT, a marker of spinal Mns (Barber *et al.* 1984), alongside labelling for primary PNN components, including various CSPGs and the acclaimed “universal” PNN marker WFA, in the ventral horn to elucidate the composition of PNNs associated with spinal motor circuitry.

3.2.1: Characterisation of the normal expression and molecular composition of PNNs associated with the spinal motor pools:

a) Determine the composition of PNNs associated with the spinal motor circuitry, using a variety of CSPG markers in comparison to the acclaimed “universal” PNN marker WFA,

b) Determine the difference of PNN association in this population across the spinal levels

c) Identify the best label for PNNs associated with the afore mentioned neuronal population

3.2.2: Determine the association of PNNs with subtypes of Mns by:

a) Selectively labelling alpha and gamma Mns to categorise the expression of PNNs with these subclasses

It was found that distinct populations of Mns were surrounded by PNNs labelled by various CSPGs yet lacking WFA, indicating a difference between the composition of PNNs and associated neuronal cell types in the brain and spinal cord. PNNs were found to surround the majority of alpha Mns, suggesting that these are the main populations affected by ChABC-mediated recovery after SCI.

3.3: Results

We aim to determine the molecular heterogeneity of PNNs in the spinal cord, with a particular focus to the Mns in the VH. Spinal cord sections from three different spinal levels, cervical, thoracic and lumbar, were used to compare the spatial differences of PNNs. Alongside ChAT staining, we also stained for WFA, a common PNN marker (Koppe *et al.* 1997; Moon *et al.* 2001; Bradbury *et al.* 2002; Pizzorusso *et al.* 2002), and the CSPGs including ACAN, BCAN, NCAN, VCAN and PTPRZ.

3.3.1: WFA-positive PNNs only partially overlap with other CSPGs in the ventral motor pools

3.3.1.1: ACAN

ACAN is a CSPG in the lectican family and is widely considered to be a major component in PNNs (Morawski *et al.* 2012; Lendvai *et al.* 2013; Suttkus *et al.* 2014b). Immunohistochemical staining of ACAN core protein illustrated clear expression of PNNs surrounding ventral Mns labelled with ChAT (Figure 3.1, J-L). ACAN-positive PNNs surround approximately 85 % of ChAT-positive Mns in all levels of the spinal cord investigated (Figure 3.1, A-C). In comparison, with the use of a well-used PNN marker, WFA, it is observed that WFA-positive PNNs enwrap significantly fewer Mns (approximately 68 % of the ChAT-positive Mns) than ACAN-positive PNNs (cervical $F_{4, 15} = 495.36$, $p<0.001$; thoracic $F_{4, 15} = 80.62$, $p<0.05$; lumbar $F_{4, 15} = 249.80$, $p<0.01$; *n=4*), illustrating that WFA does not label all PNNs in the ventral motor pools. Two-way ANOVAs for each spinal level were run comparing the five categories: ACAN+, WFA+, ACAN+WFA-, ACAN+WFA+ and ACAN-WFA+ PNNs. Compounding this, the total number of ACAN-positive PNNs surrounding Mns was significantly greater than the number of ACAN+/WFA+ PNNs (cervical $p<0.001$, thoracic $p<0.05$, lumbar

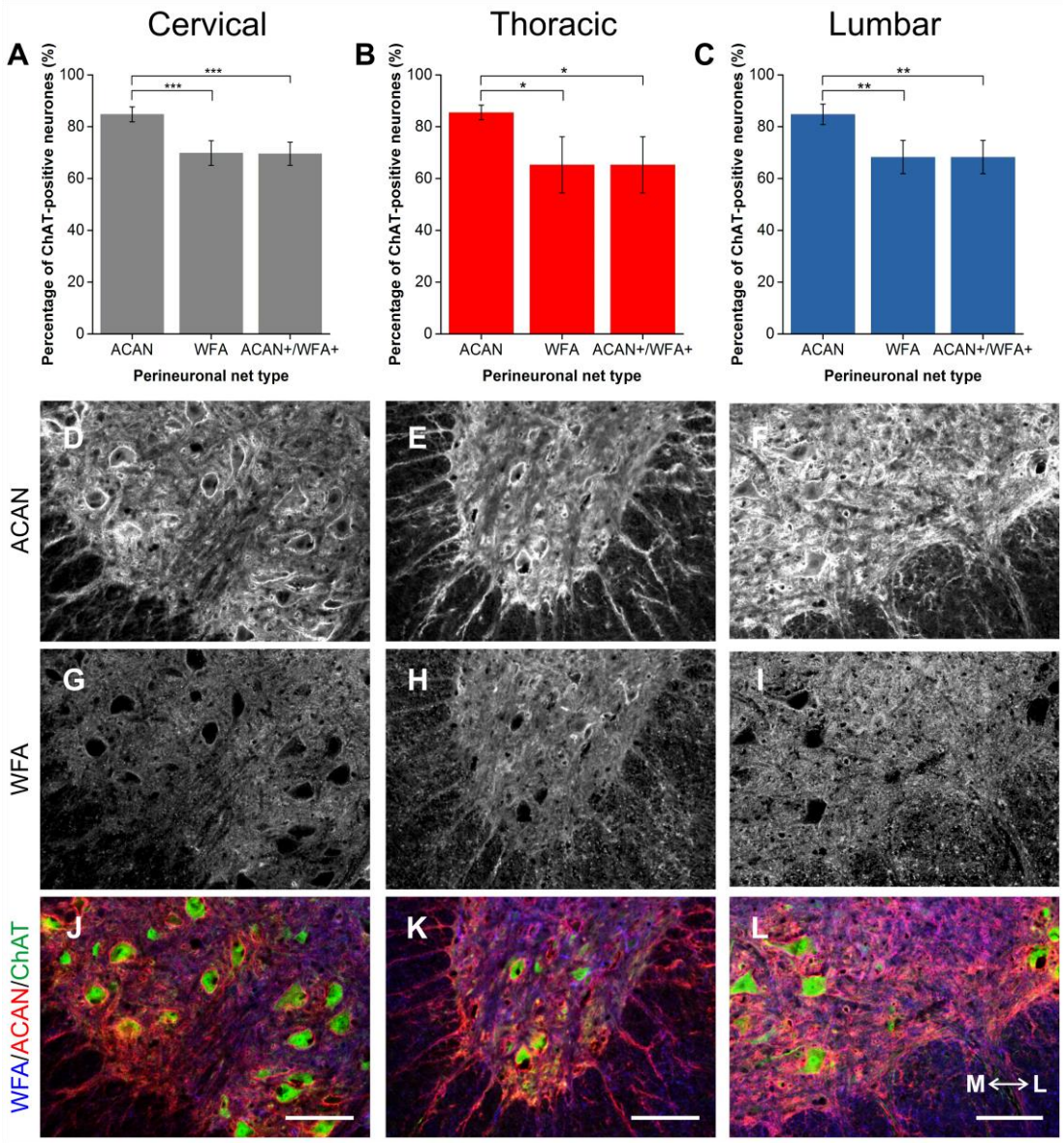

Figure 3.1: Comparison of perineuronal nets (PNNs) in the spinal ventral motor pools labelled by *Wisteria floribunda* agglutinin (WFA) and aggrecan (ACAN).

A-C) Bar graphs showing percentage of ChAT-positive neurones in the ventral motor pools surrounded by ACAN-positive and WFA-positive PNNs and their co-localisation (ACAN+/WFA+) in cervical **(A)**, thoracic **(B)** and lumbar **(C)** rat spinal cord. *Error bars ± SD; n=4. Statistics one-way ANOVA; significance levels: * p<0.05 ** p<0.01 *** p<0.001.* Confocal images showing ACAN-positive (visualised using Alexa fluor 568; **D-F**) and WFA-positive (Alexa fluor 647; **G-I**) PNNs surrounding ChAT-positive Mns (Alexa fluor 488; **J-L**) in the cervical, thoracic and lumbar spinal cord, respectively. *Scale bars, 100 µm. Medial (M) and lateral (L) orientation as illustrated.*

p<0.01; *n=4*). ACAN- and WFA-positive PNN populations appeared to overlap (Figure 3.1, D-I). Further breakdown of PNN type revealed that at each level, all PNNs that are positive for WFA co-localised with ACAN (n.s.; p=1). No PNNs were WFA-positive, ACAN-negative. The results demonstrate that ACAN labels a larger population of PNN positive Mns, and suggest that it is a better marker for PNN in the spinal cord.

3.3.1.2: BCAN

BCAN is a lectican CSPG found specifically in the CNS, and with growing evidence of its importance in regulating the plastic properties of PNNs (Favuzzi *et al.* 2017). Co-staining with ChAT-positive neurones in the VH revealed a high degree of localisation, with approximately 88 % of Mns encircled by BCAN-positive PNNs (Figure 3.2, A-C). Similar to ACAN, WFA-positive PNNs appear to denote some but not all of the BCAN-positive PNN-ensheathed Mns, labelling approximately 30 % fewer Mns than BCAN (cervical $F_{4, 20}$ = 533.62; thoracic $F_{4, 20}$ = 166.41; lumbar $F_{4, 20}$ = 321.76; all levels p<0.001; *n=5*). BCAN+/WFA+ PNNs in the motor pools appear to represent a proportion that is significantly less that the total BCAN-positive PNN population (all levels p<0.001; *n=5*). Additional categorisation again reveals that almost all WFA-positive PNNs in the motor pool co-localise with BCAN-positive PNNs.

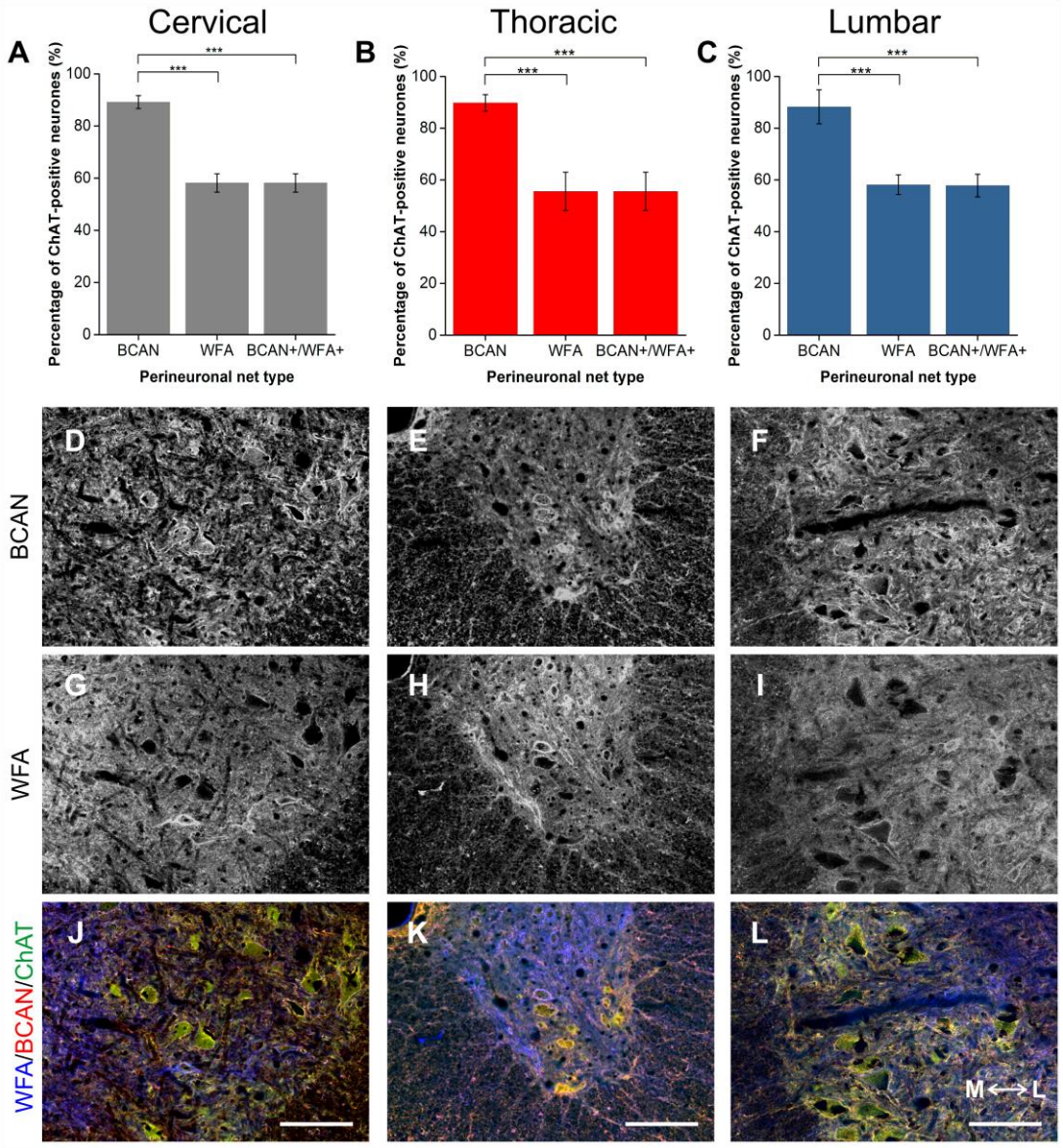

Figure 3.2: Comparison of perineuronal nets (PNNs) in the spinal ventral motor pools labelled by *Wisteria floribunda* agglutinin (WFA) and brevican (BCAN).

A-C) Bar graphs showing percentage of ChAT-positive neurones in the ventral motor pools surrounded by BCAN-positive and WFA-positive PNNs and their co-localisation (BCAN+/WFA+) in cervical **(A)**, thoracic **(B)** and lumbar **(C)** rat spinal cord. *Error bars ± SD; n=5. Statistics one-way ANOVA; significance levels: *** p<0.001.* Confocal images showing BCAN-positive (visualised using Alexa fluor 568; **D-F**) and WFA-positive (Alexa fluor 647; **G-I**) PNNs surrounding ChAT-positive Mns (Alexa fluor 488; **J-L**) in the cervical, thoracic and lumbar spinal cord, respectively. *Scale bars, 100 µm. Medial (M) and lateral (L) orientation as illustrated.*

3.3.1.3: NCAN

NCAN is a nervous system-specific lectican, like BCAN, known to be present in PNNs in the spinal cord (Asher *et al.* 2000; Deepa *et al.* 2006; Vitellaro-Zuccarello *et al.* 2007). In the VH, NCAN staining revealed PNNs encircling approximately 87 % of Mns (Figure 3.3, A-C). Echoing the trend with ACAN and BCAN, WFA-positive PNNs envelop 28 % fewer Mns than NCAN (cervical $F_{4, 20} = 172.58$; thoracic $F_{4, 20} = 73.52$; lumbar $F_{4, 20} = 505.84$; all levels $p<0.001$; $n=5$). Significantly, only approximately two-thirds of these NCAN-positive PNNs co-localise with WFA (all levels $p<0.001$; $n=5$). No WFA-positive PNNs lacking NCAN co-staining were observed, signifying that all WFA co-localised with NCAN.

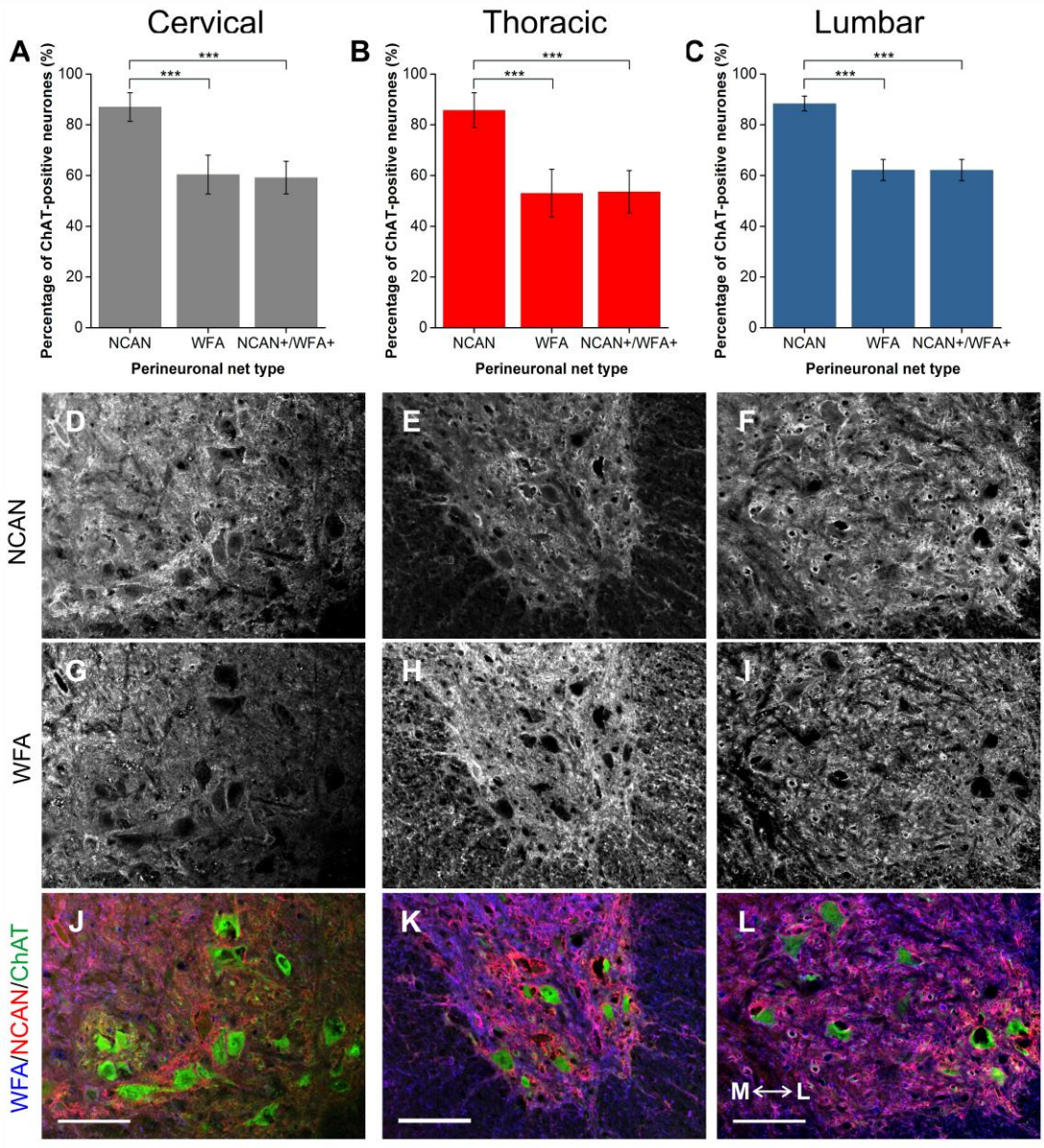

Figure 3.3: Comparison of perineuronal nets (PNNs) in the spinal ventral motor pools labelled by *Wisteria floribunda* agglutinin (WFA) and neurocan (NCAN).

A-C) Bar graphs showing percentage of ChAT-positive neurones in the ventral motor pools surrounded by NCAN-positive and WFA-positive PNNs and their co-localisation (NCAN+WFA+) in cervical **(A)**, thoracic **(B)** and lumbar **(C)** rat spinal cord. *Error bars ± SD; n=5. Statistics one-way ANOVA; significance levels: *** p<0.001.* Confocal images showing NCAN-positive (visualised using Alexa fluor 568; **D-F**) and WFA-positive (Alexa fluor 647; **G-I**) PNNs surrounding ChAT-positive Mns (Alexa flour 488; **J-L**) in the cervical, thoracic and lumbar spinal cord, respectively. *Scale bars, 100 µm. Medial (M) and lateral (L) orientation as illustrated.*

3.3.1.4: VCAN

VCAN staining reveals strong diffuse ECM expression in both the white and gray matter of the spinal cord due to its expression in the nodes of Ranvier (Dours-Zimmermann *et al.* 2009; Asher *et al.* 2002; Deepa *et al.* 2006). VCAN does not show strong PNN staining in laminae other than the VH. In the VH, VCAN-positive PNNs surround approximately 82 % of Mns at all spinal levels (Figure 3.4, A-C). WFA and VCAN populations of PNNs showed a strong overlap at all spinal levels (Figure 3.4, D-L). However, all WFA-positive PNNs co-localised with VCAN with a significant population of VCAN-positive PNNs WFA-negative (cervical $F_{4, 15} = 994.08$; thoracic $F_{4, 15} = 132.44$; lumbar $F_{4, 15} = 279.20$; all levels $p<0.001$; *n=4*).

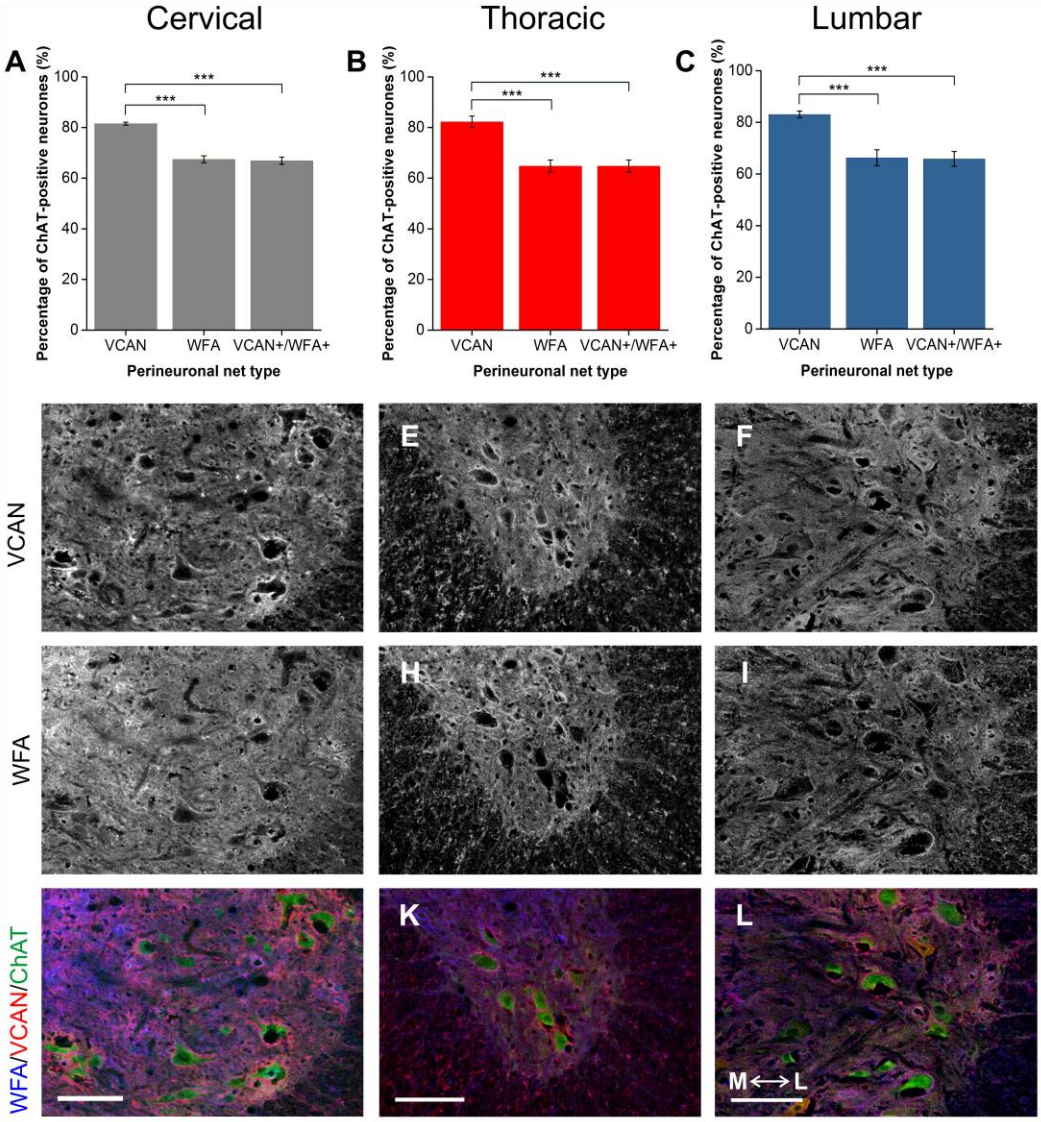

Figure 3.4: Comparison of perineuronal nets (PNNs) in the spinal ventral motor pools labelled by *Wisteria floribunda* agglutinin (WFA) and versican (VCAN).

A-C) Bar graphs showing percentage of ChAT-positive neurones in the ventral motor pools surrounded by VCAN-positive and WFA-positive PNNs and their co-localisation (VCAN+/WFA+) in cervical **(A)**, thoracic **(B)** and lumbar **(C)** rat spinal cord. *Error bars ± SD, n=4. Statistics one-way ANOVA; significance levels: * p<0.05 ** p<0.01 *** p<0.001.* Confocal images showing VCAN-positive (visualised using Alexa fluor 568; **D-F**) and WFA-positive (Alexa fluor 647; **G-I**) PNNs surrounding ChAT-positive Mns (Alexa fluor 488; **J-L**) in the cervical, thoracic and lumbar spinal cord, respectively. *Scale bars, 100 µm. Medial (M) and lateral (L) orientation as illustrated.*

3.3.1.5: PTPRZ

Phosphacan or PTPRZ is a non-HA binding CSPG that represents the extracellular domain of protein tyrosine phosphatase receptor zeta (PTPRZ) modified by glial cells (Maurel *et al.* 1994; Dwyer *et al.* 2015) and has been found to be present in WFA-positive PNNs in the cerebral cortex (Haunsø *et al.* 1999; Deepa *et al.* 2006; Vitellaro-Zuccarello *et al.* 2007). Immunohistochemistry showed that PTPRZ is also found in PNNs in the ventral motor pool, surrounding approximately 76 % of Mns in all levels of the cord studied (Figure 3.5, A-C). However, in all levels of the spinal cord investigated, PTPRZ-positive PNNs still surrounded 15 % more Mns than WFA (cervical $F_{4, 15} = 128.77$; thoracic $F_{4, 15} = 1066.95$; lumbar $F_{4, 15} = 234.34$; all levels $p<0.01$; *n=4*). Approximately 82 % of PTPRZ-positive PNNs were also labelled by WFA, representing a significantly lower proportion of the total observed PTPRZ-positive PNNs in the motor pool (all levels $p<0.05$; *n=4*).

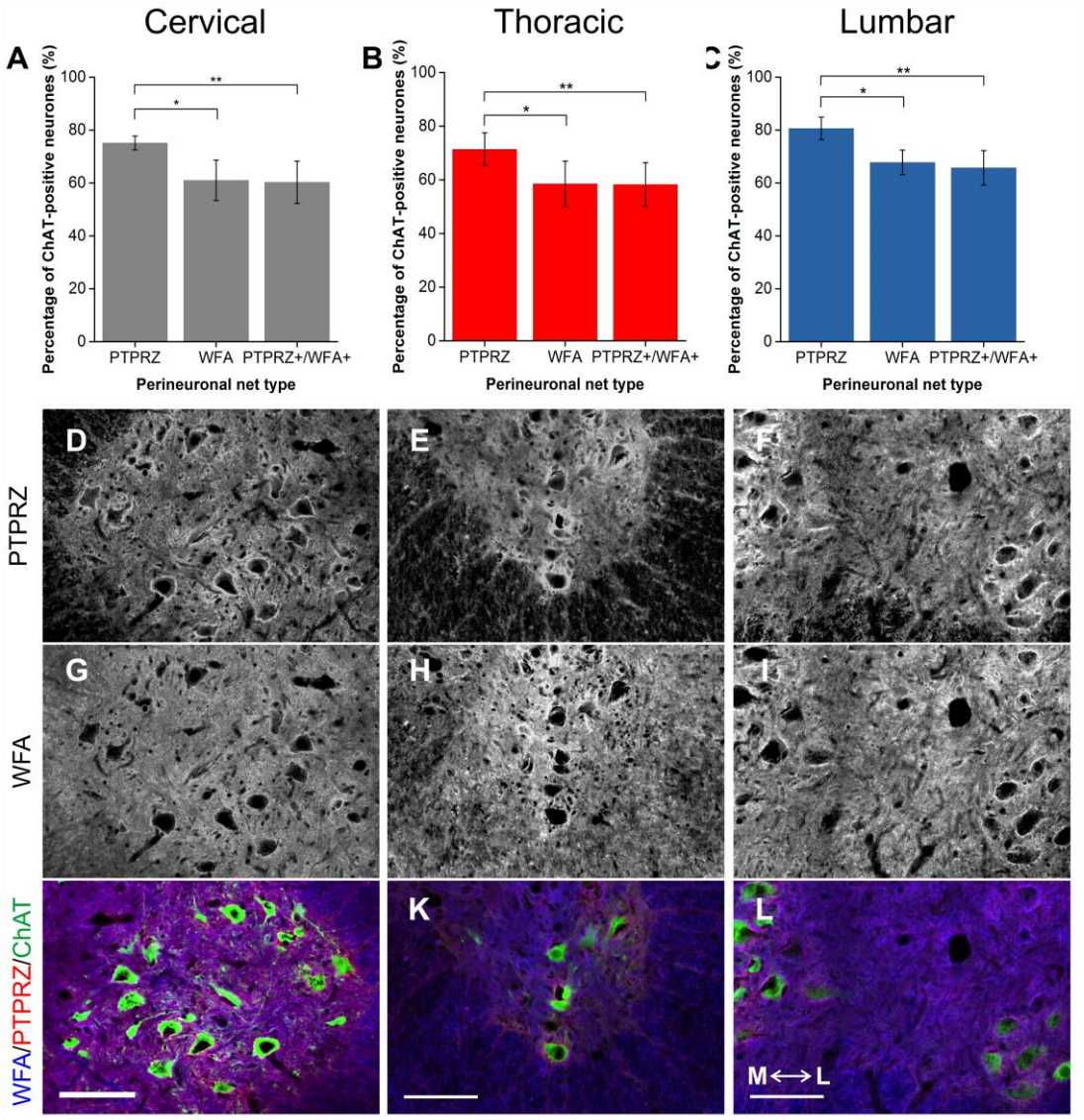

Figure 3.5: Comparison of perineuronal nets (PNNs) in the spinal ventral motor pools labelled by *Wisteria floribunda* agglutinin (WFA) and phosphacan (PTPRZ).

A-C) Bar graphs showing percentage of ChAT-positive neurones in the ventral motor pools surrounded by PTPRZ -positive and WFA-positive PNNs and their co-localisation (PTPRZ+/WFA+) in cervical **(A)**, thoracic **(B)** and lumbar **(C)** rat spinal cord. *Error bars ± SD; n=4. Statistics one-way ANOVA; significance levels: * p<0.05 ** p<0.01.* Confocal images showing PTPRZ-positive (visualised using Alexa fluor 568; D**-F**) and WFA-positive (Alexa fluor 647; **G-I**) PNNs surrounding ChAT-positive Mns (Alexa fluor 488; **J-L**) in the cervical, thoracic and lumbar spinal cord, respectively. *Scale bars, 100 µm. Medial (M) and lateral (L) orientation as illustrated.*

3.3.2: Distinct populations of CSPG-positive yet WFA-negative PNNs in the motor pools

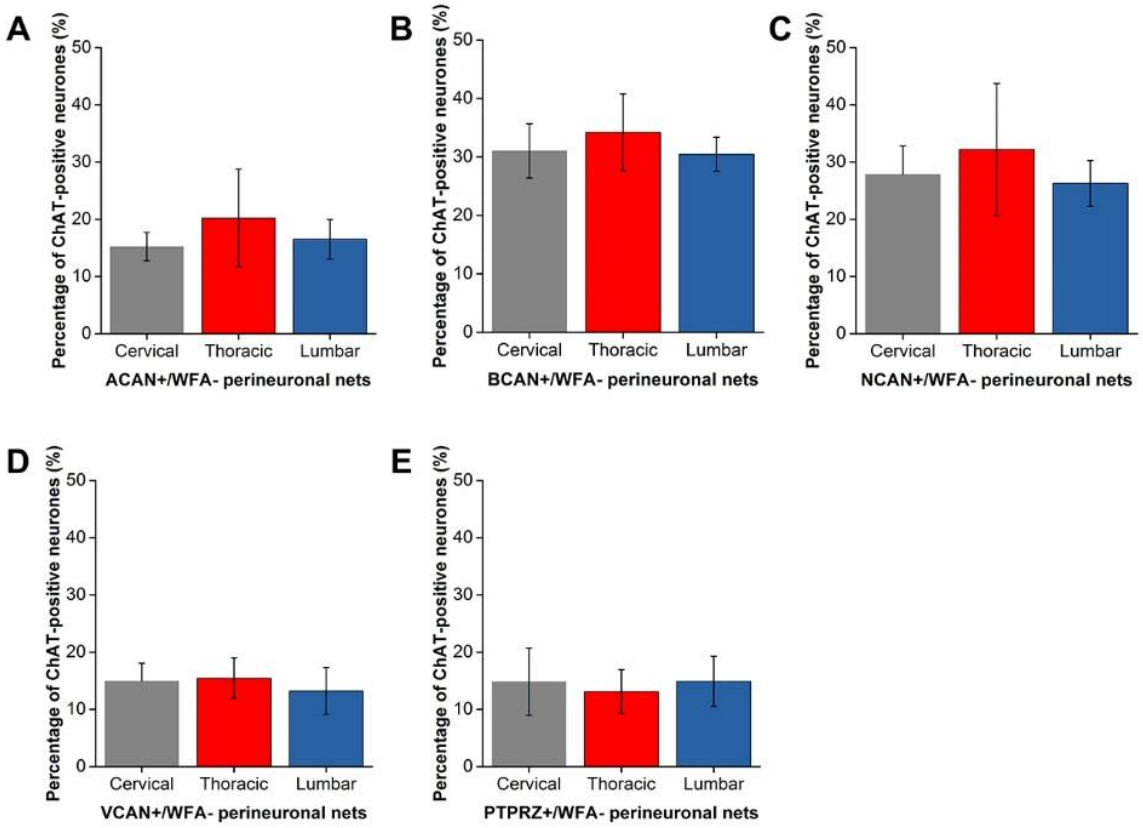

Figure 3.6: A proportion of perineuronal nets (PNNs) in the spinal motor pools is negative for Wisteria floribunda agglutinin (WFA).

Percentage of ChAT-positive (visualised using Alexa fluor 488) motoneurones in the ventral motor pools in the cervical, thoracic and lumbar spinal cord surrounded by CSPG-positive (Alexa fluor 568), WFA-negative (Alexa fluor 647) PNNs. **A)** Aggrecan (ACAN, *n=4*); **B)** brevican (BCAN, *n=5*); **C)** neurocan (NCAN, *n=5*); **D)** versican (VCAN, *n=4*); and **E)** phosphacan (PTPRZ*, n=4*). *Error bars ± SD. Statistics one-way ANOVA; n.s.*

For each CSPG investigated, a significant percentage of Mns were surrounded by PNNs that were CSPG-positive yet WFA-negative (all levels, all CSPGs $p<0.001$). The percentage of Mns with WFA-negative PNNs varies with CSPG (Figure 3.6). While ACAN+/WFA-, VCAN+/WFA- and PTPRZ+/WFA- PNNs encircled roughly 15 % of Mns (Figure 3.6, A, D and E), a higher percentage of Mns (approximately 30 %) appeared to be surrounded by BCAN+/WFA- and NCAN+/WFA- PNNs (Figure 3.6, B

and C). Overall, the results suggest that in the ventral motor pools, WFA does not denote all PNNs, and instead distinct populations of Mns with CSPG-positive WFA-negative PNNs exist.

3.3.3: Alpha Mns, not gamma Mns, are preferentially surrounded by PNNs

Using NeuN and ChAT co-labelling, Mns in the spinal ventral motor pools were selectively labelled as either alpha (NeuN-positive) or gamma (NeuN-negative) (Friese *et al.* 2009; Smith *et al.* 2015). It was observed that approximately 70-80 % of ChAT-positive Mns were NeuN-positive (Figure 3.7 and Figure 3.8), suggesting that they are alpha Mns. Firstly, as the universal marker for PNNs, WFA was used to determine the number of PNNs surrounding each Mn subtype. Similarly to results above, WFA-positive PNNs surrounded approximately 60 % of all Mns with approximately 98 % of these PNNs surrounding NeuN-positive Mns (alphas; Figure 3.7A-C). In other words, a significant proportion of alpha Mns (~72 %) were associated with WFA-positive PNNs (cervical $F_{3, 8} = 3127.82$; thoracic $F_{3, 8} = 68.75$; lumbar $F_{3, 8} = 120.09$; cervical and lumbar $p<0.001$, thoracic $p<0.05$; *n=3*). As previous findings illustrated that in the ventral motor pools, WFA did not label all Mns, ACAN was also used to identify PNNs around each Mn subtype. Again most PNNs (95 %) surrounded alpha Mns (Figure 3.8, A-C). ACAN-positive PNNs encircled roughly 90 % of alpha Mns, suggesting that PNN-positive Mns and alpha Mns are the same population. Approximately, 14 % of gamma Mns were surrounded by WFA+ or ACAN + PNNs, representing approximately 3.3 % of the total Mn population.

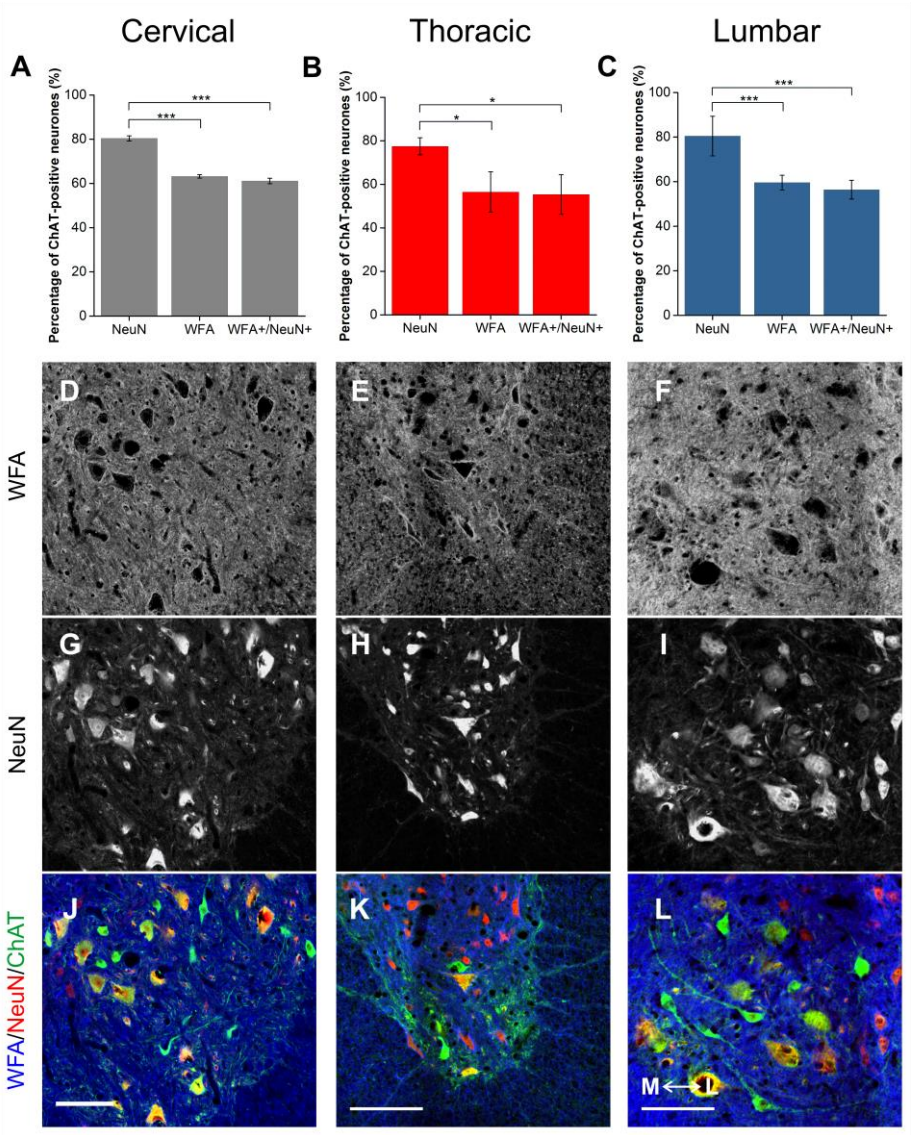

Figure 3.7: *Wisteria floribunda* agglutinin (WFA)-positive PNNs surrounded some but not all alpha motoneurones (Mns).

A-C) Bar graphs showing percentage of ChAT-positive Mns in the ventral motor pools surrounded by NeuN, WFA-positive PNNs and their co-localisation (WFA+/NeuN+) in cervical **(A)**, thoracic **(B)** and lumbar **(C)** rat spinal cord. NeuN and ChAT co-localisation denotes alpha Mns. *Error bars ± SD; n=3. Statistics one-way ANOVA; significance levels: * p<0.05 ** p<0.01 *** p<0.001.* Confocal images showing WFA-positive PNNs (visualised using Alexa fluor 647; **D-F**) surrounding NeuN-positive (Alexa fluor 568; **G-I**) PNNs and ChAT-positive Mns (Alexa fluor 488; **J-L**) in the cervical, thoracic and lumbar spinal cord, respectively. *Scale bars, 100 µm. Medial (M) and lateral (L) orientation as illustrated.*

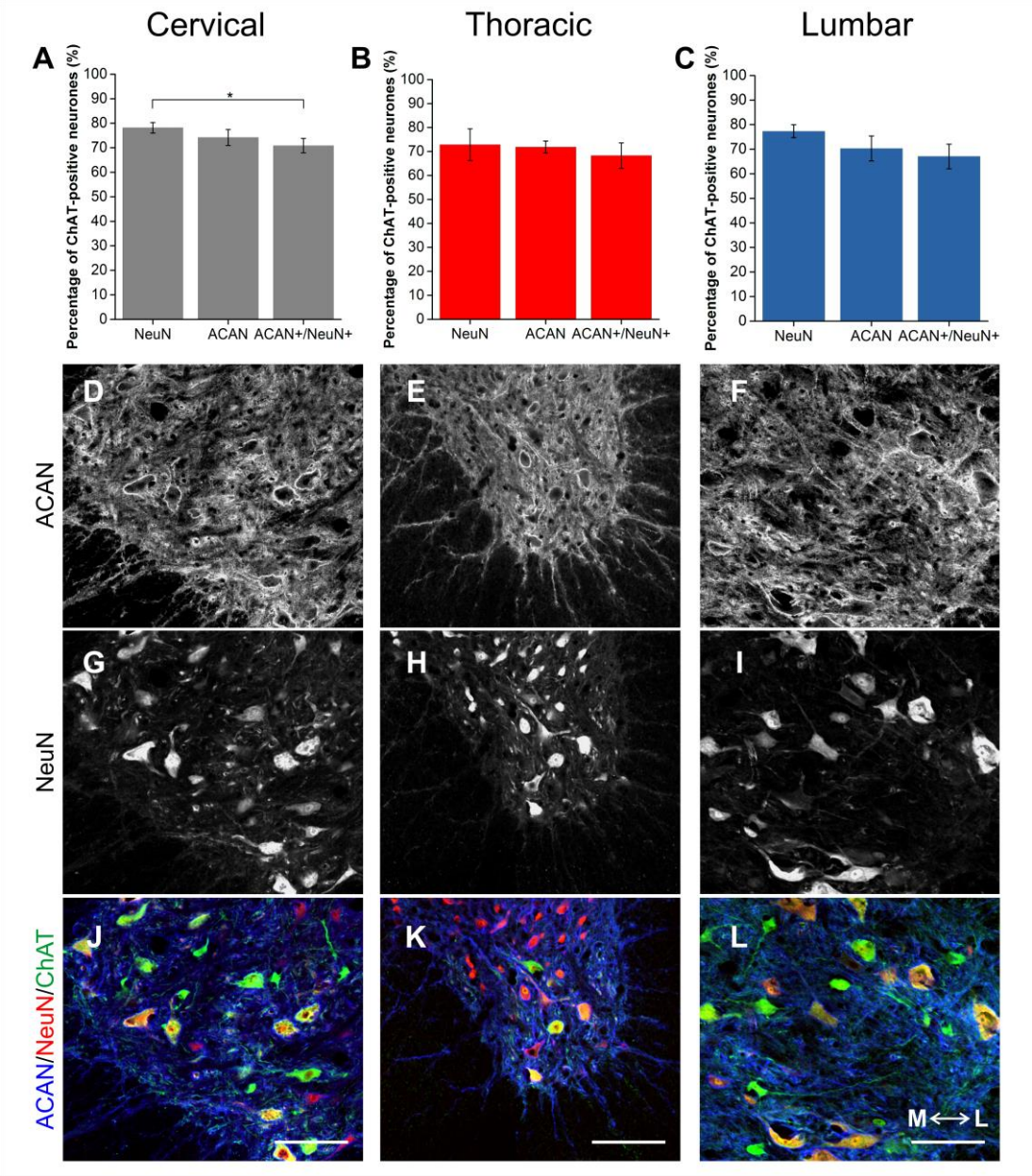

Figure 3.8: Aggrecan (ACAN)-positive PNNs surrounded most alpha motoneurones (Mns).

A-C) Bar graphs showing percentage of ChAT-positive Mns in the ventral motor pools surrounded by NeuN, ACAN-positive PNNs and their co-localisation (ACAN+/NeuN+) in cervical **(A)**, thoracic **(B)** and lumbar **(C)** rat spinal cord. NeuN and ChAT co-localisation denotes alpha Mns. *Error bars ± SD; n=3. Statistics one-way ANOVA; significance levels: * p<0.05.* Confocal images showing ACAN-positive PNNs (visualised using Alexa fluor 647; **D-F**) surrounding NeuN-positive (Alexa fluor 568; **G-I**) PNNs and ChAT-positive Mns (Alexa fluor 488; **J-L**) in the cervical, thoracic and lumbar spinal cord, respectively. *Scale bars, 100 µm. Medial (M) and lateral (L) orientation as illustrated.*

3.4: Discussion

As removal of PNNs in the spinal cord after injury enhances motor recovery, we looked to investigate the expression of PNNs and their heterogeneity in spinal Mns; the final order neurones for the control of voluntary movement. This is the first investigation to systemically and semi-quantitatively compare the differences of CSPG- or WFA-positive PNN Mns in the ventral motor pools. Mns were identified using an antibody against ChAT to label cholinergic neurones alongside markers for PNN components and the acclaimed universal PNN marker WFA in comparison. We demonstrated that a high proportion of Mns in the ventral spinal cord are surrounded by PNNs, particularly alpha Mns. Unexpectedly, the universal marker for PNNs, WFA, did not label all of the PNNs with distinct populations of Mns surrounded by CSPG-positive yet WFA-negative PNNs. Instead, ACAN labelled more PNNs in the ventral motor pools and appeared to be a better marker for PNNs in the spinal cord. This suggests that, in contrast to the brain, WFA does not label the majority of PNN neurones in the ventral spinal cord and that studies using WFA in the spinal cord may be underestimating the number of PNNs.

3.4.1: PNNs in the spinal ventral motor pools

Previous studies have described ventral Mns as the most conspicuous neuronal population in the spinal cord to be surrounded by PNNs and this appears to be conserved across mammalian species (Galtrey *et al.* 2008; Wang *et al.* 2011a; Jäger *et al.* 2013; Smith *et al.* 2015; Mueller *et al.* 2016). Despite this, few studies have actually investigated the proportion of PNNs in the ventral motor pools and those that do use varying markers to determine this. Comparable to our own methods, using ChAT as a specific Mn marker, a similar proportion of ventral Mns was observed to be surrounded by PNNs to that found in our study (~80 %) has been reported in non-human primates (75 %), using WFA (Mueller *et al.* 2016), and in human (71 %) spinal

cord, using ACAN (Jäger *et al.* 2013). In rats, however, this distribution has been investigated with the general neuronal marker (NeuN) using size and ventral location to identify Mns alongside WFA lectin staining to characterise PNN expression, resulting in estimates of only 30 % of Mns associated with PNNs (Galtrey *et al.* 2008). This is likely to underestimate for two reasons: 1) without a Mn-specific neuronal marker small sized Mns, including NeuN-negative gamma Mns (Friese *et al.* 2009; Shneider *et al.* 2009), would have been absent from these counts, and 2) WFA does not appear to label all PNNs in the rat spinal cord. Indeed, our findings suggest that PNNs are present in almost 80 % of the ChAT-positive Mns.

Although others have implicated that PNNs only surround large cell-bodied Mns in the motor pools, i.e., alpha Mns and not gamma Mns (Galtrey *et al.* 2008; Smith *et al.* 2015), we are the first to systematically categorise the proportion of specific Mn-subtypes associated with PNNs at different levels of the spinal cord. Despite driving the same goal endpoint of voluntary muscle control, alpha and gamma Mns represent distinct populations of Mns within the ventral motor pools, differing in both electrical and molecular properties (Eccles *et al.* 1960; Friese *et al.* 2009; Manuel and Zytnicki 2011; Misawa *et al.* 2012). These differences also include the innervation of different muscle targets, with alpha Mns responsible for force generation though contraction of extrafusal fibres whereas gamma Mns innervate the intrafusal fibres regulating muscle spindle sensitivity. The high proportion of enveloped alpha Mns likely reflects the importance of the role of PNNs in providing synaptic stabilisation of inputs from the specific spinal circuitry and consequent contractile innervation of key muscle groups. Exercise increases PNN thickness around Mns in the spinal cord, thereby further supporting its synaptic inputs, but induces the opposite effect on brain PNNs, therefore promoting synaptic changes (Smith *et al.* 2015). After SCI, the stabilisation of synaptic plasticity conferred by PNNs instead becomes another mechanism inhibiting regenerative attempts and compensatory rearrangements of spared fibres.

We suggest that ChABC-mediated removal of PNNs in SCI models is therefore able to induce a high degree of enhanced plasticity of synaptic connections to the above mentioned populations of Mns contributing to the observed improvement of most functional motor recovery studies.

3.4.2: Differences in PNNs between the brain and spinal cord

It is generally assumed that PNNs in the brain and the spinal cord are the same. While in the brain, WFA does not always co-localise with ACAN as previously discussed, other CSPG-positive PNNs always co-localise with WFA. Here, we demonstrate differences in the composition of PNNs between the brain and spinal cord, where ACAN and other CSPGs denote subclasses of Mns in the spinal cord lacking WFA. This study recommends that future staining for PNNs associated with the spinal motor pools, particularly SCI studies utilising therapies that modify PNNs such as ChABC, should seek alternatives to WFA to avoid underestimating total PNN number.

Additionally, brain PNNs are well known to target small fast-spiking inhibitory interneurones playing a modulatory role in the brain (Härtig, Brauer and Brückner 1992). In sharp contrast, the associated neuronal populations studied here are large cell bodied neurones acting as the primary endpoint of neural control of the somatic motor system. Other neuronal cell types such as calbindin-positive Renshaw cells in the ventral spinal cord are surrounded by PNNs (Vitellaro-Zuccarello *et al.* 2007), further implicating the role of PNNs in stabilisation of connections within the spinal motor circuitry. In a recent systematic review of the CNS, motor regions, including the cerebellum and spinal cord, were more likely to have a higher proportion of neurones surrounded by PNNs than sensory structures (Mueller *et al.* 2016). It is possible that PNNs may have different roles in different parts of the nervous system or with different neuronal populations.

3.4.3: Composition of PNNs in the spinal motor pools

Staining with the lectin WFA and antibodies for various CSPG core proteins revealed two distinct types of distributions throughout the grey matter: diffuse extracellular staining and a bright 'halo' of pericellular expression identifying the PNNs. The overall distributions of immunoreactivities for the CSPGs investigated and ChAT were generally similar to previous descriptions (Deepa *et al.* 2006; Barber *et al.* 1984; Vitellaro-Zuccarello *et al.* 2007; Galtrey *et al.* 2008). We showed that all of the CSPGs investigated were present in PNNs surrounding spinal Mns. These were also found to be present to varying degrees, indicating heterogeneity of PNNs in the motor pools.

ACAN in particular has been previously reported to be present in PNNs surrounding Mns (Kalb and Hockfield 1988; Matthews *et al.* 2002; Vitellaro-Zuccarello *et al.* 2007), as well as BCAN, NCAN, VCAN and PTPRZ. It is estimated that VCAN begins to appear in PNNs around the Mns from postnatal day 8 (Bignami, Perides and Rahemtulla 1993). Studies in the brain and spinal cord show that ACAN is present in all PNNs and generally co-localises with WFA expression (Deepa *et al.* 2006; Galtrey *et al.* 2008; Giamanco, Morawski and Matthews 2010). However, consistent with all CSPGs investigated, WFA does not appear to show all PNN-associated neurones in the ventral motor pools. As WFA is supposed to bind to the CS-GAG sugar GalNAc (Härtig, Brauer and Brückner 1992), it should bind to all CSPGs and therefore denote all PNNs. A recent study suggested that sulphation of CS-GAGs may influence WFA labelling, after overexpression of CS-C (CS-6S) during development induced the formation of structurally impaired PNNs that were WFA-negative (Miyata *et al.* 2012). However, binding of WFA has previously been shown to be dependent on the presence of ACAN (Giamanco, Morawski and Matthews 2010) and recently other studies in various regions of the brain including the hippocampus have reported PNNs with ACAN labelling but no WFA binding (Ueno *et al.* 2017; Yamada and Jinno 2017). In the spinal cord, we observed a lack of WFA in ACAN-positive PNNs to a similar

degree to that observed in the CA1 area of the hippocampus (Yamada and Jinno 2017), appearing to denote distinct populations of Mns. ACAN is understood to be a 'full-time' CSPG component of PNNs. While this study has also demonstrated that ACAN has a high association to PNNs within the spinal motor pools, the heterogeneity of PNNs in various CNS regions could be further explored in relation to ACAN. As there is a vast degree of heterogeneity of CS-GAGs within CSPGs, further research is required to determine the conditions and exact epitopes for WFA binding. It is possible that the molecular composition of CSPGs within PNNs may confer functional subclasses of Mns.

The expression of many PNN components such has ACAN, BCAN and Tn-R show differences in expression between various brain regions (Dauth *et al.* 2016). Indeed expression of CSPGs in PNNs across the spinal laminae has also been shown to display differential expression (Vitellaro-Zuccarello *et al.* 2007; Galtrey *et al.* 2008). PNNs are a dynamic network of ECM components. Activity-dependant modulation has been demonstrated where the thickness of PNNs surrounding spinal Mns increases in response to exercise or rehabilitative training (Wang *et al.* 2011a; Smith *et al.* 2015). This is likely conveyed through dynamic regulation of CSPGs and/or CS-GAGs within the PNNs. There is a growing concept that the properties of the ECM have an important influence in both healthy and pathological states. Though it is beyond the scope of this study, it is hoped that further research of PNN heterogeneity in CNS regions may help to unravel the functionality of these ECM components and their alterations in disease states.

3.4.4: Further research and conclusions

Despite the clinical relevance of PNNs targeted for CNS repair and regeneration, particularly in locomotor recovery models of SCI, the functional relationship between PNNs and the motor system is still mostly unexplored. Further research is required to

look at the normal functional properties of PNNs surrounding Mns. Additionally, the molecular heterogeneity of PNNs displayed in spinal Mns may indicate a functional role. However, understanding how the varying molecular heterogeneity of PNNs affects CNS functions, is a topic still in its infancy.

Though this study begins to address a research gap surrounding the properties of PNNs in the spinal cord, much characterisation remains to be done. While ChABC has been an invaluable investigative tool for understanding the role of PNNs in promoting plasticity and functional recovery after SCI, there are clinical limitations to its therapeutic use. It is hoped that insights into the properties of PNNs and their role in the spinal cord could aid the generation of alternative and non-invasive strategies for targeted PNN removal to enhance functional recovery post-injury.

Chapter 4: Enhancing functional recovery using novel non-invasive PNN inhibition

4.1: Introduction

Regaining lost functions after a SCI remains the ultimate goal for developing therapies. However, this requires overcoming intrinsic and extrinsic obstacles to plasticity and regeneration in order to acquire new functional connections. A wide variety of approaches have been investigated to enhance plasticity and/or regeneration to treat neurological injury. However, the great pitfall for many prospective treatments is that not all plasticity is positive and even when anatomical changes are observed, these do not always produce functional benefit (Maier *et al.* 2009; Fouad *et al.* 2013).

Amongst the most promising potential treatments is the bacterial enzyme ChABC which digests a family of repulsive guidance molecules, CSPGs. Various CSPGs are upregulated in the ECM in response to injury both rostral and caudal to lesion site (Andrews *et al.* 2012; Buss *et al.* 2009) and importantly are also found abundantly as part of a specialised lattice-like structure called PNNs (Carulli *et al.* 2006; Deepa *et al.* 2006; Giamanco, Morawski and Matthews 2010). PNNs are key plasticity regulators that form around specific groups of neurones at the termination of developmental plasticity to provide stability of functional mature synapses (Carulli *et al.* 2010; Pizzorusso *et al.* 2002).

Over the past two decades, it has been extensively demonstrated that ChABC-mediated digestion of PNNs induces a window of plasticity improving functional recovery after both chronic and acute SCI (Bradbury *et al.* 2002; Zhao *et al.* 2011; Hu *et al.* 2018). Given the complexity of the injury-induced mechanisms inhibitory to repair, a single therapy is unlikely to provide a ‘cure’ to SCI. Therefore, notably, ChABC has demonstrated additive functional benefits in combination with various treatments, including trophic factors, anti-Nogo immunotherapy (Zhao *et al.* 2013) and particularly with rehabilitative training (García-Alías *et al.* 2009; Wang *et al.* 2011a; Warren *et al.* 2018).

However, ChABC is an invasive therapy and may pose significant hurdles regarding human application. As a heat-sensitive protein (Tester, Plaas and Howland 2007; Chen, Li and Yuan 2015), ChABC is degraded by the body (~ 8 d half-life), requiring invasive re-applications to the injury site resulting in further damage and inflammation (Mountney *et al.* 2013). Recent studies have attempted to overcome this, by creating heat-stable ChABC, firstly with mutation of ChABC by Accorda Therapeutics (Patents: World Intellectual Property Organisation #WO2005087920A2; Canada #CA2525804C; USA including #10323240 and #9987340) (Caggiano *et al.* 2005; Iseda *et al.* 2008; Wang *et al.* 2011a; Rosenzweig *et al.* 2019) and independently with stabilisation of ChABC using the sugar, trelulose (Lee, McKeon and Bellamkonda 2010; Hu *et al.* 2018) or alternatively by maintaining a fresh supply of ChABC by incorporating into a lenti-viral vector for expression (Zhao *et al.* 2011; Muir *et al.* 2010; Burnside *et al.* 2018), the latter of which poses ethical concerns as a treatment to an already vulnerable population. Despite its shortcomings, ChABC has been recently approved for clinical use for the treatment of slipped or herniated disc under the name Condoliase (Chiba *et al.* 2018; Matsuyama *et al.* 2018) and has recently proved efficacious in a canine clinical trial for SCI (Hu *et al.* 2018). Whilst ChABC is a powerful experimental tool that has demonstrated the positive functional improvements of removing PNNs, it would be beneficial to explore alternative avenues of removing PNNs.

Alternative methods attempt to modulate the effects of inhibitory CSPG signalling through the PTPσ and LAR receptors, using ISP or ILP respectively (Lang *et al.* 2015; Dyck *et al.* 2018; Tran *et al.* 2018). While not as invasive as intraparenchymal delivery, these peptides also require daily subcutaneous injection, which is known to raise multiple issues with patient compliance with translation to clinical application due to both the frequency and invasiveness of application (Brod, Rousculp and Cameron 2008; Lang *et al.* 2015; Tran *et al.* 2018). However, whilst blockade of these

receptors may play a role in preventing the collapse of growth cones necessary for the formation of new synapses, other inhibitory CSPG receptors such as NgR would also need to be modulated (Dickendesher *et al.* 2012; Lang *et al.* 2015). Additionally, PNNs remain present and able to confer physical constraints to plasticity of circuitry.

This study uses a currently licensed small molecule and looks to investigate the off-label use as a non-invasive small molecule PNN inhibitor (PNNi) for treatment of SCI. PNNi will be used as a method of removing PNNs to enhance plasticity for recovery by interrupting the molecular turnover of the PNN. Preliminary unpublished pilot work showed that after a 10-day trial of i.p. and oral (via gavage) PNNi administration in the adult rat, PNNs were downregulated in the spinal cord, particularly in the VH. The downregulation was a lot weaker in the brain, further indicating that there are differences in the properties of PNNs in the brain and spinal cord. The following study therefore aims to investigate the efficacy of a novel method of PNN removal to enhance systemic plasticity to improve functional recovery in an acute SCI model. As rehabilitative training is the only viable clinical therapy known to enhance recovery and is known to shape enhanced plasticity, this study also looked to investigate the compatibility of PNNi and locomotor training as a combination therapy.

4.2: Aims

The main aim of this chapter was to determine the functional recovery achieved with PNNi administration and in combination with rehabilitative treadmill training after acute SCI. However, firstly, to complete preliminary studies, the behavioural effects of acute PNNi administration on intact healthy adult rats was determined. These were investigated using a variety of different techniques.

4.2.1: Investigate the functional motor and sensory effects of acute systemic PNN removal to the uninjured animal

a) Determine the sensory and motor response to 10 days PNNi administration in the intact rat using behavioural tests such as the Von Frey assay and the horizontal ladder

4.2.2: Promoting plasticity for functional recovery after acute SCI using novel PNN inhibitor (PNNi)

c) Determine the efficacy of chronic PNNi in promoting functional recovery in combination with rehabilitation by accessing the recovery of HL locomotor activity:

   i. using periodic assessment of locomotor stepping using the BBB HL locomotor score for rats

   ii. Assess stepping of both HL and FL using horizontal ladder

   iii. HL sensory recovery using the Von Frey assay

d) Determine the effect of consolidation of PNNs after a sustained period of PNNi removal (8 weeks PNNi treatment) in combination with rehabilitation:

i. using the behavioural parameters detailed above

ii. Additional periodic assessment of the HL stepping using the horizontal ladder at key time points

4.3: Results

PNNi is an already licensed non-invasive therapy for a non-CNS related disease. The following results illustrate the functional motor and sensory changes observed in response to acute and chronic oral feeding of PNNi to intact rats and rats with a moderate acute mid-thoracic Cx injury. The von Frey assay was used to determine 50% HL withdrawal threshold (Chaplan *et al.* 1994) – an indicator of HL nociceptive sensitivity to mechanical stimuli. Motor functions were assessed using the specialised open field test for HL locomotion for SCI rats, the BBB HL locomotor scale (Basso, Beattie and Bresnahan 1995), as well as using a skilled walking task, the horizontal ladder (Metz and Whishaw 2009).

4.3.1: 10 days PNNi dosing: functional sensory but not motor changes to the intact rat

Does systemic PNN removal affect normal sensation and motor functions? To investigate this, adult female Lister Hooded rats (*n=11*) were given 10 days of oral PNNi treatment. Comparison to a pre-treatment baseline (7.9 ± 2.73 g) with the same rats, revealed that acute PNN removal decreased the withdrawal threshold to 5.5 ± 2.03 g (Figure 4.1A), indicating a significant 30 % increase in sensitivity ($t(10) = 2.76$; $p<0.05$; *n=11*). Acute PNNi administration did not appear to alter body weight over time (Figure 4.1B; n.s.; p=1; *n=11*).

Open field locomotor testing revealed no differences with 10 days PNNi treatment with all animals achieving top scores of 21 in the BBB scale (n.s.; p=1, *n=11*). When a more skilled walking task was used to assess locomotion, HL locomotor activity also appeared consistent between treated and untreated animals (Figure 4.1C; n.s.; p<1; *n=7 non-treated and n=11 10d PNNi treatment*), with correct stepping (green) approximately 93 % of the time, with slips (yellow) and misses (red) making up ~5 %

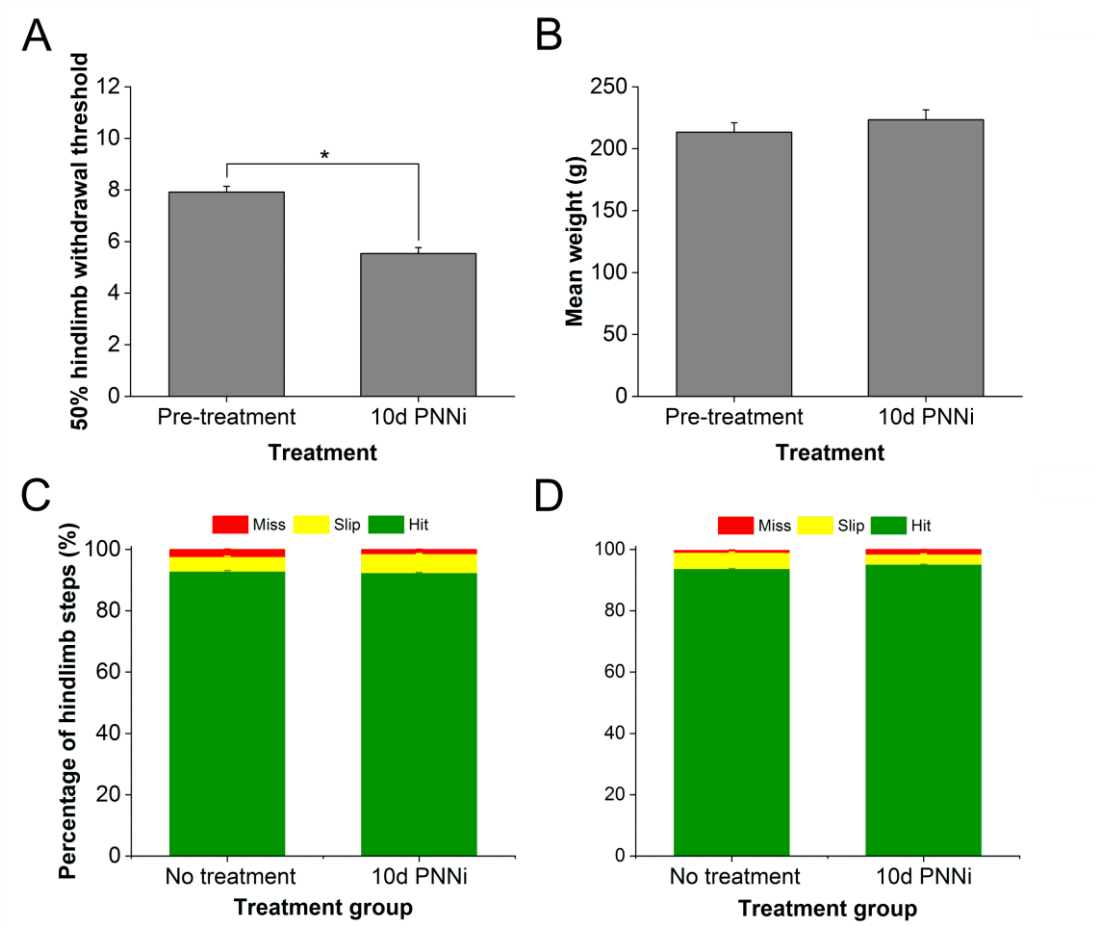

Figure 4.1: Sensory but not motor functional changes in response to 10 days administration of PNNi to the intact rat.

A) Acute administration of PNNi appears to increase sensitivity. Bar graph showing mean 50 % withdrawal threshold for the left-right hindpaws determined from von Frey assays before and 1 day after acute oral PNNi treatment. *Error bars are ±SEM; n=11 for pre- and post-PNNi treatment. Statistics paired Student's t-test; significance levels: *p<0.05 (p=0.02).* **B)** Bar graph showing no change in mean weight of rats before and after acute PNNi treatment. *Error bars are ±SD; n=11 for pre- and post-PNNi treatment.* **C-D)** Stacked bar graphs showing classification of **(C)** hindlimb and **(D)** forelimb steps on the horizontal ladder in non-treated and 10 days treated animals. No detrimental changes were observed to fine motor control. Error bars *±SEM. Statistics two-tailed Student's t-test (n=7 for non-treated and n=11 for acute PNNi treated animals); significance levels: * p<0.05.*

and ~2 % of all steps, respectively. Similarly, FL performance was unaffected by acute PNNi removal (Figure 4.1D; n.s.; p<1; *n=7 non-treated and n=11 10d PNNi treatment*), with ~2 % missed, ~4 % slipped and ~94 % correct steps. Regardless of

treatment, HL and FL function performed equally as well. The results revealed that acute removal of PNNs in the normal adult rat slightly increases sensitivity in the limbs tested but does not affect locomotor function. No other behavioural differences were observed.

4.3.2: PNNi to promote functional recovery in acute SCI model alongside rehabilitation

The following will examine the behavioural changes in an acute mid-thoracic Cx injury model to investigate the efficacy of the novel compound PNNi in increasing functional recovery, in combination with treadmill training. The following experimental paradigms will first focus on a timeline where animals were given oral treatments from the day of injury until termination of the study (chronic PNNi; *n=124*), followed by an investigation into recovery after PNN reconsolidation (8 week PNNi; *n=18*) where PNNi was given from day of injury for a total of eight weeks.

4.3.2.1: All treatment groups sustained comparable Cx impact

All animals received a laminectomy at vertebral level T8 with those in Cx treatment groups also sustaining a moderate Cx injury of ~200 kilodynes (kdyn) at spinal level T9 using an Infinite Horizon (IH) impactor. Slight variabilities arise in experimental Cx injuries due to factors such as animal positioning, surgical technique and control over impact. Unlike other devices which rely on displacement, the IH impactor is a force-controlled device which displaces a small diameter steel tip towards the exposed and stabilised spinal cord to the limit of the pre-set force and then immediately withdraws preventing any secondary impact (Scheff and Roberts 2009). The impactor's force sensor generates actual force impact data from each Cx injury which are shown in Figure 4.2A and C to illustrate reproducibility and variation between groups. In the chronic PNNi study, an average Cx of 207 kdyn was sustained with no difference

between groups (Figure 4.2A; n.s., p = 0.21). Animals receiving eight weeks PNNi also received a mean Cx of 207 kdyn (Figure 4.2C; n.s.; p = 0.11).

4.3.2.2: PNNi administration does not alter age-associated gain in mass

Neither acute (Figure 4.1B), chronic (Figure 4.2B) or 8 weeks (Figure 4.2D) PNNi dosing appeared to impact body weight over time. The body mass of all groups increased over time from an average of 243 ± 20 g on the day of surgery (0 days post injury, DPI) to 282 ± 22 g after 10 weeks (Figure 4.2B). Neither PNNi treated groups or other injured groups showed a difference from Sham animals, suggesting normal growth over time. Slight decreases in weight were observed within the first week post-injury, in comparison to sham control animals, mostly under 5 % reduction in body mass from the day of surgery (Figure 4.2B, D). Locomotion from 0 – 7 DPI was significantly reduced (see HL locomotor scoring; Figure 4.4) and therefore may have resulted in reduced food and water consumption despite also being given soaked diet to rectify this.

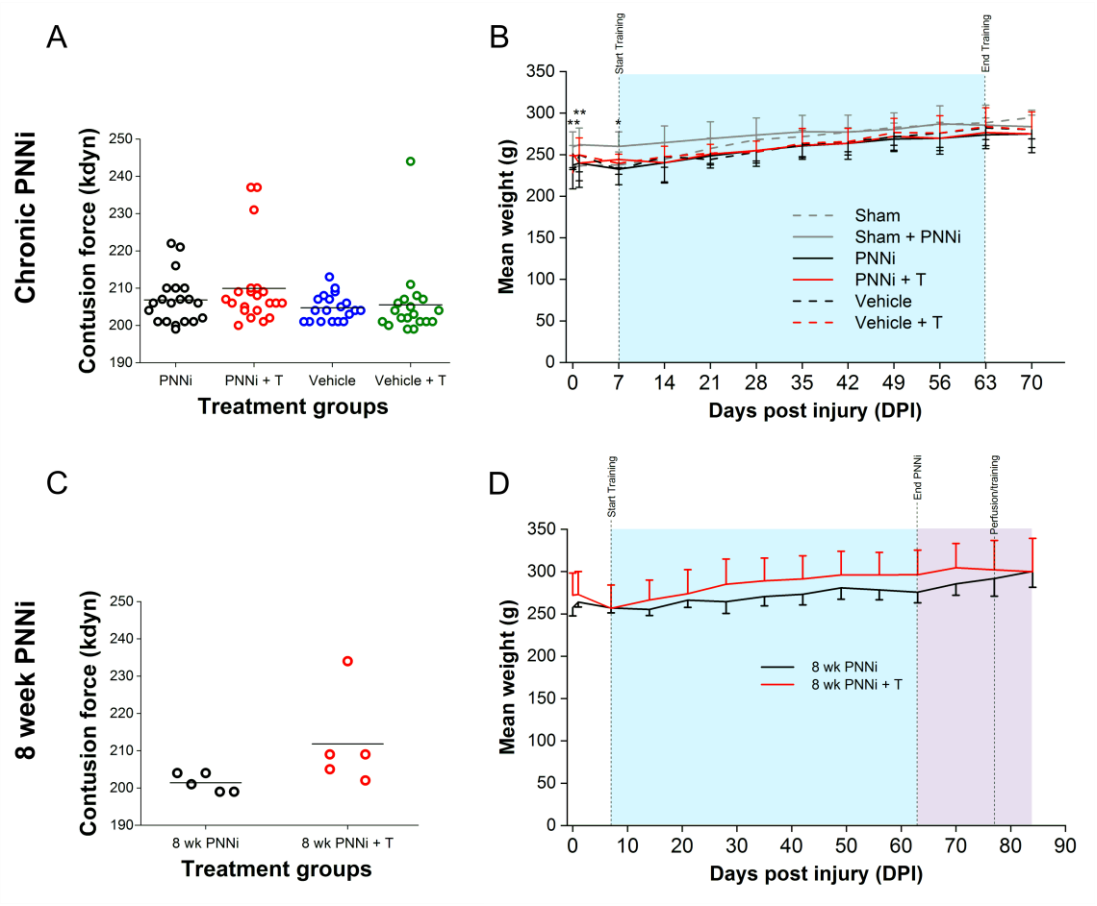

Figure 4.2: Grouped animals received a similar spinal cord contusion (Cx) and drug treatments did not affect weight.

Cx force data (moderate mid-thoracic Cx of 200 kilodynes; kdyn) using the Infinite Horizon impactor **(A, C)** and weight changes post-injury **(B, D)** for experimental groups receiving drug treatment from injury day until termination date (**A:** *n= 18, 21, 19 and 17 for groups;* **B:** *n= 18, 18, 18, 21, 19, 17 for groups, respectively*) and for a period of 8 weeks (**C-D**; *n= 5 per group*). The differences in Cx received between groups **(A, C)** were not significant. ***A:*** *on-way ANOVA.* ***B, D****: statistics two-way mixed factorial ANOVA; where significance levels: *p<0.05 **p<0.01 and ***p<0.001.* ***C:*** *statistics two-tailed Student's t-test.* ***B, D:*** *Error bars are ±SEM.*

4.3.2.3: Chronic PNNi-induced hyperplasticity hampers motor and sensory improvements

4.3.2.3.1: Chronic PNNi-induced hyperplasticity hampers sensory improvements

All injured groups responded to an average of 14.9 ± 0.53 g withdrawal threshold. An increase in withdrawal HL threshold was observed with injury from the intact threshold of 9.9 ± 0.64 g ($F_{6, 145}$ = 5.44; p<0.01 for PNNi, PNNi + T and Vehicle + T and p<0.001 for Vehicle; Figure 4.3 A), corresponding to a decrease in HL sensitivity in comparison to intact control animals.

Although not significant, both sham groups appeared to have a slight decrease in HL sensitivity denoted by the small increase in HL withdrawal threshold to 12.0 ± 0.96 g for Sham animals and even further for Sham + PNNi to 13.4 ± 0.75 g. Interestingly, these sham groups did not appear to show differences in comparison to the injured groups. The intact animals were lighter than all of the other experimental groups ($F_{6, 145}$ = 26.32; p<0.001; Figure 4.3).

4.3.2.3.2: Chronic PNNi induces no improvements to HL motor function, but no deficit to FL

To assess differences in skilled locomotor functions, the walking performance of animals crossing a novel arrangement of irregular rungs on a horizontal ladder was filmed and analysed. Both HL and FL functions were investigated.

As expected, the ladder performance illustrated significant differences between injured and non-injured control groups in all HL measures analysed (p<0.001; Figure 4.3C), representing a significant decrease in HL motor function after a moderate mid-thoracic injury. Average steps were correct approximately 93.7 ± 0.49 %, with 4.78 ± 0.39 % slips and 1.48 ± 0.23 % misses for non-injured animals. In contrast, injured groups displayed 43.5 ± 2.33 % correct steps, 25.5 ± 1.03 % slips and 31.0 ± 2.26 %

misses. Chronic PNNi or rehabilitative treatments showed no difference from injured vehicle control (Figure 4.3C; n.s.; p=1).

As PNNi is administered orally, FL ladder performance was also analysed to assess the effects of chronic PNN removal throughout the spinal cord. Overall FL performance was much better than the HL in injured animals with approximately 92.0 ± 0.96 % correct FL steps in comparison to 43.5 ± 2.33 % for the HL, reflecting the level of the injury (Figure 4.3C - D). However, slight locomotor deficits were observed in the FL between Vehicle groups and non-injured control groups that were not observed with PNNi treated groups. The injured Vehicle control animals showed significantly more misses (1.92 ± 0.32 %) than uninjured control animals (0.39 ± 0.50 %; $F_{6, 129} = 5.33$; $p<0.001$; Figure 4.3D). Animals that received training only (Vehicle + T) missed 1.62 ± 0.41 % of the FL steps which was significantly more than Sham (0.32 ± 0.14 %) and intact (0.34 ± 0.19 %) animals ($p<0.01$; Figure 4.3D). Though chronic PNNi treated animals did not have significant improvements compared to the vehicle control animals, their FL stepping was not significantly different from uninjured animals. It is expected that minor deficits in FL performance may arise as a result of mid-thoracic Cx due to the interruption of ascending intraspinal proprioceptive connections between the FL and HL, as well as a direct consequence of HL errors. However, this data may suggest that PNNi induces a degree of improvement of FL performance after injury.

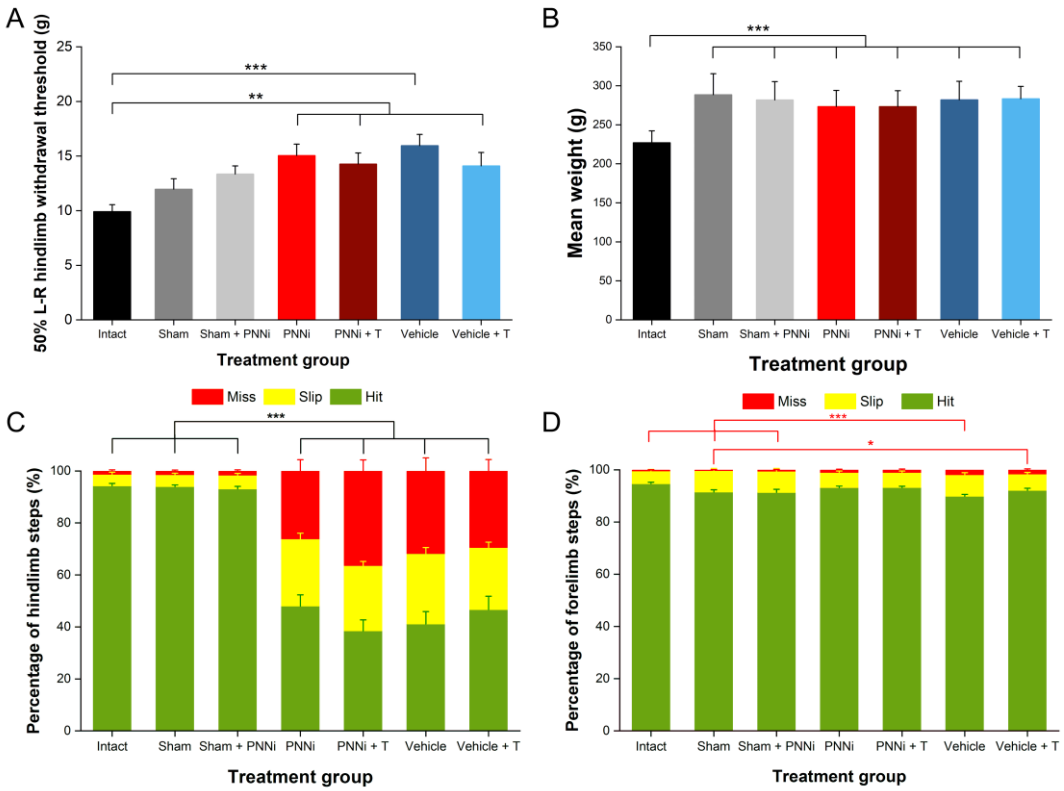

Figure 4.3: Chronic PNNi-induced hyperplasticity hampers sensory and motor functional improvements 9 weeks after acute mid-thoracic moderate contusion (Cx) injury.

A) Bar graph showing mean 50% withdrawal threshold for the left-right hind paws determined from von Frey assays performed at 9 weeks post-surgery. Cx injury induced an increase in 50% withdrawal threshold. *Error bars are ±SEM; n= 28, 25, 19, 20, 21, 19, 20 for groups, respectively.* **B)** Bar graph showing no change in mean weight of rats 9 weeks post-injury. *Error bars are ±SD; n= 28, 25, 19, 20, 21, 19, 20 for groups, respectively.* **C-D)** Stacked bar graphs showing classification of **(B)** hindlimb (HL) and **(C)** forelimb (FL) steps on the horizontal ladder 9 weeks post-injury. **C)** Deficits in HL function observed with injury, with no differences between PNNi and vehicle treatments. **D)** Systemic PNNi removal does not detriment FL stepping. Increased FL misses where observed with both vehicle groups in comparison to non-injured groups, but not with PNNi groups. *For groups, n=15, 23, 19, 20, 20, 19 and 20, respectively. For **C-D)**, error bars are ±SEM. For all graphs, statistics one-way ANOVA; significance levels: *p<0.05 **p<0.01 and ***p<0.001.*

4.3.2.3.3: Spontaneous recovery of weight bearing and plantar stepping

Weekly BBB scoring was performed weekly to observe periodic changes to HL locomotor ability after a mid-thoracic moderate Cx. A baseline BBB score was

established before injury/surgery to ensure that all animals had no locomotor defects. The day after injury, BBBs were again scored to provide an injury baseline in order to equally weight treatment groups and to ensure animals were injured.

Mid-thoracic Cx injury acutely decreased HL locomotor ability with a mean BBB score of approximately 3.2 ± 0.27 at 1 DPI (Greenhouse Geisser $F_{28, 654} = 55.43$; $p<0.001$; Figure 4.4A). By 7 DPI, the mean BBB score for injured animals was 7.93 ± 0.24, corresponding to sweeping of the HLs or plantar placement of the hindpaws but without weight support in some animals (Basso, Beattie and Bresnahan 1995). In all treatment groups HL function improved over the eight-week assessment period (Greenhouse Geisser $F_{5.5, 654} = 662.29$; $p<0.001$). All injured animals demonstrated strong weight support by their HLs at approximately 21 DPI (Figure 4.4B). By 28 DPI, locomotor recovery began to plateau, with a mean BBB score of 10.8 ± 0.2 (Figure 4.4A) when approximately 82 % of animals were able to plantar step (Figure 4.4C). All injured animals were able to plantar step by the end of the assessment paradigm. Figure 4.4A-C show clear spontaneous recovery encompassing rapid regaining of weight bearing ability and a more gradual recovery of plantar stepping. For all injured groups, BBB scoring plateaued at approximately 11 to 12, corresponding with the observation of strong plantar stepping and occasional FL-HL coordination. Training groups showed the earliest emergence of coordination at 14 DPI (~ 13 % of animals), approximately one week earlier than non-trained injured animals (Figure 4.4D). All treatment groups showed a trend of increasing percentage of animals able to achieve FL-HL coordination over time, however, this was not necessarily cumulative. Due to the nature of BBB scoring, animal behaviour is voluntary and limited to a timeframe of four minutes and inevitably may not always be reflective of what the animal is capable of.

Despite improvements over time, both sham control groups achieved significantly higher BBB scores than injured groups at all time points after injury with near to

perfect scores (Greenhouse Geisser $F_{28, 654} = 55.43$; $p<0.001$; Figure 4.4A). No clear differences in HL performance were observed between treatments given to injured animals (n.s.; Figure 4.4A). However, an overall group difference was observed with PNNi treatment to sham animals in comparison to sham controls, where those receiving PNNi displayed a better HL performance ($p<0.001$; Figure 4.4A).

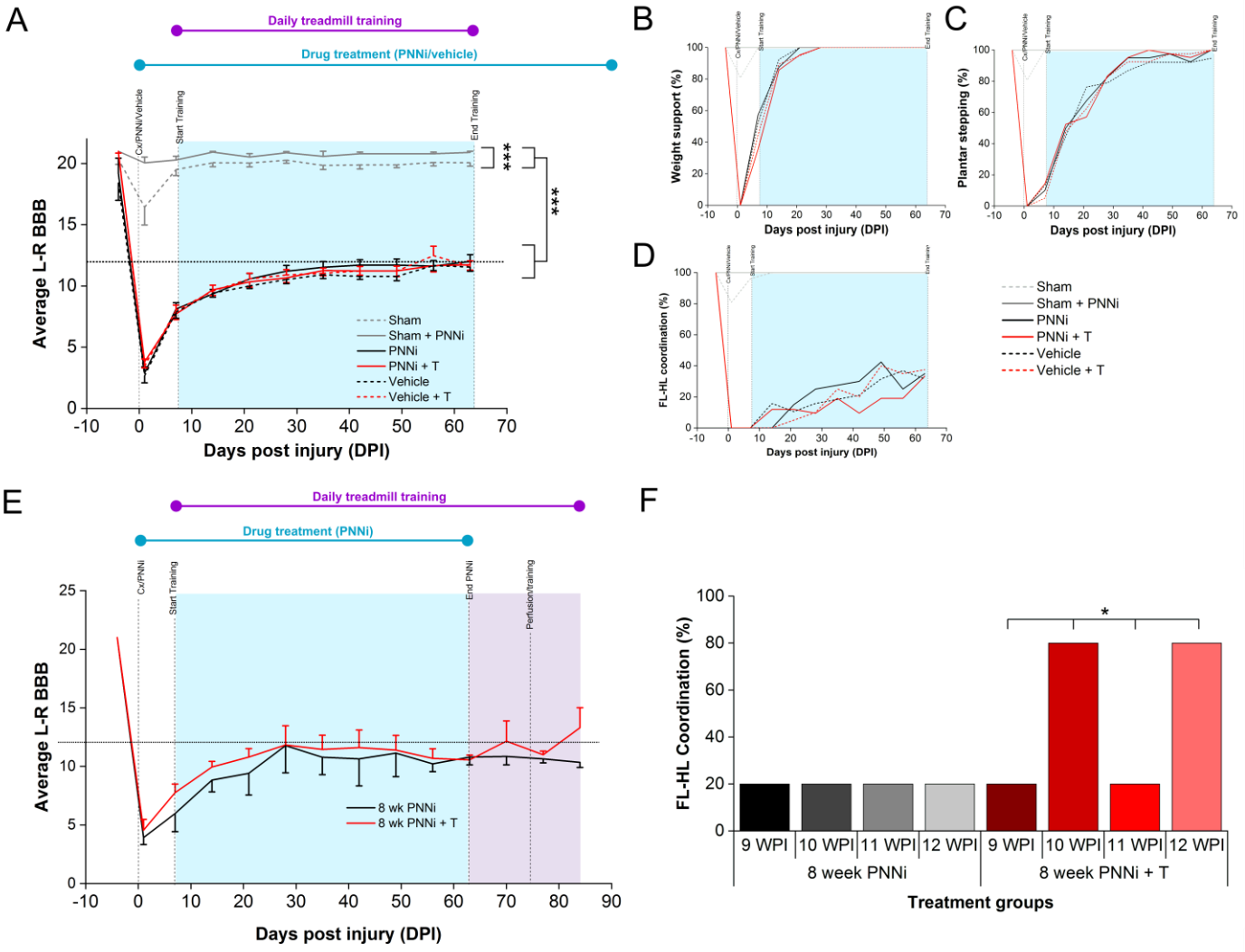
A
Daily treadmill training
Drug treatment (PNNi/vehicle)
Cx/PNNi/Vehicle
Start Training
End Training
***
***
Average L-R BBB
Days post injury (DPI)
Sham
Sham + PNNi
PNNi
PNNi + T
Vehicle
Vehicle + T
B
Weight support (%)
Days post injury (DPI)
C
Plantar stepping (%)
Days post injury (DPI)
D
FL-HL coordination (%)
Days post injury (DPI)
Sham
Sham + PNNi
PNNi
PNNi + T
Vehicle
Vehicle + T
E
Daily treadmill training
Drug treatment (PNNi)
Cx/PNNi
Start Training
End PNNi
Perfusion/training
Average L-R BBB
8 wk PNNi
8 wk PNNi + T
Days post injury (DPI)
F
*
FL-HL Coordination (%)
9 WPI
10 WPI
11 WPI
12 WPI
9 WPI
10 WPI
11 WPI
12 WPI
8 week PNNi
8 week PNNi + T
Treatment groups

Figure 4.4: Limiting PNNi administration alongside sustained rehabilitation allows further HL recovery.

Assessment of hindlimb (HL) locomotor function after a mid-thoracic moderate contusion (Cx) injury using left- right (L-R) limb average Basso, Beattie and Bresnahan (BBB). Treatment groups are defined in Table 2.3. **A)** Injury immediately induced a decline in HL locomotor ability. When PNNi was administered until the end of the experimental paradigm, all injured groups showed improvement of HL motor function, plateauing at approximately 28 DPI. PNNi treatment did not demonstrate significant benefits in the HL locomotor ability when compared to vehicle treated rats. *Error bars are ±SEM; n=18, 18, 18, 21, 19, 17 for groups, respectively. Statistics two-way mixed factorial ANOVA; significance levels: *p<0.05 **p<0.01 and ***p<0.001.* **B)** Percentage of animals able to weight bear over time, derived from BBB scoring. **C)** Percentage of animals able to plantar step over time, derived from BBB scoring. **D)** Percentage of animals able to forelimb-hindlimb (FL-HL) coordinate over time, derived from BBB scoring. **E)** However, when PNNi treatment was terminated 2-3 weeks before the end of the experiments (8 weeks PNNi treatment) allowing for PNN reformation, a further HL improvement was observed with animals that had continued rehabilitative training. *Error bars are ±SEM; n=9 for both groups. Statistics two-way mixed factorial ANOVA; significance levels: *p<0.05 **p<0.01 and ***p<0.001.* **F)** Bar graph showing the percentage of animals that were able to achieve FL-HL coordination at 9 weeks post-injury (WPI) at the end of PNNi administration and 12 WPI. Animals that sustained further rehabilitation training (8 week PNNi + T) showed a large increase in percentage able to coordinate from 9 WPI to 12 WPI. *Statistics chi squared test; significance levels: *p<0.05 **p<0.01 and ***p<0.001.*

4.3.3: Regulating plasticity by limited administration of PNNi alongside rehabilitation allows further HL recovery

As illustrated above, hyperplasticity induced by chronic PNNi treatment limited motor and sensory improvements after Cx injury. Therefore, a small study was performed where PNNi was administered in a limited treatment window and behavioural tests were continued to allow for PNN consolidation. The effect of PNN consolidation on sensory and motor function will be studied (see paradigm in Figure 2.1B).

4.3.3.1: 8-week PNNi with sustained rehabilitation allows improvement of FL-HL co-ordination

Weekly BBB scoring was performed for 8 week PNNi and 8 week PNNi + T animals for twelve weeks (Figure 4.4E). Similar HL functional improvements were observed over time as those for other injured groups, previously illustrated in Figure 4.4A, with recovery plateauing at 11.8 ± 1.53 (8 week PNNi) and 11.8 ± 1.18 (8 week PNNi + T) at approximately 28 DPI. Training and PNNi appeared to show a trend of earlier establishment of weight-bearing between 7 and 21 DPI ($F_{4, 69}$ = 0.57; p = 1; Figure 4.4E).

From one week after cessation of PNNi, animals receiving sustained rehabilitation showed trends of increased HL locomotor capability, particularly FL-HL coordination (p = 0.1; Figure 4.4E-F). Two weeks after the end of PNNi administration (approximately 77 DPI), tracing surgeries were performed, including i.m. injections into the left HL muscles, as described in section 2.3.5.1: Surgical injection of retrograde and anterograde tracers. This caused inflammation in the traced HL in animals receiving sustained rehabilitative treatment only, which appeared to adversely affect HL locomotor scoring in the subsequent BBB scoring that week. However, by the next BBB scoring at 84 DPI, 8 week PNNi + T animals had recovered from their surgeries and more than surpassed their pre-tracing best BBB score with 13.3 ± 1.72. 8 week PNNi treated animals showed no further improvements in HL

locomotor function from cessation of PNNi treatment (p = 0.06). At 9 WPI, approximately 20 % of animals in both groups achieved FL-HL coordination. 8 week PNNi animals as described previously, showed no increase in animals achieving coordination with PNN consolidation (X^2 *(3, n = 20*) 0, p = 1; Figure 4.4F). However, when combined with sustained rehabilitative training, the percentage of animals achieving coordination increased to approximately 80 % at 12 WPI (X^2 *(3, n = 20*) 10.3, p<0.05; Figure 4.4F).

4.3.3.2: Motor changes observed with sustained rehabilitation after 8-week PNNi administration

To assess the effect of PNN consolidation on fine motor skills, HL horizontal ladder performance was assessed at 9 WPI, at the end of PNNi administration, and at 12 WPI, approximately three weeks after the end of PNNi administration (Figure 4.5A).

Overall, in this study, HL locomotor performance was improved with sustained training. The percentage of misses decreased dramatically with rehabilitation, from 44.1 ± 8.34 % (8 week PNNi) to 7.94 ± 4.17 % (8 week PNNi + T) at 9 WPI ($F_{1, 8}$ = 9.67, p<0.05, *n = 5 per group*; Figure 4.5A). At 12 WPI, this difference was still observed but neither group changed with PNN consolidation. Approximately 21.6 ± 3.96 % (8 week PNNi) and 23.1 ± 4.00 % (8 week PNNi + T) of steps were slipped at 9 WPI, similar to performance at 12 WPI ($F_{1, 8}$ = 120.53, n.s., p=1), suggesting that slipping was unaffected by either training or cessation of PNNi administration. Average steps were correct 34.3 ± 14.5 % in 8 week PNNi animals (9 WPI) and this increased significantly with training at both time points, with 68.9 ± 7.57 % correct steps displayed by 8 week PNNi + T animals ($F_{1, 8}$ = 8.07, p<0.05). Inverse to the percentage of missed steps, more correct steps were performed with training but no further improvement was observed with PNN consolidation at 12 WPI.

4.3.3.3: No changes in sensory function observed with a limited window of PNNi administration

Sensory function was also evaluated at both 9 and 12 WPI to investigate the effect of PNN consolidation after a window of plasticity on the 50 % HL withdrawal threshold (Figure 4.5B). No difference was found between trained and untrained animals at either time point with values of approximately 14.2 ± 2.90 g for 8 week PNNi and 15.9 ± 1.79 g for 8 week PNNi + T ($F_{1, 8}$ = 47.85, p = 1, *n=5 per group*, Figure 4.5B) suggesting that rehabilitative training did not affect HL withdrawal threshold. Additionally, the 50 % withdrawal threshold did not change in the three weeks since PNNi cessation for either group, with 50 % withdrawal thresholds of 14.8 ± 1.37 g at 9 WPI and 15.3 ± 3.15 g at 12 WPI ($F_{1, 8}$ = 47.85, p = 1, *n=5 per group*).

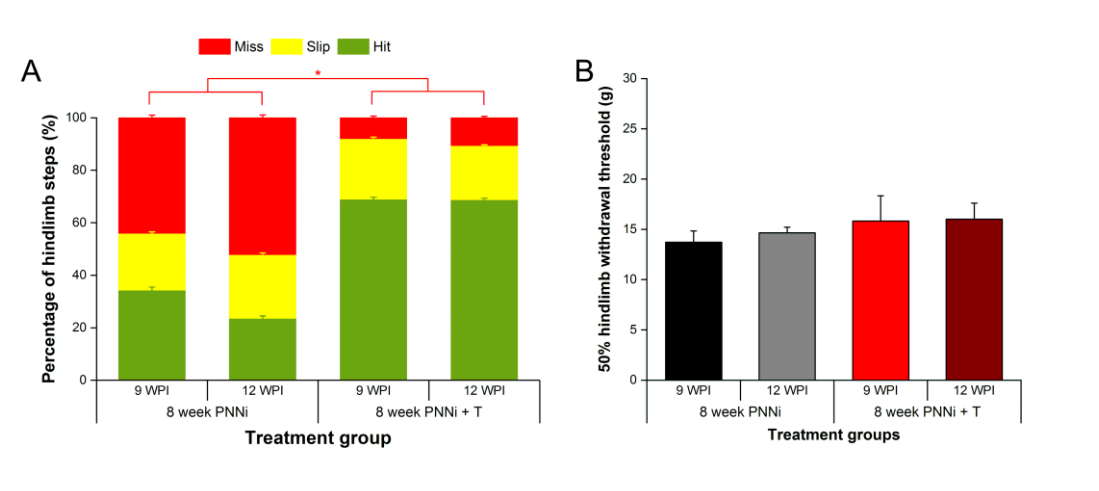

Figure 4.5: Motor but not sensory differences observed with rehabilitative training at 9 and 12 weeks after acute mid-thoracic moderate contusion injury.

A) Stacked bar graph showing classification of hindlimb steps on the horizontal ladder at 9- and 12-weeks post-injury (WPI). Deficits in HL function observed with injury are improved with access to sustained rehabilitative training. Consolidation of PNNs did not induce improvement for either group. **B)** Bar graph showing the left-right average 50% withdrawal threshold for the plantar hindpaws determined from von Frey assays performed at 9 and 12 WPI. Consolidation of PNNs after

termination of PNNi treatment does not induce sensory changes. *Error bars are ± SEM. For all graphs, n=5 per group; statistics two-way mixed factorial ANOVA; significance levels: *p<0.05 **p<0.01 and ***p<0.001.*

4.4: Discussion

This chapter aimed to investigate the effect of a novel and non-invasive method to remove PNNs on sensory and motor functions, firstly, in the intact rat and then its efficacy in improving these functions after an acute mid-thoracic Cx injury, by using a variety of behavioural assessments.

In healthy adult rats, acute administration of PNNi did appear to enhance plasticity, resulting in an increase in HL sensitivity but did not alter functional performance of fine motor skills (Figure 4.1). While PNNi is an already licensed pharmacological drug, the dose administered in these studies is higher than its clinical use. Crucially, chronic and acute PNNi treatment did not induce changes in weight beyond normal growth, particularly for an already vulnerable, injured population of rats (Figure 4.2B, D).

This is the first study to assess the use of this novel small molecular PNN inhibitor, PNNi, and its effectiveness for promoting functional recovery in a SCI model. A Cx injury model was utilised as clinically this is the most prevalent human SCI sustained (Kumar *et al.* 2018). Figure 4.2A and C demonstrated the reproducibility of a moderate Cx injury sustained by animals in each of the treatment paradigms, using the commercially available Infinite Horizon impactor (Scheff and Roberts 2009). Weekly behavioural assessments in an open field environment mapped the progression of HL locomotor function after the moderate (200 kdyn) Cx injury (Figure 4.4). This revealed the extent of spontaneous recovery and contributions from the treatments given in each paradigm, as well as demonstrating the effect of sham surgeries on locomotor function. Using a more sensitive motor function test like the horizontal ladder, effectively illustrated that PNNi mediated plasticity throughout the spinal system, influencing both HL and FL motor performance (Figure 4.3C-D). Assessment of sensory functions, by defining mechanical thresholds, revealed that while mid-thoracic injury induced deficits in HL sensation, as expected, PNNi-mediated plasticity neither improved or caused further impairments to HL sensory

function (Figure 4.3A). As an oral drug, PNNi permitted investigation of motor and sensory functional recovery after a defined period of PNN removal (Figure 4.4E-F Figure 4.5). The effect of PNN formation after an extended window of plasticity after CNS injury has, as of yet, been poorly investigated. This is a question that is essential to be addressed for the progression of therapies harnessing PNN-mediated plasticity to the clinic.

4.4.1: PNNi-mediated plasticity in intact systems induced transient changes in some functions

Application of ChABC causes removal of PNNs surrounding the injection site in both injured and uninjured animals, inducing a local environment permissive to plastic changes (Barritt *et al.* 2006; Bartus *et al.* 2014; Pizzorusso *et al.* 2002; Galtrey *et al.* 2007; Soleman *et al.* 2012). In this study, plasticity was observed in sensory systems in uninjured animals following acute PNNi administration, however, by nine weeks no difference in HL sensitivity was observed between PNNi treated and untreated sham controls. This suggests enhancement of plasticity induced a transient change in the sensory circuitry that recovered to normal sensory levels due to sustained plasticity in the uninjured system. This is partially supported by evidence describing no change, after lentiviral ChABC delivery to the cord, to mechanical or thermal thresholds in uninjured animals even after three months (Bartus *et al.* 2014). Similarly, bacterial ChABC application appeared not to induce any sprouting of peripheral afferents in uninjured animals (Barritt *et al.* 2006). No sprouting was also observed in CST or 5-HT fibres, which corroborates with the lack of change detected in motor functions following acute and chronic PNNi treatment to unlesioned animals in this study. However, single injection of ChABC to the intact cerebellum revealed transient sprouting between 7 and 21 days post injection (Corvetti and Rossi 2005), supporting the PNNi-mediated functional changes observed. It is important to note that lentiviral

ChABC induces sustained and much more widespread removal of PNNs in comparison to bacterial ChABC, which requires repeated injection to sustain PNN degradation (Bartus *et al.* 2014). The anatomical studies carried out by Barritt et al. (2006), investigated sprouting of these systems at a single time point, after partial recovery of PNNs and their components (Brückner *et al.* 1998; Lin *et al.* 2008), so may have underestimated or missed the transient sprouting in intact systems. However, as functional changes were observed in sensory and not in motor systems, it is also possible that different fibres or systems have varying sensitivities or capacities to sprouting in response to removal of plasticity restricting mechanisms. Additionally, in intact systems the absence of injury mechanisms or experience driving connections, sprouting may not establish functional connections.

4.4.2: Robust spontaneous recovery masks additional benefits of rehabilitative training

Robust spontaneous recovery was observed following a mid-thoracic moderate Cx injury, similar to that observed in the literature (Franz *et al.* 2014; Carter *et al.* 2016; Scheff *et al.* 2003), plateauing with the achievement of plantar stepping. Regaining FL-HL coordination represented the glass ceiling of this injury model. Animals receiving rehabilitation training were, therefore, quadrupedally trained, as evidence suggests that engagement of the FLs improves HL function after injury and strengthens intralimb coordination, via plasticity of intraspinal and intersegmental circuitry, including propriospinal neurones (Shah *et al.* 2013). The short propriospinal neurones that help mediate cervical and lumbar connectivity are particularly vulnerable to mid-thoracic SCI, suggesting that functional recovery can be mediated by the recovery of these intraspinal circuits following loss of descending control (Courtine *et al.* 2009; Bareyre *et al.* 2004). Interestingly, in this study, rehabilitation did not appear to promote any further enhancements in motor function compared to

that spontaneously reacquired, even after assessment of fine motor performance. The effect of rehabilitation therapy in incomplete injuries demonstrate contradictory results, with many reporting positive outcomes but others no change (Fouad *et al.* 2000; Battistuzzo *et al.* 2012; Liu *et al.* 2008; Park *et al.* 2010). A systematic review suggested that this could be dose dependant and that treadmill training beginning in a critical period of 1-2 WPI and lasting at least 8 weeks, similar to that utilised in this study, was most likely to result in enhancements of function (Battistuzzo *et al.* 2012). However, others suggest that 'self-training' in over-ground walking by cage activity may confound the differences between trained and untrained animals, by reaching a ceiling effect and not as a result of task-specificity (Fouad *et al.* 2000; Kuerzi *et al.* 2010; Dobkin *et al.* 2006; DeBow *et al.* 2003).

4.4.3: Systemic PNN removal induces mal-adaptive plasticity against functional benefit

The ability of PNNi to induce a period of plasticity has been demonstrated by the transient changes in sensory function observed in unlesioned animals. Sustained local removal of PNNs using lentiviral ChABC administration is able to enhance motor function performance in some SCI models (Bartus *et al.* 2014; García-Alías *et al.* 2009). However, shorter periods of ChABC application resulted in less beneficial results, frequently providing evidence of anatomical but not functional recovery (Tom *et al.* 2009; Führmann *et al.* 2018; Barritt *et al.* 2006). These studies indicate that prolonged removal of PNNs is necessary to facilitate functional improvements. However, chronic PNNi administration failed to induce recovery greater than spontaneously reacquired HL motor functions, after assessment of both gross and fine motor functions. PNNi affects the spinal cord systemically, not local to injury like intrathecal ChABC injections. Horizontal ladder performance revealed that FL performance was positively affected by PNNi administration and demonstrated

evidence of plasticity post-injury. The systemic plasticity induced promoted changes in FL function that were able to overcome detriments to FL performance as a result of HL motor impairments. These results suggest that increasing the area of plasticity in the spinal cord could drive more compensatory mechanisms, such as improving FL performance in response to HL slips and falls.

Combination treatment of rehabilitation and PNN removal in this study did not provide synergistic enhancement of motor functions, in contrast with prominent studies using task-specific rehabilitation and ChABC (García-Alías *et al.* 2009; Wang *et al.* 2011a). Despite this, it was important to demonstrate that PNNi could be used alongside rehabilitative training, using classical time points, without detriment to functional recovery, unlike other plasticity enhancing treatments (Maier *et al.* 2009). However, like the anti-Nogo-A studies, optimisation of timing and duration may be required to maximise behavioural recovery.

Like motor function, PNNi did not induce any long term adverse changes in HL mechanical sensitivity. The moderate Cx model used in this study did not appear to induce mechanical allodynia, as frequently reported (Yoon *et al.* 2004; Kanno *et al.* 2014; Carter *et al.* 2016), instead showing injury-induced sensitivity deficits in response to mechanical stimuli (Wang *et al.* 2011a). However, as lack of sensory recovery was observed, it also suggests that PNNi-induced plasticity does not induce mechanical allodynia. In support of these findings, ChABC-mediated PNN removal also provokes no change in response to either mechanical or thermal stimuli after SCI (Bartus *et al.* 2014; Lee, McKeon and Bellamkonda 2010; Barritt *et al.* 2006; Wang *et al.* 2011a).

It was expected that removal of PNNs around spinal populations, such as Mns, using systemic PNNi, would improve FL-HL coordination after mid-thoracic contusion by allowing changes to the synaptic inputs and electrical properties for these neurones. Motor improvements of the injured control rats plateaued before reacquisition of FL-

HL coordination which is dependent on recovery of intraspinal propriospinal neurones between cervical and lumbar motor pools that are disproportionally affected by mid-thoracic injury. The widespread removal of PNNs by PNNi should render the environment more favourable for recovery of this cervical-lumbar connectivity. While it is possible that the anatomical recovery of the necessary neuronal populations was not adequate to enhance recovery of sensory or motor functions, PNN formation is responsible for the stabilisation and maturation of new connections formed during development (Carulli *et al.* 2010; Pizzorusso *et al.* 2002; Miyata *et al.* 2012). Therefore, whilst a sustained period of PNN removal is necessary to permit plastic and regenerative changes to the spared circuitry, prolonged removal, particularly in such a large area, may render the formation of these new synapses temporary without consolidation by PNNs. Whilst some of the mechanisms of the effects of PNNi on functional recovery will be explored in the next chapter (Chapter 5: The mechanistic changes induced by systemic PNNi inhibition), other experiments will look to determine the anatomical recovery of the CST. Future experiments could label or trace the propriospinal neurones to understand the condition of cervical-lumbar connectivity and its contribution to the failure of PNNi to induce further functional recovery.

4.4.4: Stabilisation of PNNs after a window of plasticity permits further changes in motor functions

Development of PNN removing therapies has primarily sought to increase the thermal stability or increase the expression of the enzyme ChABC to enhance the period of plasticity for further recovery. The advent of the lentiviral gene delivery system for ChABC has achieved this goal (Bartus *et al.* 2014). However, recovery reaches a plateau and does not continue to increase for as long as plasticity is enhanced (Bartus

et al. 2014). Maintaining heightened plasticity levels may also render the system vulnerable to maladaptive effects (García-Alías *et al.* 2009).

In this study, PNNi was given for a period of 8 weeks, defining both the opening and closure of a plasticity window. The turnover of PNN components is rapid; with CSPGs beginning to recover approximately seven to ten days after removal (Lin *et al.* 2008) and HA even more rapidly in about two days (Fraser, Laurent and Laurent 1997). Therefore, it was proposed that the effects of PNN reformation could be assessed from two weeks after the end of PNNi administration. No further changes were observed in sensory function with consolidation of PNNs with or without sustained rehabilitative training. However, whilst no further motor recovery was observed in animals that had only received PNNi treatment, those that received sustained rehabilitative training showed trends of improvement from one week after PNNi treatment ended. This was consistent with the recovery of some PNN components (Lin *et al.* 2008; Brückner *et al.* 1998) and suggests that whilst new connections were consolidated by PNN formation, the adaptive plasticity provided by continued rehabilitation was able to strengthen the synaptic connections and confer further functional motor improvements (Lynskey, Belanger and Jung 2008). PNNs are dynamic structures, with constant synthesis of components, such as HA, to replenish temporal degradation and maintain synaptic stability. It is important to note that PNNi and rehabilitation have differential effects on PNNs, with PNNi removing PNNs through disruption of component turnover, whereas exercise increases the expression of PNN components in the spinal cord (Smith *et al.* 2015; Wang *et al.* 2011a). Therefore, it is likely that the recovery of PNNs after cessation of PNNi could have been accelerated by rehabilitation, conferring a dual role in both stabilisation of connections and the driving of functional connectivity.

The trends in motor improvement observed here may have been limited due to the study's design where after unilateral intramuscular tracing injections it was observed

that the affected HL was highly inflamed in animals with sustained rehabilitation only and may have consequently impaired HL function. Additionally, as it can take up to six weeks for all the PNN components to recover after ChABC treatment (Brückner *et al.* 1998; Corvetti and Rossi 2005; Lin *et al.* 2008), it would be beneficial to repeat this study to increase n numbers, omitting surgeries mid-behavioural tests, and to keep animals for longer to see if they continue to improve. This additional time may be necessary for further recovery of animals given only 8 weeks PNNi treatment. A key question is whether the window of plasticity could be further optimised as plateaus in motor function were observed from four to six weeks post-injury. However, a recent study that developed an immune evasive 'switch' for delivery of ChABC, proposes that longer term PNN removal (eight weeks) is necessary for recovery of more skilled tasks and was associated with greater recovery of descending tracts (Burnside *et al.* 2018).

4.4.5: Conclusions

The data presented here provides evidence that PNNi is capable of inducing plasticity. After a mid-thoracic Cx injury, rehabilitation-induced acceleration of PNN reformation is required after a defined period of enhanced plasticity to induce functional motor improvements. This improvement was observed at 84 DPI in our preliminary testing and therefore future experiments will be designed with a longer duration of training post-PNNi administration to promote further functional benefit. PNNi treatment induced no adverse long term effects on pain pathways. As aforementioned, this study represents the first time that this drug has been used in this pathology and the results above illustrate that the use of PNNi for acute SCI requires further optimisation to promote recovery. However, importantly PNNi administration appeared to be compatible with rehabilitation and this sustained training was essential for the motor improvements observed with PNN reformation.

Continued study into this small molecule inhibitor remains an attractive option due to its availability as an already licensed pharmacological treatment. Optimisation for off-label use can utilise data from essential preliminary tests such as LD50 for example that are already available. This study showed that the higher dose used here induced no adverse effects on weight. Assessment of the extent of PNN removal in specific CNS regions will need to be made and will begin to be addressed in the following chapter, along with exploration of changes in descending and intraspinal innervation.

Chapter 5: The mechanistic changes induced by systemic PNNi inhibition

5.1: Introduction

Whilst experimental SCI is no longer incurable, with a myriad of treatments attributed to cause functional recovery of motor and/or sensory behaviours, much of the mechanisms by which this occurs are still relatively unknown. After injury, spontaneous sprouting of damaged spinal circuitry occurs but is limited by intrinsic and extrinsic capabilities of regeneration in the CNS. The exact contributions of plasticity and regeneration of severed descending fibres and local spinal circuitry required to confer functional recovery is yet to be determined and defines the central caveat to plasticity-enhancing therapies, in that anatomical changes are not always auspicious to recovery.

Removal of PNNs in the vicinity of the lesion site is well documented to benefit both functional and anatomical recovery after SCI by promoting the sprouting and reorganisation of descending tracts, such as the CST, and spared intraspinal circuitry (Bradbury *et al.* 2002; Barritt *et al.* 2006; García-Alías *et al.* 2009; Carter, McMahon and Bradbury 2011; García-Alías *et al.* 2015). Shaping this ChABC-induced recovery using task-specific rehabilitation, in both acute (García-Alías *et al.* 2009) and chronic (Wang *et al.* 2011a) SCI models, provides further functional and organisational enhancements (García-Alías *et al.* 2015). The previous chapter demonstrated that systemic removal of PNNs, using PNNi, was also capable of inducing functional plasticity. However, further investigation is required to look at the extent of PNN removal and circuitry plasticity.

Whilst SCI greatly impacts transmission of descending modulation and control of functions below the level of injury, other regions in the CNS are also affected (Freund *et al.* 2011; Freund *et al.* 2013; Wu *et al.* 2014; Jure and Labombarda 2017). Whilst changes to the somatosensory cortex have been explored following SCI, showing cortical reorganisation, specifically large-scale expansion of the facial sensory representation following injury to the dorsal columns innervating the hand (Jain,

Catania and Kaas 1997; Jain *et al.* 2000; Tandon *et al.* 2009; Kao *et al.* 2009), other regions, such as the primary motor cortex (M1) and premotor regions, also contain a highly organised topographical representation of motor movements (Penfield and Boldrey 1937; Neafsey *et al.* 1986; Graziano 2016). It is well established that cortical regions associated with sensorimotor activity are subject to functional and structural plasticity in response to sensorimotor learning (Kleim, Barbay and Nudo 1998; Plautz, Milliken and Nudo 2000; Kleim *et al.* 2004) and neuronal injury (Nudo and Milliken 1996; Jain, Catania and Kaas 1997; Jain *et al.* 2000). Activity-based plasticity drives the expansion of movements after task-specific training, not just repetitive use, to be represented over a larger cortical area (Plautz, Milliken and Nudo 2000). This creates variation between healthy uninjured individuals, each with their own personal profile of skilled learning, for example, the exaggeration of the somatosensory area dedicated to the hand in Braille readers (Pascual-Leone and Torres 1993), but there is still a general area that is associated with certain topographical body regions and behavioural actions (Plautz, Milliken and Nudo 2000; Graziano 2016).

Studies investigating somatotopic cortical motor representations have generally focused on structural changes following stroke (Nudo and Milliken 1996), peripheral nerve injury (Sanes, Suner and Donoghue 1990) and limb amputations (Cohen *et al.* 1991; Wu and Kaas 1999). In all of the above described cases, large-scale cortical reorganisation occurred, in particular expansion of the remaining functioning areas was induced, such as shoulder and face, into the denervated FL area after a FL amputation, for example (Cohen *et al.* 1991; Wu and Kaas 1999). The primary motor cortex or sensorimotor cortex in rodents has biological significance to SCI recovery, because it gives rise to CST projections to the spinal cord, which are key for skilled motor functions (Lemon *et al.* 1998; Anderson, Gunawan and Steward 2007). Therefore, this study will look to investigate the remodelling of motor representations in response to mid-thoracic incomplete SCI and the shaping of this by sensorimotor

experience given as rehabilitative training, as well as the effect of plasticity enhancement by PNNi. The intact normal cortical motor representation has been well described in many rat strains, including Wistar, Sprague Dawley and Long Evans rats, and has revealed some strain differences (Neafsey *et al.* 1986; Paxinos and Watson 2006; Fonoff *et al.* 2009; VandenBerg *et al.* 2002). However, the sensorimotor map of Lister Hooded rat has not been well characterised, therefore firstly, a baseline motor map needs to be developed to compare to.

5.2: Aims

The following investigation aims to firstly, confirm the removal of PNNs mediated by PNNi administration by labelling a variety of different PNN components in key CNS regions and to examine consequent changes in inhibitory-excitatory balance in the VH. The contributions of regeneration/plasticity of descending tracts that have been interrupted during SCI, particularly the CST and their functional plasticity will be investigated using cortical mapping by ICMS and neuronal tracing.

5.2.1: Assess the effect of chronic PNNi administration on PNNs in the cortex and spinal cord

5.2.2: Determine the efficacy of PNNi in promoting plasticity and regeneration after acute SCI using:

i. Immunohistochemistry

ii. Electrophysiology (to assess functional pathways)

iii. Anterograde neuronal tracing

5.3: Results

The following results will investigate if oral administration of PNNi removes PNN components in key areas in the CNS and explore the mechanisms induced by enhancement of plasticity after a mid-thoracic Cx injury. The animals used for the following experiments followed the paradigms detailed in section 2.3: Acute contusive SCI and have previously been used for unilateral ICMS motor mapping experiments (see Figure 5.7-9).

5.3.1: Chronic PNNi treatment alters expression of PNN components in the VH and cortex

These investigations primarily aimed to confirm the effect of PNNi on the expression of key PNN components in specific CNS regions. Spinal sections from T4-6 (rostral to the Cx lesion) and transverse brain sections were immunohistochemically labelled, for each of the previously described chronic treatments, to elucidate injury-induced changes from therapeutic alterations. A general neuronal stain (NeuN) (Kim, Adelstein and Kawamoto 2009) was used alongside the 'universal PNN marker' WFA, one of the principal CSPG components, ACAN, as well as for HA, using hyaluronan binding protein (HABP). The intensities of WFA, ACAN and HABP are displayed as a percentage of sham control animals to show relative changes to normal expression.

5.3.1.1: Systemic PNNi treatment reduces number of PNNs and extracellular HA levels in the VH

After SCI, much of the focus of recovery looks at progression of locomotor skills. The VH contains neuronal cell types critical to motor control, such as spinal Mns, which are also known to be associated with PNNs (Vitellaro-Zuccarello *et al.* 2007; Galtrey *et al.* 2008; Irvine and Kwok 2018). Therefore, the following explores changes to key PNN components within the VH immediately rostral to the lesion site (Figure 5.1 – 3). The data in Figure 5.1B and Figure 5.2B may be underpowered in terms of animal

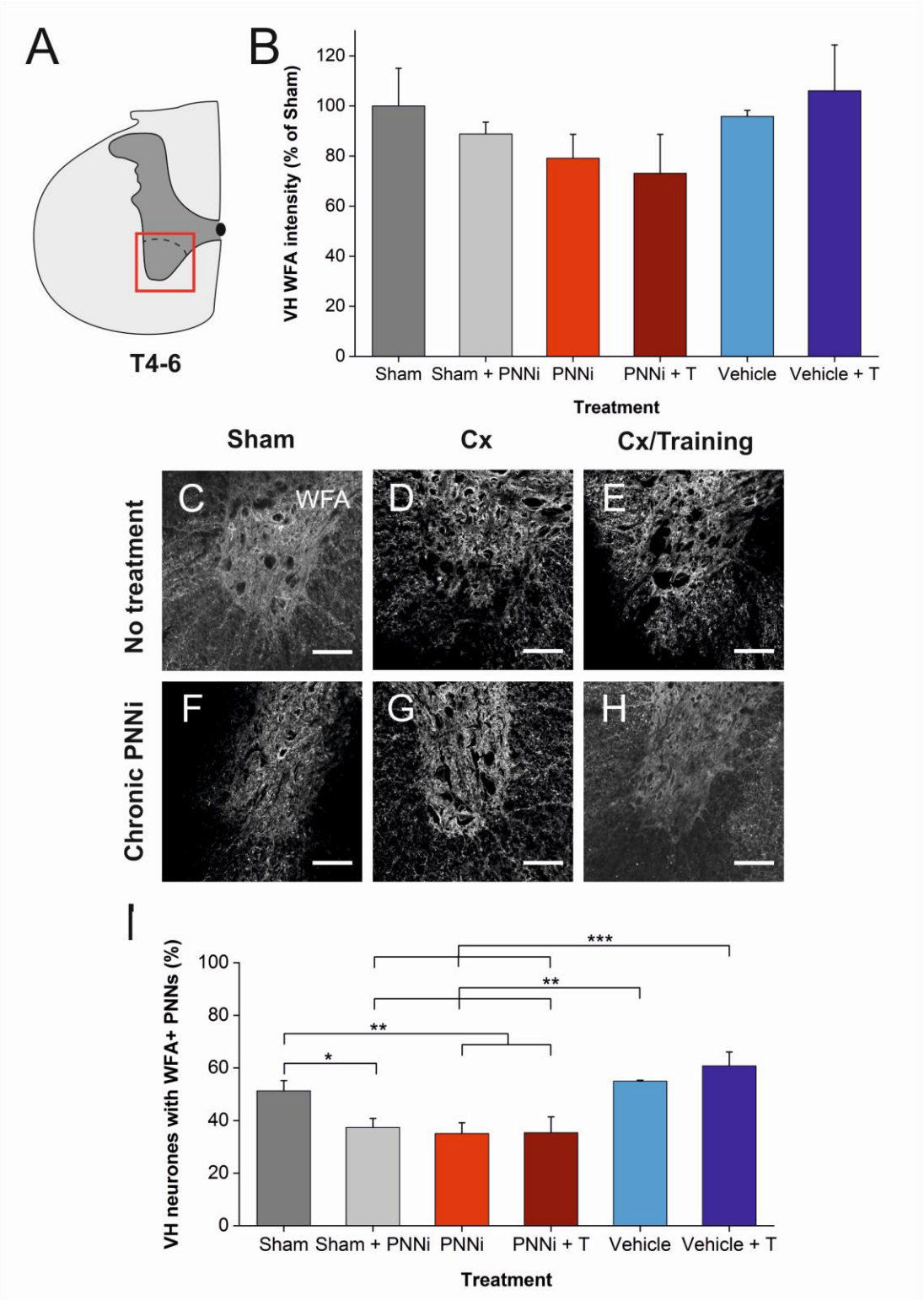

Figure 5.1: Chronic PNNi treatment preferentially reduces expression of *Wisteria floribunda* agglutinin (WFA)-positive PNNs in the ventral horn (VH). **A)** Rat spinal cord sections (T4-6) obtained at 12 weeks post-injury were stained and intensity was analysed in the VH (denoted by red box). **B)** WFA intensity (visualised using Alexa fluor 488) in the VH shows a trend of reduction in animals treated with PNNi after injury. Confocal images showing global WFA expression is unchanged rostral to injury **(C-E).** PNNi-treated sham **(F)** animals also show no

change in overall WFA expression. Whereas, injured animals, treated with PNNi alone **(G)** or with combination treatment of PNNi and training **(H)**, showed slight but not significant reductions in WFA expression in the VH. **I)** However, PNNi decreases number of WFA-positive PNNs, particularly after injury. *Scale bars, 100 µm. For all graphs, error bars ± SD; n=3 per treatment group. Statistics one-way ANOVA; significance levels: * p<0.05 ** p<0.01 *** p<0.001.*

number used (*n = 3*), however, a total of ten sections were used to minimise intensity variation. Future experiments will repeat these investigations using additional animals from the study.

5.3.1.1.1: Decreases in number of PNN positive neurons but not the general loose ECM after chronic PNNi treatment

WFA is thought to label all CSPGs and therefore all PNNs, through binding to a key sugar residue (GalNAc) present in the CS-GAG disaccharide subunit (Härtig, Brauer and Brückner 1992). However, recent publications cast doubt on this and suggest that the binding conditions for WFA may be more complex (Giamanco, Morawski and Matthews 2010; Miyata *et al.* 2012; Ueno *et al.* 2017; Yamada and Jinno 2017; Irvine and Kwok 2018). Tissue from injured animals was obtained at 12 WPI. Cx injury alone (95.8 ± 2.41 %) or with rehabilitation training (106 ± 18.3 %) did not appear to alter WFA intensity in the spinal cord ($F_{5, 17} = 3.09$; p=1; Figure 5.1B - E), suggesting that CSPG levels in the ventral ECM were similar to normal expression (100 ± 15.1 %) rostral to the chronic lesion environment. Additionally, in unlesioned animals that received chronic PNNi administration, global levels of WFA staining in the ventral ECM did not significantly reduce (88.4 ± 4.72 %; p=1; Figure 5.1B, C, F). However, whilst not significant, some reduction of WFA intensity in the ECM was observed with PNNi administration after injury (Figure 5.1B, G-H). PNNi administration alone (79.1 ± 9.53 %) and in combination with rehabilitative training (73.1 ± 15.6 %) appeared to reduce WFA intensity in comparison to injured animals receiving rehabilitation (p=0.31 and p=0.10, respectively). PNNi and training combination also displayed a

slight reduction of WFA binding in relative to expression of CSPGs in the VH of sham animals (p=0.32). Overall, PNNi displayed little influence on WFA level to the ventral ECM, suggesting the level of WFA binding in the loose ECM in the VH remained similar.

Unlike loose ECM, PNNs are aggregated ECM wrapped on the surface of sub-populations of neurones and the assembly of PNNs are regulated at the molecular level. Here, the number of PNN positive neurons stained by WFA was counted. Unlike the lack of significant change in loose ECM, a decrease in the number of WFA-positive PNNs was observed between PNNi treated groups and all untreated controls ($F_{5, 17}$ = 20.93; Figure 5.1I). Without pharmacological treatment approximately 55.7 ± 3.20 % neurones, labelled using NeuN, were surrounded by WFA-positive PNNs. In contrast, following chronic PNNi treatment only 35.9 ± 4.18 % of neurones remained associated with PNNs. These results indicate that PNNi preferentially affects the binding of WFA to the usually highly aggregated ECM of the PNNs rather than impacting intensity seen in the loose ECM.

5.3.1.1.2: Lack of ACAN in PNNs but not in the ventral ECM after PNNi treatment

ACAN is an abundant hyaluronan binding CSPG (Yamaguchi 2000), known to be present at high levels in the spinal ventral motor pools (Vitellaro-Zuccarello *et al.* 2007; Galtrey *et al.* 2008). As reported in Chapter 3, ACAN surrounds more in neurons with PNN in the ventral motor pools of normal animals than WFA (Irvine and Kwok 2018). After Cx injury (94.3 ± 10.8 %) or with PNNi administration to unlesioned animals (85.8 ± 9.23 %), ACAN levels appeared unchanged from normal expression in the ECM ($F_{5, 17}$ = 1.70; p=1; Figure 5.2B-F). However, with chronic PNNi treatment to acutely injured animals, slight yet not significant reductions in ACAN expression were observed (73.1 ± 5.40 %), relative to sham animals (100 ± 21.5 %; p= 0.32; Figure 5.2B, C, G). Whereas, addition of rehabilitation, to form a combination

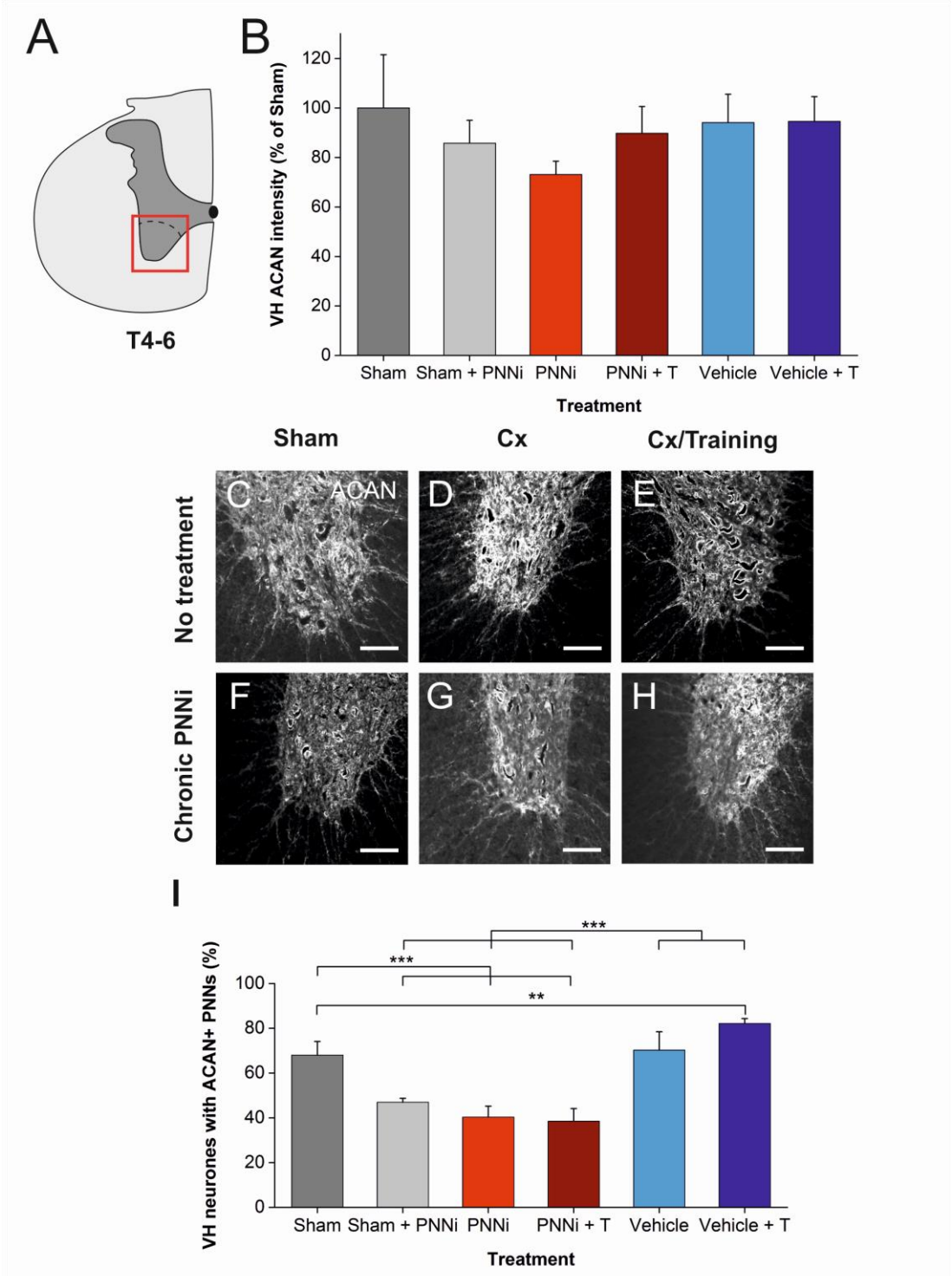

Figure 5.2: Chronic PNNi treatment preferentially reduces expression of aggrecan (ACAN)-positive PNNs in the ventral horn (VH).

A) Rat spinal cord sections (T4-6) obtained at 12 weeks post-injury were stained and intensity was analysed in the VH (denoted by red box). **B)** ACAN intensity (visualised using Alexa fluor 568) in the VH appears to decrease slightly in animals treated with PNNi. Confocal images showing ACAN expression is unchanged rostral to injury **(C-E).** Whereas, PNNi treated sham **(F)** and injured animals **(G)** show minimal reductions in ACAN expression in the VH. When combined with

training, ACAN showed no change from normal expression **(H).** *Scale bars, 100 µm.* **I)** PNNi decreases number of ACAN-positive PNNs, particularly after injury. *For all graphs, error bars ± SD; n=3 per treatment group. Statistics one-way ANOVA; significance levels: * p<0.05 ** p<0.01 *** p<0.001.*

treatment regime, appeared to increase the expression of ACAN in the ventral ECM to control levels (89.8 ± 10.98 %; p=1; Figure 5.2B, H).

Whilst minimal changes in ACAN expression were observed in the loose ECM in the VH, PNNi induced similar effects to the number of PNN-positive neurons as illustrated above with WFA binding. As expected, ACAN-positive PNNs were highly associated with neurones in the VH (73.0 ± 2.79 %; Figure 5.2I). With PNNi administration, a more drastic decrease in PNN envelopment was observed, to a similar level of approximately 40.2 ± 3.53 % ($F_{5, 17}$ = 128.07; Figure 5.2I). Rehabilitative treatment, in the absence of PNNi treatment, has the opposite influence on PNNi expression, increasing the number of ACAN-positive PNNs by approximately 20 % to 83.4 ± 1.09 % of neurones (p<0.01; Figure 5.2I).

5.3.1.1.3: PNNi downregulates HA expression in the ECM of the VH

HA exists as ubiquitous polysaccharide chains that act as a major component in ECM structure, as well as an essential scaffold for the formation of PNNs (Kwok, Carulli and Fawcett 2010). Immunohistochemical staining was performed using the HA probe, HABP, adapted from the HA binding region of the lectican core protein (Ripellino *et al.* 1985). After a mid-thoracic Cx injury, animals receiving either vehicle treatment alone (77.0 ± 15.4 %) or along with treadmill training (77.9 ± 28.9 %) showed close to normal HA expression approximately three months after injury ($F_{5, 17}$ = 10.18; p=1; Figure 5.3B-E). However, chronic PNNi administration in unlesioned (29.8 ± 6.1 %) and injured animals (27.6 ± 4.4 %) displayed decreased levels of HA in the VH compared to sham control intensities (100 ± 16.9 %; p<0.01 for both; Figure 5.3B, F-G) and both vehicle treatments (p<0.05 for both; Figure 5.3B). Although

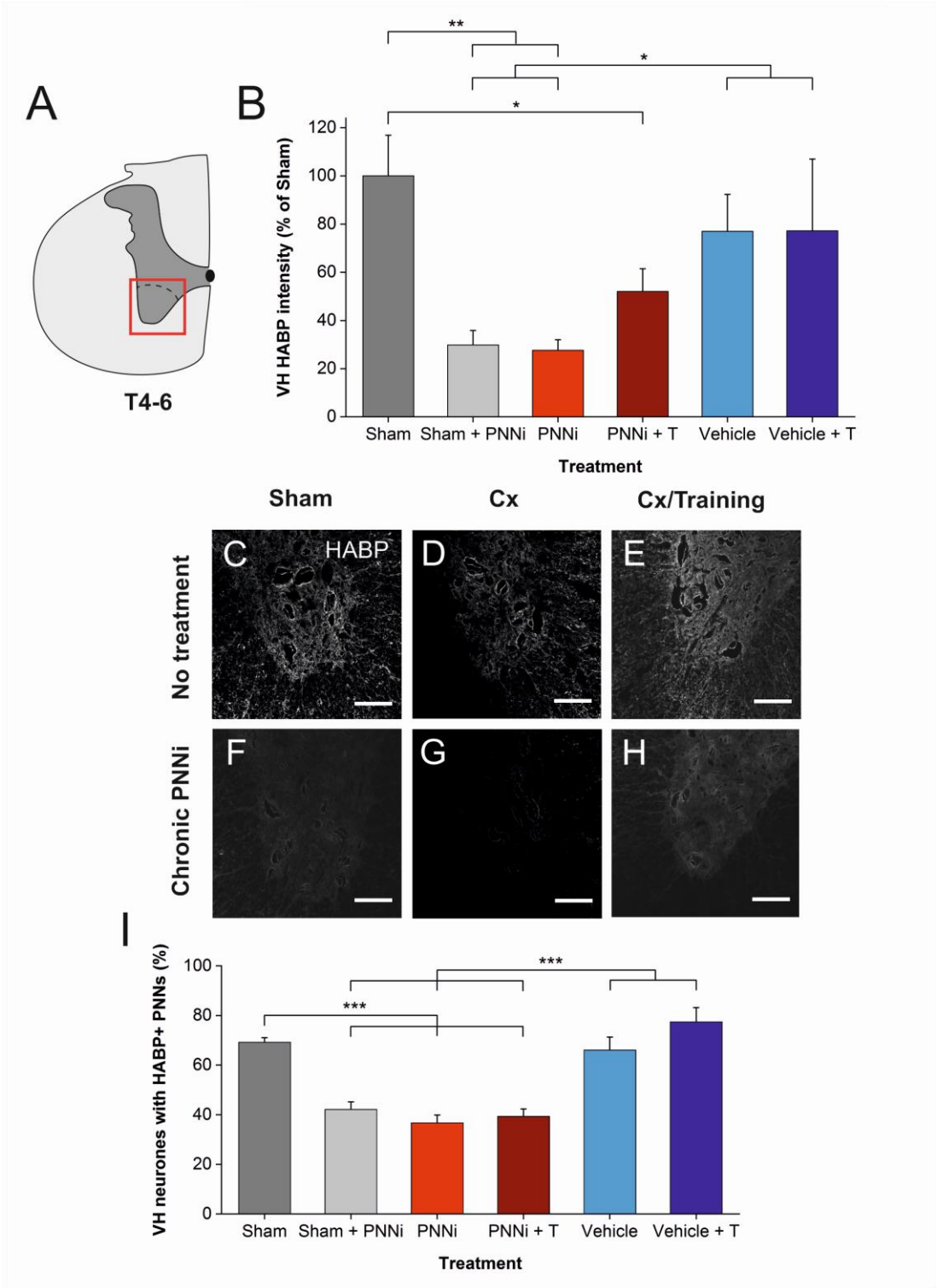

Figure 5.3: Chronic PNNi treatment reduced expression of hyaluronan binding protein (HABP) in the ventral horn (VH) ECM.

A) Rat spinal cord sections (T4-6) obtained at 12 weeks post-injury were stained and intensity was analysed in the VH (denoted by red box). **B)** HABP intensity (visualised using Alexa fluor 488) in the VH appears to decrease in animals treated with PNNi. *Error bars ± SD; n=3 per treatment group. Statistics one-way ANOVA;*

*significance levels: * p<0.05 ** p<0.01 *** p<0.001.* Confocal images showing HABP expression is unchanged with injury **(C-E).** Whereas, PNNi treated sham **(F)** and injured animals **(G)** show global HABP reduction in the VH. When combined with training, HABP levels seem to recover from PNNi treatment **(H).** *Scale bars, 100 µm.* **I)** PNNi decreases number of HABP-positive PNNs. *For all graphs, error bars ± SD; n=3 per treatment group. Statistics one-way ANOVA; significance levels: * p<0.05 ** p<0.01 *** p<0.001.*

combination treatment of training and PNNi expressed only 52.1 ± 9.4 % of normal levels of HA (sham p<0.05), a partial recovery of HA was observed in the VH, with levels comparable to vehicle and training control animals. Notably, whilst HABP decreased throughout the ECM, some PNNs appear to still be present, consistent with the results above. However, whilst PNNs are present, these do appear to have an attenuated intensity (Figure 5.3C-H). PNNi significantly decreased the number of HABP-positive PNNs compared to untreated animals by approximately 40 % ($F_{5, 17}$ = 61.6; p<0.001; Figure 5.3I).

5.3.1.2: Chronic PNNi treatment and contusive SCI reduce expression of key PNN components in the sensorimotor cortex

The sensorimotor cortex is known to be susceptible to structural plasticity in response to neuronal injury or task-specific training. The following looks to, firstly, investigate the effect of neuronal injury and rehabilitative training on the expression of PNN components to determine whether they contribute to the associated plastic changes. Secondly, the following looks to determine whether systemic PNNi administration extends its effects to the sensorimotor cortex.

5.3.1.2.1: WFA binding is reduced in the sensorimotor cortex after injury and PNNi treatment

WFA-positive PNNs were mostly localised to layers II –VI of the rat sensorimotor cortex (Figure 5.4C), similar to that observed in other studies (Orlando and Raineteau

2015; Ueno *et al.* 2017; Quattromani *et al.* 2018; Ueno *et al.* 2019). WFA binding shows robust expression throughout the cortical layers with strong PNN staining (Figure 5.4A-C). After Cx injury, WFA binding dramatically decreases to 39.7 ± 8.64 % of the normal expression in the cortical ECM, which is unchanged by rehabilitation treatment (51.7 ± 21.4 %; $F_{5, 17} = 8.41$, $p<0.01$ for Vehicle and $p<0.05$ for Vehicle + T; Figure 5.4B-E). Chronic PNNi treatment to unlesioned animals revealed a similar decrease in cortical WFA levels, to 43.1 ± 11.0 % of sham control ($p<0.05$; Figure 5.4B-C, F). The downregulating effects of SCI and PNNi administration do not appear to be additive, as a parallel decrease in WFA expression was observed with PNNi treatment of injured animals (46.2 ± 15.3 %; $p<0.05$; Figure 5.4B, G). The biggest decrease of WFA binding in the sensorimotor cortex was found with combination treatment (23.0 ± 3.82 %; $p<0.001$; Figure 5.4B, H). WFA-positive PNNs remained present in all samples, despite reduced WFA intensity after injury and PNNi treatment, although did appear attenuated, particularly after combination treatment (Figure 5.4C-H). This suggests that rehabilitative training is capable of inducing further plastic changes in response to injury, only in the presence of the plasticity enhancing drug, PNNi.

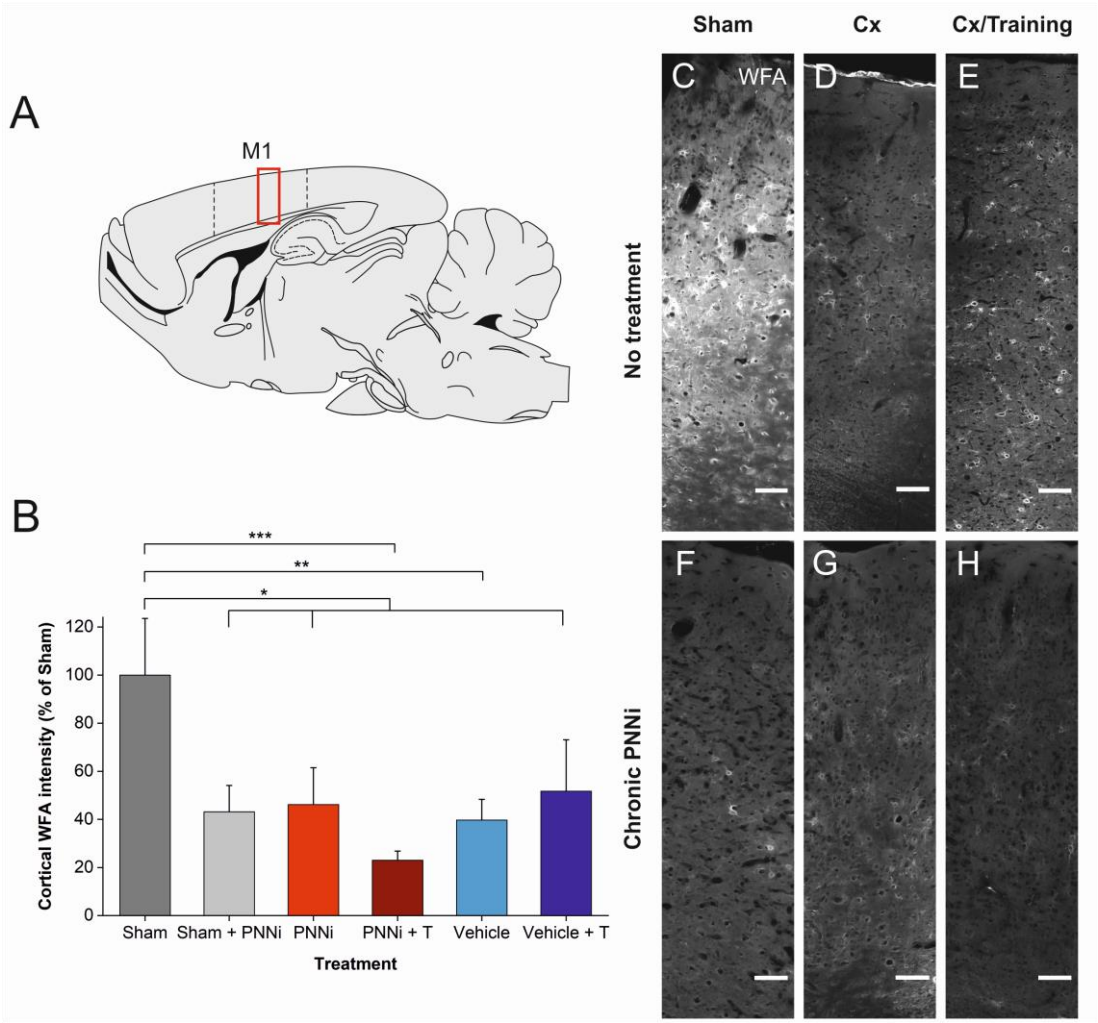

Figure 5.4: Chronic PNNi treatment and mid-thoracic contusion (Cx) injury independently reduce expression of perineuronal nets (PNNs) labelled by *Wisteria floribunda* agglutinin (WFA) in the sensorimotor cortex.

A) Rat brain sections obtained at 12 weeks post-injury were stained and a 400 x 1500 µm area from the M1 sensorimotor cortex was imaged (denoted by red box). **B)** Cortical WFA intensity (visualised using Alexa fluor 488) decreased with PNNi treatment and with Cx injury. *Error bars ± SD; n=3 per treatment group. Statistics one-way ANOVA; significance levels: * p<0.05 ** p<0.01 *** p<0.001.* Confocal images showing strong PNN expression in Sham animals **(C)**, in contrast to Vehicle **(D)**, Vehicle + T **(E)**, Sham + PNNi **(F)**, PNNi **(G)**, and PNNi + T **(H)** treatment groups. *Scale bars, 100 µm.*

5.3.1.2.2: Cortical ACAN expression is downregulated in response to injury and PNNi administration

Similar to WFA, ACAN was observed throughout layers II – VI, labelling PNNs, as observed in the literature (McRae *et al.* 2007; Madinier *et al.* 2014; Ueno *et al.* 2017). Parallel to the trend displayed by cortical WFA binding, Cx injury induced downregulation of ACAN in the sensorimotor cortex (37.8 ± 7.52 %; $F_{5, 17}$ = 6.56; $p<0.05$; Figure 5.5A-D). However, unlike above, treadmill training appeared to have upregulated cortical ACAN expression after injury (56.2 ± 14.5 %;), as it was no longer significantly different from sham animals (100 ± 24.9 %; p= 0.17; Figure 5.5B-E). PNNi administration to sham animals, again, mirrored WFA binding patterns, with a decrease in ACAN levels to 41.9 ± 6.42 % of normal expression ($p<0.05$; Figure 5.5 B, F). However, when PNNi treatment alone (31.3 ± 30.1 %) and in combination with training (28.7 ± 10.6 %) were given to injured animals, ACAN levels decreased further, relative to sham control (Figure 5.5G-H). This was suggestive of a slight additive effect of neuronal injury and PNNi administration on downregulation of ACAN in the sensorimotor cortex, resulting in further enhancement of plasticity.

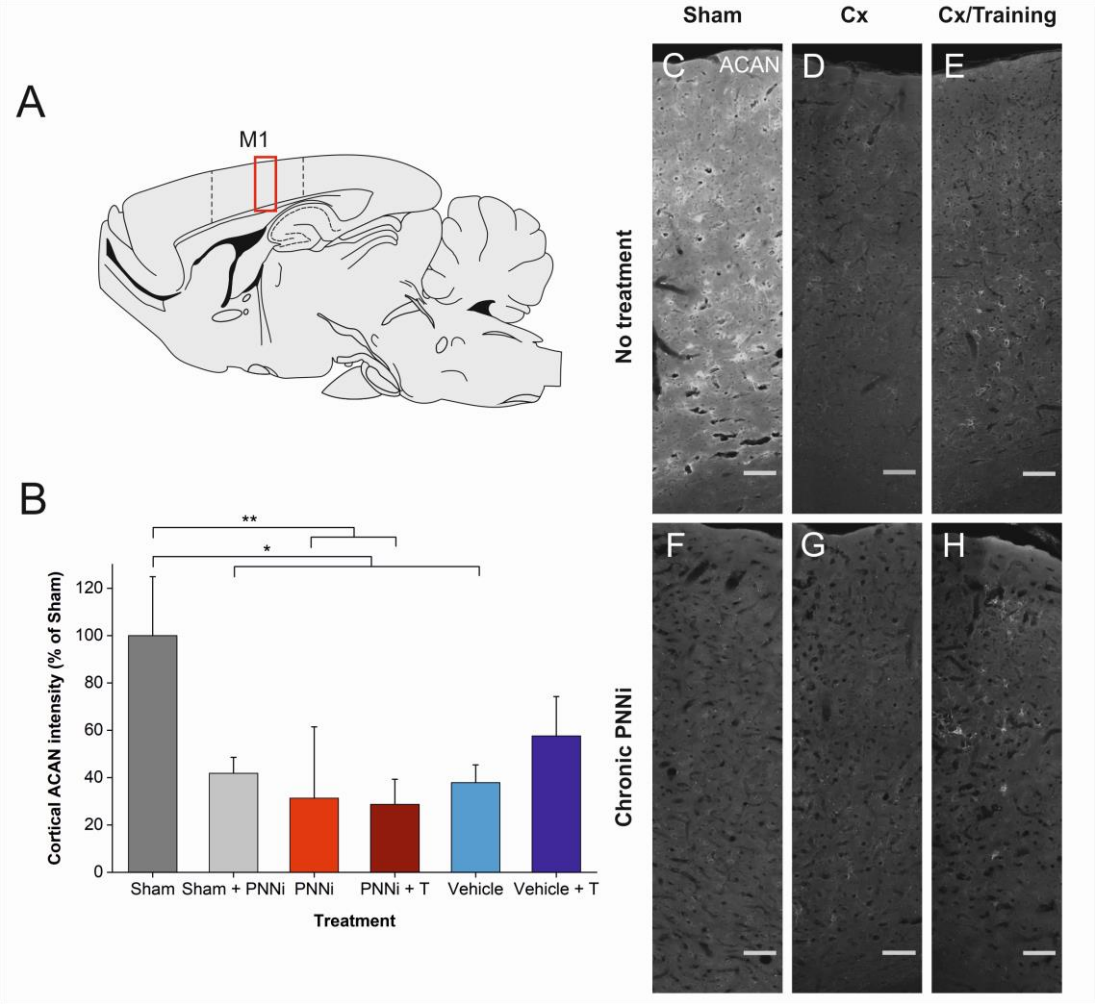

Figure 5.5: Chronic PNNi treatment and mid-thoracic contusion (Cx) spinal cord injury independently reduce expression of perineuronal nets (PNNs) labelled by aggrecan (ACAN) in the sensorimotor cortex.

A) Rat brain sections obtained at 12 weeks post-injury were stained and a 400 x 1500 µm area from the M1 sensorimotor cortex was imaged (denoted by red box). **B)** Cortical ACAN intensity (visualised using Alexa fluor 568) decreased with PNNi treatment and with Cx injury. *Error bars ± SD; n=3 per treatment group. Statistics one-way ANOVA; significance levels: * p<0.05 ** p<0.01 *** p<0.001.* Confocal images showing strong PNN expression in Sham animals **(C)**, in contrast to Cx injured animals with Vehicle treatment **(D)**. This was partially recovered with rehabilitation in Vehicle + T animals **(E)**. Chronic PNNi treated groups: Sham + PNNi **(F)**, PNNi **(G)**, and PNNi + T **(H)** also display decreased ACAN expression. *Scale bars, 100 µm.*

5.3.1.2.3: HA expression in the sensorimotor cortex is relatively unchanged with neuronal injury or PNNi administration

As a ubiquitous glycan, HABP labelling illustrated expression throughout the cortical ECM, as well as forming a ring-like halo around NeuN-positive cells, characteristic of PNNs. Whilst CSPG content, as revealed by WFA and ACAN staining, was downregulated in response to mid-thoracic Cx injury, as illustrated above, HA content remains unchanged (89.6 ± 9.68 %), even with rehabilitative training (101.6 ± 18.2 %; $F_{5, 17}$ = 2.70; p=1; Figure 5.6A-E). Additionally, PNNi administration, whilst there may appear to be slight decreases in HA expression, does not show a significant difference with that of normal expression, in either lesioned (72.0 ± 10.7 %; p=1) or unlesioned animals (64.0 ± 32.0 %; p= 0.55; Figure 5.6B, F-G). However, combination training also does not confer additional effects on HA expression (61.9 ± 13.5 %; p= 0.43; Figure 5.6B, H). These results indicate that PNNi has a minimal effect on expression of HA in the sensorimotor cortex, suggesting that PNNi preferentially downregulates HA in the spinal cord.

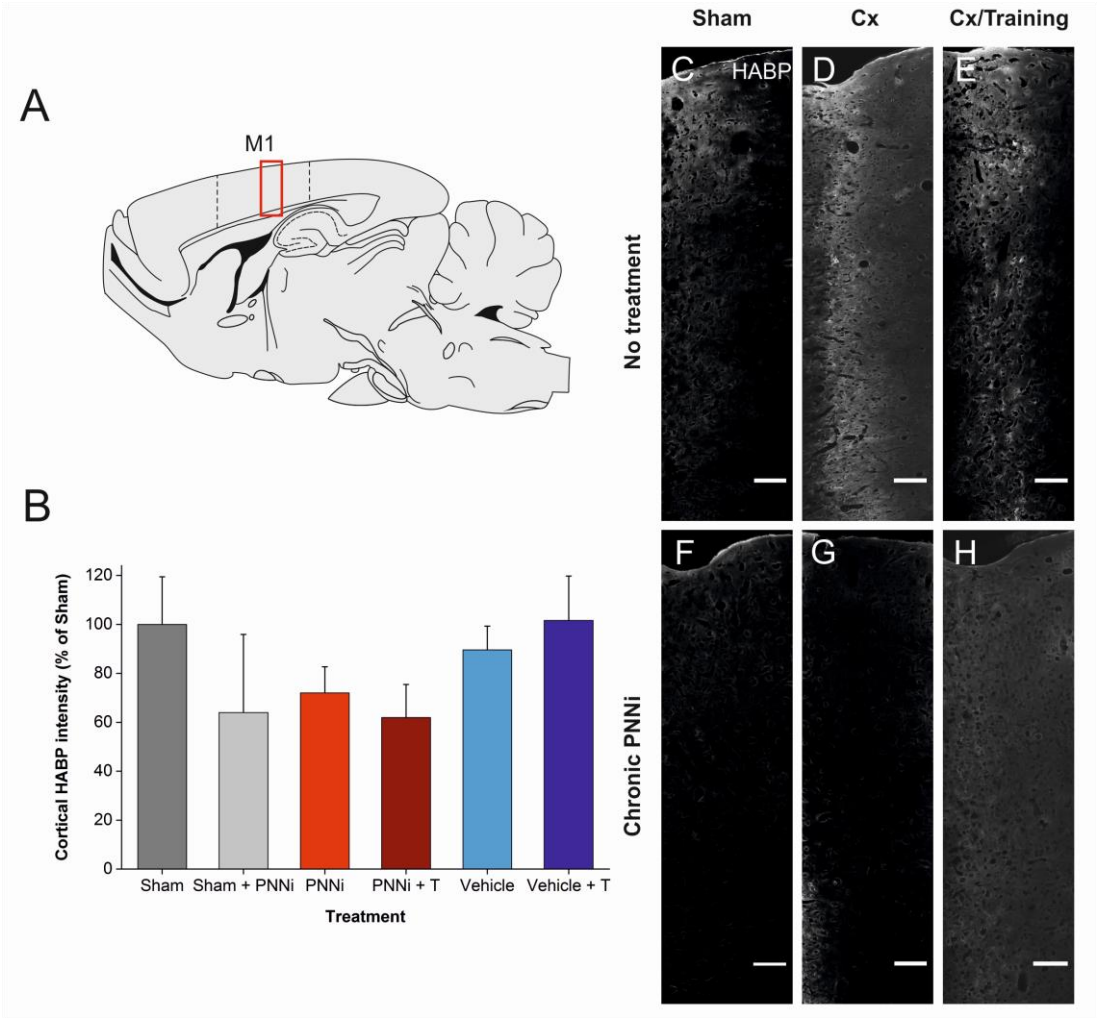

Figure 5.6: Chronic PNNi treatment does not appear to downregulate expression of hyaluronan (HA), labelled by hyaluronan binding protein (HABP) in the sensorimotor cortex.

A) Rat brain sections obtained at 12 weeks post-injury were stained and a 400 x 1500 µm area from the M1 sensorimotor cortex was imaged (denoted by red box). **B)** Cortical HABP intensity (visualised using Alexa fluor 488) showed minor but not significant decreases with PNNi treatment and not with Cx injury. *Error bars ± SD; n=3 per treatment group. Statistics one-way ANOVA; significance levels: * p<0.05 ** p<0.01 *** p<0.001.* Confocal images showing strong HA expression in the ECM and also some PNN structure in Sham animals **(C)**. This is unchanged with Cx injured animals with Vehicle treatment **(D)**, as well as with rehabilitation in Vehicle + T animals **(E)**. Chronic PNNi treated groups: Sham + PNNi **(F)**, PNNi **(G)**, and PNNi + T **(H)** also display minimal if any differences in HA expression. *Scale bars, 100 µm.*

5.3.2: Investigating functional reorganisation of the motor cortex as a measure of corticospinal (CST) connections

To compare changes to the functional reorganisation of the cortical motor map with injury and plasticity enhancing therapies, a baseline representation for adult Lister Hooded rats was generated. ICMS mapping of the right sensorimotor cortex (revealed by an approximately 10 x 5 mm craniotomy; illustrated in Figure 5.7A, Figure 5.8A and Figure 5.9A) in the intact adult rat successfully elicited movements that could be classified into three main categories: HL, FL and facial (F) movements. In some areas, stimulation elicited more than one type of movement but for clarity the following figures each illustrate a single type of movement and the corresponding heat maps denote the percentage of animals at each location stimulated for which the movement was evoked. Trunk movement was almost never elicited and when it occurred often denoted a grounding issue to be corrected. Minimum and mean cortical stimulation thresholds showed no difference between treatment groups (Table 5.1). However, groups receiving training did appear to show a trend of increased minimum stimulation thresholds for FL, suggesting a shift in the inhibitory-excitatory balance as a higher level of excitatory current was required to evoke movements. Many of the following ICMS plots will be qualitatively assessed due to ongoing statistical analysis looking to quantify the change in location and area of the various representations.

5.3.2.1: Disruption of cortical control of HL movements post-injury.

In the intact female adult Lister Hooded rat, HL movements were successfully evoked within a concise area immediately caudal to bregma and approximately 1 mm to 3.5 mm lateral to midline (Figure 5.7B). HL movements generally encompassed flexion of the major leg joints or digits. The HL representation was mostly conserved after sham surgeries, although with a decrease in area was observed with PNNi treatment, from 9.77 ± 1.74 mm^2 to 3.64 ± 1.26 mm^2 ($F_{8, 36}$ = 37.5; $p<0.001$; Figure 5.7C,

Table 5.1: Average cortical stimulation thresholds to elicit hindlimb (HL), forelimb (FL) or facial (F) movements.

Measurements for minimum (min) and mean cortical thresholds were recorded from intracortical microstimulation experiments performed on each group at 9 weeks or 15 weeks (for 8 week (wk) PNNi and 8 week PNNi + T treatment groups only). Where dashes are shown, the movement was unable to be elicited. *For groups, Intact n=4, Sham n=4, Vehicle n=4, Vehicle + Training n=4, Sham + PNNi n=5, PNNi n=4, PNNi + Training n=5, 8 week PNNi n=3 and 8 week PNNi + T n=3.*

	Cortical stimulation thresholds (µA)								
	Intact	**Sham**	**Sham + PNNi**	**PNNi**	**PNNi + T**	**Vehicle**	**Vehicle + T**	**8 wk PNNi**	**8 wk PNNi + T**
Min HL	5.25 ± 2.22	7.60 ± 1.52	6.00 ± 2.00	-	-	-	-	-	-
Mean HL	16.8 ± 1.13	16.1 ± 1.67	15.8 ± 2.08	-	-	-	-	-	-
Min FL	4.00 ± 2.58	6.80 ± 1.64	5.60 ± 1.52	7.38 ± 1.11	7.50 ± 0.74	7.30 ± 2.28	8.10 ± 1.43	5.33 ± 0.58	6.00 ± 1.73
Mean FL	16.32 ± 1.61	16.13 ± 1.08	14.85 ± 1.72	19.32 ± 4.74	16.72 ± 1.70	18.28 ± 8.00	17.53 ± 2.48	12.46 ± 1.32	12.67 ± 0.43
Min F	5.25 ± 1.71	6.60 ± 2.07	6.20 ± 1.30	7.00 ± 2.94	15.4 ± 13.8	6.70 ± 0.45	10.6 ± 4.51	6.00 ± 1.00	5.33 ± 1.15
Mean F	17.0 ± 0.91	17.3 ± 1.02	15.3 ± 1.82	17.9 ± 2.60	21.4 ± 10.7	15.1 ± 1.74	19.9 ± 4.61	12.8 ± 0.89	13.1 ± 0.84

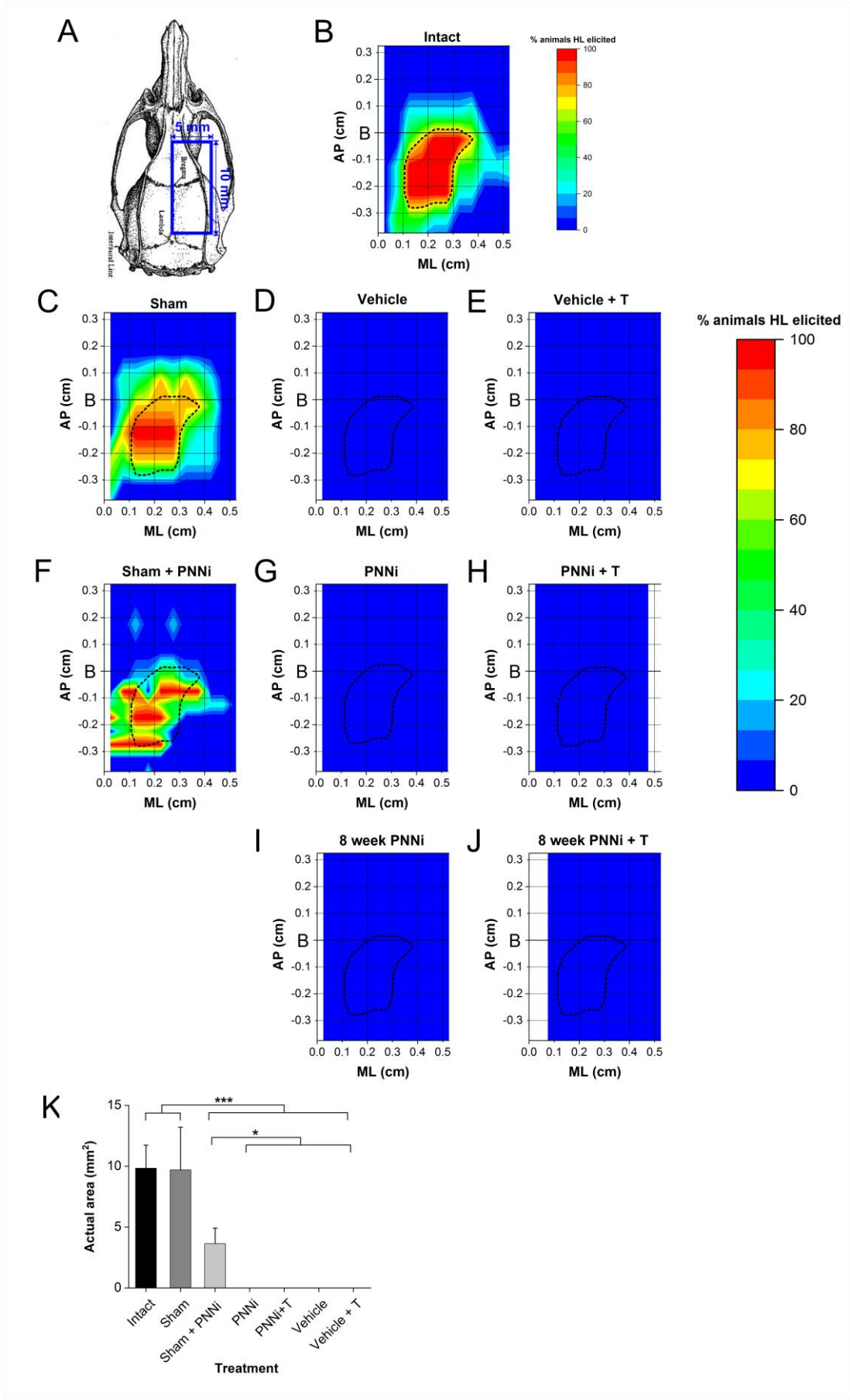
A
5 mm
10 mm
Bregma
Lambda
Intact
% animals HL elicited
B
AP (cm)
ML (cm)
C
Sham
D
Vehicle
E
Vehicle + T
F
Sham + PNNi
G
PNNi
H
PNNi + T
I
8 week PNNi
J
8 week PNNi + T
K
Actual area (mm²)
Intact
Sham
Sham + PNNi
PNNi
PNNi+T
Vehicle
Vehicle + T
Treatment
***
*

Figure 5.7: Disruption of cortical control of hindlimb (HL) movements post-injury.

Intracortical microstimulation (ICMS) was performed at stereotaxic coordinates within a craniotomy 5 mm above and below bregma (labelled B on each scale) on the right hemisphere **(A)** approximately 11 weeks **(C-H)** or 15 weeks **(I-J)** after a mid-thoracic moderate contusion injury. Individual ICMS maps were combined to give the representative heat maps for each group showing the percentage of animals for each stereotaxic coordinate where HL movements were able to be elicited. A baseline HL cortical map was generated for Lister Hooded rats (**B**; with dotted outline in **C-J**) to compare the functional plasticity of groups with no treatment **(C-E)**, chronic PNNi administration **(F-H)** and 8-week PNNi treatment **(I-J)**. HL movements were unable to be elicited after spinal cord injury. **K)** Average area (mm^2) of the HL representation for each treatment group. *Error bars ± SD. Statistics one-way ANOVA; significance levels: * p<0.05 ** p<0.01 *** p<0.001. For groups, Intact **(B)** n=4, Sham **(C)** n=4, Vehicle **(D)** n=4, Vehicle + Training **(E)** n=4, Sham + PNNi **(F)** n=5, PNNi **(G)** n=4, PNNi + Training **(H)** n=5, 8 week PNNi **(I)** n=3 and 8 week PNNi + T **(J)** n=3.*

F and K). This variation between animals was amplified with the addition of PNNi administration (Figure 5.7F). After a mid-thoracic Cx injury, HL movements were unable to be elicited upon stimulation (Figure 5.7D). No single or combination treatment were able to recovery cortical stimulation of HL movements (Figure 5.7E, G-J), despite behavioural results showing recovery of walking.

5.3.2.2: FL shifts into HL area of motor cortex after Cx injury

FL movements were elicited from an area rostral to bregma and 2 mm to 5 mm lateral to midline in the intact Lister Hooded rat and, as denoted in black and white dashed lines, formed a border with the HL motor representation (Figure 5.8B). FL flexion of the shoulder, bicep, wrist and digits were the most commonly evoked FL movements. In sham animals, this representation was mostly conserved, however, displayed a slight shift towards the midline (Figure 5.8C). Approximately, 30-50% of intact animals also were able to have FL movements evoked in this region. When sham animals were given a plasticity enhancing drug (PNNi), variability of FL response increased

(Figure 5.8F). However, the main site of FL representation (red) remained the same albeit reduced in size, from approximately 4.82 mm^2 with sham and intact animals to 3.88 mm^2 with Sham + PNNi. Additionally, an isolated area 1 to 3 mm caudal to bregma, previously representing HL (black lines), elicited FL movement, suggesting heightened cortical plasticity in comparison to sham control. With mid-thoracic Cx injury, the core FL representation decreased in size (from 4.82 mm^2 with sham and intact animals to 4.08 mm^2 for vehicle treatment) and the FL area shifted rostrally into the HL representation (Figure 5.8D). PNNi-induced cortical plasticity (chronic PNNi), as demonstrated with Sham + PNNi animals, did not appear to considerably alter or further enhance injury-induced plasticity, as indicated by the similar shift observed with PNNi and Vehicle animals (Figure 5.8D, G).

Rehabilitative training, in contrast, showed further expansion of the FL area into that of the HL (Figure 5.8E). Animals receiving training showed better defined stimulation sites, suggesting that task-specific rehabilitative training enhances injury-induced cortical plasticity, driving remodelling of the map in the same way. Animals receiving both PNNi and training showed similar changes, again with all animals in the group eliciting FL movements in the same new rostral stimulation sites (Figure 5.8H). The FL area appeared even further remodelled with combination treatment and had shifted medially by approximately 1 mm compared to intact animals. Additionally, combination treatment also appeared to elicit FL movements in the barrel cortex (approximately 1 to 4 mm rostral to bregma, 4 to 5 mm medial to midline).

When PNNi was given for only 8 weeks (limited PNNi paradigm), FL movements were evoked in most of the area stimulated rostral to bregma area (1 to 5 mm lateral to midline; Figure 5.8I). This area extended continuously along the lateral edge of the craniotomy (Figure 5.8A) to elicit FL movements in the barrel cortex, similarly to PNNi + T and also encompassed much of the area lateral to the HL representation. 8-week

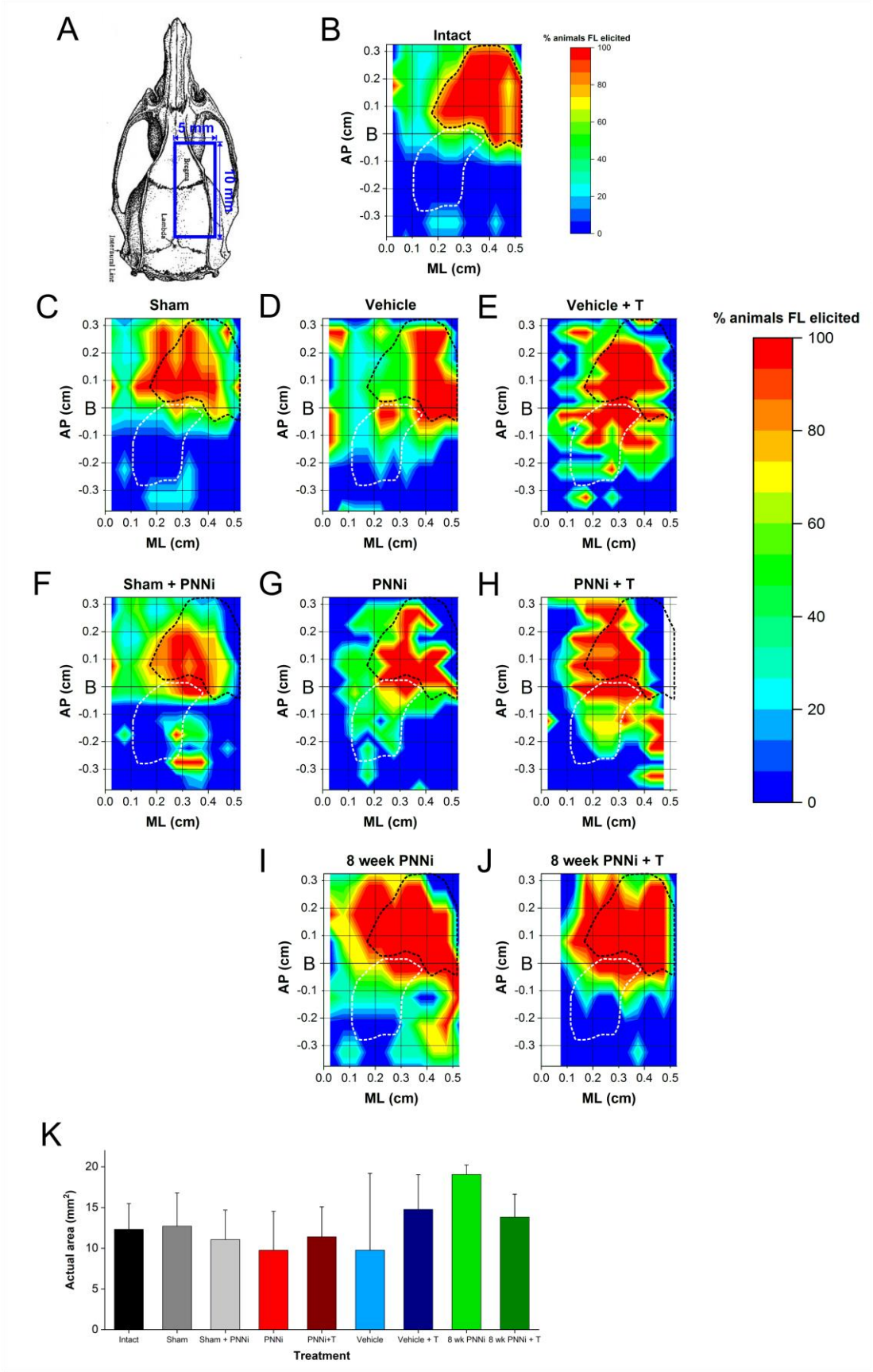
A
5 mm
10 mm
Bregma
Lambda
Interparietal Line
B
Intact
% animals FL elicited
100
80
60
40
20
0
AP (cm)
ML (cm)
C
Sham
D
Vehicle
E
Vehicle + T
F
Sham + PNNi
G
PNNi
H
PNNi + T
I
8 week PNNi
J
8 week PNNi + T
K
Actual area (mm²)
Intact
Sham
Sham + PNNi
PNNi
PNNi+T
Vehicle
Vehicle + T
8 wk PNNi
8 wk PNNi + T
Treatment

Figure 5.8: Forelimb (FL) shifts into hindlimb (HL) area of motor cortex after injury.

Intracortical microstimulation (ICMS) was performed at stereotaxic coordinates within a craniotomy 5 mm above and below bregma (labelled B on each scale) on the right hemisphere **(A)** approximately 11 weeks **(C-H)** or 15 weeks **(I-J)** after a mid-thoracic moderate contusion injury. Individual ICMS maps were combined to give the representative heat maps for each group showing the percentage of animals for each stereotaxic coordinate where FL movements were able to be elicited. A baseline FL cortical map was generated for Lister Hooded rats (**B**; black dotted outline in **C-J**) to compare the functional plasticity of groups with no treatment **(C-E)**, chronic PNNi administration **(F-H)** and 8-week PNNi treatment **(I-J)**. After spinal cord injury, FL movements were elicited in areas that previously elicited HL movements (baseline HL map shown in white dotted outline **B-J**). **K)** Average area (mm^2) of the FL representation for each treatment group. *Error bars ± SD. Statistics one-way ANOVA; significance levels: * p<0.05 ** p<0.01 *** p<0.001. For groups, Intact **(B)** n=4, Sham **(C)** n=4, Vehicle **(D)** n=4, Vehicle + Training **(E)** n=4, Sham + PNNi **(F)** n=5, PNNi **(G)** n=4, PNNi + Training **(H)** n=5, 8 week PNNi **(I)** n=3 and 8 week PNNi + T **(J)** n=3.*

PNNi treatment displayed a trend of increased FL area (Figure 5.8K). In comparison to vehicle (9.76 ± 9.43 mm^2) and PNNi (9.75 ± 4.78 mm^2), the average area of FL representation for 8-week PNNi was 19.07 ± 1.15 mm^2. Like all injured groups, FL shifted into the HL area, however, this was considerably less pronounced. The well-defined appearance of this map suggests that a restricted PNNi treatment window permitted consolidation of new connections.

The combination of 8-week PNNi administration and sustained rehabilitative training produced minimal remodelling in comparison to intact animals (Figure 5.8I). However, the FL representation expanded to encompass the rostral to bregma area and displays slight extension into the HL area, alluding to the trend observed with mid-thoracic Cx injury.

5.3.2.3: Facial representation in sensorimotor cortex expands after Cx injury

Whisker twitching as well as jaw and eye were evoked predominantly in the barrel cortex (caudal to bregma, 3.5 to 5 mm lateral to midline) and in the rostral area immediately lateral to midline in intact animals (Figure 5.9B). Sham surgeries caused both of these sites to expand, with the rostral site expanding laterally and the caudal barrel cortex expanding medially (Figure 5.9C). PNNi treatment did not change this remodelling of the F representation in sham animals considerably, although it did appear to increase variability between animals (Figure 5.9F). Injury on the other hand induced wide scale remodelling with F movements evoked virtually across the entire stimulation area tested and encroached into the HL representation (white lines; Figure 5.9D). In parallel, PNN removal in Cx animals displayed widespread F representation including the HL area, however, these were located in discrete pockets and were less variable between animals (Figure 5.9G).

Rehabilitation after injury caused remodelling similar to sham animals (Figure 5.9E), suggesting that the adaptive plasticity induced by treadmill training shapes the reorganisation in a way similar to intact animals. PNNi and locomotor training, in stark contrast, evoked very little F movements throughout all of the area tested (0.48 ± 0.50 mm^2; Figure 5.9H), showing a reduction in total average area compared to the sham control (10.9 ± 2.93 mm^2; $F_{8, 35} = 8.15$; $p<0.05$; Figure 5.9K). Both Vehicle + Training (1.49 ± 1.72 mm^2) and PNNi + Training (0.48 ± 0.50 mm^2) treatment groups displayed a reduction in the average size of the rostral F representation in comparison to 8.35 ± 3.29 mm^2 in injured control animals, from ($F_{6, 29} = 4.68$; $p<0.05$ for Vehicle + Training; $p<0.01$ for PNNi + Training; Figure 5.9L).

8 week limited PNNi treatment caused overall expansion of the average F area in comparison to all chronic treatment groups and control animals ($F_{8, 35} = 8.15$; $p<0.05$; Figure 5.9I, K). When continued rehabilitative training was applied to this paradigm,

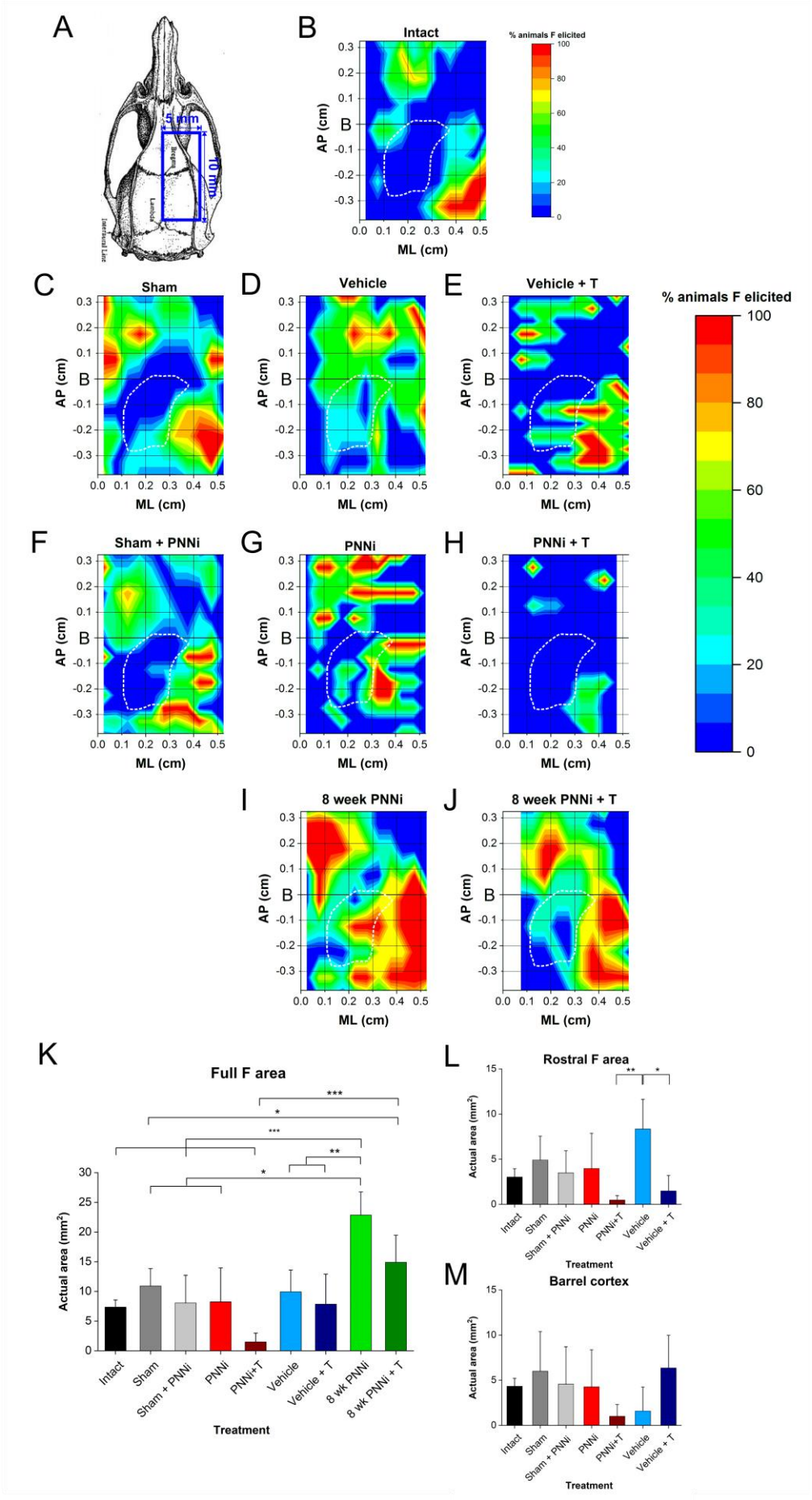
A
5 mm
10 mm
Bregma
Lambda
B
Intact
% animals F elicited
AP (cm)
ML (cm)
C
Sham
D
Vehicle
E
Vehicle + T
F
Sham + PNNi
G
PNNi
H
PNNi + T
I
8 week PNNi
J
8 week PNNi + T
K
Full F area
Actual area (mm²)
Intact
Sham
Sham + PNNi
PNNi
PNNi+T
Vehicle
Vehicle + T
8 wk PNNi
8 wk PNNi + T
Treatment
L
Rostral F area
M
Barrel cortex

Figure 5.9: Facial (F) cortical area expands with contusion (Cx) injury.
Intracortical microstimulation (ICMS) was performed at stereotaxic coordinates within a craniotomy 5 mm above and below bregma (labelled B on each scale) on the right hemisphere **(A)** approximately 11 weeks **(C-H)** or 15 weeks **(I-J)** after a mid-thoracic moderate Cx injury. Individual ICMS maps were combined to give the representative heat maps for each group showing the percentage of animals for each stereotaxic coordinate where F movements were able to be elicited. A baseline F cortical map was generated for Lister Hooded rats **(B)** to compare the functional plasticity of groups with no treatment **(C-E)**, chronic PNNi administration **(F-H)** and 8-week PNNi treatment **(I-J)**. After Cx injury, the F cortical map extended to regions all over the area mapped **(D & G)**, including the former hindlimb (HL) representation (baseline HL map shown in white dotted outline **B-J**). Average F area (mm^2) for the full stimulation area **(K)**, rostral F representation **(L)** and for the barrel cortex **(M)** for all treatment groups. *Error bars ± SD. Statistics one-way ANOVA; significance levels: * p<0.05 ** p<0.01 *** p<0.001. For groups, Intact **(B)** n=4, Sham **(C)** n=4, Vehicle **(D)** n=4, Vehicle + Training **(E)** n=4, Sham + PNNi **(F)** n=5, PNNi **(G)** n=4, PNNi + Training **(H)** n=5, 8 week PNNi **(I)** n=3 and 8 week PNNi + T **(J)** n=3.*

the areas reduced but still showed a slightly expanded and defined F representation at the barrel cortex (Figure 5.9J). Interestingly, the 8 week PNNi + Training paradigm (14.9 ± 1.49 mm^2) showed increased total average F area, in contrast to 1.49 ± 1.49 mm^2, with chronic PNNi + T treated animals ($F_{8, 35}$ = 8.15; p<0.01; Figure 5.9K), suggesting further remapping driven by rehabilitation after the recovery of PNNs. Breakdown of the rostral and barrel cortex was no longer possible as both the rostral F area and barrel cortex appeared to expand towards each other into the HL representation (white lines) for both 8 week PNNi groups and showed large areas where F movements were evoked by all animals within these groups (Figure 5.9I-J).

5.3.3: Shifts in excitatory – inhibitory balance rostral to Cx injury

In the CNS, control over neuronal circuits is maintained by the balance of excitatory and inhibitory neurotransmission, primarily mediated by glutamate and GABA/glycine release, respectively. After SCI, death of neurones in both intraspinal circuitry and

modulating tracts leads to dysregulation of this balance both rostral and caudal to the lesion site (Berrocal *et al.* 2014). Similarly, PNN removal has also been shown to dysregulate this balance (Lensjo *et al.* 2017). The following looks to explore the excitatory-inhibitory balance in the spinal levels where the effects of PNNi have been illustrated, above.

5.3.3.1: PNNi and injury-associated increases in excitatory intraspinal connections are pruned with rehabilitative training

Glutamate is the most abundant neurotransmitter in the CNS, conferring powerful and excitatory synaptic transmission (Fonnum 1984). Identification of glutamatergic synaptic terminals using vesicular glutamate transporter 2 (VGLUT2) (Takamori *et al.* 2001) primarily labels intraspinal connections in the spinal cord (Oliveira *et al.* 2003; Todd *et al.* 2003; Alvarez *et al.* 2004; Landry *et al.* 2004; Persson *et al.* 2006). Expression of VGLUT2 was found to be distributed across the whole of gray matter in the cord, including an abundant presence in the VH, similar to results in other studies (Varoqui *et al.* 2002; Oliveira *et al.* 2003; Todd *et al.* 2003; Alvarez *et al.* 2004; Herzog *et al.* 2004; Persson *et al.* 2006). Cx injury considerably increased excitatory VGLUT2-positive connections (171.2 ± 1.53 %), and with rehabilitative training this decreased to normal levels (109.6 ± 21.0 %; $F_{5, 17}$ = 11.86; Figure 5.10A-E). PNNi treatment to unlesioned animals independently induced increases in VGLUT2-positive connections in the VH to 155.9 ± 16.4 % ($p<0.05$; Figure 5.11B, F), suggesting plastic changes to the intraspinal circuitry. The plastic effect of PNNi appeared to be additive in an injured environment, as further elevation of VGLUT2 connectivity in the VH was observed, with combination treatment inducing a partial reduction relative to normal expression ($p<0.05$; Figure 5.10B, H). This may be indicative of pruning of the new connections to functional connections following rehabilitative training.

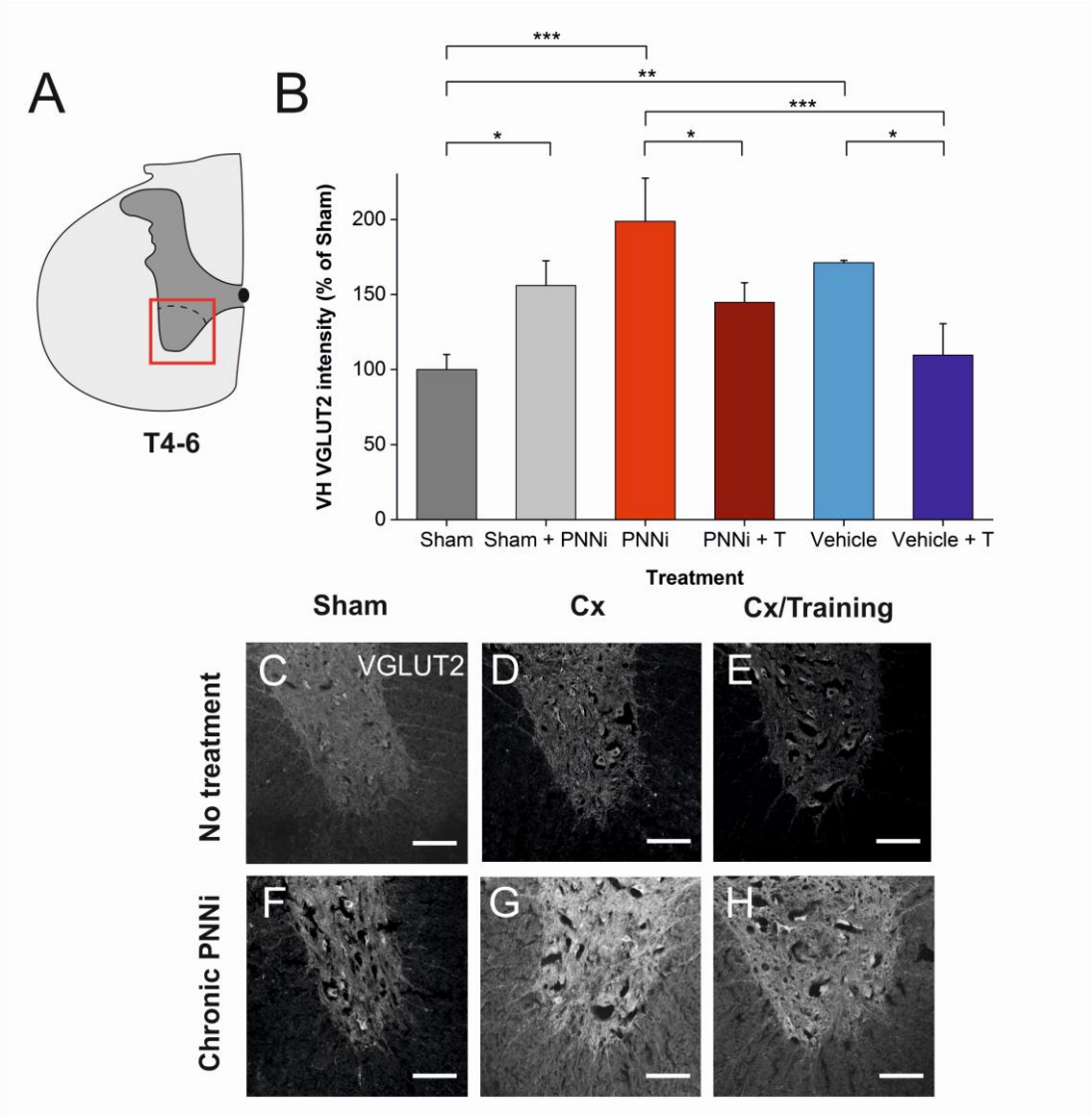

Figure 5.10: **PNNi treatment and injury increased excitatory connections in the ventral horn (VH), labelled by vesicular glutamate transporter 2 (VGLUT2), decreased with rehabilitative training, rostral to a mid-thoracic contusive (Cx) injury.**

A) Rat spinal cord sections (T4-6) obtained at 12 weeks post-injury were stained and intensity was analysed in the VH (denoted by red box). **B)** VGLUT2 intensity (visualised using Alexa fluor 568) in the VH increased with PNNi and after Cx injury. Rehabilitative training reduced VGLUT2 intensity. *Error bars ± SD; n=3 per treatment group. Statistics one-way ANOVA; significance levels: * p<0.05 ** p<0.01 *** p<0.001.* Confocal images showing VGLUT2 expression appeared to increase with injury and PNNi treatment, but is reduced with training **(C-E).** Chronic PNNi treatment induced increased VGLUT2 expression in sham **(F)** and greatly increased in Cx injured animals **(G)**. PNNi + T **(H)** combination decreased VGLUT2 expression in the VH. *Scale bars, 100 µm.*

5.3.3.2: GABAergic connections increase in the VH with combination treatment post-Cx injury

Gamma-aminobutyric acid (GABA) is a major inhibitory transmitter in the mature CNS, principally regulating neuronal excitability (Roberts 1975). GABA is synthesised by the enzyme, glutamate decarboxylase (GAD), that is found in two isoforms in the synaptic terminal and the cell body (Erlander *et al.* 1991). These are differentially expressed throughout the spinal cord laminae (Mackie *et al.* 2003). The following therefore uses an antibody labelling both GAD65 and 67 isoforms to identify inhibitory synaptic boutons in the spinal cord. Rostral to the lesion site, the normal expression of GABAergic boutons did not appear to be altered after mid-thoracic Cx injury (111.8 ± 18.9 %), even with the addition of rehabilitation (108.4 ± 21.9 %; $F_{5, 17} = 6.22$; p=1; Figure 5.11A-E). Enhancement of plastic capabilities with addition of PNNi to lesioned (77.9 ± 9.27 %) or unlesioned (69.3 ± 36.3 %) animals also did not appear to significantly influence GABAergic connectivity in the VH (p=1 for both; Figure 5.11B, F-G). Interestingly, massive upregulation of GAD65/67-positive boutons was observed in the VH of animals receiving combination treatment, to 181.0 ± 44.0 % of that observed in control conditions ($p<0.05$; Figure 5.11B, H). Addition of rehabilitative training more than doubled the inhibitory synaptic boutons in comparison to animals given only PNNi after Cx ($p<0.01$). These findings illustrate that exercise training only influenced changes in the number of inhibitory boutons in the presence of the plasticity enhancing drug PNNi, suggesting that experience is necessary to drive changes in the circuitry.

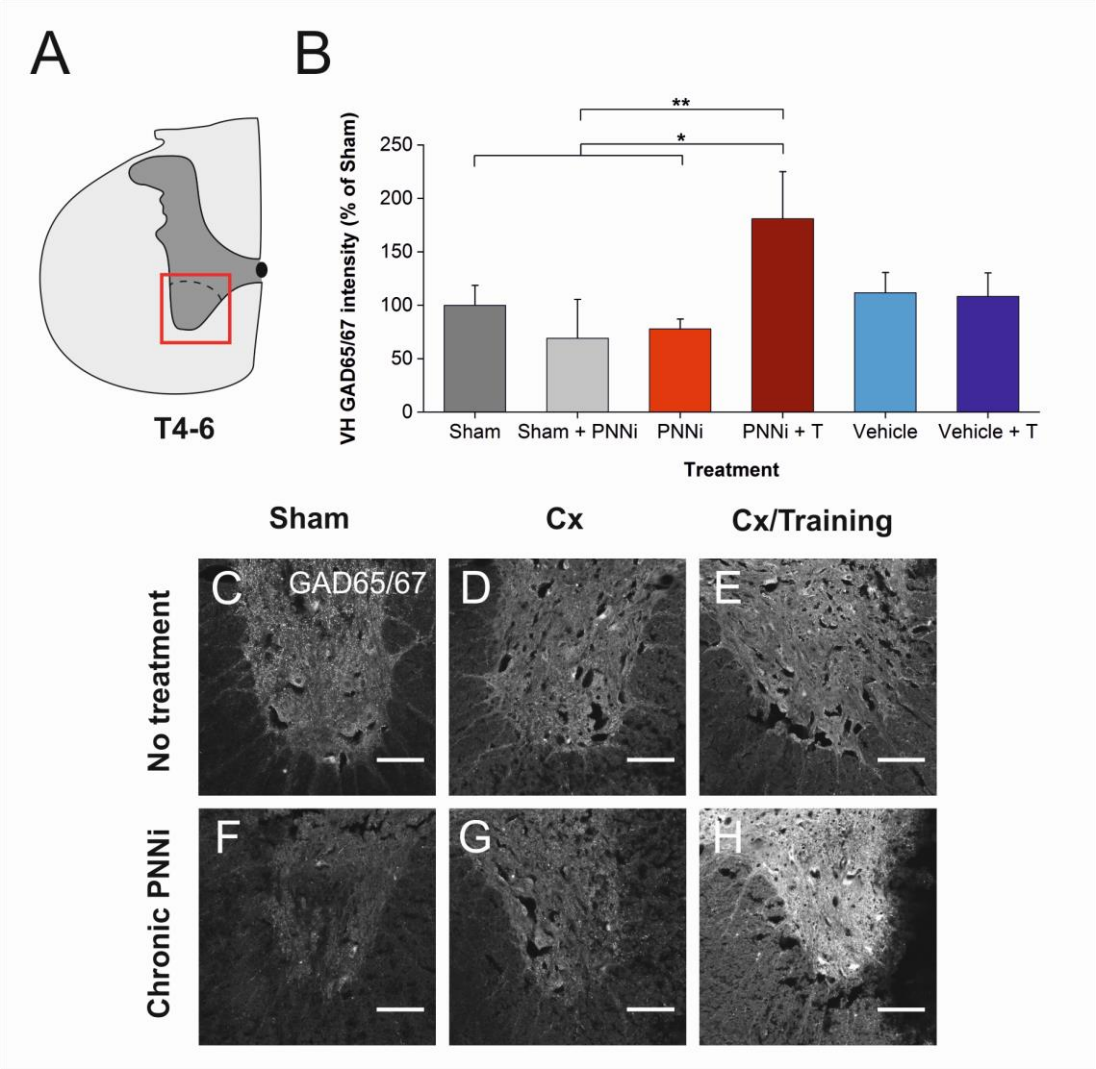

Figure 5.11: Combination treatment increased inhibitory connections labelled by glutamate decarboxylase isoforms 65 and 67 (GAD65/67) in the ventral horn (VH) rostral to a mid-thoracic contusive (Cx) injury.

A) Rat spinal cord sections (T4-6) obtained at 12 weeks post-injury were stained and intensity was analysed in the VH (denoted by red box). **B)** GAD65/67 intensity (visualised using Alexa fluor 568) in the VH increased with PNNi and rehabilitative combination treatment in comparison to other PNNi treated animals. *Error bars ± SD; n=3 per treatment group. Statistics one-way ANOVA; significance levels: * p<0.05 ** p<0.01 *** p<0.001.* Confocal images showing GAD 65/67 expression is unchanged with injury **(C-E).** Chronic PNNi treatment induced slightly decreased GAD65/67 expression in sham **(F)** and Cx injured animals **(G)**. Whereas, PNNi + T **(H)** combination strongly increased GAD65/67 expression in the VH. *Scale bars, 100 µm.*

5.3.4: Regenerative capability of descending fibres to be assessed in 3D

As discussed above, the CST is a descending motor tract that plays a large role in voluntary skilled functions, such as reaching and grasping, in the rat and in humans (Anderson, Gunawan and Steward 2007; Lemon *et al.* 1998; Lemon 2008). Reacquisition of skilled motor functions has been shown to correlate with regeneration of the CST (Weidner *et al.* 2001). Therefore, in this study, recovery of CST is to be assessed using anterograde tracing with BDA that has been injected into the HL motor cortex of the right brain hemisphere (Figure 5.12A). The stereotaxic coordinates for these intracortical injections were calculated using data from Long Evans rats (Neafsey *et al.* 1986), but later it was confirmed, using ICMS experiments, that the HL motor cortex for Lister hooded rats is located in the same area (Figure 5.7B). Tissue clearing protocols based on the iDISCO+ method were optimised for BDA traced tissue and visualised using the light sheet microscopy in order to assess recovery of the CST after mid-thoracic Cx in 3D (Renier *et al.* 2014). The preliminary images displayed in Figure 5.12B-E reveal that the anterograde tracing with BDA from the HL motor cortex was able to travel to reach the thoracic cord in the time from injection to termination of experiment. Additionally, this method was able to detect single CST axons travelling in the dorsal funiculus in both the cervical and thoracic spinal cord (Figure 5.12D-E). This method will be applied in future experiments to SCI tissue detailed in this thesis to assess recovery of the CST proximal to the lesion site and use the number of CST axons traversing the cervical spinal cord as control.

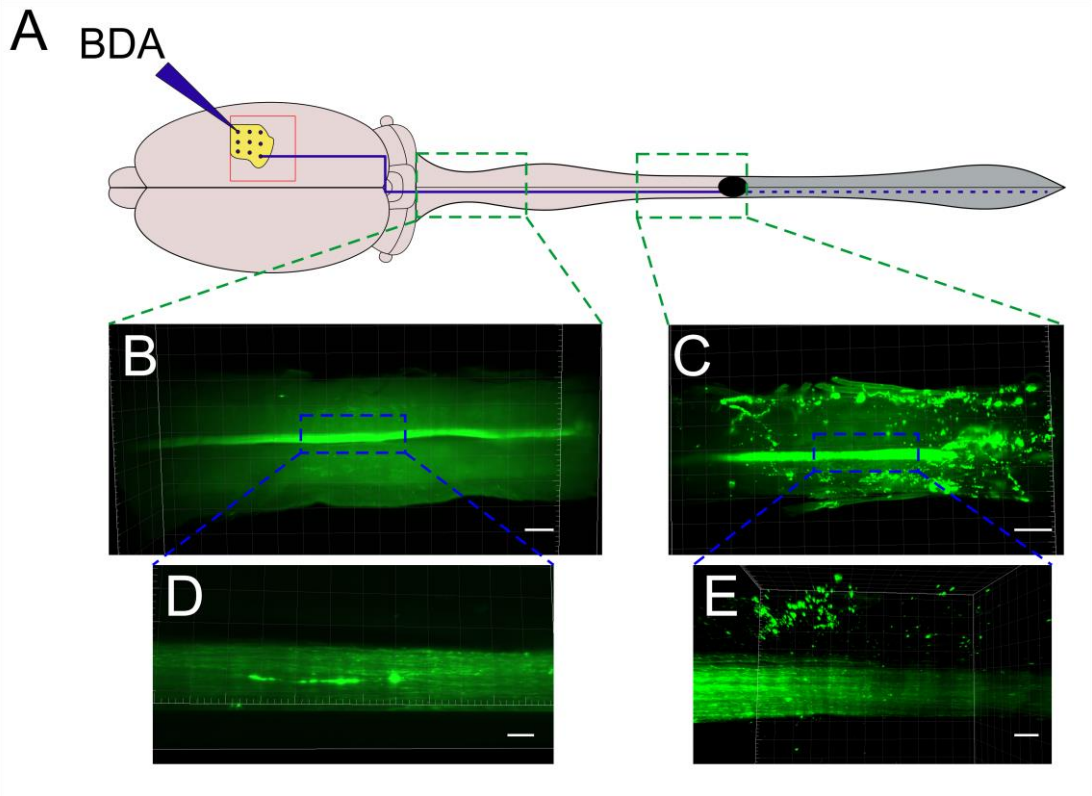

Figure 5.12: Corticospinal tract (CST) is revealed using anterograde tracing with biotin dextran amine (BDA) following mid-thoracic contusion injury.

A) BDA was injected into the right hindlimb motor cortex approximately 10 weeks post injury. Animals were perfused two weeks later to allow time for tracer to travel down the spinal cord. Sections of the cervical **(B, D)** and thoracic **(C, E)** spinal cord approximately 1 cm in length were subjected to tissue clearing protocols and visualised using Alexa fluor 568. 3D reconstruction of images of these spinal sections revealed CST axons travelling in the dorsal funiculus of the cervical and thoracic spinal cord, clearly seen in **D – E.** *Scale bars, **B)** 500 µm, **C)** 700 µm, **D)** 50 µm, **E)** 100 µm***.**

5.4: Discussion

This chapter aimed to elucidate some of the mechanisms by which PNNi mediates its effects when chronically given to animals after an acute mid-thoracic Cx injury.

Firstly, the effect of injury and PNNi treatment on key extracellular molecules that contribute to PNN architecture was able to be visualised and measured in the VH and the sensorimotor cortex. Using WFA and ACAN as markers for CSPGs revealed that, at a chronic injury time point, expression of these components in the ECM had returned to normal levels, rostral to the lesion site (Figure 5.1 & Figure 5.2). Total HA in either the ECM of the VH or the sensorimotor cortex also appeared to be unchanged by injury (Figure 5.3 & Figure 5.6). However, in the sensorimotor cortex, both WFA and ACAN revealed downregulation of CSPGs 12 weeks after injury (Figure 5.4 & Figure 5.5), suggesting a mechanism by which neuronal injury predisposes this area to structural remodelling.

After PNNi treatment, WFA and ACAN levels remained relatively unaltered and instead labelled fewer PNNs in the VH (Figure 5.1 & Figure 5.2). In the sensorimotor cortex, PNNi conferred independent reductions in CSPG expression in the ECM but did not appear to confer significantly additive reductions with injury (Figure 5.4 & Figure 5.5). HABP staining after PNNi treatment revealed downregulation of HA in the ECM of the VH but not the sensorimotor cortex (Figure 5.3 & Figure 5.6). These experiments confirmed that PNNi preferentially removed PNNs in the spinal cord, in contrast to the sensorimotor cortex. The actions of PNNi appeared to be specific to PNNs in the VH, resulting in minimal effects to CSPG content in the loose ECM (Figure 5.1 & Figure 5.2).

Secondly, functional connectivity of the CST was assessed using ICMS and revealed extensive functional and structural plasticity independently mediated by neuronal injury and plasticity enhancing mechanisms such as PNNi and training. Stimulation

of the HL motor representation failed to elicit HL movements after any post-injury treatment paradigm, suggesting that functional cortical control of HL muscles was unable to be established (Figure 5.7), despite the presumed sparing of alternative pathways, such as the cortico-reticulospinal pathway that project to the lumbar cord. The ICMS technique appeared to mainly evoke flexion, and not extension movements, in contrast to optogenetic stimulation of the sensorimotor cortex (Asboth *et al.* 2018), suggesting that the movement types elicited are technique specific. Optogenetic stimulation has also been shown to evoke HL extension in mice, even after severe thoracic Cx (Asboth *et al.* 2018). This electrophysiological preparation allowed the observation of functional remodelling of the HL area by expansion of the face and FL areas, alongside the complex interaction of neuronal injury, rehabilitative training and the plasticity enhancing drug, PNNi (Figure 5.8 & Figure 5.9).

Thirdly, this study begins to elucidate the contributions of PNNi-mediated plasticity, particularly in combination with rehabilitative training, to intraspinal changes to the neuronal circuitry by examining changes to global excitatory and inhibitory connectivity (Figure 5.10 & Figure 5.11).

5.4.1: PNNi limits synthesis of HA leading to partial removal of PNNs in the spinal cord

One of the central themes for research promoting recovery after SCI implicates extracellular molecules such as CSPGs as inhibitory to regeneration and plasticity. In this study, observations of WFA binding and ACAN expression after injury and chronic treatment paradigms suggest that CSPG expression returns to normal in the ECM within 12 weeks after injury. This is consistent with studies that show that whilst CSPGs such as NCAN, NG2 and VCAN increase both near and distal to the lesion site in acute SCI (Jones, Margolis and Tuszynski 2003; Andrews *et al.* 2012), the

expression of most CSPGs is downregulated to normal levels with progression to chronic injury, even close to the lesion site (Tang, Davies and Davies 2003). ACAN, in particular, is acutely downregulated at the lesion epicentre and normal expression is maintained rostral and caudal to a mid-thoracic Cx lesion (Andrews *et al.* 2012).

Whilst some slight trends of CSPG reduction were observed in the loose ECM of the VH with PNNi treatment, in summary, PNNi appears not to affect long-term ACAN core protein or CS-GAGs expression in the ECM. However, a partial removal of all PNNs in the VH was observed (Figure 5.1I &Figure 5.2I). Echoing the observations made in Chapter 3, ACAN labelled more PNNs in the VH than WFA (Irvine and Kwok 2018) and in this study a 40 % and 30 % reduction of ACAN- and WFA-positive PNNs was observed, respectively. However, the primary effect of PNNi in the spinal cord was the reduction of HA expression in both the loose ECM and PNNs. The deposition of HA as a pericellular coat is an essential prerequisite for the assembly of other PNN components, including CSPGs, into an aggregated structure (Kwok, Carulli and Fawcett 2010). Therefore, the high degree of HA downregulation but concurrent maintenance of CSPG levels with the reduction of PNN positive neurones with all stains suggests that the reduction of WFA- and ACAN-positive PNNs likely reflects the absence of the HA backbone of the PNN to bind to.

PNNi induced a partial, but not total abolition of HA production in the spinal cord, with approximately 25 % of original levels remaining. This provides an explanation for the incomplete removal of PNNs observed with WFA and ACAN staining. PNNi treatment reveals two different populations of PNN-associated neurone in the VH: one that is sensitive to PNNi-mediated removal of HA and another that are still producing the HA backbone necessary for the structural integrity of PNNs. In the spinal cord, the HAS1 and HAS3 isoforms are temporally expressed during development (Kwok *et al.* 2011). This could represent a mechanism through which PNNi affects the expression of some but not all HA in the spinal cord and as different isoforms of HAS are responsible

for production of different lengths of HA chains (Kwok *et al.* 2011), and could also illustrate heterogeneity of PNN structure.

5.4.2: Partial removal of PNNs allows plasticity of connections in the spinal cord

Previous studies have demonstrated that removal of PNNs, via enzymatic digestion by ChABC, is capable of stimulating long distance regeneration and local plastic changes in the spinal circuitry, correlating with functional recovery (Bradbury *et al.* 2002; Barritt *et al.* 2006; García-Alías *et al.* 2009; Wang *et al.* 2011a; Starkey *et al.* 2012; Bartus *et al.* 2014; García-Alías *et al.* 2015). This is the first study to show that PNNi is capable of inducing intraspinal changes to excitatory or inhibitory connectivity with or without spinal lesion.

The effect of injury and locomotor training on the excitatory/inhibitory balance in the ventral motor pools is relatively better explored caudal to the injury than rostral. After complete transection, the GAD67-positive or 'F-type' boutons are upregulated to lumbar Mns and across the lumbar cord (Tillakaratne *et al.* 2002; Ichiyama *et al.* 2011). The additional severance of descending excitatory pathways, such as the CST, rubrospinal, vestibulospinal and reticulospinal tracts (Du Beau *et al.* 2012), results in a net loss of excitatory drive to the HL locomotor circuity. Locomotor training in transection injury models induces a gross shift towards excitation of alpha Mns, due to a decreased inhibitory and increased excitatory influence, including a rise in VGLUT1-positive proprioceptive afferent contacts (Ichiyama *et al.* 2011; Alvarez *et al.* 2004; Tillakaratne *et al.* 2002).

Abundant VGLUT2-positive boutons are also known to be present on the surface of ventral Mns (Alvarez *et al.* 2004) and, alongside VGLUT1-positive inputs, comprise a population of glutamatergic 'S-type' inputs to the motor pools (Ichiyama *et al.* 2011).

The origin of some of the VGLUT2 terminals in the ventral motor pools may be interneurons in the medioventral cord, thought to be implicated in locomotor central pattern generators (Bannatyne *et al.* 2003; Kullander *et al.* 2003). VGLUT2 is the main transporter in the spinal cord, consistent with its proposed localisation in the spinal cord's numerous excitatory interneurons (Alvarez *et al.* 2004; Oliveira *et al.* 2003; Todd *et al.* 2003; Landry *et al.* 2004; Persson *et al.* 2006). Changes to VGLUT2-positive inputs therefore may indicate the plasticity of intraspinal circuitry.

This data illustrated that PNNi induced plasticity of excitatory intraspinal connectivity to the thoracic VH of unlesioned animals. Spontaneous increase of excitatory interneurons was also observed after injury, and this was further increased by PNNi treatment after injury, suggesting that additional plastic changes occurred due to concurrent PNN removal. However, intraspinal excitatory connections were decreased by locomotor training both with and without PNNi combination, signifying use-dependant pruning of these new synapses to functional connections. Interestingly, changes to inhibitory modulation of spinal circuitry rostral to the injury only changed in an environment of enhanced plasticity that was also primed by training.

These intraspinal plastic changes, whilst not in primary locomotor areas, signify an independent area of the spinal cord proximal to the injury site in which PNNi was able to induce plasticity despite only partial removal of PNNs. These results correlate with unpublished results, where PNNi administration has been shown to improve memory (unpublished results from Centre of Reconstructive Neurosciences, The Czech Academy of Sciences, Prague, Czech Republic), again with an incomplete removal of PNNs in the brain. These experiments were also able to illustrate the synergistic role of PNNi and locomotor training on uninjured intraspinal circuitry. Further research looking at the change in balance of excitatory/inhibitory inputs to the specific neuronal populations, such as ventral Mns, in key locomotor areas, such as the cervical and

lumbar spinal cord, could allow the exploration of differing effects of PNNi on FL and HL function. Additionally, investigation into the ECM changes with PNNi in the lumbar cord, as well as the cervical spinal segments, could aid in understanding the functional motor changes observed in HL, FL and their failure to improve coordination.

5.4.3: Structural reorganisation in the sensorimotor cortex is mediated by removal of PNNs

Frequently positron emission tomography (PET) and functional MRI scans have been used to investigate sensorimotor cortical reorganisation after SCI in humans (Bruehlmeier *et al.* 1998; Jurkiewicz *et al.* 2007) and increasingly in rodents (Ghosh *et al.* 2009a; Sydekum *et al.* 2009; Sydekum *et al.* 2014; Ghosh *et al.* 2009b), in replacement of ICMS techniques that were originally used to generate cortical maps (Penfield and Boldrey 1937). Total sensorimotor cortical activation is greater in paraplegic brains than in tetraplegics, illustrating that the level of lesion and remaining actions or movements directly correlates with remaining skilled task capacity (Bruehlmeier *et al.* 1998; Monfils, Plautz and Kleim 2005; Tandon *et al.* 2009).

In the mid-thoracic Cx model used in this study, HL movements were unable to be elicited by ICMS, indicating a lack of functional CST projections traversing the lesion site, regardless of treatment paradigm. Future investigations will confirm this via neuronal tracing analysis. It should be noted that the motor map is thought to reflect the capacity of the system in carrying out skilled motor tasks, and is not a reflection of movement capability (Monfils, Plautz and Kleim 2005), as all animals in this study were able to carry out HL locomotion. Following injury, FL representation expanded into the HL region, although this occurred to a lesser degree in animals where PNNi was given for a limited duration. At this level and severity of injury, the FL appears to compensate for reduced HL function, particularly in the absence of CST connectivity

caudal to the lesion. Other studies in a parallel injury model were similarly able to induce FL but not HL movements when stimulating the HL area (Frost *et al.* 2015; Ghosh *et al.* 2009a), and somatosensory representations also have been shown to remodel in the same way (Endo *et al.* 2007). However, single unit activity was able to be recorded in the HL cortical area approximately 4 WPI – a much earlier time point than investigated in this study. These findings demonstrate that remodelling of the HL representation after mid-thoracic lesion is rapid and suggest that lack of evoked HL response is reflective of a loss of synapses and not neurones at the cortical level (Ghosh *et al.* 2012; Yagüe *et al.* 2014). Neuronal tracing of axons originating from the cortical HL area revealed that after a mid-thoracic transection of the dorsal funiculus, expansion of the FL area and loss of HL response correlated with the spouting of CST collaterals onto spinal interneurons in the cervical spinal cord (Fouad *et al.* 2001), indicating that cortical motor remodelling may reflect CST plasticity.

The F motor representations also expanded in all injured animals, overlapping with the FL representation as well as into the HL area. Remodelling post-injury is known to be reflective of the motor experience (Nishibe *et al.* 2015; Nudo and Milliken 1996; Plautz, Milliken and Nudo 2000). As animals were orally fed either vehicle or PNNi twice daily, it is proposed that these animals may have accidentally received task-specific training in holding or acceptance of the syringe and/or daily stimulation of whiskers. This response appeared to be particularly exaggerated in animals with limited PNNi treatment, suggesting consolidation of these new connections. However, the stark reduction of F movements that were able to be elicited in animals with combination treatment, suggests that in the absence of PNNs and without specific training on the F area, the lack of consolidation of synapses may have induced withdrawal of existing synapses.

The ICMS experiments shown here support evidence from the literature that proposed that after a neuronal injury the sensorimotor cortex is able to modulate

various mechanisms of plasticity restriction to promote remodelling shaped by early post-injury experiences (Nishibe *et al.* 2015; Kleim *et al.* 2002). CST neurones originate in layer V in the sensorimotor cortex (Nudo and Masterton 1990), and our data illustrates that whilst PNNs were present throughout the cortical layers, they displayed greatest expression in these same layers. Analysis of PNN components in the sensorimotor cortex revealed independent and not additive downregulation of ACAN and the 'universal' PNN marker WFA with injury and with PNNi treatment, concurrent with the structural reorganisation illustrated in these conditions by ICMS motor mapping. However, PNNs also appeared to be downregulated in layers other than layer V spinally projecting neurones, which may be suggestive of intracortical plasticity. Notably, other studies also implicate PNNs in experience driven plasticity of the cortical motor representation. Along the transition areas between FL and HL areas, PNNs surrounding parvalbumin-positive cells have been reported as thinner and fainter but not reduced in number after SCI injury (Orlando and Raineteau 2015). PNNs are a dynamic structure and thickness of net structure has been proposed to modulate the level of plasticity restriction mediated, therefore supporting reorganisation of connections as the FL expands into the HL representation. Locomotor training has been demonstrated to have differential effects on PNN expression in the brain and spinal cord (Smith *et al.* 2015), parallel to the trends in PNN components observed in the VH and sensorimotor cortex above. Downregulation of PNNs in the sensorimotor cortex as a response to exercise training may provide part of the mechanism through which exercise and injury are able to induce plasticity in the sensorimotor cortex (Smith *et al.* 2015). As injury, PNNi and locomotor training all appear to independently modulate expression of CSPGs, and as a result PNN structure, this may explain why the effects in combination were not additive.

PNNs are not the only plasticity restricting mechanism to be modulated by injury. Transection of the spinal cord induced downregulation of NgR and upregulation of BDNF in the denervated HL somatosensory area, correlating with expansion of FL into HL area (Endo *et al.* 2007). These modulatory responses were found highly localised to layer V sensorimotor neurones, and further compounds the evidence that injury promotes sensorimotor cortex plasticity by downregulating plasticity restriction mechanisms. Further study into how neuronal injury modulates these mechanisms in the sensorimotor cortex could reveal endogenous methods to promote plasticity in other areas of the CNS. While it was observed that thoracic injury was able to regulate plasticity enhancing mechanisms in the sensorimotor cortex, this region is known to remain plastic and experience-dependent throughout adulthood. Therefore, it is unlikely that other cortical regions, such as the visual cortex, where the termination of developmental plasticity by PNNs are well studied, will also experience downregulation of PNNs in response to SCI.

5.4.4: PNNi affects the ECM in the brain and spinal cord differently

This study has revealed that PNNi is able to induce plasticity in two regionally distinct areas of the CNS, and therefore is likely to also have promoted plastic changes caudal to the injury site. However, whilst PNNi appears to mediate its effects through partial removal of PNNs in both the brain and the spinal cord, the mechanisms, as revealed by the presence of PNN components in these areas, appear to be different. In the spinal cord, it has been discussed that removal of PNNs is likely due to downregulation of HA therefore preventing the unaffected levels of CSPGs from assembling into the aggregated pericellular architecture. In the sensorimotor cortex, it was revealed that HA was not depleted by PNNi. Instead, WFA and ACAN binding indicated decreased levels of CS-GAGs in the sensorimotor cortex, promoting structural plasticity. This further suggests heterogeneity in PNN formation and

structure between the brain and spinal cord. Further studies will increase the n number for these investigations using animals from this study with other terminal endpoints to reveal whether the trending effect of PNNi in the ECM is more global.

5.4.5: Conclusions

These experiments carried out allowed the effect of the complex combination of locomotor training and plasticity enhancement in an injured environment to be assessed. Many of the mechanisms of change mediated by PNNi are yet to be elucidated, including the influence of PNNi on sprouting of descending pathways and the impact of plasticity on intraspinal circuitry caudal to the injury. However, this is the first time that PNNi has been applied to the SCI pathology and this study has illustrated that PNNi appears to have different effects on ECM components in the brain and spinal cord. PNNi primarily exerts its effects in the spinal cord with minimal removal of PNNs in cortical areas such as the sensorimotor cortex. Additionally, whilst removal of PNNs was incomplete, it was revealed to be capable of promoting plasticity in two distinct and uninjured areas of the CNS, confirming that PNNi confers systemic plasticity. The effects of PNNi appear to be very specific to PNNs, in contrast to the actions of ChABC, and should allow further study into the plastic effects of PNNs without gross removal of all CSPGs. Future and ongoing work aims to visualise changes to descending modulation by CST with anterograde BDA tracing and reorganisation of synaptic inputs to Mns innervating the HL muscles, retrogradely labelled by CTB, using lightsheet microscopy. Correlations with lesion volumes, revealed using MRI, could reveal a neuroprotective role of PNNi.

Chapter 6: General Discussion

6.1: Summary of key findings

This thesis looked to explore the role of PNNs in recovery after acute SCI and to investigate the efficacy of a novel and non-invasive method of removing PNNs in promoting recovery. The primary subject of this thesis describes the anatomical and functional effects of the molecule, PNNi in its first application to the SCI pathology. HL motor recovery was observed when PNNi treatment was limited and the enhanced plasticity was shaped by exercise training. Chronic PNNi treatment induced structural plasticity and improved FL but not HL functions as plasticity was uncontrolled. The influence of PNNs on Mn subpopulations within the ventral motor pools was identified, revealing a strong relationship between alpha Mns and PNNs that is likely to be implicated in the recovery of motor functions with ChABC administration in SCI models

Importantly, this study was able to confirm that oral administration of PNNi was able to remove PNNs in both the brain and spinal cord after a clinically relevant Cx injury. This removal was partial with some populations appearing insensitive to PNNi administration. The compound induced differential and regional effects on the ECM molecules, HA and CSPGs. Interestingly, removal of some but not all PNNs was able to induce synaptic reorganisation and functional changes in regionally distinct and uninjured areas of the CNS, indicating systemic plasticity. Transient changes to sensory function in intact animals in response to systemic PNN removal were observed. Chronic PNNi allowed improvements to FL motor functions that was able to compensate for HL deficits and induced further structural reorganisation of the sensorimotor cortex. These changes are interesting as it leads to the question of how much reduction of PNNs throughout the system is sufficient to induce plasticity and whether this is dependent on removal from certain neuronal populations.

Despite this, a lack of functional recovery to HL sensory or motor functions with chronic PNNi treatment suggested that these plastic changes in different CNS regions

were not coordinated, resulting in changes to the system that were maladaptive to the recovery of lost functions. The conclusion that the systemic plasticity mediated by PNNi may bestow ‘too much’ plasticity for functional benefit led further investigations to limit the plasticity. Attempts to control the plasticity by combining chronic PNNi treatment with rehabilitative training did not confer further functional benefit but did reduce the high levels of excitatory VGLUT2 connectivity in the spinal cord induced by PNNi and injury, suggesting pruning to functional connections. Additionally, this treatment combination produced a synergistic plastic response with a strong shift towards inhibitory modulation of circuitry, correlating with the reduction of area represented by the face in the sensorimotor cortex. From these primary observations, it was concluded that the training intervention in use was able to drive plasticity in order to provide balance to the system, however, was unable to overcome the persistent and overly plastic environment in order to provide functional benefit.

As PNNi is an oral compound, the next logical step to limit plasticity was to define the duration of PNNi administration. With this experimental paradigm, it became apparent that PNN formation is necessary for maturation of new connections, reflecting the role of PNNs in normal development. Exercise training and PNNi interventions exhibited opposing influences on PNNs, with training increasing the thickness of PNN architecture but not the overall expression in contrast to the deleterious effect of PNNi. Acceleration of PNN formation by sustained rehabilitative training after the PNNi treatment window allowed trends of further motor recovery. This was positively compounded by evidence that the FL representation of the sensorimotor cortex had withdrawn from the HL region. Whilst direct stimulation of the HL was still unable to elicit this response 6 weeks after the PNNi window, neuronal tracing experiments are required to reveal the condition of the CST. Whilst these results provide promising prospects for PNNi as a treatment for SCI, further optimisation is required to provide the best behavioural benefit.

6.2: Partial but systemic removal of PNNs by PNNi renders the environment plastic

The results presented here illustrate that oral treatment with PNNi removes PNNs in the brain and spinal cord after SCI. However, this removal is partial, and the effect appears to be different between the brain and spinal cord. As PNNs are a dynamic and heterogeneous structure composed of various glycoproteins and proteoglycans, the turnover of these components affects the overall integrity of the architecture. In the spinal cord, the turnover of some PNNs appears to have been disrupted by decreased production of HA. Whilst other PNN components were found to be distributed in normal concentrations in the ECM, the absence of the HA pericellular coat that provides the backbone of the PNN structure prevented the aggregation of these other components (Figure 6.1). In the brain, PNNi appeared to alter PNNs instead by decreasing overall CSPG expression and therefore the aggregation of the highly inhibitory CSPGs into the PNN structure. From preliminary results using short

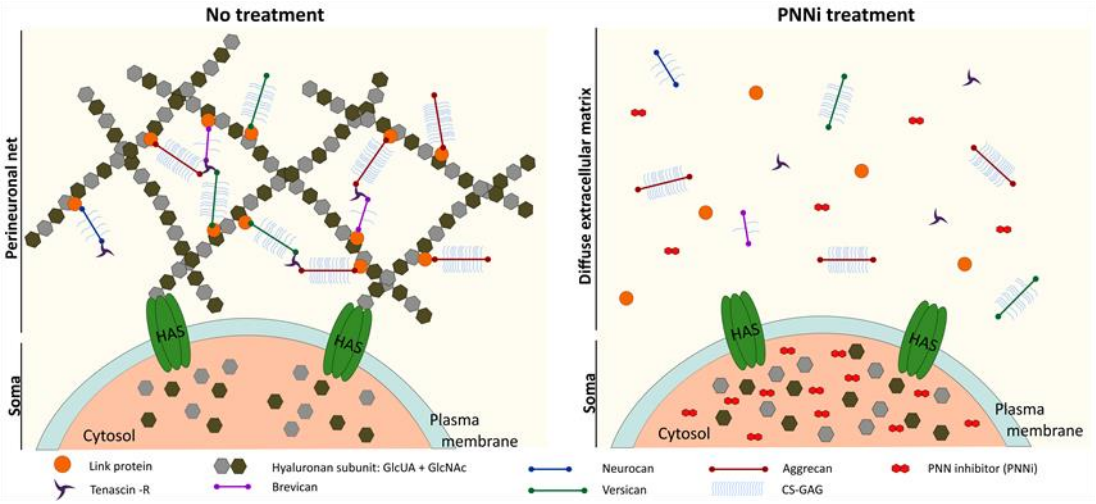

Figure 6.1: Perineuronal net (PNN) structure, modified from *(Kwok et al. 2011)*.

Without treatment, PNNs form normally around some neurones in the central nervous system after development and restrict plasticity. Chronic presence of PNN inhibitor (PNNi) disrupts the turnover of the PNNs through inhibiting the formation of critical PNN components.

term treatment with PNNi it was expected that PNNi would affect PNN expression in the spinal cord more than the brain (unpublished results, Cambridge), correlating with growing evidence that PNNs in the brain and spinal cord differ in composition. However, long term administration appears to have an accumulative effect on the brain. Further research is required is elucidate the discrepancy between these effects and to advance understanding of the mechanism of PNNi in the CNS.

Whilst PNNi and ChABC both aim to remove PNNs to enhance plasticity, the method that they go about this is very different. ChABC injection results in broad and non-specific degradation of CS-GAGs and HA in both the ECM and in PNNs (Crespo *et al.* 2007; Lin *et al.* 2008). The complete removal of inhibitory CSPGs in the ECM and PNNs has been extensively demonstrated to promote plastic and regenerative responses local to the injection site proximal to the lesion (Barritt *et al.* 2006; García-Alías *et al.* 2009; Wang *et al.* 2011a; Starkey *et al.* 2012; Bartus *et al.* 2014), including promoting reorganisation that is able to compensate for remote neuronal injury (Galtrey *et al.* 2007; Soleman *et al.* 2012). The broad effects of ChABC have also demonstrated ability to modulate the immune response and vascular remodelling (Dyck *et al.* 2018; Milbreta *et al.* 2014). Additionally, the formation of degradation products, including disaccharides and HA fragments, such as HA4, have potential neuroprotective effects (Wang *et al.* 2015b) (explored in section 1.2.2.2.4: CSPGs and glycosaminoglycans). In contrast, PNNi acts by interrupting the dynamic turnover of PNN components. In the spinal cord, the selective HA downregulation produced specific removal of some PNNs without effecting CSPG expression in the ECM. In comparison to ChABC, the effects of PNNi are therefore much more specific to PNNs and the effects of inhibitory CSPG signalling in the ECM likely remain (Dickendesher *et al.* 2012; Xu *et al.* 2015; Lang *et al.* 2015).

This study has demonstrated that the systemic effects of PNNi have allowed plastic reorganisation in sensorimotor brain areas, as well as rostral to the lesion epicentre.

These alterations to circuitry proved capable of positively affecting functional performance of the uninjured FLs after minor deficits induced by mid-thoracic Cx. The minor deficits may have been a result of HL error and/or loss of connections such as propriospinal interneurons. PNNi treatment induced changes that made the FL performance of these injured animals to be comparable to sham and intact animals. However, whilst HL functional recovery was not observed to be greater than that of spontaneous regeneration, the anatomical effects of PNNi caudal to the injury is yet to be explored. Crucially, PNNi demonstrates that specifically removing some but not all PNNs in the spinal cord is capable of promoting plasticity, in contrast to the broad and non-specific removal of CS-GAGs and HA in both the ECM and PNNs by ChABC (Crespo *et al.* 2007; Lin *et al.* 2008). On the other hand, ChABC-mediated plasticity is limited to the local digestion area, whereas PNNi renders plasticity throughout the system.

Theoretically, removal of PNNs from a larger area of the CNS should provide a greater scope for plasticity and thus correlate with superior functional recovery after CNS injury. This is supported, albeit on a smaller scale than mediated by PNNi, by the comparison of single dose bacterial ChABC injection versus lenti-viral ChABC, which digested a greater area proximal to the lesion as well as conferring enhanced functional recovery (Bartus *et al.* 2014). Whilst some conditional CNS KOs of PNN components do exist, including Tn-R, CTRL-1 and ACAN (Brückner *et al.* 2000; Guntinas-Lichius *et al.* 2005; Carulli *et al.* 2010; Giamanco, Morawski and Matthews 2010; Rowlands *et al.* 2018), and have demonstrated ability to enhance plasticity, few of these have investigated the effects in neuronal injury models (Guntinas-Lichius *et al.* 2005; Carulli *et al.* 2010). Of these only CTRL-1 KO animals have been applied to CNS injury models and unfortunately the effects exhibited in this study are limited to assessments of sprouting and not to functional recovery (Carulli *et al.* 2010). Whilst not clinically relevant, applying CNS injury models to these conditional KO may help

to elucidate the different effects between partial and complete systemic removal of PNNs in the CNS on functional recovery.

6.3: Adaptive and maladaptive plasticity: a balancing act

The ability to render the CNS malleable to change is an essential prerequisite for many developing therapies aiming to restore lost functions after SCI. However, whilst adaptive changes that reach a threshold to which they are beneficial to recovery are the primary goal, enhancement of plasticity can leave the system vulnerable to maladaptive alterations if not carefully shaped.

In this study, it has been demonstrated that PNNi was able to promote plasticity throughout the CNS, resulting in adaptive modifications to the motor control of the FL after mid-thoracic Cx injury. However, plasticity in HL innervating regions remained functionally neutral and importantly did not result in maladaptive outcomes such as hyperreflexia, spasticity and allodynia. The absence of HL recovery likely indicates that anatomical reorganisation did not meet the threshold of functional new connections to alter behaviour. This was supported by attempts to shape the malleable circuitry mediated by PNNi by using involuntary active exercise. Combination with training intervention provided balance of inputs to spinal circuitry and resulted in faster recovery of weight support when compared to untrained PNNi treated animals (Figure 4.4E). The functional disparity of PNNi throughout the CNS additionally indicated independent plasticity of different and disconnected regions resulting in an uncoordinated system. Training is well documented to modulate and coordinate neuronal activity through various means, such as changes to electrophysiological properties of lumbar Mns, excitatory drive from intraspinal locomotor central pattern generators and structural reorganisation of the sensorimotor cortex (Barbeau and Rossignol 1987; Tillakaratne *et al.* 2002; Dobkin *et al.* 2006; Girgis *et al.* 2007; Barrière *et al.* 2008; Beaumont *et al.* 2008; Ichiyama *et al.* 2008; Kao *et al.* 2011; Shah *et al.* 2013). However, a major caveat of studies utilising task-specific rehabilitation is whether the program is strenuous enough to provide further behavioural gains. Further investigations utilising higher intensity or

increased number of rehabilitation training sessions may be necessary to control and coordinate the PNNi-mediated plasticity for optimal behavioural benefit.

ChABC remains the primary tool for removal of PNNs in the various developmental and injury models (Moon *et al.* 2001; Bradbury *et al.* 2002; Pizzorusso *et al.* 2002; Barritt *et al.* 2006; Galtrey *et al.* 2007; McRae *et al.* 2007; Tester and Howland 2008; García-Alías *et al.* 2009; Wang *et al.* 2011a; Zhao *et al.* 2011; Soleman *et al.* 2012; Starkey *et al.* 2012; Bartus *et al.* 2014; Cheng *et al.* 2015; Burnside *et al.* 2018; Warren *et al.* 2018). Whilst much of the last few decades has focused on establishing means to sustain removal of PNNs by ChABC through the development of thermal stabilised and lenti-viral delivery systems (Lee, McKeon and Bellamkonda 2010; Muir *et al.* 2010; Zhao *et al.* 2011; Bartus *et al.* 2014; Hu *et al.* 2018), only recently have efforts been made to control the duration of PNN removal (Burnside *et al.* 2018). Subpopulations of mammalian neurones have evolved to form PNNs for a reason. Therefore, whilst removing PNNs proximal to the lesion site using ChABC enhances plasticity essential for the development of new and compensatory connections (Bartus *et al.* 2014; Starkey *et al.* 2012), this recovery eventually plateaus and sustained plasticity is unfavourable to clinical translation. Whilst development of the doxycycline inducible regulatory switch revealed that long term removal of PNNs by ChABC was required for optimal functional recovery, crucially the effects of allowing PNNs to re-establish in this principal study were not investigated (Burnside *et al.* 2018).

This study therefore represents the first investigation to control PNN-mediated plasticity in a SCI model by defining a long-term window of PNN removal and examining the influence of PNN consolidation on behavioural functions. Similar to the Burnside study above, this study defined long term PNN removal as a period of 8 weeks (Burnside *et al.* 2018). However, unlike ChABC, during this period PNNi was unable to provide improvements to functional deficits caudal to the injury. Systemic

removal of PNNs rendered an environment that was overly plastic and simultaneous training interventions was inadequate in shaping the response to a degree capable of functional changes. Further trying to control plasticity by limiting the duration of PNNi treatment, appeared to induce further motor recovery with PNN consolidation, only in combination with sustained rehabilitation. As training positively modulates PNN expression in the spinal cord (Smith *et al.* 2015; Wang *et al.* 2011a), and motor recovery did not improve in the timescale given in animals without sustained training, it is suspected that exercise accelerated the reformation of PNNs. The reconsolidation of PNNs would stabilise any new connections whilst simultaneously exercise training would provide coordination of neuronal activity in these reorganised spinal circuits. Unfortunately, the scope of the study did not allow this HL motor recovery to peak and therefore future investigations aim to repeat this and extend the amount of time after cessation of PNNi to allow greater PNN recovery. The effects of PNN consolidation also appeared to reduce structural plasticity in the sensorimotor cortex, particularly when shaped by sustained rehabilitation and minimised expansion of the FL into the HL area. The cortical remodelling of the FL representation returned to that of unlesioned animals, coinciding with the further HL motor recovery detailed above. The anatomical repercussions of this remodelling on the CST remain to be investigated using neuronal tracing techniques.

Whilst these results reveal the importance of PNNs in maturation of modified circuitry, this highlights how much is still unknown about the underlying mechanisms of shaping plasticity and how much change in circuitry is necessary for shifts in behavioural outcomes. Activity based therapies are one of the best methods to increase control of plasticity, therefore intensification and/or more frequent rehabilitative session alongside further optimisation of duration of PNN removal could better shape recovery.

6.4: Motor circuitry is highly sensitive to PNN modulation

ChABC has been extensively used to enzymatically remove PNNs in the spinal cord and to induce motor recovery following SCI (Bradbury *et al.* 2002; Barritt *et al.* 2006; García-Alías *et al.* 2009; Lee, McKeon and Bellamkonda 2010; Carter, McMahon and Bradbury 2011; Wang *et al.* 2011a; Zhao *et al.* 2011; Bosch *et al.* 2012; Zhao *et al.* 2013; Bartus *et al.* 2014; James *et al.* 2015; Burnside *et al.* 2018; Rosenzweig *et al.* 2019). However, as many of the neuronal populations in the spinal cord associated with PNNs remain either unidentified or not well defined, the impact of PNN removal on specific populations is relatively unknown.

Unpublished results (University of Leeds) demonstrate that plasticity of synaptic inputs to Mns after ChABC treatment correlate with motor improvements after severe mid-thoracic Cx injury. However, this study was the first to reveal that the high association of PNNs with alpha Mns underlies the dramatic impact of ChABC on this population. Therefore, removal of PNNs is likely to affect synaptic inputs to these neurones and modulate motor functions. Other studies also implicate exercise training in the modulation of PNNs with motor circuitry at multiple CNS levels (Wang *et al.* 2011a; Orlando and Raineteau 2015; Smith *et al.* 2015). This study provides supporting evidence of the differential modulation of PNNs in the brain and spinal cord. As exercise training increased HA levels but not PNN number in the spinal cord, despite depletion by PNNi, it can be proposed that exercise plays a role in the modulation of PNN components and the resulting thickness of the net structure but not in formation. This corroborates with the refining effect of exercise observed on synaptic connections to Mns. Further research is required to elucidate how the effect of net thickness influences synaptic inputs to Mns as well as exactly how exercise could help to elucidate the mechanism through which exercise modulates the dynamic structure of PNNs. As PNNs are also implicated in providing stability of inputs to the recurrent inhibitory circuit as Renshaw cells, which are also known to be

enwrapped by PNNs (Vitellaro-Zuccarello *et al.* 2007). Removal or exercise-mediated modulation of PNNs likely alters synaptic inputs and therefore underlies changes to the excitability of Mns (Moore *et al.* 2015; Shefner *et al.* 1992). The low association of PNNs with gamma Mns, in contrast to that of alpha Mns, likely reflects increased plasticity of their synapses, suggesting that they could play a greater role in adapting and changing the motor response after SCI. Further experiments are required to understand the role of gamma Mns after injury, including characterisation of their changing electrical properties using electrophysiological experiments.

Assessment of the heterogeneity of PNN expression indicated that studies identifying PNNs using the 'universal PNN marker' WFA underestimate total number of PNNs, highlighting the need to extend research into its binding properties (Miyata *et al.* 2012; Härtig, Brauer and Brückner 1992). Whilst it is known that much of the heterogeneity of PNNs is provided by the different lecticans that bind to HA (Yamaguchi 2000; Gama *et al.* 2006; Kitagawa 2014), chronic PNNi treatment revealed subclasses of PNNs insensitive to HA removal. As some HA but not all was affected, this indicated that PNNs in the VH also display heterogeneity in HA production, such as HAS isoforms, which can also confer differential functional properties due to differing sizes produced (Kwok *et al.* 2011; Cyphert, Trempus and Garantziotis 2015). However, the functional impact of much of PNN heterogeneity is relatively unknown but extended research could help to elucidate which neurones still are surrounded by PNNs after PNNi treatment.

6.5: Future perspectives and clinical relevance of PNNi

The experiments in this thesis were primarily designed to explore the efficacy of a novel and non-invasive method of PNN removal in enhancement of recovery after acute SCI. This is the first time PNNi is applied to a SCI model. A Cx model was used as this is the most prevalent clinical injury phenotype and is easily experimentally replicated using controlled Cx devices such as the IH impactor. Rats more closely model the human pathophysiology of SCI than other rodents (Metz *et al.* 2000; Stammers, Liu and Kwon 2012) where size, morphology and white matter sparing have been directly related to preservation of functions. However, experimentally injuries are given dorsally and in the thoracic region of the cord, and in contrast, injuries present most frequently to the human condition in the cervical spinal cord and from the ventral aspect (Kumar *et al.* 2018). Other larger animals are used now in late-stage preclinical studies before humans, such as the recent canine clinical trial for ChABC (Hu *et al.* 2018). However, rats were appropriate for this study as the first use of PNNi in this pathology.

This study demonstrates that PNNi is able to induce anatomical and functional alterations to the spinal cord circuitry, and is therefore suitable for exploration as a treatment for SCI. Importantly, this investigation has demonstrated that this compound is not only compatible with rehabilitation but requires shaping by training for optimal effects. Forthcoming studies will test the efficacy of this compound in opening a window of plasticity in chronic Cx models and to further optimise the timing of PNN removal required for the best functional recovery. The systemic nature of PNNi also proves efficacious in promoting plasticity in the brain and could therefore be applied to other brain-related pathologies, such as improving memory retention (Romberg *et al.* 2013; Yang *et al.* 2015), or improving recovery after traumatic brain injury or stroke (Moon *et al.* 2001; Soleman *et al.* 2012; Gherardini, Gennaro and Pizzorusso 2013; Harris *et al.* 2013).

The effect of ChABC has been well established and whilst it has a broad effect by both digesting CSPGs in the loose ECM and targeting the plasticity modulating effects of PNNs (Crespo *et al.* 2007; Lin *et al.* 2008), it also conveys a dual role in promoting recovery. The immunomodulating and ultimately neuroprotective role of ChABC degradation in the acute and sub-acute lesion site minimises neurodegeneration leading to a greater sparing of tissue and therefore more tissue to effectively 'work with' or reorganise (Milbreta *et al.* 2014). Whilst not currently available in this study, lesion analysis will provide greater insights into the effects of PNNi on the general lesion environment and tissue sparing. Extending research into the effects of PNNi on CSPG secretion by astrocytes and modulation of immune cells would expand understanding of the mechanisms of PNNi in SCI pathology but unfortunately is beyond the reach of what this principal/primary SCI study was able to accomplish.

Importantly other models of attenuated PNN formation throughout the CNS, such as CNS-specific deletions of CRTL1 and Tn-R, show a lack of detriment to normal behaviours and crucially did not appear to cause motor impairment in intact animals (Carulli *et al.* 2010; Brückner *et al.* 2000). This corroborates the observations we observed with short and long term PNNi treatment in intact animals. However, PNNi instigates removal of HA in the spinal cord. As HA is a highly ubiquitous glycan and is essential to the ECM throughout the body, PNNi may also exert HA depleting properties to other peripheral tissues, such as cartilage or the liver (Cyphert, Trempus and Garantziotis 2015; Fraser, Laurent and Laurent 1997; Toole 2004). Whilst PNNi at the currently licensed dose appears not to cause damage to peripheral tissues, this study uses a higher dose and appears to be able to act in tissues within the blood brain barrier. Tissues have been sampled from the chronic and short term PNNi administration studies to investigate the effect on key organs including cartilage, liver, kidney and smooth muscle. As the dose of PNNi used for the *in vivo* investigations detailed in this thesis were derived from preliminary studies *in vitro* and previous

animal experiments, it is possible that if PNNi negatively effects peripheral tissues the dose could be optimised. This could represent another method for control the plasticity mediated by PNNi in the CNS.

6.6: Final conclusions

In conclusion, the contents of this thesis have achieved the aims of identifying a population of neurones likely responsible for motor recovery after removal of PNNs in SCI, as well as assessing the efficacy of the novel and non-invasive compound, PNNi in functional recovery after a clinically relevant acute Cx injury. Firstly, it has been demonstrated that PNNi is able to remove some but not all PNNs throughout the CNS. This partial removal of PNNs is capable of enhancing structural and functional plasticity in regionally specific and uninjured areas of the CNS. Due to the high level of association of PNNs with alpha Mns, removal of PNNs likely induces alterations to alpha Mns and their corresponding motor circuitry which modifies the excitatory properties of these neurones and consequently the contractility of their associated muscle groups. However, as PNNi-mediated plasticity occurs independently in different regions, the system is unable to coordinate these changes into functional improvements of deficits caudal to the contusive injury and is further limited by the presence of other inhibitory mechanisms, such as Nogo-A. Further study into the neuroanatomical changes after PNNi treatment to the injured CNS is required to elucidate the mechanism behind the functional changes observed. Attempts to shape and control the overly plastic environment rendered by PNNi with rehabilitative training and limiting the duration of PNN removal are able to allow motor recovery. This study provides evidence that PNNi represents a novel and non-invasive alternative to ChABC, conferring specific removal of PNNs in the CNS. However, further optimisation of the PNNi regime is required to better control and drive plasticity to promote the best possible behavioural recovery after SCI.

Appendix 1: BBB HL locomotor scoring

The following marking and scoring sheets for the open field HL locomotor scoring sheet are taken or modified from (Basso, Beattie and Bresnahan 1995). Behavioural results using this locomotor test can be found in sections 4.3.2.3.3: Spontaneous recovery of weight bearing and plantar stepping and 4.3.3.1: 8-week PNNi with sustained rehabilitation allows improvement of FL-HL co-ordination.

STEPS			
DORSAL		PLANTAR	
L	R	L	R
PASSES			
COORDINATED		UNCOORDINATED	
TOE CLEARANCE			
L		R	
TOE DRAG			
L		R	

STEPS			
DORSAL		PLANTAR	
L	R	L	R
PASSES			
COORDINATED		UNCOORDINATED	
TOE CLEARANCE			
L		R	
TOE DRAG			
L		R	

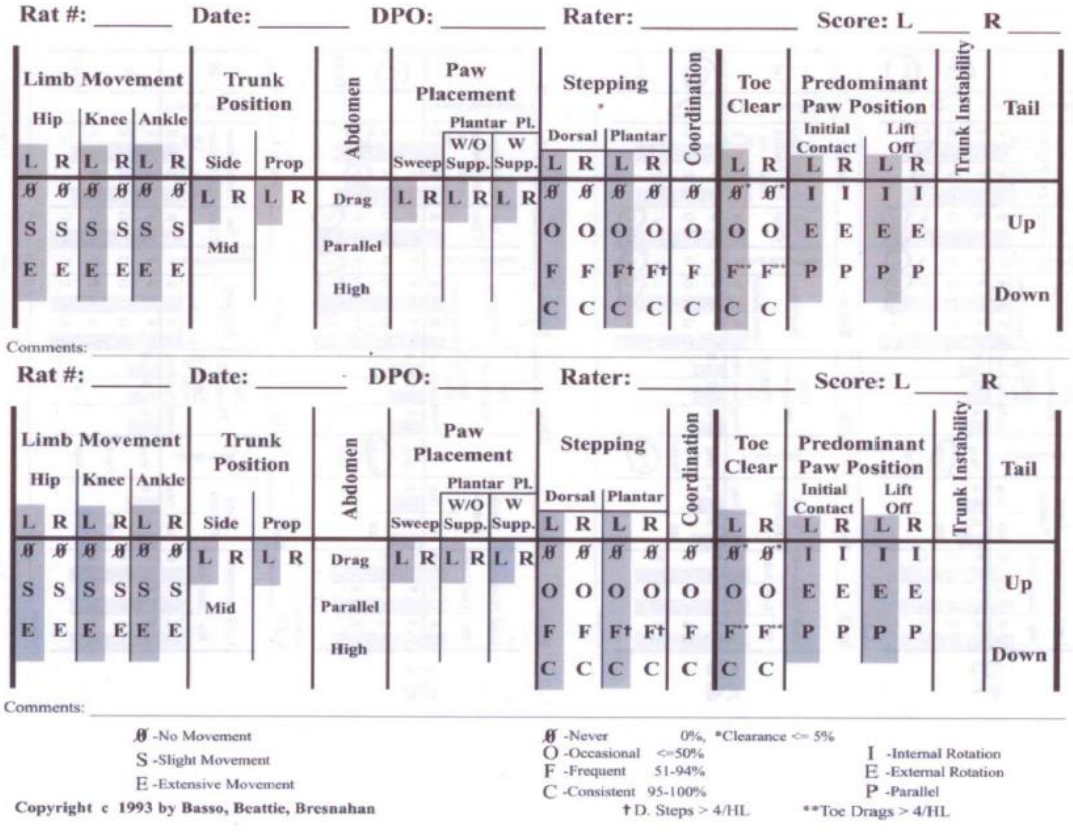

DESCRIPTIONS AND DEFINITIONS
FOR THE
BASSO, BEATTIE BRESNAHAN LOCOMOTOR RATING SCALE

0 No observable hind limb (HL) movement

1 Slight movement of one or two joints, usually the hip &/or knee

2 Extensive movement of one joint or

Extensive movement of one joint and slight movement of one other joint

3 Extensive movement of two joints

4 Slight movement of all three joints of the HL

5 Slight movement of two joints and extensive movement of the third

6 Extensive movement of two joints and slight movement of the third

7 Extensive movement of all three joints of the HL

8 Sweeping with no weight support

or

Plantar placement of the paw with no weight support

9 Plantar placement of the paw with weight support in stance only (i.e. when stationary)

or

Occasional, Frequent or Consistent weight supported dorsal stepping and no plantar stepping

10 Occasional weight supported plantar steps, no FL-HL coordination

11 Frequent to consistent weight supported plantar steps and no FL-HL coordination

12 Frequent to consistent weight supported plantar steps and occasional FL-HL coordination

13 Frequent to consistent weight supported plantar steps and frequent FL-HL coordination

14 Consistent weight supported plantar steps, consistent FL-HL coordination; and Predominant paw position during locomotion is rotated (internally or externally) when it makes initial contact with the surface as well as just before it is lifted off at the end of stance or

Frequent plantar stepping, consistent FL~HL coordination and occasional dorsal stepping

15 Consistent plantar stepping and Consistent FL-HL coordination; and, No toe clearance or occasional toe clearance during forward limb advancement Predominant paw position is parallel to the body at initial contact

16 Consistent plantar stepping and Consistent FL-HL coordination during gait; and Toe clearance occurs frequently during forward limb advancement Predominant paw position is parallel at initial contact and rotated at lift off

Revised *2/25/94*

17 Consistent plantar stepping and Consistent FL-HL coordination during gait; and Toe clearance occurs frequently during forward limb advancement Predominant paw position is parallel at initial contact and lift off

18 Consistent plantar stepping and Consistent FL-HL coordination during gait; and Toe clearance occurs consistently during forward limb advancement Predominant paw position is parallel at initial contact and rotated at lift off

19 Consistent plantar stepping and Consistent FL-HL coordination during gait; and Toe clearance occurs consistently during forward limb advancement Predominant paw position is parallel at initial contact and lift off; and, Tail is down part or all of the time

20 Consistent plantar stepping and Consistent coordinated gait; consistent toe clearance; Predominant paw position is parallel at initial contact and lift off; and Trunk instability Tail consistently up

21 Consistent plantar stepping and Coordinated gait, consistent toe clearance, predominant paw position is parallel throughout stance, consistent trunk stability; tail consistently up

DEFINITIONS

Slight:	partial joint movement through less than 1/2 the range of joint motion
Extensive:	movement through more than half of the range of joint motion
Sweeping:	rhythmic movement of HL in which all three joints are extended, then fully flex and extend again; animal is usually side-lying and plantar surface of paw may or may not contact the ground; no weight support across the HL is evident
No Weight Support:	no contraction of the extensor muscles of the HL during plantar placement of the paw; or no elevation of the hindquarter
Weight Support:	contraction of the extensor muscles of the HL during plantar placement of the paw; or, elevation of the hindquarter
Plantar Stepping:	The paw is in ***plantar*** contact with weight support then the HL is advanced forward and *plantar* contact with weight support is re-established
Dorsal Stepping:	Weight is supported through the dorsal surface of the paw at some point in the step cycle.
F-HL Coordination:	For every FL step a HL step is taken and the HLs alternate
Occasional:	less than or equal to half *≤50%*
Frequent:	more than half but not always; 51-94%
Consistent:	nearly always or always; 95-100%
Trunk Instability:	Lateral weight shifts which cause waddling from side to side or a partial collapse of the trunk.

Revised *2/25/94*

Appendix 2: Jointly authored publication

The following attached publication (Irvine and Kwok 2018) contains results displayed in Chapter 3: Characterisation of perineuronal nets in the spinal motor pools.

Irvine SF, Kwok JCF. *Perineuronal Nets in Spinal Motoneurones: Chondroitin Sulphate Proteoglycan around Alpha Motoneurones*. International Journal of Molecular Sciences. 2018; 19(4):1172.

International Journal of
Molecular Sciences

MDPI

Article

Perineuronal Nets in Spinal Motoneurones: Chondroitin Sulphate Proteoglycan around Alpha Motoneurones

Sian F. Irvine [1] and Jessica C. F. Kwok [1,2,*]

[1] School of Biomedical Sciences, University of Leeds, Leeds LS2 9JT, UK; bs11sfi@leeds.ac.uk
[2] Centre of Reconstructive Neurosciences, Institute of Experimental Medicine, The Czech Academy of Sciences, Prague 4, Czech Republic
* Correspondence: J.Kwok@leeds.ac.uk; Tel.: +44-0113-343-9802

Received: 28 February 2018; Accepted: 7 April 2018; Published: 12 April 2018

Abstract: Perineuronal nets (PNNs) are extracellular matrix structures surrounding neuronal sub-populations throughout the central nervous system, regulating plasticity. Enzymatically removing PNNs successfully enhances plasticity and thus functional recovery, particularly in spinal cord injury models. While PNNs within various brain regions are well studied, much of the composition and associated populations in the spinal cord is yet unknown. We aim to investigate the populations of PNN neurones involved in this functional motor recovery. Immunohistochemistry for choline acetyltransferase (labelling motoneurones), PNNs using *Wisteria floribunda* agglutinin (WFA) and chondroitin sulphate proteoglycans (CSPGs), including aggrecan, was performed to characterise the molecular heterogeneity of PNNs in rat spinal motoneurones (Mns). CSPG-positive PNNs surrounded ~70–80% of Mns. Using WFA, only ~60% of the CSPG-positive PNNs co-localised with WFA in the spinal Mns, while ~15–30% of Mns showed CSPG-positive but WFA-negative PNNs. Selective labelling revealed that aggrecan encircled ~90% of alpha Mns. The results indicate that (1) aggrecan labels spinal PNNs better than WFA, and (2) there are differences in PNN composition and their associated neuronal populations between the spinal cord and cortex. Insights into the role of PNNs and their molecular heterogeneity in the spinal motor pools could aid in designing targeted strategies to enhance functional recovery post-injury.

Keywords: perineuronal nets; spinal cord; alpha motoneurone; gamma motoneurone; chondroitin sulphate proteoglycans

1. Introduction

Perineuronal nets (PNNs) are dense specialised extracellular matrix (ECM) structures that surround neuronal sub-populations throughout the central nervous system (CNS). First described by Golgi as reticular structures in the late 1800s [1], PNNs have since been implicated in pathologies of various neurological disorders, including Alzheimer's disease, epilepsy and schizophrenia [2–5], as well as in traumatic CNS injuries [6], particularly spinal cord injury (SCI) models [7,8]. A key role of PNNs is their involvement in the termination of developmental plasticity, where they form an interdigitating mesh with mature somatic and dendritic contacts to confer synaptic stabilisation [9–11].

PNNs are composed of a compact arrangement of a variety of neural ECM proteoglycans and proteins [12,13]. These components primarily consist of chondroitin sulphate proteoglycans (CSPGs) including the hyaluronan (HA) binding CSPGs called lecticans, bound upon a long HA backbone and stabilised by the HA and proteoglycan link proteins (HAPLNs) and tenascin-R [14]. Upon this basic PNN structure, the binding of other CSPGs (such as phosphacan) are thought to provide much

of the heterogeneity of PNNs [15]. CSPGs are composed of chondroitin sulphate glycosaminoglycan (CS-GAG) chains attached to a core protein that differentiates the various CSPGs from one another [15]. CS-GAGs confer a further vast degree of heterogeneity through variation of expression, chain length and sulphation patterns, even to the same core protein [16,17].

Although many studies have investigated the molecular heterogeneity of PNNs in distinct neuronal populations in regions of the brain [18–21], much of the composition and associated populations in the spinal cord is relatively unknown. Similar to the brain [22], in the spinal cord many of the known cells enwrapped by PNNs are fast-spiking inhibitory parvalbumin (PV)-positive interneurones (approximately half) [23,24], and have also been associated with calbindin-positive Renshaw cells [22]. However, in contrast to the brain, reports suggest that PNNs in the spinal cord also surround cells with large neuronal cell bodies, particularly within the ventral horn likely representing motoneurones (Mns) [22,25–27]. Mns are a heterogeneous population of neurones with the main subclasses, alpha and gamma Mns, innervating contractile extrafusal fibres and proprioceptive intrafusal fibres within the motor unit, respectively [28].

Enzymatic removal of PNNs using chondroitinase ABC (ChABC) after CNS injury has been shown in multiple models, predominately SCI, to reopen a window of plasticity to promote improvements in motor functions [7,8]. Regeneration of descending tracts can contribute to this functional recovery [29,30]; however, the extent and mechanism of changes in local spinal circuitry attributing to this recovery remains unclear. Additionally, studies also implicate exercise and rehabilitative training to activity-dependant modulation of PNNs in the ventral motor pools [31,32], suggesting a relationship between PNNs and Mns that is important for normal motor functions.

This study therefore aims to investigate the normal expression and molecular composition of PNNs in the spinal motor pools; the population of PNN-associated neurones in the spinal cord likely to be involved in functional motor recovery after SCI, and to identify the best PNN marker for this population. Immunohistochemical staining was performed using antibodies against choline acetyltransferase (ChAT), a marker of spinal Mns [33], alongside labelling for primary PNN components, including various CSPGs and the acclaimed "universal" PNN marker *Wisteria floribunda* agglutinin (WFA), to elucidate the composition of PNNs associated with spinal motor circuitry. Selective staining for the primary functional Mn subclasses was combined with PNN labelling to categorise PNN expression within the motor pool. It was found that distinct populations of Mns were surrounded by PNNs labelled by various CSPGs yet lacking WFA, indicating a difference between the composition of PNNs and associated neuronal cell types in the brain and spinal cord. PNNs were found to surround the majority of alpha Mns, suggesting that these are the main populations affected by ChABC-mediated recovery after SCI.

2. Results

We aim to determine the molecular heterogeneity of PNNs in the spinal cord, with a particular focus to the Mns in the ventral horn. Spinal cord sections from three different spinal levels, cervical, thoracic and lumbar, were used to compare the spatial differences of PNNs. Alongside ChAT staining, we also stained for WFA, a common PNN marker [6,7,10,34], and for CSPGs including aggrecan (ACAN), brevican (BCAN), neurocan (NCAN), versican (VCAN) and phosphacan (PTPRZ).

2.1. WFA-Positive PNNs Only Partially Overlap with Other CSPGs in the Ventral Motor Pools

2.1.1. ACAN

ACAN is a CSPG in the lectican family and is widely considered to be a major component in PNNs [2,35,36]. Immunohistochemical staining of ACAN core protein illustrated clear expression of PNNs surrounding ventral Mns labelled with ChAT (Figure 1J–L). ACAN-positive PNNs surrounded approximately 85% of ChAT-positive Mns in all levels of the spinal cord investigated (Figure 1A–C). In comparison, WFA-positive PNNs enwrapped significantly fewer Mns (approximately 68% of the

ChAT-positive Mns) than ACAN-positive PNNs (cervical $p < 0.001$, thoracic $p < 0.05$ and lumbar $p < 0.01$; $n = 4$), illustrating that WFA does not label all PNNs in the ventral motor pools. Compounding this, the total number of ACAN-positive PNNs surrounding Mns was significantly greater than the number of ACAN+/WFA+ PNNs (cervical $p < 0.001$, thoracic $p < 0.05$, lumbar $p < 0.01$; $n = 4$). ACAN and WFA PNN populations appeared to overlap (Figure 1D–I). Further breakdown of PNN type revealed that, at each level, all PNNs that are positive for WFA co-localised with ACAN (n.s.; $p = 1$). No investigated PNNs were WFA-positive and ACAN-negative. The results demonstrate that ACAN labels a larger population of PNN-positive Mns, and suggest that it is a better marker for PNN in the spinal cord.

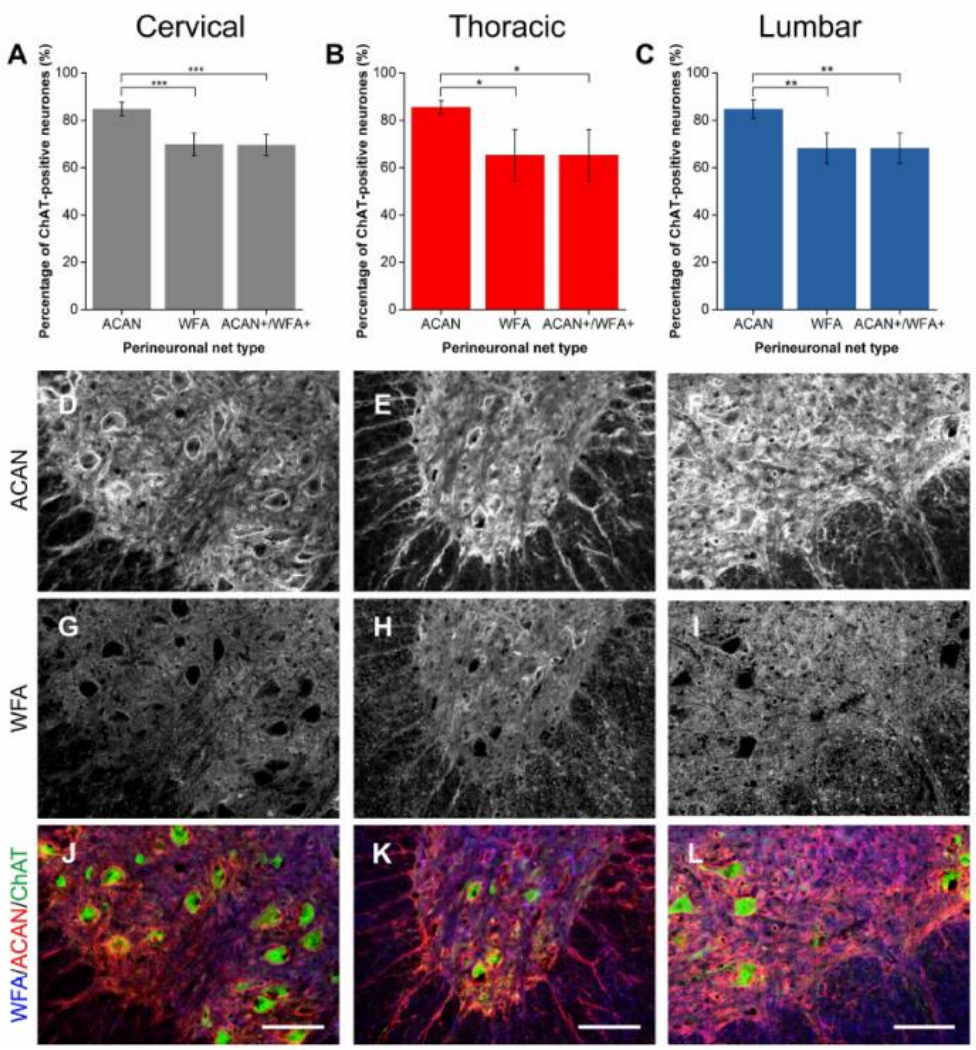

Figure 1. Comparison of perineuronal nets (PNNs) in the spinal ventral motor pools labelled by *Wisteria floribunda* agglutinin (WFA) and aggrecan (ACAN). (**A**–**C**) Bar graphs showing percentage of ChAT-positive motoneurones (Mns) in the ventral motor pools surrounded by ACAN-positive and WFA-positive PNNs and their co-localisation (ACAN+/WFA+) in cervical (**A**), thoracic (**B**) and lumbar (**C**) rat spinal cord. Error bars ± SD; $n = 4$. Statistics one-way ANOVA; significance levels: * $p < 0.05$, ** $p < 0.01$, *** $p < 0.001$. Confocal images showing ACAN-positive (**D**–**F**) and WFA-positive (**G**–**I**) PNNs surrounding ChAT-positive Mns (**J**–**L**) in the cervical, thoracic and lumbar spinal cord, respectively. Scale bars, 100 µm.

2.1.2. BCAN

BCAN is a lectican CSPG found specifically in the CNS with growing evidence of its importance in regulating the plastic properties of PNNs [37]. Co-staining with ChAT-positive neurones in the ventral horn revealed a high degree of localisation, with approximately 88% of Mns encircled by BCAN-positive PNNs (Figure 2A–C). Similar to ACAN, WFA-positive PNNs appeared to denote some but not all of the BCAN-positive PNN-ensheathed Mns, labelling approximately 30% fewer Mns than BCAN (all levels $p < 0.001$; $n = 5$). BCAN+/WFA+ PNNs in the motor pools appeared to represent a proportion that is significantly less that the total BCAN-positive PNN population (all levels $p < 0.001$; $n = 5$). Additional categorisation again revealed that all WFA-positive PNNs in the motor pool co-localised with BCAN-positive PNNs.

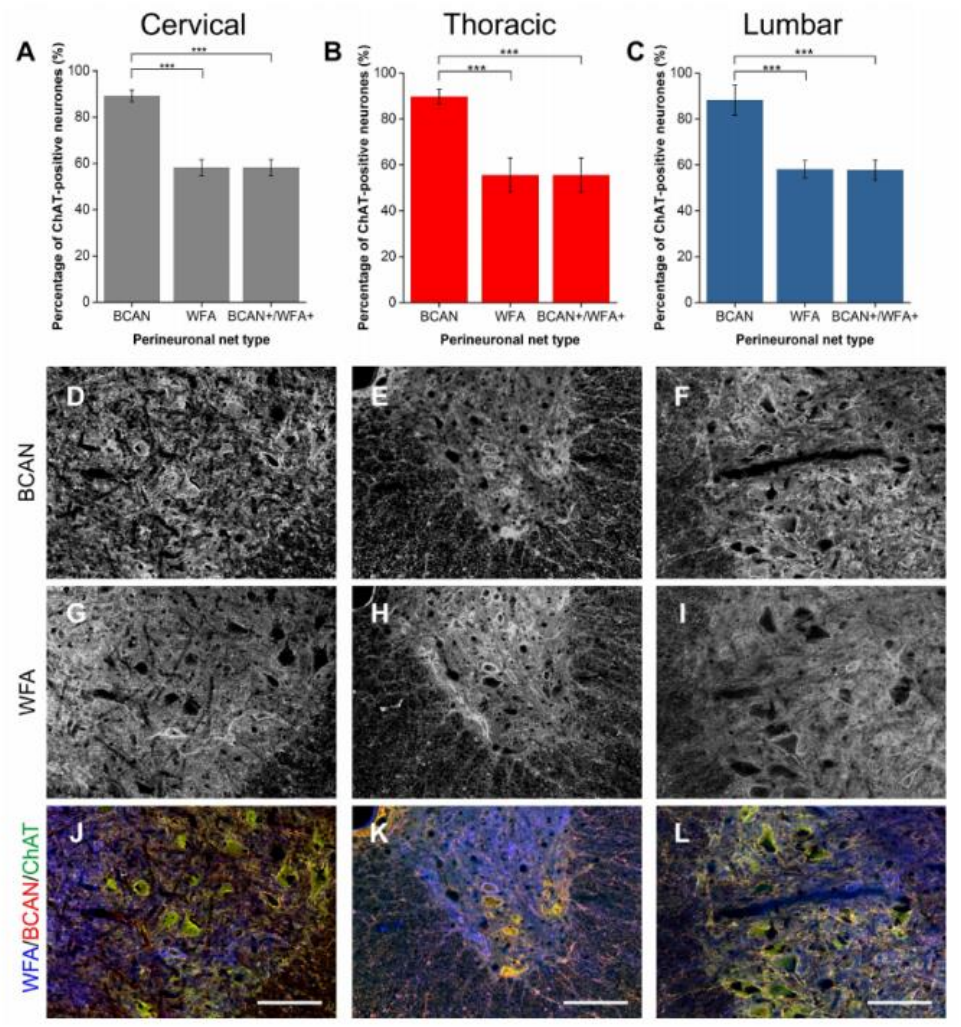

Figure 2. Comparison of perineuronal nets (PNNs) in the spinal ventral motor pools labelled by *Wisteria floribunda* agglutinin (WFA) and brevican (BCAN). (**A**–**C**) Bar graphs showing percentage of ChAT-positive motoneurones (Mns) in the ventral motor pools surrounded by BCAN-positive and WFA-positive PNNs and their co-localisation (BCAN+/WFA+) in cervical (**A**), thoracic (**B**) and lumbar (**C**) rat spinal cord. Error bars ± SD; $n = 5$. Statistics one-way ANOVA; significance levels: *** $p < 0.001$. Confocal images showing BCAN-positive (**D**–**F**) and WFA-positive (**G**–**I**) PNNs surrounding ChAT-positive Mns (**J**–**L**) in the cervical, thoracic and lumbar spinal cord, respectively. Scale bars, 100 µm.

2.1.3. NCAN

NCAN is a nervous system-specific lectican, like BCAN, known to be present in PNNs in the spinal cord [18,22,38]. In the ventral horn, NCAN staining revealed PNNs encircling approximately 87% of Mns (Figure 3A–C). Echoing the trend with ACAN and BCAN, WFA-positive PNNs enveloped 28% fewer Mns than NCAN (all levels $p < 0.001$; $n = 5$). Significantly, only approximately two-thirds of these NCAN-positive PNNs co-localised with WFA (all levels $p < 0.001$; $n = 5$). No WFA-positive PNNs lacking NCAN co-staining were observed, signifying that all WFA co-localised with NCAN.

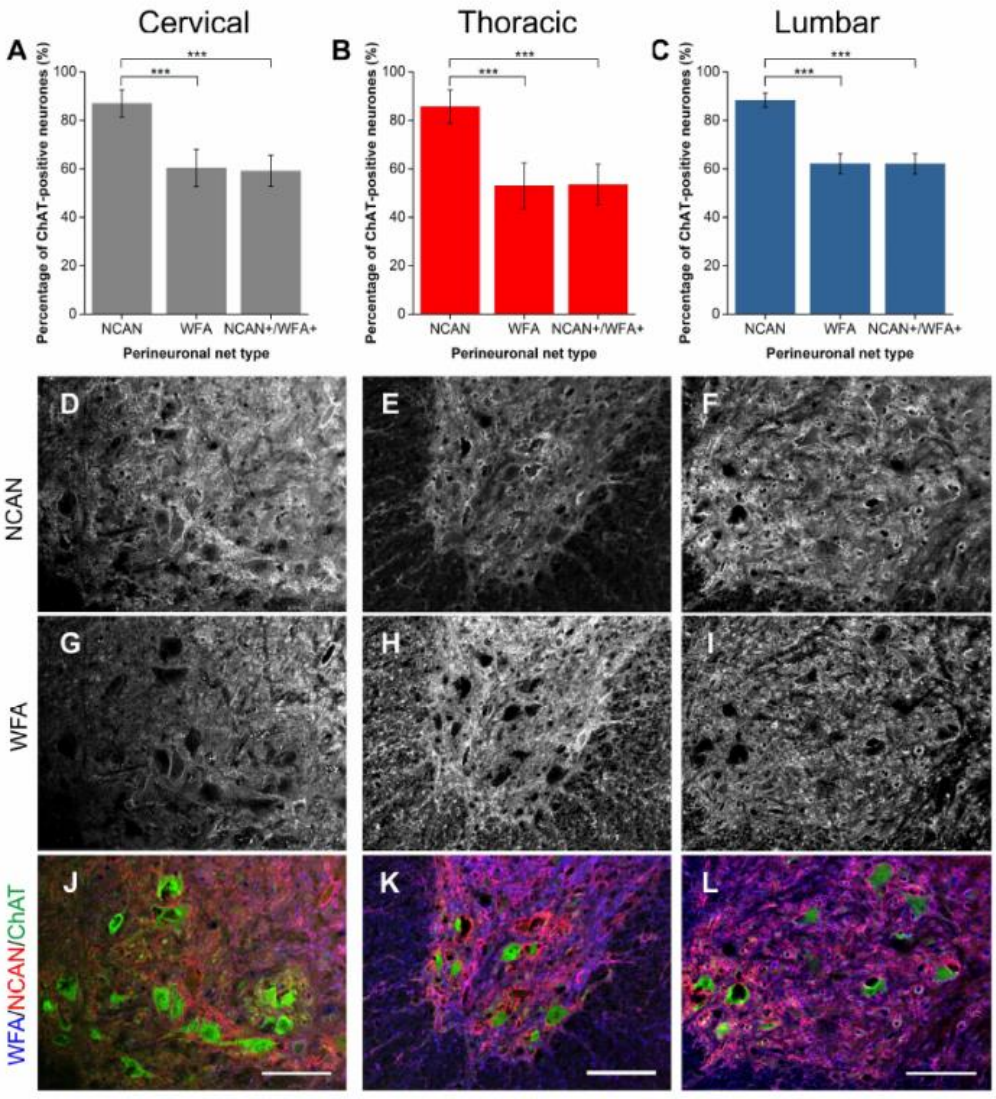

Figure 3. Comparison of perineuronal nets (PNNs) in the spinal ventral motor pools labelled by *Wisteria floribunda* agglutinin (WFA) and neurocan (NCAN). (**A**–**C**) Bar graphs showing percentage of ChAT-positive motoneurones (Mns) in the ventral motor pools surrounded by NCAN-positive and WFA-positive PNNs and their co-localisation (NCAN+WFA+) in cervical (**A**), thoracic (**B**) and lumbar (**C**) rat spinal cord. Error bars ± SD; $n = 5$. Statistics: one-way ANOVA; significance levels: *** $p < 0.001$. Confocal images showing NCAN-positive (**D**–**F**) and WFA-positive (**G**–**I**) PNNs surrounding ChAT-positive Mns (**J**–**L**) in the cervical, thoracic and lumbar spinal cord, respectively. Scale bars, 100 µm.

2.1.4. VCAN

VCAN staining revealed intense diffuse ECM expression in both the white and gray matter of the spinal cord due to its expression in the nodes of Ranvier [18,39,40]. VCAN did not show strong PNN staining in laminae other than the ventral horn. In the ventral horn, VCAN-positive PNNs surrounded approximately 82% of Mns at all spinal levels (Figure 4A–C). WFA and VCAN populations of PNNs showed a clear overlap at all spinal levels (Figure 4D–L). However, all WFA-positive PNNs co-localised with VCAN with a significant population of VCAN-positive PNNs WFA-negative (all levels $p < 0.001$; $n = 4$).

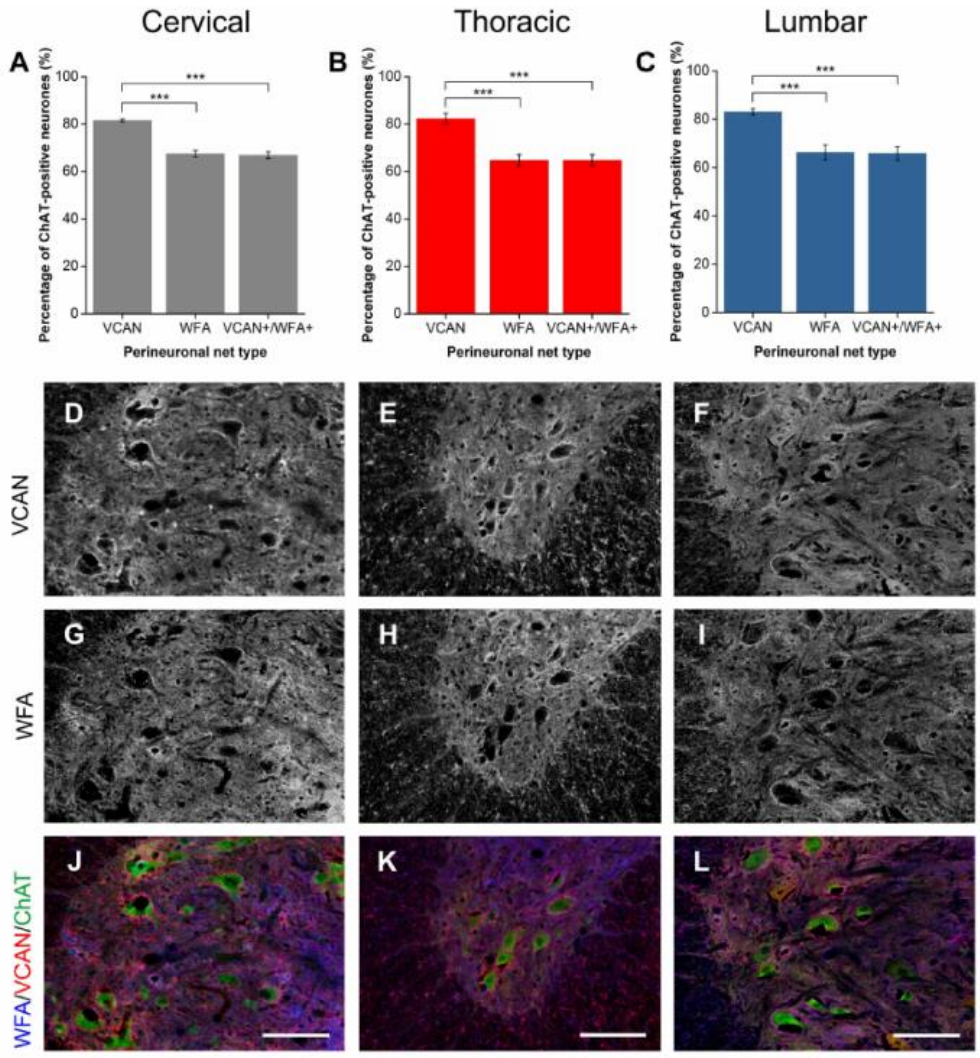

Figure 4. Comparison of perineuronal nets (PNNs) in the spinal ventral motor pools labelled by *Wisteria floribunda* agglutinin (WFA) and versican (VCAN). (A-C) Bar graphs showing percentage of ChAT-positive motoneurones (Mns) in the ventral motor pools surrounded by VCAN-positive and WFA-positive PNNs and their co-localisation (VCAN+/WFA+) in cervical (**A**), thoracic (**B**) and lumbar (**C**) rat spinal cord. Error bars ± SD, $n = 4$. Statistics: one-way ANOVA; significance levels: * $p < 0.05$, ** $p < 0.01$, *** $p < 0.001$. Confocal images showing VCAN-positive (**D**–**F**) and WFA-positive (**G**–**I**) PNNs surrounding ChAT-positive Mns (**J**–**L**) in the cervical, thoracic and lumbar spinal cord, respectively. Scale bars, 100 µm.

2.1.5. PTPRZ

Phosphacan or PTPRZ is a non-HA binding CSPG that represents the extracellular domain of protein tyrosine phosphatase receptor zeta (PTPRZ) modified by glial cells [41,42] and has been found to be present in WFA-positive PNNs in the cerebral cortex [18,22,43]. Immunohistochemistry showed that PTPRZ is also found in PNNs in the ventral motor pool, surrounding approximately 76% of Mns in all levels of the cord studied (Figure 5A–C). However, in all levels of the spinal cord investigated, PTPRZ-positive PNNssurrounded 15% more Mns than WFA (all levels $p < 0.01$; $n = 4$), reiterating the trend shown by the lecticans above. Approximately 82% of PTPRZ-positive PNNs were also labelled by WFA, representing a significantly lower proportion of the total observed PTPRZ-positive PNNs in the motor pool (all level $p < 0.05$; $n = 4$).

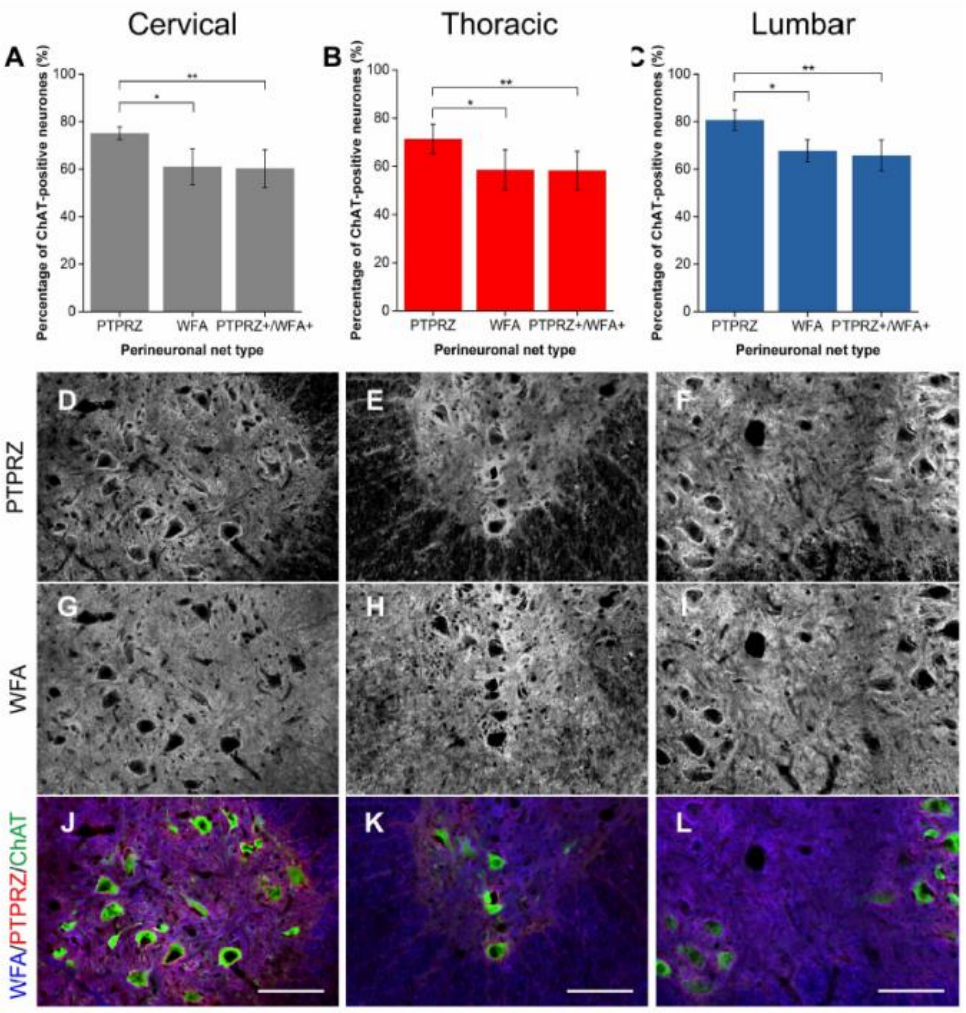

Figure 5. Comparison of perineuronal nets (PNNs) in the spinal ventral motor pools labelled by *Wisteria floribunda* agglutinin (WFA) and phosphacan (PTPRZ). (**A**–**C**) Bar graphs showing percentage of ChAT-positive motoneurones (Mns) in the ventral motor pools surrounded by PTPRZ-positive and WFA-positive PNNs and their co-localisation (PTPRZ+/WFA+) in cervical (**A**), thoracic (**B**) and lumbar (**C**) rat spinal cord. Error bars ± SD; $n = 4$. Statistics: one-way ANOVA; significance levels: * $p < 0.05$, ** $p < 0.01$. Confocal images showing PTPRZ-positive (**D**–**F**) and WFA-positive (**G**–**I**) PNNs surrounding ChAT-positive Mns (**J**–**L**) in the cervical, thoracic and lumbar spinal cord, respectively. Scale bars, 100 µm.

2.2. Distinct Populations of CSPG-Positive yet WFA-Negative PNNs in the Motor Pools

For each CSPG investigated, a significant percentage of Mns were surrounded by PNNs that were CSPG-positive yet WFA-negative (all levels, all CSPGs $p < 0.001$). The percentage of Mns with WFA-negative PNNs varied with CSPG investigated (Figure 6). While ACAN+/WFA−, VCAN+/WFA− and PTPRZ+/WFA− PNNs encircled roughly 15% of Mns (Figure 6A,D,E), a higher percentage of Mns (approximately 30%) appeared to be surrounded by BCAN+/WFA− and NCAN+/WFA− PNNs (Figure 6B,C). Overall, the results suggest that in the ventral motor pools, WFA does not denote all PNNs, and instead distinct populations of Mns with CSPG-positive, WFA-negative PNNs exist.

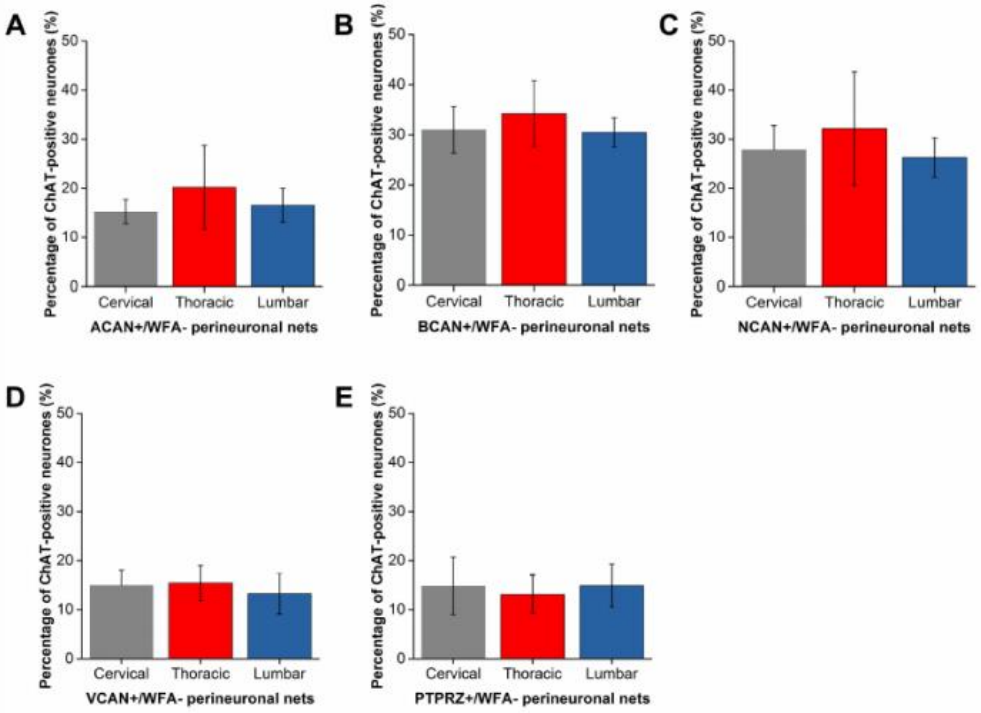

Figure 6. A proportion of perineuronal nets (PNNs) in the spinal motor pools were negative for *Wisteria floribunda* agglutinin (WFA). Percentage of ChAT-positive motoneurones in the ventral motor pools in the cervical, thoracic and lumbar spinal cord surrounded by CSPG-positive, WFA-negative PNNs. (**A**) Aggrecan (ACAN, $n = 4$); (**B**) brevican (BCAN, $n = 5$); (**C**) neurocan (NCAN, $n = 5$); (**D**) versican (VCAN, $n = 4$); and (**E**) phosphacan (PTPRZ, $n = 4$). Error bars ± SD. Statistics one-way ANOVA; n.s.

2.3. Alpha Mns Are Preferentially Surrounded by PNNs

Using NeuN and ChAT co-labelling, Mns in the spinal ventral motor pools were selectively labelled as either alpha (NeuN-positive) or gamma (NeuN-negative) [31,44]. It was observed that approximately 70–80% of ChAT-positive Mns were NeuN-positive (Figures 7 and 8), signifying thealpha Mn population. Firstly, as the universal marker for PNNs, WFA was used to determine the number of PNNs surrounding each Mn subtype. Similarly to the results above, WFA-positive PNNs surrounded approximately 60% of all Mns with approximately 98% of these PNNs surrounding NeuN-positive Mns (alphas; Figure 7A–C). In other words, a significant proportion of alpha Mns (~72%) were associated with WFA-positive PNNs (cervical and lumbar $p < 0.001$, thoracic $p < 0.05$; $n = 3$). As previous findings illustrated that in the ventral motor pools, WFA did not label all Mns, ACAN was also used to identify PNNs around Mn subtype. Again, most PNNs (95%) surrounded

alpha Mns (Figure 8A–C). ACAN-positive PNNs encircled roughly 90% of alpha Mns, suggesting that PNN-positive Mns and alpha Mns are the same population.

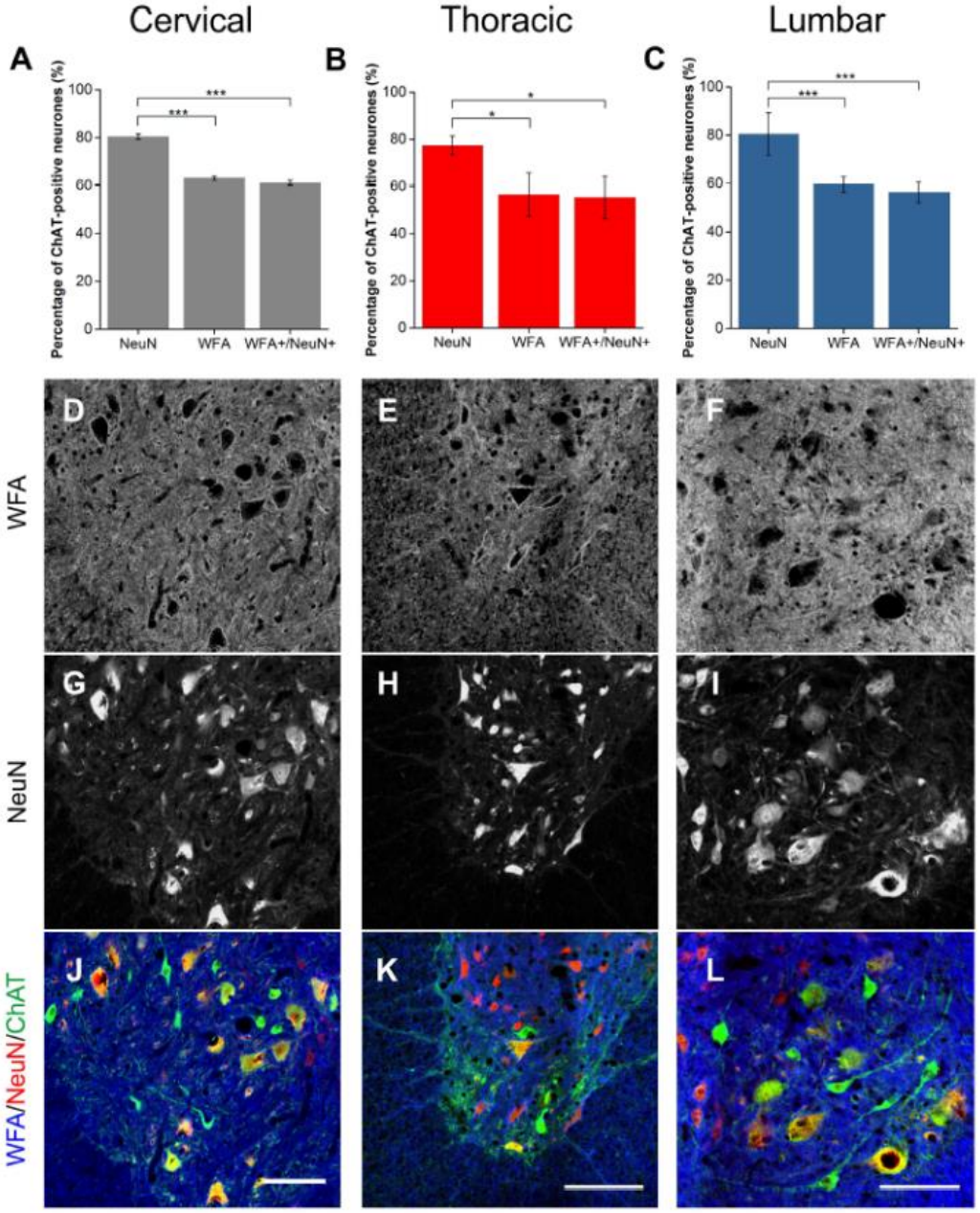

Figure 7. *Wisteria floribunda* agglutinin (WFA)-positive PNNs surrounded some but not all alpha motoneurones (Mns). (**A**–**C**) Bar graphs showing percentage of ChAT-positive Mns in the ventral motor pools surrounded by NeuN, WFA-positive PNNs and their co-localisation (WFA+/NeuN+) in cervical (**A**), thoracic (**B**) and lumbar (**C**) rat spinal cord. NeuN and ChAT co-localisation denotes alpha Mns. Error bars ± SD; $n = 3$. Statistics: one-way ANOVA; significance levels: * $p < 0.05$, *** $p < 0.001$. Confocal images showing WFA-positive PNNs (**D**–**F**) surrounding NeuN-positive (**G**–**I**) PNNs and ChAT-positive Mns (**J**–**L**) in the cervical, thoracic and lumbar spinal cord, respectively. Scale bars, 100 µm.

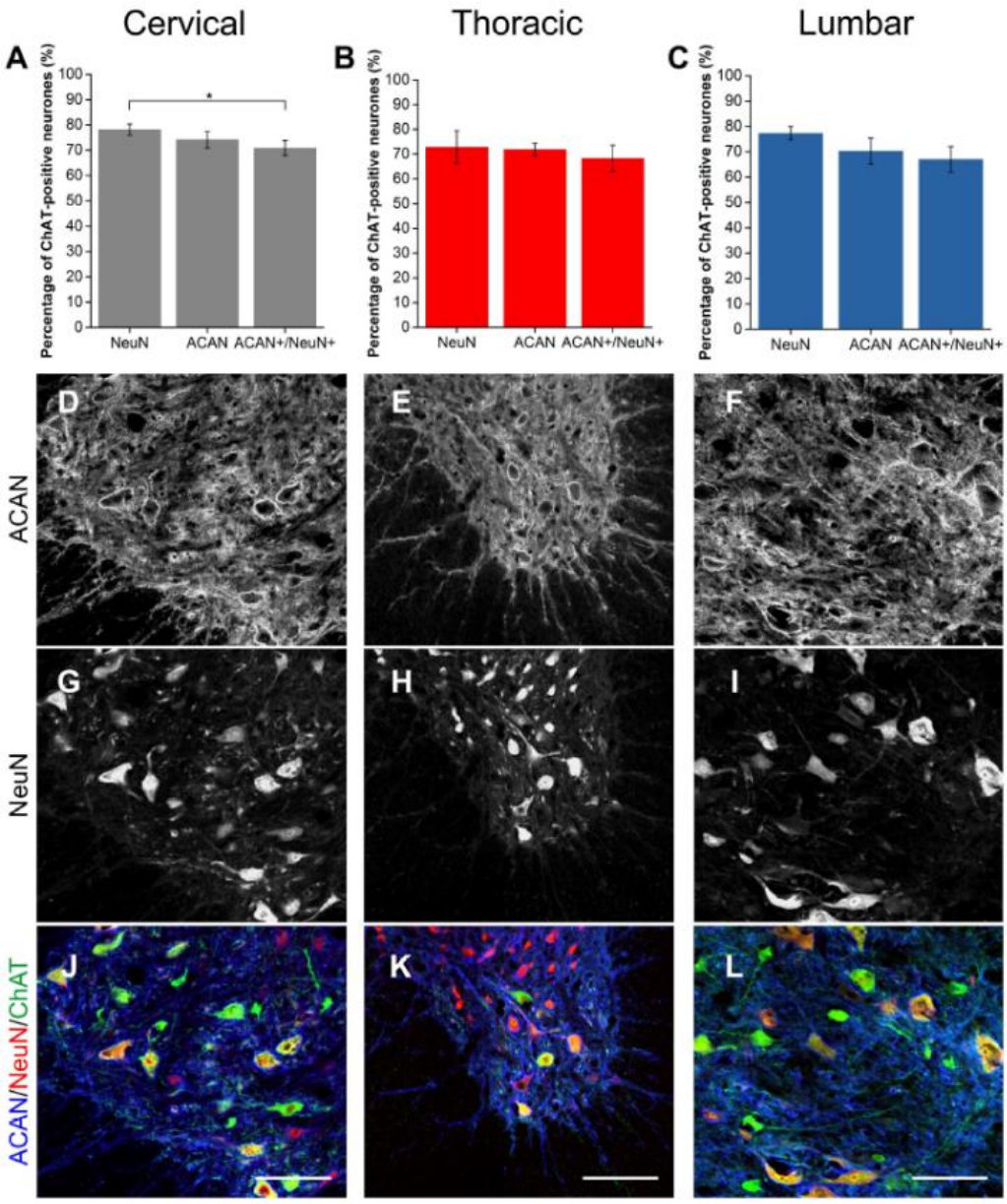

Figure 8. Aggrecan (ACAN)-positive PNNs surrounded most alpha motoneurones (Mns). (**A**–**C**) Bar graphs showing percentage of ChAT-positive Mns in the ventral motor pools surrounded by NeuN, ACAN-positive PNNs and their co-localisation (ACAN+/NeuN+) in cervical (**A**), thoracic (**B**) and lumbar (**C**) rat spinal cord. NeuN and ChAT co-localisation denotes alpha Mns. Error bars ± SD; $n = 3$. Statistics: one-way ANOVA; significance levels: * $p < 0.05$. Confocal images showing ACAN-positive PNNs (**D**–**F**) surrounding NeuN-positive (**G**–**I**) PNNs and ChAT-positive Mns (**J**–**L**) in the cervical, thoracic and lumbar spinal cord, respectively. Scale bars, 100 µm.

3. Discussion

As removal of PNNs in the spinal cord after injury enhances motor recovery, we looked to investigate the expression of PNNs and their heterogeneity in spinal Mns; the final order neurones for

the control of voluntary movement. This is the first article to systemically and quantitatively compare the differences of CSPG- or WFA-positive PNN Mns in the ventral motor pools. Mns were identified using an antibody against ChAT to label cholinergic neurones alongside markers for PNN components and the acclaimed universal PNN marker WFA in comparison. We demonstrated that a high proportion of Mns in the ventral spinal cord were surrounded by PNNs, particularly alpha Mns. Unexpectedly, the universal marker for PNNs, WFA, did not label all of the PNNs with distinct populations of Mns surrounded by CSPG-positive yet WFA-negative PNNs. This suggests that, in contrast to the brain, WFA does not label the majority of PNN neurones in the ventral spinal cord and that studies using WFA in the spinal cord may be underestimating the number of PNNs.

3.1. PNNs in the Spinal Ventral Motor Pools

Previous studies have described ventral Mns as the most conspicuous neuronal population in the spinal cord to be surrounded by PNNs and this appears to be conserved across mammalian species [25,31,32,45,46]. Despite this, few studies have actually investigated the proportion of PNNs in the ventral motor pools and those that do use varying markers to determine this. Comparable to our own methods, using ChAT as a specific Mn marker, a similar proportion of ventral Mns was observed to be surrounded by PNNs to that found in our study (~80%) has been reported in non-human primates (75%), using WFA [45], and in human (71%) spinal cord, using ACAN [46]. In rats, however, this distribution has been investigated with the general neuronal marker (NeuN) using size and ventral location to identify Mns alongside WFA lectin staining to characterise PNN expression, resulting in estimates of only 30% of Mns associated with PNNs [25]. This is likely to underestimate for two reasons: (1) without a Mn-specific neuronal marker small sized Mns, including NeuN-negative gamma Mns [44,47], would have been absent from these counts, and (2) WFA does not appear to label all PNNs in the rat spinal cord. Indeed, our findings suggest that PNNs are present in almost 80% of the ChAT-positive Mns.

Although others have implicated that PNNs only surround large cell-bodied Mns in the motor pools, i.e., alpha Mns and not gamma Mns [25,31], we are the first to systematically categorise the proportion of specific Mn-subtypes associated with PNNs at different levels of the spinal cord. Despite contributing to the same goal of voluntary muscle control, alpha and gamma Mns represent distinct populations of Mns within the ventral motor pools, differing in both electrical and molecular properties [28,44,48,49]. These differences also include the innervation of different muscle targets, with alpha Mns responsible for force generation though contraction of extrafusal fibres whereas gamma Mns innervate the intrafusal fibres regulating muscle spindle sensitivity. The high proportion of enveloped alpha Mns revealed likely reflects the importance of the role of PNNs in providing synaptic stabilisation of inputs from the specific spinal circuitry and consequent contractile innervation of key muscle groups. After SCI, the stabilisation of synaptic plasticity conferred by PNNs instead becomes another mechanism inhibiting regenerative attempts and compensatory rearrangements of spared fibres. We suggest that ChABC-mediated removal of PNNs in SCI models is therefore able to induce a high degree of enhanced plasticity of synaptic connections to the abovementioned populations of alpha Mns contributing to the observed improvement of most functional motor recovery studies.

3.2. Differences in PNNs between the Brain and Spinal Cord

It is generally assumed that PNNs in the brain and the spinal cord are the same. While in the brain, WFA does not always co-localise with ACAN as previously discussed, other CSPG-positive PNNs always co-localise with WFA. Here, we demonstrate differences in the composition of PNNs between the brain and spinal cord, where ACAN and other CSPGs denote subclasses of Mns in the spinal cord lacking WFA. This study recommends that future staining for PNNs associated with the spinal motor pools, particularly SCI studies utilising therapies that modify PNNs such as ChABC, should seek alternatives to WFA to avoid underestimating total PNN number.

Additionally, brain PNNs are well known to target small fast-spiking inhibitory interneurones playing a modulatory role in the brain [50]. In sharp contrast, the associated neuronal populations studied here are large cell bodied neurones acting as the primary endpoint of neural control of the somatic motor system. Other neuronal cell types such as calbindin-positive Renshaw cells in the ventral spinal cord are surrounded by PNNs [22], further implicating the role of PNNs in stabilisation of connections within the spinal motor circuitry. In a recent systematic review of the CNS, motor regions, including the cerebellum and spinal cord, were more likely to have a higher proportion of neurones surrounded by PNNs than sensory structures [45]. It is possible that PNNs may have different roles in different parts of the nervous system or with different neuronal populations.

3.3. Composition of PNNs in the Spinal Motor Pools

Staining with the lectin WFA and antibodies for various CSPG core proteins revealed two distinct types of distributions throughout the grey matter: diffuse extracellular staining and a bright 'halo' of pericellular expression identifying the PNNs. The overall distributions of immunoreactivities for the CSPGs investigated and ChAT were generally similar to previous descriptions [18,22,25,33]. We showed that all of the CSPGs investigated were present in PNNs surrounding spinal Mns. These were also found to be present to varying degrees, indicating heterogeneity of PNNs in the motor pools.

ACAN in particular has been previously reported to be present in PNNs surrounding Mns [22,51,52], as well as BCAN, NCAN, VCAN and PTPRZ. It is estimated that VCAN begins to appear in PNNs around the Mns from postnatal day 8 [53]. Studies in the brain and spinal cord show that ACAN is present in all PNNs and generally co-localises with WFA expression [12,18,25]. However, consistent with all CSPGs investigated, WFA does not appear to show all PNN-associated neurones in the ventral motor pools. As WFA is supposed to bind to the CS-GAG sugar *N*-acetylgalactosamine (GalNAc) [50], it should bind to all CSPGs and therefore denote all PNNs. However, binding of WFA has previously been shown to be dependent on the presence of ACAN [12] and recently other studies in various regions of the brain, including the hippocampus, have reported PNNs with ACAN labelling but no WFA binding [21,54]. In the spinal cord, we observed a lack of WFA in ACAN-positive PNNs to a similar degree to that observed in the CA1 area of the hippocampus [21], appearing to denote distinct populations of Mns. As there is a vast degree of heterogeneity of CS-GAGs within CSPGs, further research is required to determine the conditions of WFA binding. It is possible that the molecular composition of CSPGs within PNNs may confer functional subclasses of Mns.

The expression of many PNN components such as ACAN, BCAN and tenascin-R show differences in expression between various brain regions [55]. In particular, BCAN is usually found at the para-nodal regions and has been shown to regulate the localisation of potassium channels and AMPA receptors [37]. The mechanism of how brevican performs these functions remains to be determined. Expression of CSPGs in PNNs across the spinal laminae has also been shown to display differential expression [22,25]. PNNs are a dynamic network of ECM components. Activity-dependant modulation has been demonstrated where the thickness of PNNs surrounding spinal Mns increases in response to exercise or rehabilitative training [31,32]. This is likely conveyed through dynamic regulation of CSPGs and/or CS-GAGs within the PNNs. There is a growing concept that the properties of the ECM have an important influence in both healthy and pathological states. Though it is beyond the scope of this study, it is hoped that further research into the heterogeneity of PNNs in CNS regions may help to unravel the functionality of these ECM components and their alterations in disease states.

3.4. Further Research and Conclusions

Despite the clinical relevance of PNNs targeted for CNS repair and regeneration, particularly in locomotor recovery models of SCI, the functional relationship between PNNs and the motor system is still mostly unexplored. Further research is required to look at the normal functional properties of PNNs surrounding Mns. Additionally, the molecular heterogeneity of PNNs displayed in spinal Mns

may indicate a functional role. However, understanding how the varying molecular heterogeneity of PNNs affects CNS functions is a topic still in its infancy.

Though this study begins to address a research gap surrounding the properties of PNNs in the spinal cord, much characterisation remains to be done. While ChABC has been an invaluable investigative tool for understanding the role of PNNs in promoting plasticity and functional recovery after SCI, there are clinical limitations to its therapeutic use. It is hoped that insights into the properties of PNNs and their role in the spinal cord could aid the generation of alternative and non-invasive strategies for targeted PNN removal to enhance functional recovery post-injury.

4. Materials and Methods

4.1. Animals

Female Lister Hooded rats (200–250 g; n = 5) were obtained from Charles River Laboratories (Canterbury, UK) and were housed in groups in Central Biomedical Services (University of Leeds) in a temperature controlled environment (20 ± 1 °C), with a 12 h light/dark cycle (lights on at 07:00). Access to food and water was *ad libitum*. All procedures and experiments complied with the UK Animals (Scientific Procedures) Act 1986.

4.2. Tissue Preparation

Animals were given an overdose of sodium pentobarbital (Pentoject; Henry Schein; 200 mg/kg; intraperitoneal injection) to deeply anaesthetise without halting cardiac function. A transcardial perfusion [56] was then performed using sodium phosphate buffer (PB; 0.12 M sodium phosphate monobasic; 0.1 M NaOH; pH 7.4) followed by 4% paraformaldehyde (PFA; in PB; pH 7.4) for tissue fixation. The spinal cord was dissected out, post-fixed in PFA (4%; 4 °C) overnight and cryoprotected in 30% sucrose solution (30% v/w sucrose in PB; 4 °C) until tissue saturation. The appropriate cervical (C3-T1), mid-thoracic and lumbar (L1-6) spinal cord segments were removed and frozen in optimum temperature medium (OCT; Leica FSC 22 Frozen Section Media; Leica Biosystems) before storage at −80 °C until sectioning. Tissue was cut using a cryostat (Leica CM1850; Leica Biosystems) into 40 µm transverse sections. Sections were serially collected into 48-well plates containing physiological buffer solution (PBS; 0.13 M NaCl, 0.7 M sodium phosphate dibasic, 0.003 M sodium phosphate monobasic; pH 7.4) to remove the OCT before being transferred to 30% sucrose solution for storage at 4 °C.

4.3. Staining Procedures

Immunohistochemical techniques were used to label for cells in the spinal cord containing ChAT and the PNNs surrounding subsets of these cells labelled by biotinylated *Wisteria floribunda* agglutinin (bio-WFA) and CSPG components, including ACAN, BCAN and NCAN (Table 1). ChAT was used for Mn identification [57] whilst WFA is universally used as a marker for PNNs [10,12].

At room temperature (RT), free-floating sections were washed three times for 5 min each in Tris-buffered saline (TBS; 0.1 M tris base, 0.15 M NaCl; pH 7.4) to remove sucrose residue. Tissue was then blocked in 0.3% TBST (1× TBS solution and 0.3% v/v Triton X-100) and 3% normal donkey serum (NDS; v/v) for two hours. The sections were then transferred to co-incubate at 4 °C in blocking buffer (3% NDS in 0.3% TBST; pH 7.4) containing the following primary antibodies: anti-ChAT (goat; Millipore; 1:500; 48 h), biotin-conjugated *Wisteria floribunda* agglutinin (bio-WFA; Sigma; 1:150; 24 h) and either ACAN (rabbit; Millipore; 1:250; 24 h), BCAN (mouse; DSHB; 1:500; 24 h), NCAN (mouse; DSHB; 1:100; 24 h), VCAN (mouse; DSHB; 1:100; 24 h) or PTPRZ (mouse; DSHB; 1:80; 24 h) (Table 1).

Table 1. Immunohistochemical detection of extracellular matrix components and neuronal markers, including concentration (conc.) of antibody used.

Detected Component	Marker	Host	Antibody Conc.	Source	Characterisation
CSPGs					
Aggrecan (mouse ACAN core protein)	Anti-ACAN	Rabbit polyclonal IgG	500 µg/mL	Millipore #AB1031	WB[2] (Lendvai et al., 2013 & Sutkus et al., 2014)
Brevican (BCAN; mouse cell-line derived recombinant human Brevican)	Anti-BCAN	Sheep polyclonal IgG	1 mg/mL	R&D Systems #AF4009	WB[2] (R&D Systems data sheet)
Neurocan (NCAN; N-terminal epitope)	Anti-NCAN	Mouse monoclonal IgG	369 µg/mL	DSHB[1] #1F6	WB[2] (Asher et al., 2000 & Deepa et al., 2006)
Versican (VCAN; hyaluronate-binding region)	Anti-VCAN	Mouse monoclonal IgG	169 µg/mL	DSHB[1] #12C5	WB[2] (Asher et al., 2002 & Deepa et al., 2006)
Phosphacan (PTPRZ)	Anti- PTPRZ	Mouse monoclonal IgG	165 µg/mL	DSHB[1] #3F8	WB[2] (Deepa et al., 2006 & Vitellaro-Zuccarello et al., 2006)
Lectins					
N-acetylgalactosamine (GalNAc)	Biotinylated *Wisteria floribunda* agglutinin (WFA)	N/A	2 mg/mL	Sigma #L1766	Koppe et al., 1996
Neuronal markers					
Choline acetyltransferase (ChAT)	Anti-ChAT	Goat polyclonal IgG	-	Millipore #AB144P	-
Neuron-specific nuclear protein (NeuN)	Anti-NeuN	Mouse monoclonal IgG	1 mg/mL	Millipore #MAB377	WB[2] (Jin et al., 2003)

[1] DSHB, Developmental Studies Hybridoma Bank, University of Iowa, USA. [2] WB, Western blotting.

Immunostaining was routinely carried out using tissue from different animals and differing spinal segments. The combinations carried out in this study used the formula: ChAT—Bio-WFA—CSPG marker using various antibodies from Table 1, including for the lecticans ACAN, BCAN, NCAN and VCAN. To differentiate between alpha and gamma Mns [31,44], ChAT was co-stained with anti-NeuN (mouse; Millipore; 1:500; 24 h). Antibodies requiring 24-h incubation were added and mixed well 48 h into a 72-h incubation with ChAT, using the protocols as above. To visualise each primary antibody staining, the tissue was then co-incubated with the appropriate species of fluorescent-conjugated secondary antibodies (1:500; 2 h; RT; Table 2).

Table 2. Fluorescent-conjugated secondary antibodies (2 mg/mL) used for immuno-detection of primary antibodies.

Antibody	Host	Source
Alexa fluor 488	chicken anti-goat IgG	Invitrogen #A21467
Alexa fluor 568	donkey anti-mouse IgG	Invitrogen #A31571
Alexa fluor 568	donkey anti-rabbit IgG	Invitrogen #A10042
Alexa fluor 568	donkey anti-sheep IgG	Invitrogen #A21099
Alexa fluor 647	*Streptavidin*-conjugated	Invitrogen #S32357

4.4. Image Acquisition and Quantification Methods

The fluorophores used to label the spinal cord sections were visualised using a Zeiss LSM 880 (upright) confocal microscope and were used to generate tile scans of the entire spinal cord transverse section at 20× magnification (1.03 µs per pixel, averaging: 4). ChAT-positive cells and co-localisation with WFA-positive PNNs and other CSPG-positive PNNs were counted using the Cell Counter plugin (Kurt de Vos; https://imagej.nih.gov/ij/plugins/cell-counter.html) in the software FIJI [58]. Mns were identified by location within the ventral horn of ChAT-positive cellular staining. All ChAT-positive cells were individually counted and sequentially analysed for presence of PNN staining. PNNs were only counted around ChAT-positive neurones and were identified by the presence of intense staining as a bright 'halo' directly adjacent to the perimeter of ChAT-positive cells. Positive PNN staining was categorised into three classes: (1) only WFA-positive, (2) only positive for the appropriate CSPG stain or (3) WFA-positive and CSPG-positive. For differentiation of alpha and gamma Mns, cells co-localising both ChAT and NeuN staining where taken as alpha Mns whereas the absence of NeuN denoted gamma Mns [44,59].

4.5. Experimental Design and Statistical Analysis

A minimum of three sections per spinal level (cervical, thoracic or lumbar) per animal ($n = 5$) were stained and imaged, maintaining the same confocal microscopy settings per staining procedure. All counts per section were normalised by the number of ChAT-positive cells before averaging per animal. All data sets were analysed with OriginPro 2016 scientific graphing and data analysis software (OriginLab, Northampton, MA, USA), where results were statistically significant given that $p < 0.05$. To test the influence of spinal cord level on PNN expression and for differences between PNN types, results were pooled and analysed using one-way ANOVA, with Bonferroni correction for between-groups multiple comparison.

Acknowledgments: This work was financed by grants from the Wings for Life Foundation, The University of Leeds 110 Years Scholarship and the European Union-the Operational Programme Research, Development and Education in the framework of the project "Centre of Reconstructive Neuroscience", registration number CZ.02.1.01/0.0./0.0/15_003/0000419. The authors declare no competing financial interests.

Author Contributions: Jessica C. F. Kwok and Sian F. Irvine conceived and designed the experiments; Sian F. Irvine performed the experiments and analysed the data; Jessica C. F. Kwok contributed reagents/materials/analysis tools; Sian F. Irvine wrote the paper with amendments by Jessica C. F. Kwok.

Conflicts of Interest: The authors declare no conflict of interest. The funding sponsors had no role in the design of the study; in the collection, analyses, or interpretation of data; in the writing of the manuscript, and in the decision to publish the results.

Abbreviations

ACAN	Aggrecan core protein
BCAN	Brevican core protein
ChAT	Choline acetyltransferase
ChABC	Chondroitinase ABC
CNS	Central nervous system
CS-GAG	Chondroitin sulphate glycosaminoglycan
CSPGs	Chondroitin sulphate proteoglycans
ECM	Extracellular matrix
GalNAc	*N*-acetylgalactosamine
HA	Hyaluronic acid/hyaluronan
Mn	Motoneurone
NeuN	Neuron-specific nuclear protein
NCAN	Neurocan core protein
PTPRZ	Phosphacan/protein tyrosine phosphatase receptor zeta
PNN	Perineuronal net
Mn	Motoneurone
SCI	Spinal cord injury
VCAN	Versican core protein
WFA	*Wisteria floribunda* agglutinin

References

1. Celio, M.R.; Spreafico, R.; De Biasi, S.; Vitellaro-Zuccarello, L. Perineuronal nets: Past and present. *Trends Neurosci.* **1998**, *21*, 510–515. [CrossRef]
2. Suttkus, A.; Rohn, S.; Weigel, S.; Glöckner, P.; Arendt, T.; Morawski, M. Aggrecan, link protein and tenascin-R are essential components of the perineuronal net to protect neurons against iron-induced oxidative stress. *Cell Death Dis.* **2014**, *5*. [CrossRef] [PubMed]
3. Cabungcal, J.-H.H.; Steullet, P.; Morishita, H.; Kraftsik, R.; Cuenod, M.; Hensch, T.K.; Do, K.Q. Perineuronal nets protect fast-spiking interneurons against oxidative stress. *Proc. Natl. Acad. Sci. USA* **2013**, *110*, 9130–9135. [CrossRef] [PubMed]
4. Pantazopoulos, H.; Berretta, S. In Sickness and in Health: Perineuronal Nets and Synaptic Plasticity in Psychiatric Disorders. *Neural Plast.* **2016**, *2016*, 9847696. [CrossRef] [PubMed]
5. McRae, P.A.; Porter, B.E. The perineuronal net component of the extracellular matrix in plasticity and epilepsy. *Neurochem. Int.* **2012**, *61*, 963–972. [CrossRef] [PubMed]
6. Moon, L.D.F.; Asher, R.A.; Rhodes, K.E.; Fawcett, J.W. Regeneration of CNS axons back to their target following treatment of adult rat brain with chondroitinase ABC. *Nat. Neurosci.* **2001**, *4*, 465–466. [CrossRef] [PubMed]
7. Bradbury, E.J.; Moon, L.D.; Popat, R.J.; King, V.R.; Bennett, G.S.; Patel, P.N.; Fawcett, J.W.; McMahon, S.B. Chondroitinase ABC promotes functional recovery after spinal cord injury. *Nature* **2002**, *416*, 636–640. [CrossRef] [PubMed]
8. García-Alías, G.; Barkhuysen, S.; Buckle, M.; Fawcett, J.W. Chondroitinase ABC treatment opens a window of opportunity for task-specific rehabilitation. *Nat. Neurosci.* **2009**, *12*, 1145–1151. [CrossRef] [PubMed]
9. Carulli, D.; Pizzorusso, T.; Kwok, J.C.; Putignano, E.; Poli, A.; Forostyak, S.; Andrews, M.R.; Deepa, S.S.; Glant, T.T.; Fawcett, J.W. Animals lacking link protein have attenuated perineuronal nets and persistent plasticity. *Brain* **2010**, *133*, 2331–2347. [CrossRef] [PubMed]
10. Pizzorusso, T.; Medini, P.; Berardi, N.; Chierzi, S.; Fawcett, J.W.; Maffei, L. Reactivation of ocular dominance plasticity in the adult visual cortex. *Science* **2002**, *298*, 1248–1251. [CrossRef] [PubMed]
11. Tsien, R.Y. Very long-term memories may be stored in the pattern of holes in the perineuronal net. *Proc. Natl. Acad. Sci. USA* **2013**, *110*, 12456–12461. [CrossRef] [PubMed]

12. Giamanco, K.A.; Morawski, M.; Matthews, R.T. Perineuronal net formation and structure in aggrecan knockout mice. *Neuroscience* **2010**, *170*, 1314–1327. [CrossRef] [PubMed]
13. Kwok, J.C.; Carulli, D.; Fawcett, J.W. In vitro modeling of perineuronal nets: Hyaluronan synthase and link protein are necessary for their formation and integrity. *J. Neurochem.* **2010**, *114*, 1447–1459. [CrossRef] [PubMed]
14. Kwok, J.C.; Dick, G.; Wang, D.; Fawcett, J.W. Extracellular matrix and perineuronal nets in CNS repair. *Dev. Neurobiol.* **2011**, *71*, 1073–1089. [CrossRef] [PubMed]
15. Yamaguchi, Y. Lecticans: Organizers of the brain extracellular matrix. *Cell. Mol. Life Sci.* **2000**, *57*, 276–289. [CrossRef] [PubMed]
16. Kitagawa, H. Using sugar remodeling to study chondroitin sulfate function. *Biol. Pharm. Bull.* **2014**, *37*, 1705–1712. [CrossRef] [PubMed]
17. Gama, C.I.; Tully, S.E.; Sotogaku, N.; Clark, P.M.; Rawat, M.; Vaidehi, N.; Goddard, W.A.; Nishi, A.; Hsieh-Wilson, L.C. Sulfation patterns of glycosaminoglycans encode molecular recognition and activity. *Nat. Chem. Biol.* **2006**, *2*, 467–473. [CrossRef] [PubMed]
18. Deepa, S.S.; Carulli, D.; Galtrey, C.; Rhodes, K.; Fukuda, J.; Mikami, T.; Sugahara, K.; Fawcett, J.W. Composition of perineuronal net extracellular matrix in rat brain: A different disaccharide composition for the net-associated proteoglycans. *J. Biol. Chem.* **2006**, *281*, 17789–17800. [CrossRef] [PubMed]
19. Carulli, D.; Rhodes, K.E.; Brown, D.J.; Bonnert, T.P.; Pollack, S.J.; Oliver, K.; Strata, P.; Fawcett, J.W. Composition of perineuronal nets in the adult rat cerebellum and the cellular origin of their components. *J. Comp. Neurol.* **2006**, *494*, 559–577. [CrossRef] [PubMed]
20. Fader, S.M.; Imaizumi, K.; Yanagawa, Y.; Lee, C.C. Wisteria Floribunda Agglutinin-Labeled Perineuronal Nets in the Mouse Inferior Colliculus, Thalamic Reticular Nucleus and Auditory Cortex. *Brain Sci.* **2016**, *6*, 13. [CrossRef] [PubMed]
21. Yamada, J.; Jinno, S. Molecular heterogeneity of aggrecan-based perineuronal nets around five subclasses of parvalbumin-expressing neurons in the mouse hippocampus. *J. Comp. Neurol.* **2017**, *525*, 1234–1249. [CrossRef] [PubMed]
22. Vitellaro-Zuccarello, L.; Bosisio, P.; Mazzetti, S.; Monti, C.; De Biasi, S. Differential expression of several molecules of the extracellular matrix in functionally and developmentally distinct regions of rat spinal cord. *Cell Tissue Res.* **2007**, *327*, 433–447. [CrossRef] [PubMed]
23. Brauer, K.; Härtig, W.; Bigl, V.; Brückner, G. Distribution of parvalbumin-containing neurons and lectin-binding perineuronal nets in the rat basal forebrain. *Brain Res.* **1993**, *631*, 167–170. [CrossRef]
24. Yamada, J.; Ohgomori, T.; Jinno, S. Perineuronal nets affect parvalbumin expression in GABAergic neurons of the mouse hippocampus. *Eur. J. Neurosci.* **2015**, *41*, 368–378. [CrossRef] [PubMed]
25. Galtrey, C.M.; Kwok, J.C.; Carulli, D.; Rhodes, K.E.; Fawcett, J.W. Distribution and synthesis of extracellular matrix proteoglycans, hyaluronan, link proteins and tenascin-R in the rat spinal cord. *Eur. J. Neurosci.* **2008**, *27*, 1373–1390. [CrossRef] [PubMed]
26. Bertolotto, A.; Manzardo, E.; Guglielmone, R. Immunohistochemical mapping of perineuronal nets containing chondroitin unsulfate proteoglycan in the rat central nervous system. *Cell Tissue Res.* **1996**, *283*, 283–295. [CrossRef] [PubMed]
27. Takahashi-Iwanaga, H.; Murakami, T.; Abe, K. Three-dimensional microanatomy of perineuronal proteoglycan nets enveloping motor neurons in the rat spinal cord. *J. Neurocytol.* **1998**, *27*, 817–827. [CrossRef] [PubMed]
28. Manuel, M.; Zytnicki, D. Alpha, beta and gamma motoneurons: Functional diversity in the motor system's final pathway. *J. Integr. Neurosci.* **2011**, *10*, 243–276. [CrossRef] [PubMed]
29. Zhao, R.-R.R.; Andrews, M.R.; Wang, D.; Warren, P.; Gullo, M.; Schnell, L.; Schwab, M.E.; Fawcett, J.W. Combination treatment with anti-Nogo-A and chondroitinase ABC is more effective than single treatments at enhancing functional recovery after spinal cord injury. *Eur. J. Neurosci.* **2013**, *38*, 2946–2961. [CrossRef] [PubMed]
30. Barritt, A.W.; Davies, M.; Marchand, F.; Hartley, R.; Grist, J.; Yip, P.; McMahon, S.B.; Bradbury, E.J. Chondroitinase ABC Promotes Sprouting of Intact and Injured Spinal Systems after Spinal Cord Injury. *J. Neurosci.* **2006**, *26*, 10856–10867. [CrossRef] [PubMed]

31. Smith, C.C.; Mauricio, R.; Nobre, L.; Marsh, B.; Wüst, R.C.; Rossiter, H.B.; Ichiyama, R.M. Differential regulation of perineuronal nets in the brain and spinal cord with exercise training. *Brain Res. Bull.* **2015**, *111*, 20–26. [CrossRef] [PubMed]
32. Wang, D.; Ichiyama, R.M.; Zhao, R.; Andrews, M.R.; Fawcett, J.W. Chondroitinase combined with rehabilitation promotes recovery of forelimb function in rats with chronic spinal cord injury. *J. Neurosci.* **2011**, *31*, 9332–9344. [CrossRef] [PubMed]
33. Barber, R.P.; Phelps, P.E.; Houser, C.R.; Crawford, G.D.; Salvaterra, P.M.; Vaughn, J.E. The morphology and distribution of neurons containing choline acetyltransferase in the adult rat spinal cord: An immunocytochemical study. *J. Comp. Neurol.* **1984**, *229*, 329–346. [CrossRef] [PubMed]
34. Koppe, G.; Bruckner, G.; Hartig, W.; Delpech, B.; Bigl, V. Characterization of proteoglycan-containing perineuronal nets by enzymatic treatments of rat brain sections. *Histochem. J.* **1997**, *29*, 11–20. [CrossRef] [PubMed]
35. Morawski, M.; Brückner, G.; Arendt, T.; Matthews, R.T. Aggrecan: Beyond cartilage and into the brain. *Int. J. Biochem. Cell Biol.* **2012**, *44*, 690–693. [CrossRef] [PubMed]
36. Lendvai, D.; Morawski, M.; Négyessy, L.; Gáti, G.; Jäger, C.; Baksa, G.; Glasz, T.; Attems, J.; Tanila, H.; Arendt, T.; et al. Neurochemical mapping of the human hippocampus reveals perisynaptic matrix around functional synapses in Alzheimer's disease. *Acta Neuropathol.* **2013**, *125*, 215–229. [CrossRef] [PubMed]
37. Favuzzi, E.; Marques-Smith, A.; Deogracias, R.; Winterflood, C.M.; Sánchez-Aguilera, A.; Mantoan, L.; Maeso, P.; Fernandes, C.; Ewers, H.; Rico, B. Activity-Dependent Gating of Parvalbumin Interneuron Function by the Perineuronal Net Protein Brevican. *Neuron* **2017**, *95*. [CrossRef] [PubMed]
38. Asher, R.A.; Morgenstern, D.A.; Fidler, P.S.; Adcock, K.H.; Oohira, A.; Braistead, J.E.; Levine, J.M.; Margolis, R.U.; Rogers, J.H.; Fawcett, J.W. Neurocan is upregulated in injured brain and in cytokine-treated astrocytes. *J. Neurosci.* **2000**, *20*, 2427–2438. [CrossRef] [PubMed]
39. Dours-Zimmermann, M.T.; Maurer, K.; Rauch, U.; Stoffel, W.; Fässler, R.; Zimmermann, D.R. Versican V2 Assembles the Extracellular Matrix Surrounding the Nodes of Ranvier in the CNS. *J. Neurosci.* **2009**, *29*, 7731–7742. [CrossRef] [PubMed]
40. Asher, R.A.; Morgenstern, D.A.; Shearer, M.C.; Adcock, K.H.; Pesheva, P.; Fawcett, J.W. Versican is upregulated in CNS injury and is a product of oligodendrocyte lineage cells. *J. Neurosci.* **2002**, *22*, 2225–2236. [PubMed]
41. Maurel, P.; Rauch, U.; Flad, M.; Margolis, R.K.; Margolis, R.U. Phosphacan, a chondroitin sulfate proteoglycan of brain that interacts with neurons and neural cell-adhesion molecules, is an extracellular variant of a receptor-type protein tyrosine phosphatase. *Proc. Natl. Acad. Sci. USA* **1994**, *91*, 2512–2516. [CrossRef] [PubMed]
42. Dwyer, C.A.; Katoh, T.; Tiemeyer, M.; Matthews, R.T. Neurons and Glia Modify Receptor Protein-tyrosine Phosphatase ζ (RPTPζ)/Phosphacan with Cell-specific O-Mannosyl Glycans in the Developing Brain. *J. Biol. Chem.* **2015**, *290*, 10256–10273. [CrossRef] [PubMed]
43. Haunsø, A.; Celio, M.R.; Margolis, R.K.; Menoud, P.-A. Phosphacan immunoreactivity is associated with perineuronal nets around parvalbumin-expressing neurones. *Brain Res.* **1999**, *834*, 219–222. [CrossRef]
44. Friese, A.; Kaltschmidt, J.A.; Ladle, D.R.; Sigrist, M.; Jessell, T.M.; Arber, S. Gamma and alpha motor neurons distinguished by expression of transcription factor Err3. *Proc. Natl. Acad. Sci. USA* **2009**, *106*, 13588–13593. [CrossRef] [PubMed]
45. Mueller, A.L.; Davis, A.; Sovich, S.; Carlson, S.S.; Robinson, F.R. Distribution of *N*-Acetylgalactosamine-Positive Perineuronal Nets in the Macaque Brain: Anatomy and Implications. *Neural Plast.* **2016**, *2016*. [CrossRef] [PubMed]
46. Jäger, C.; Lendvai, D.; Seeger, G.; Brückner, G.; Matthews, R.T.; Arendt, T.; Alpár, A.; Morawski, M. Perineuronal and perisynaptic extracellular matrix in the human spinal cord. *Neuroscience* **2013**, *238*, 168–184. [CrossRef] [PubMed]
47. Shneider, N.A.; Brown, M.N.; Smith, C.A.; Pickel, J.; Alvarez, F.J. Gamma motor neurons express distinct genetic markers at birth and require muscle spindle-derived GDNF for postnatal survival. *Neural Dev.* **2009**, *4*, 42. [CrossRef] [PubMed]
48. Eccles, J.C.; Eccles, R.M.; Iggo, A.; Lundberg, A. Electrophysiological studies on gamma motoneurones. *Acta Physiol. Scand.* **1960**, *50*, 32–40. [CrossRef] [PubMed]

49. Misawa, H.; Hara, M.; Tanabe, S.; Niikura, M.; Moriwaki, Y.; Okuda, T. Osteopontin is an alpha motor neuron marker in the mouse spinal cord. *J. Neurosci. Res.* **2012**, *90*, 732–742. [CrossRef] [PubMed]
50. Härtig, W.; Brauer, K.; Brückner, G. Wisteria floribunda agglutinin-labelled nets surround parvalbumin-containing neurons. *Neuroreport* **1992**, *3*, 869–872. [CrossRef] [PubMed]
51. Kalb, R.G.; Hockfield, S. Molecular evidence for early activity-dependent development of hamster motor neurons. *J. Neurosci.* **1988**, *8*, 2350–2360. [CrossRef] [PubMed]
52. Matthews, R.T.; Kelly, G.M.; Zerillo, C.A.; Gray, G.; Tiemeyer, M.; Hockfield, S. Aggrecan glycoforms contribute to the molecular heterogeneity of perineuronal nets. *J. Neurosci.* **2002**, *22*, 7536–7547. [PubMed]
53. Bignami, A.; Perides, G.; Rahemtulla, F. Versican, a hyaluronate-binding proteoglycan of embryonal precartilaginous mesenchyma, is mainly expressed postnatally in rat brain. *J. Neurosci. Res.* **1993**, *34*, 97–106. [CrossRef] [PubMed]
54. Ueno, H.; Suemitsu, S.; Okamoto, M.; Matsumoto, Y.; Ishihara, T. Sensory experience-dependent formation of perineuronal nets and expression of Cat-315 immunoreactive components in the mouse somatosensory cortex. *Neuroscience* **2017**, *355*, 161–174. [CrossRef] [PubMed]
55. Dauth, S.; Grevesse, T.; Pantazopoulos, H.; Campbell, P.H.; Maoz, B.M.; Berretta, S.; Parker, K.K. Extracellular matrix protein expression is brain region dependent. *J. Comp. Neurol.* **2016**, *524*, 1309–1336. [CrossRef] [PubMed]
56. Gage, G.J.; Kipke, D.R.; Shain, W. Whole animal perfusion fixation for rodents. *J. Vis. Exp.* **2012**. [CrossRef] [PubMed]
57. Phelps, P.E.; Barber, R.P.; Houser, C.R.; Crawford, G.D.; Salvaterra, P.M.; Vaughn, J.E. Postnatal development of neurons containing choline acetyltransferase in rat spinal cord: An immunocytochemical study. *J. Comp. Neurol.* **1984**, *229*, 347–361. [CrossRef] [PubMed]
58. Schindelin, J.; Arganda-Carreras, I.; Frise, E.; Kaynig, V.; Longair, M.; Pietzsch, T.; Preibisch, S.; Rueden, C.; Saalfeld, S.; Schmid, B.; et al. Fiji: An open-source platform for biological-image analysis. *Nat. Meth.* **2012**, *9*, 676–682. [CrossRef] [PubMed]
59. Mullen, R.J.; Buck, C.R.; Smith, A.M. NeuN, a neuronal specific nuclear protein in vertebrates. *Development* **1992**, *116*, 201–211. [PubMed]

References

ACKERY, A., C. TATOR and A. KRASSIOUKOV. 2004. A Global Perspective on Spinal Cord Injury Epidemiology. *Journal of Neurotrauma,* **21**(10), pp.1355–1370.

ADAMS, K. L. and V. GALLO. 2018. The diversity and disparity of the glial scar. *Nat Neurosci,* **21**(1), pp.9-15.

AKBARI, M., M. KHAKSARI, M. REZAEEZADEH-ROUKERD, M. MIRZAEE and M. NAZARI-ROBATI. 2017. Effect of chondroitinase ABC on inflammatory and oxidative response following spinal cord injury. *Iranian journal of basic medical sciences,* **20**(7), pp.806-812.

ALILAIN, W. J., K. P. HORN, H. HU, T. E. DICK and J. SILVER. 2011. Functional regeneration of respiratory pathways after spinal cord injury. *Nature,* **475**, p196.

ALIZADEH, A., S. M. DYCK and S. KARIMI-ABDOLREZAEE. 2019. Traumatic Spinal Cord Injury: An Overview of Pathophysiology, Models and Acute Injury Mechanisms. *Frontiers in neurology,* **10**, pp.282-282.

ALLUIN, O., H. DELIVET-MONGRAIN, M.-K. K. GAUTHIER, M. G. FEHLINGS, S. ROSSIGNOL and S. KARIMI-ABDOLREZAEE. 2014. Examination of the combined effects of chondroitinase ABC, growth factors and locomotor training following compressive spinal cord injury on neuroanatomical plasticity and kinematics. *PloS one,* **9**(10).

ALVAREZ, F. J., R. M. VILLALBA, R. ZERDA and S. P. SCHNEIDER. 2004. Vesicular glutamate transporters in the spinal cord, with special reference to sensory primary afferent synapses. **472**(3), pp.257-280.

ANDERSON, K. D., A. GUNAWAN and O. STEWARD. 2007. Spinal pathways involved in the control of forelimb motor function in rats. *Exp Neurol,* **206**(2), pp.318-31.

ANDERSON, M. A., J. E. BURDA, Y. REN, Y. AO, T. M. O'SHEA, R. KAWAGUCHI, G. COPPOLA, B. S. KHAKH, T. J. DEMING and M. V. SOFRONIEW. 2016. Astrocyte scar formation aids central nervous system axon regeneration. *Nature,* **532**(7598), pp.195-200.

ANDREWS, E. M., R. J. RICHARDS, F. Q. YIN, M. S. VIAPIANO and L. B. JAKEMAN. 2012. Alterations in chondroitin sulfate proteoglycan expression occur both at and far from the site of spinal contusion injury. *Experimental neurology,* **235**(1), pp.174-187.

ANKENY, D. P., K. M. LUCIN, V. M. SANDERS, V. M. MCGAUGHY and P. G. POPOVICH. 2006. Spinal cord injury triggers systemic autoimmunity: evidence for chronic B lymphocyte activation and lupus-like autoantibody synthesis. *J Neurochem,* **99**(4), pp.1073-87.

ASAHI, M., X. WANG, T. MORI, T. SUMII, J. C. JUNG, M. A. MOSKOWITZ, M. E. FINI and E. H. LO. 2001. Effects of matrix metalloproteinase-9 gene knock-out on the proteolysis of blood-brain barrier and white matter components after cerebral ischemia. *J Neurosci,* **21**(19), pp.7724-32.

ASBOTH, L., L. FRIEDLI, J. BEAUPARLANT, C. MARTINEZ-GONZALEZ, S. ANIL, E. REY, L. BAUD, G. PIDPRUZHNYKOVA, M. A. ANDERSON, P. SHKORBATOVA, L. BATTI, S. PAGES, J. KREIDER, B. L. SCHNEIDER, Q. BARRAUD and G. COURTINE. 2018. Cortico-reticulo-spinal circuit reorganization enables functional recovery after severe spinal cord contusion. *Nat Neurosci,* **21**(4), pp.576-588.

ASHER, R. A., D. A. MORGENSTERN, P. S. FIDLER, K. H. ADCOCK, A. OOHIRA, J. E. BRAISTEAD, J. M. LEVINE, R. U. MARGOLIS, J. H. ROGERS and J. W. FAWCETT. 2000. Neurocan is upregulated in injured brain and in cytokine-treated astrocytes. *J Neurosci,* **20**(7), pp.2427-38.

ASHER, R. A., D. A. MORGENSTERN, M. C. SHEARER, K. H. ADCOCK, P. PESHEVA and J. W. FAWCETT. 2002. Versican is upregulated in CNS injury and is a product of oligodendrocyte lineage cells. *J Neurosci,* **22**(6), pp.2225-36.

ASHER, R. A., R. J. SCHEIBE, H. D. KEISER and A. BIGNAMI. 1995. On the existence of a cartilage-like proteoglycan and link proteins in the central nervous system. *Glia,* **13**(4), pp.294-308.

ASPBERG, A., C. BINKERT and E. RUOSLAHTI. 1995. The versican C-type lectin domain recognizes the adhesion protein tenascin-R. *Proceedings of the National Academy of Sciences of the United States of America,* **92**(23), pp.10590-10594.

ATCHA, Z., C. ROURKE, A. H. NEO, C. W. GOH, J. S. LIM, C.-C. C. AW, E. R. BROWNE and D. J. PEMBERTON. 2010. Alternative method of oral dosing for rats.

Journal of the American Association for Laboratory Animal Science : JAALAS, **49**(3), pp.335-343.

AUSTIN, J. W., C. GILCHRIST and M. G. FEHLINGS. 2012. High molecular weight hyaluronan reduces lipopolysaccharide mediated microglial activation. *Journal of neurochemistry,* **122**(2), pp.344-355.

BAI, F., H. PENG, J. D. ETLINGER and R. J. ZEMAN. 2010. Partial functional recovery after complete spinal cord transection by combined chondroitinase and clenbuterol treatment. *Pflügers Archiv - European Journal of Physiology,* **460**(3), pp.657-666.

BALMER, T. S., V. M. CARELS, J. L. FRISCH and T. A. NICK. 2009. Modulation of perineuronal nets and parvalbumin with developmental song learning. *The Journal of neuroscience : the official journal of the Society for Neuroscience,* **29**(41), pp.12878-12885.

BANNATYNE, B. A., S. A. EDGLEY, I. HAMMAR, E. JANKOWSKA and D. J. MAXWELL. 2003. Networks of inhibitory and excitatory commissural interneurons mediating crossed reticulospinal actions. *The European journal of neuroscience,* **18**(8), pp.2273-2284.

BÁRBARA-BATALLER, E., J. L. MÉNDEZ-SUÁREZ, C. ALEMÁN-SÁNCHEZ, J. SÁNCHEZ-ENRÍQUEZ and M. SOSA-HENRÍQUEZ. 2018. Change in the profile of traumatic spinal cord injury over 15 years in Spain. *Scandinavian journal of trauma, resuscitation and emergency medicine,* **26**(1), pp.27-27.

BARBEAU, H. and S. ROSSIGNOL. 1987. Recovery of locomotion after chronic spinalization in the adult cat. *Brain research,* **412**(1), pp.84-95.

BARBER, R. P., P. E. PHELPS, C. R. HOUSER, G. D. CRAWFORD, P. M. SALVATERRA and J. E. VAUGHN. 1984. The morphology and distribution of neurons containing choline acetyltransferase in the adult rat spinal cord: An immunocytochemical study. *Journal of Comparative Neurology,* **229**(3), pp.329-346.

BAREYRE, F. M., M. KERSCHENSTEINER, O. RAINETEAU, T. C. METTENLEITER, O. WEINMANN and M. E. SCHWAB. 2004. The injured spinal cord spontaneously forms a new intraspinal circuit in adult rats. *Nature neuroscience,* **7**(3), pp.269-277.

BARRIÈRE, G., H. LEBLOND, J. PROVENCHER and S. ROSSIGNOL. 2008. Prominent role of the spinal central pattern generator in the recovery of locomotion after partial spinal cord injuries. *Journal of Neuroscience,* **28**(15), pp.3976-3987.

BARRITT, A. W., M. DAVIES, F. MARCHAND, R. HARTLEY, J. GRIST, P. YIP, S. B. MCMAHON and E. J. BRADBURY. 2006. Chondroitinase ABC Promotes Sprouting of Intact and Injured Spinal Systems after Spinal Cord Injury. *The Journal of Neuroscience,* **26**(42), pp.10856-10867.

BARTUS, K., N. D. JAMES, A. DIDANGELOS, K. D. BOSCH, J. VERHAAGEN, R. J. YÁÑEZ-MUÑOZ, J. H. ROGERS, B. L. SCHNEIDER, E. M. MUIR and E. J. BRADBURY. 2014. Large-Scale Chondroitin Sulfate Proteoglycan Digestion with Chondroitinase Gene Therapy Leads to Reduced Pathology and Modulates Macrophage Phenotype following Spinal Cord Contusion Injury. *The Journal of Neuroscience,* **34**(14), pp.4822-4836.

BASSO, D. M., M. S. BEATTIE and J. C. BRESNAHAN. 1995. A sensitive and reliable locomotor rating scale for open field testing in rats. *Journal of neurotrauma,* **12**(1), pp.1-21.

BATTISTUZZO, C. R., R. J. CALLISTER, R. CALLISTER and M. P. GALEA. 2012. A Systematic Review of Exercise Training To Promote Locomotor Recovery in Animal Models of Spinal Cord Injury. *Journal of Neurotrauma,* **29**(8), pp.1600-1613.

BEAUMONT, E., S. KALOUSTIAN, G. ROUSSEAU and B. CORMERY. 2008. Training improves the electrophysiological properties of lumbar neurons and locomotion after thoracic spinal cord injury in rats. *Neuroscience research,* **62**(3), pp.147-154.

BECERRA, J. L., W. R. PUCKETT, E. D. HIESTER, R. M. QUENCER, A. E. MARCILLO, M. J. POST and R. P. BUNGE. 1995. MR-pathologic comparisons of wallerian degeneration in spinal cord injury. *AJNR Am J Neuroradiol,* **16**(1), pp.125-33.

BEKKU, Y., W. D. SU, S. HIRAKAWA, R. FASSLER, A. OHTSUKA, J. S. KANG, J. SANDERS, T. MURAKAMI, Y. NINOMIYA and T. OOHASHI. 2003. Molecular cloning of Bral2, a novel brain-specific link protein, and immunohistochemical colocalization with brevican in perineuronal nets. *Mol Cell Neurosci,* **24**(1), pp.148-59.

BELLER, J. A., B. KULENGOWSKI, E. M. KOBRAEI, G. CURINGA, C. M. CALULOT, A. BAHRAMI, T. M. HERING and D. M. SNOW. 2013. Comparison of sensory neuron growth cone and filopodial responses to structurally diverse aggrecan variants, in vitro. *Experimental neurology,* **247**, pp.143-157.

BERARDI, N., T. PIZZORUSSO and L. MAFFEI. 2000. Critical periods during sensory development. *Current Opinion in Neurobiology,* **10**(1), pp.138-145.

BERROCAL, Y. A., V. W. ALMEIDA, R. PUENTES, E. P. KNOTT, J. F. HECHTMAN, M. GARLAND and D. D. PEARSE. 2014. Loss of central inhibition: implications for behavioral hypersensitivity after contusive spinal cord injury in rats. *Pain research and treatment,* **2014**, pp.178278-178278.

BERTOLOTTO, A., E. MANZARDO and R. GUGLIELMONE. 1996. Immunohistochemical mapping of perineuronal nets containing chondroitin unsulfate proteoglycan in the rat central nervous system. *Cell and Tissue Research,* **283**(2), pp.283-295.

BEURDELEY, M., J. SPATAZZA, H. H. C. LEE, S. SUGIYAMA, C. BERNARD, A. A. DI NARDO, T. K. HENSCH and A. PROCHIANTZ. 2012. Otx2 Binding to Perineuronal Nets Persistently Regulates Plasticity in the Mature Visual Cortex. *The Journal of Neuroscience,* **32**(27), pp.9429-9437.

BIGNAMI, A., G. PERIDES and F. RAHEMTULLA. 1993. Versican, a hyaluronate-binding proteoglycan of embryonal precartilaginous mesenchyma, is mainly expressed postnatally in rat brain. *Journal of Neuroscience Research,* **34**(1), pp.97-106.

BILGEN, M., R. ABBE, S. J. LIU and P. A. NARAYANA. 2000. Spatial and temporal evolution of hemorrhage in the hyperacute phase of experimental spinal cord injury: in vivo magnetic resonance imaging. *Magn Reson Med,* **43**(4), pp.594-600.

BORISOFF, J. F., C. C. CHAN, G. W. HIEBERT, L. OSCHIPOK, G. S. ROBERTSON, R. ZAMBONI, J. D. STEEVES and W. TETZLAFF. 2003. Suppression of Rho-kinase activity promotes axonal growth on inhibitory CNS substrates. *Mol Cell Neurosci,* **22**(3), pp.405-16.

BOSCH, K. D., E. J. BRADBURY, J. VERHAAGEN, J. W. FAWCETT and S. B. MCMAHON. 2012. Chondroitinase ABC promotes plasticity of spinal reflexes following peripheral nerve injury. *Experimental neurology,* **238**(1), pp.64-78.

BOTELHO, R. V., J. W. DANIEL, J. L. L. BOULOSA, B. O. COLLI, R. D. L. FARIAS, O. J. MORAES, W. E. PIMENTA, C. H. RIBEIRO, F. R. RIBEIRO, M. A. TARICCO, M. V. CARVALHO and W. M. BERNARDO. 2009. [Effectiveness of methylprednisolone in the acute phase of spinal cord injuries--a systematic review of randomized controlled trials]. *Revista da Associação Médica Brasileira (1992),* **55**(6), pp.729-737.

BOZZELLI, P. L., S. ALAIYED, E. KIM, S. VILLAPOL and K. CONANT. 2018. Proteolytic Remodeling of Perineuronal Nets: Effects on Synaptic Plasticity and Neuronal Population Dynamics. *Neural plasticity,* **2018**, pp.5735789-5735789.

BRADBURY, E. J., L. D. MOON, R. J. POPAT, V. R. KING, G. S. BENNETT, P. N. PATEL, J. W. FAWCETT and S. B. MCMAHON. 2002. Chondroitinase ABC promotes functional recovery after spinal cord injury. *Nature,* **416**(6881), pp.636-640.

BRAUER, K., W. HÄRTIG, V. BIGL and G. BRÜCKNER. 1993. Distribution of parvalbumin-containing neurons and lectin-binding perineuronal nets in the rat basal forebrain. *Brain research,* **631**(1), pp.167-170.

BROD, M., M. ROUSCULP and A. CAMERON. 2008. Understanding compliance issues for daily self-injectable treatment in ambulatory care settings. *Patient preference and adherence,* **2**, pp.129-136.

BROUDE, E., M. MCATEE, M. S. KELLEY and B. S. BREGMAN. 1997. c-Jun expression in adult rat dorsal root ganglion neurons: differential response after central or peripheral axotomy. *Exp Neurol,* **148**(1), pp.367-77.

BROWN, J. M., J. XIA, B. ZHUANG, K.-S. CHO, C. J. ROGERS, C. I. GAMA, M. RAWAT, S. E. TULLY, N. UETANI, D. E. MASON, M. L. TREMBLAY, E. C. PETERS, O. HABUCHI, D. F. CHEN and L. C. HSIEH-WILSON. 2012. A sulfated carbohydrate epitope inhibits axon regeneration after injury. **109**(13), pp.4768-4773.

BROWN, P. J., R. J. MARINO, G. J. HERBISON and J. F. DITUNNO, JR. 1991. The 72-hour examination as a predictor of recovery in motor complete quadriplegia. *Arch Phys Med Rehabil,* **72**(8), pp.546-8.

BROWN, T. G. and C. S. SHERRINGTON. 1912. On the instability of a cortical point. *Proceedings of the Royal Society of London. Series B, Containing Papers of a Biological Character,* **85**(579), pp.250-277.

BRÜCKNER, G., A. BRINGMANN, W. HÄRTIG, G. KÖPPE, B. DELPECH and K. BRAUER. 1998. Acute and long-lasting changes in extracellular-matrix chondroitin-sulphate proteoglycans induced by injection of chondroitinase ABC in the adult rat brain. *Experimental Brain Research,* **121**(3), pp.300-310.

BRÜCKNER, G., J. GROSCHE, S. SCHMIDT, W. HÄRTIG, R. U. MARGOLIS, B. DELPECH, C. I. SEIDENBECHER, R. CZANIERA and M. SCHACHNER. 2000. Postnatal development of perineuronal nets in wild-type mice and in a mutant deficient in tenascin-R. *The Journal of comparative neurology,* **428**(4), pp.616-629.

BRUEHLMEIER, M., V. DIETZ, K. L. LEENDERS, U. ROELCKE, J. MISSIMER and A. CURT. 1998. How does the human brain deal with a spinal cord injury? *European Journal of Neuroscience,* **10**(12), pp.3918-3922.

BUNGE, R. P., W. R. PUCKETT, J. L. BECERRA, A. MARCILLO and R. M. QUENCER. 1993. Observations on the pathology of human spinal cord injury. A review and classification of 22 new cases with details from a case of chronic cord compression with extensive focal demyelination. *Adv Neurol,* **59**, pp.75-89.

BUNGE, R. P., W. R. PUCKETT and E. D. HIESTER. 1997. Observations on the pathology of several types of human spinal cord injury, with emphasis on the astrocyte response to penetrating injuries. *Adv Neurol,* **72**, pp.305-15.

BURNS, A. S., R. J. MARINO, A. E. FLANDERS and H. FLETT. 2012. Clinical diagnosis and prognosis following spinal cord injury. *Handb Clin Neurol,* **109**, pp.47-62.

BURNSIDE, E. R., F. DE WINTER, A. DIDANGELOS, N. D. JAMES, E. C. ANDREICA, H. LAYARD-HORSFALL, E. M. MUIR, J. VERHAAGEN and E. J. BRADBURY. 2018. Immune-evasive gene switch enables regulated delivery of chondroitinase after spinal cord injury. *Brain,* **141**(8), pp.2362-2381.

BUSS, A., K. PECH, B. A. KAKULAS, D. MARTIN, J. SCHOENEN, J. NOTH and G. A. BROOK. 2009. NG2 and phosphacan are present in the astroglial scar after human traumatic spinal cord injury. *BMC neurology,* **9**, p32.

CABUNGCAL, J.-H. H., P. STEULLET, H. MORISHITA, R. KRAFTSIK, M. CUENOD, T. K. HENSCH and K. Q. DO. 2013. Perineuronal nets protect fast-spiking interneurons against oxidative stress. *Proceedings of the National Academy of Sciences of the United States of America,* **110**(22), pp.9130-9135.

CAGGIANO, A. O., M. P. ZIMBER, A. GANGULY, A. R. BLIGHT and E. A. GRUSKIN. 2005. Chondroitinase ABCI improves locomotion and bladder function following contusion injury of the rat spinal cord. *J Neurotrauma,* **22**(2), pp.226-39.

CARTER, L. M., S. B. MCMAHON and E. J. BRADBURY. 2011. Delayed treatment with chondroitinase ABC reverses chronic atrophy of rubrospinal neurons following spinal cord injury. *Experimental neurology,* **228**(1), pp.149-156.

CARTER, L. M., M. L. STARKEY, S. F. AKRIMI, M. DAVIES, S. B. MCMAHON and E. J. BRADBURY. 2008. The Yellow Fluorescent Protein (YFP-H) Mouse Reveals Neuroprotection as a Novel Mechanism Underlying Chondroitinase ABC-Mediated Repair after Spinal Cord Injury. *The Journal of Neuroscience,* **28**(52), pp.14107-14120.

CARTER, M. W., K. M. JOHNSON, J. Y. LEE, C. E. HULSEBOSCH and Y. S. GWAK. 2016. Comparison of Mechanical Allodynia and Recovery of Locomotion and Bladder Function by Different Parameters of Low Thoracic Spinal Contusion Injury in Rats. *The Korean journal of pain,* **29**(2), pp.86-95.

CARULLI, D., T. PIZZORUSSO, J. C. KWOK, E. PUTIGNANO, A. POLI, S. FOROSTYAK, M. R. ANDREWS, S. S. DEEPA, T. T. GLANT and J. W. FAWCETT. 2010. Animals lacking link protein have attenuated perineuronal nets and persistent plasticity. *Brain : a journal of neurology,* **133**(Pt 8), pp.2331-2347.

CARULLI, D., K. E. RHODES, D. J. BROWN, T. P. BONNERT, S. J. POLLACK, K. OLIVER, P. STRATA and J. W. FAWCETT. 2006. Composition of perineuronal nets in the adult rat cerebellum and the cellular origin of their components. *Journal of Comparative Neurology,* **494**(4), pp.559-577.

CATZ, A., M. ITZKOVICH, E. AGRANOV, H. RING and A. TAMIR. 1997. SCIM--spinal cord independence measure: a new disability scale for patients with spinal cord lesions. *Spinal Cord,* **35**(12), pp.850-6.

CATZ, A., M. ITZKOVICH, A. TAMIR, O. PHILO, F. STEINBERG, H. RING, J. RONEN, R. SPASSER and R. GEPSTEIN. 2002a. [SCIM--spinal cord independence measure (version II): sensitivity to functional changes]. *Harefuah,* **141**(12), pp.1025-31, 1091.

CATZ, A., M. THALEISNIK, B. FISHEL, J. RONEN, R. SPASSER, Y. FOLMAN, E. L. SHABTAI and R. GEPSTEIN. 2002b. Recovery of neurologic function after spinal cord injury in Israel. *Spine (Phila Pa 1976),* **27**(16), pp.1733-5.

CELIO, M. R. and I. BLUMCKE. 1994. Perineuronal nets--a specialized form of extracellular matrix in the adult nervous system. *Brain Res Brain Res Rev,* **19**(1), pp.128-45.

CELIO, M. R., R. SPREAFICO, S. DE BIASI and L. VITELLARO-ZUCCARELLO. 1998. Perineuronal nets: past and present. *Trends in neurosciences,* **21**(12), pp.510-515.

CHAPLAN, S. R., F. W. BACH, J. W. POGREL, J. M. CHUNG and T. L. YAKSH. 1994. Quantitative assessment of tactile allodynia in the rat paw. *Journal of neuroscience methods,* **53**(1), pp.55-63.

CHEN, Z., Y. LI and Q. YUAN. 2015. Expression, purification and thermostability of MBP-chondroitinase ABC I from Proteus vulgaris. *International journal of biological macromolecules,* **72**, pp.6-10.

CHENG, C.-H., C.-T. LIN, M.-J. LEE, M.-J. TSAI, W.-H. HUANG, M.-C. HUANG, Y.-L. LIN, C.-J. CHEN, W.-C. HUANG and H. CHENG. 2015. Local Delivery of High-Dose Chondroitinase ABC in the Sub-Acute Stage Promotes Axonal Outgrowth and Functional Recovery after Complete Spinal Cord Transection. *PLOS ONE,* **10**(9), pe0138705.

CHERIYAN, T., D. J. RYAN, J. H. WEINREB, J. CHERIYAN, J. C. PAUL, V. LAFAGE, T. KIRSCH and T. J. ERRICO. 2014. Spinal cord injury models: a review. *Spinal cord,* **52**(8), pp.588-595.

CHIBA, K., Y. MATSUYAMA, T. SEO and Y. TOYAMA. 2018. Condoliase for the Treatment of Lumbar Disc Herniation: A Randomized Controlled Trial. *Spine,* **43**(15), pp.E869-E876.

CHOO, A. M., J. LIU, Z. LIU, M. DVORAK, W. TETZLAFF and T. R. OXLAND. 2009. Modeling spinal cord contusion, dislocation, and distraction: characterization of vertebral clamps, injury severities, and node of Ranvier deformations. *J Neurosci Methods,* **181**(1), pp.6-17.

COHEN, D. M., C. B. PATEL, P. AHOBILA-VAJJULA, L. M. SUNDBERG, T. CHACKO, S.-J. LIU and P. A. NARAYANA. 2009. Blood-spinal cord barrier permeability in experimental spinal cord injury: dynamic contrast-enhanced MRI. *NMR in biomedicine,* **22**(3), pp.332-341.

COHEN, L. G., S. BANDINELLI, T. W. FINDLEY and M. HALLETT. 1991. Motor reorganisation after upper limb amputation in man: a study with focal magnetic stimulation. *Brain,* **114**(1), pp.615-627.

CONRAD, S., H. J. SCHLUESENER, K. TRAUTMANN, N. JOANNIN, R. MEYERMANN and J. M. SCHWAB. 2005. Prolonged lesional expression of RhoA and RhoB following spinal cord injury. *Journal of Comparative Neurology,* **487**(2), pp.166-175.

CORVETTI, L. and F. ROSSI. 2005. Degradation of chondroitin sulfate proteoglycans induces sprouting of intact purkinje axons in the cerebellum of the adult rat. *J Neurosci,* **25**(31), pp.7150-8.

COURTINE, G., Y. GERASIMENKO, R. VAN DEN BRAND, A. YEW, P. MUSIENKO, H. ZHONG, B. SONG, Y. AO, R. M. ICHIYAMA, I. LAVROV, R. R. ROY, M. V. SOFRONIEW and V. R. EDGERTON. 2009. Transformation of nonfunctional spinal circuits into functional states after the loss of brain input. *Nat Neurosci,* **12**(10), pp.1333-42.

CRESPO, D., R. A. ASHER, R. LIN, K. E. RHODES and J. W. FAWCETT. 2007. How does chondroitinase promote functional recovery in the damaged CNS? *Exp Neurol,* **206**(2), pp.159-71.

CROSS, A. K., G. HADDOCK, C. J. STOCK, S. ALLAN, J. SURR, R. A. BUNNING, D. J. BUTTLE and M. N. WOODROOFE. 2006. ADAMTS-1 and -4 are up-regulated following transient middle cerebral artery occlusion in the rat and their expression is modulated by TNF in cultured astrocytes. *Brain Res,* **1088**(1), pp.19-30.

CYPHERT, J. M., C. S. TREMPUS and S. GARANTZIOTIS. 2015. Size Matters: Molecular Weight Specificity of Hyaluronan Effects in Cell Biology. *Int J Cell Biol,* **2015**, p563818.

DAUTH, S., T. GREVESSE, H. PANTAZOPOULOS, P. H. CAMPBELL, B. M. MAOZ, S. BERRETTA and K. K. PARKER. 2016. Extracellular matrix protein expression is brain region dependent. *Journal of Comparative Neurology,* **524**(7), pp.1309-1336.

DAVID, S. and A. J. AGUAYO. 1981. Axonal elongation into peripheral nervous system "bridges" after central nervous system injury in adult rats. *Science,* **214**(4523), pp.931-3.

DE CASTRO, R. C., JR., C. L. BURNS, D. J. MCADOO and A. M. ROMANIC. 2000. Metalloproteinase increases in the injured rat spinal cord. *Neuroreport,* **11**(16), pp.3551-4.

DE WINTER, F., J. C. KWOK, J. W. FAWCETT, T. T. VO, D. CARULLI and J. VERHAAGEN. 2016. The Chemorepulsive Protein Semaphorin 3A and Perineuronal Net-Mediated Plasticity. *Neural Plast,* **2016**, p3679545.

DE WINTER, F., M. OUDEGA, A. J. LANKHORST, F. P. HAMERS, B. BLITS, M. J. RUITENBERG, R. J. PASTERKAMP, W. H. GISPEN and J. VERHAAGEN. 2002. Injury-induced class 3 semaphorin expression in the rat spinal cord. *Exp Neurol,* **175**(1), pp.61-75.

DEBOW, S. B., M. L. DAVIES, H. L. CLARKE and F. COLBOURNE. 2003. Constraint-induced movement therapy and rehabilitation exercises lessen motor deficits and volume of brain injury after striatal hemorrhagic stroke in rats. *Stroke,* **34**(4), pp.1021-6.

DEEPA, S. S., D. CARULLI, C. GALTREY, K. RHODES, J. FUKUDA, T. MIKAMI, K. SUGAHARA and J. W. FAWCETT. 2006. Composition of Perineuronal Net Extracellular Matrix in Rat Brain A DIFFERENT DISACCHARIDE COMPOSITION FOR THE NET-ASSOCIATED PROTEOGLYCANS. *Journal of Biological Chemistry,* **281**(26), pp.17789-17800.

DERGHAM, P., B. ELLEZAM, C. ESSAGIAN, H. AVEDISSIAN, W. D. LUBELL and L. MCKERRACHER. 2002. Rho Signaling Pathway Targeted to Promote Spinal Cord Repair. **22**(15), pp.6570-6577.

DICK, G., C. L. TAN, J. N. ALVES, E. M. EHLERT, G. M. MILLER, L. C. HSIEH-WILSON, K. SUGAHARA, A. OOSTERHOF, T. H. VAN KUPPEVELT, J. VERHAAGEN, J. W. FAWCETT and J. C. KWOK. 2013. Semaphorin 3A binds to the perineuronal nets via chondroitin sulfate type E motifs in rodent brains. *The Journal of biological chemistry,* **288**(38), pp.27384-27395.

DICKENDESHER, T. L., K. T. BALDWIN, Y. A. MIRONOVA, Y. KORIYAMA, S. J. RAIKER, K. L. ASKEW, A. WOOD, C. G. G. GEOFFROY, B. ZHENG, C. D.

LIEPMANN, Y. KATAGIRI, L. I. BENOWITZ, H. M. GELLER and R. J. GIGER. 2012. NgR1 and NgR3 are receptors for chondroitin sulfate proteoglycans. *Nature neuroscience,* **15**(5), pp.703-712.

DITTUNO, P. L. and J. F. DITUNNO, JR. 2001. Walking index for spinal cord injury (WISCI II): scale revision. *Spinal Cord,* **39**(12), pp.654-6.

DITUNNO, J. F., JR., P. L. DITUNNO, V. GRAZIANI, G. SCIVOLETTO, M. BERNARDI, V. CASTELLANO, M. MARCHETTI, H. BARBEAU, H. L. FRANKEL, J. M. D'ANDREA GREVE, H. Y. KO, R. MARSHALL and P. NANCE. 2000. Walking index for spinal cord injury (WISCI): an international multicenter validity and reliability study. *Spinal Cord,* **38**(4), pp.234-43.

DIXON, W. J. 1980. Efficient analysis of experimental observations. *Annu Rev Pharmacol Toxicol,* **20**, pp.441-62.

DOBKIN, B., D. APPLE, H. BARBEAU, M. BASSO, A. BEHRMAN, D. DEFORGE, J. DITUNNO, G. DUDLEY, R. ELASHOFF, L. FUGATE, S. HARKEMA, M. SAULINO, M. SCOTT and G. SPINAL CORD INJURY LOCOMOTOR TRIAL. 2006. Weight-supported treadmill vs over-ground training for walking after acute incomplete SCI. *Neurology,* **66**(4), pp.484-493.

DONNELLY, D. J. and P. G. POPOVICH. 2008. Inflammation and its role in neuroprotection, axonal regeneration and functional recovery after spinal cord injury. *Experimental neurology,* **209**(2), pp.378-388.

DOURS-ZIMMERMANN, M. T., K. MAURER, U. RAUCH, W. STOFFEL, R. FÄSSLER and D. R. ZIMMERMANN. 2009. Versican V2 Assembles the Extracellular Matrix Surrounding the Nodes of Ranvier in the CNS. *The Journal of Neuroscience,* **29**(24), pp.7731-7742.

DU BEAU, A., S. SHAKYA SHRESTHA, B. A. BANNATYNE, S. M. JALICY, S. LINNEN and D. J. MAXWELL. 2012. Neurotransmitter phenotypes of descending systems in the rat lumbar spinal cord. *Neuroscience,* **227**, pp.67-79.

DUMONT, R. J., D. O. OKONKWO, S. VERMA, R. J. HURLBERT, P. T. BOULOS, D. B. ELLEGALA and A. S. DUMONT. 2001. Acute spinal cord injury, part I: pathophysiologic mechanisms. *Clinical neuropharmacology,* **24**(5), pp.254-264.

DURIGOVA, M., H. NAGASE, J. S. MORT and P. J. ROUGHLEY. 2011. MMPs are less efficient than ADAMTS5 in cleaving aggrecan core protein. *Matrix biology,* **30**(2), pp.145-153.

DWYER, C. A., T. KATOH, M. TIEMEYER and R. T. MATTHEWS. 2015. Neurons and Glia Modify Receptor Protein-tyrosine Phosphatase ζ (RPTPζ)/Phosphacan with Cell-specific O-Mannosyl Glycans in the Developing Brain. *Journal of Biological Chemistry,* **290**(16), pp.10256-10273.

DYCK, S., H. KATARIA, A. ALIZADEH, K. T. SANTHOSH, B. LANG, J. SILVER and S. KARIMI-ABDOLREZAEE. 2018. Perturbing chondroitin sulfate proteoglycan signaling through LAR and PTPσ receptors promotes a beneficial inflammatory response following spinal cord injury. *Journal of neuroinflammation,* **15**(1), pp.90-90.

ECCLES, J. C., R. M. ECCLES, A. IGGO and A. LUNDBERG. 1960. Electrophysiological studies on gamma motoneurones. *Acta Physiol Scand,* **50**, pp.32-40.

ENDO, T., C. SPENGER, T. TOMINAGA, S. BRENÉ and L. OLSON. 2007. Cortical sensory map rearrangement after spinal cord injury: fMRI responses linked to Nogo signalling. *Brain,* **130**(11), pp.2951-2961.

ERLANDER, M. G., N. J. TILLAKARATNE, S. FELDBLUM, N. PATEL and A. J. TOBIN. 1991. Two genes encode distinct glutamate decarboxylases. *Neuron,* **7**(1), pp.91-100.

ERSCHBAMER, M., K. PERNOLD and L. OLSON. 2007. Inhibiting Epidermal Growth Factor Receptor Improves Structural, Locomotor, Sensory, and Bladder Recovery from Experimental Spinal Cord Injury. **27**(24), pp.6428-6435.

EVANIEW, N., V. K. NOONAN, N. FALLAH, B. K. KWON, C. S. RIVERS, H. AHN, C. S. BAILEY, S. D. CHRISTIE, D. R. FOURNEY, R. J. HURLBERT, A. G. LINASSI, M. G. FEHLINGS, M. F. DVORAK and R. NETWORK. 2015. Methylprednisolone for the Treatment of Patients with Acute Spinal Cord Injuries: A Propensity Score-Matched Cohort Study from a Canadian Multi-Center Spinal Cord Injury Registry. *Journal of neurotrauma,* **32**(21), pp.1674-1683.

FADER, S. M., K. IMAIZUMI, Y. YANAGAWA and C. C. LEE. 2016. Wisteria Floribunda Agglutinin-Labeled Perineuronal Nets in the Mouse Inferior Colliculus, Thalamic Reticular Nucleus and Auditory Cortex. *Brain Sciences,* **6**(2), p13.

FAULKNER, J. R., J. E. HERRMANN, M. J. WOO, K. E. TANSEY, N. B. DOAN and M. V. SOFRONIEW. 2004. Reactive astrocytes protect tissue and preserve function after spinal cord injury. *The Journal of neuroscience : the official journal of the Society for Neuroscience,* **24**(9), pp.2143-2155.

FAVUZZI, E., A. MARQUES-SMITH, R. DEOGRACIAS, C. M. WINTERFLOOD, A. SÁNCHEZ-AGUILERA, L. MANTOAN, P. MAESO, C. FERNANDES, H. EWERS and B. RICO. 2017. Activity-Dependent Gating of Parvalbumin Interneuron Function by the Perineuronal Net Protein Brevican. *Neuron,* **95**(3), pp.639-655.e10.

FILLI, L., A. K. ENGMANN, B. ZÖRNER, O. WEINMANN, T. MORAITIS, M. GULLO, H. KASPER, R. SCHNEIDER and M. E. SCHWAB. 2014. Bridging the gap: a reticulo-propriospinal detour bypassing an incomplete spinal cord injury. *The Journal of neuroscience : the official journal of the Society for Neuroscience,* **34**(40), pp.13399-13410.

FISHER, D., B. XING, J. DILL, H. LI, H. H. HOANG, Z. ZHAO, X.-L. YANG, R. BACHOO, S. CANNON, F. M. LONGO, M. SHENG, J. SILVER and S. LI. 2011. Leukocyte common antigen-related phosphatase is a functional receptor for chondroitin sulfate proteoglycan axon growth inhibitors. *The Journal of neuroscience : the official journal of the Society for Neuroscience,* **31**(40), pp.14051-14066.

FONNUM, F. 1984. Glutamate: a neurotransmitter in mammalian brain. *J Neurochem,* **42**(1), pp.1-11.

FONOFF, E. T., J. F. PEREIRA, L. V. CAMARGO, C. S. DALE, R. L. PAGANO, G. BALLESTER and M. J. TEIXEIRA. 2009. Functional mapping of the motor cortex of the rat using transdural electrical stimulation. *Behavioural Brain Research,* **202**(1), pp.138-141.

FOSCARIN, S., R. RAHA-CHOWDHURY, J. W. FAWCETT and J. C. F. KWOK. 2017. Brain ageing changes proteoglycan sulfation, rendering perineuronal nets more inhibitory. *Aging (Albany NY),* **9**(6), pp.1607-22.

FOUAD, K., D. J. BENNETT, R. VAVREK and A. BLESCH. 2013. Long-term viral brain-derived neurotrophic factor delivery promotes spasticity in rats with a cervical spinal cord hemisection. *Front Neurol,* **4**, p187.

FOUAD, K., G. A. S. METZ, D. MERKLER, V. DIETZ and M. E. SCHWAB. 2000. Treadmill training in incomplete spinal cord injured rats. *Behavioural Brain Research,* **115**(1), pp.107-113.

FOUAD, K., V. PEDERSEN, M. E. SCHWAB and C. BRÖSAMLE. 2001. Cervical sprouting of corticospinal fibers after thoracic spinal cord injury accompanies shifts in evoked motor responses. *Current biology : CB,* **11**(22), pp.1766-1770.

FRANKEL, H. L., D. O. HANCOCK, G. HYSLOP, J. MELZAK, L. S. MICHAELIS, G. H. UNGAR, J. D. VERNON and J. J. WALSH. 1969. The value of postural reduction in the initial management of closed injuries of the spine with paraplegia and tetraplegia. I. *Paraplegia,* **7**(3), pp.179-92.

FRANZ, S., M. CIATIPIS, K. PFEIFER, B. KIERDORF, B. SANDNER, U. BOGDAHN, A. BLESCH, B. WINNER and N. WEIDNER. 2014. Thoracic Rat Spinal Cord Contusion Injury Induces Remote Spinal Gliogenesis but Not Neurogenesis or Gliogenesis in the Brain. *PLOS ONE,* **9**(7), pe102896.

FRASER, J. R., T. C. LAURENT and U. B. LAURENT. 1997. Hyaluronan: its nature, distribution, functions and turnover. *J Intern Med,* **242**(1), pp.27-33.

FREUND, P., E. SCHMIDLIN, T. WANNIER, J. BLOCH, A. MIR, M. E. SCHWAB and E. M. ROUILLER. 2006. Nogo-A-specific antibody treatment enhances sprouting and functional recovery after cervical lesion in adult primates. *Nat Med,* **12**(7), pp.790-2.

FREUND, P., E. SCHMIDLIN, T. WANNIER, J. BLOCH, A. MIR, M. E. SCHWAB and E. M. ROUILLER. 2009. Anti-Nogo-A antibody treatment promotes recovery of manual dexterity after unilateral cervical lesion in adult primates--re-examination and extension of behavioral data. *Eur J Neurosci,* **29**(5), pp.983-96.

FREUND, P., T. WANNIER, E. SCHMIDLIN, J. BLOCH, A. MIR, M. E. SCHWAB and E. M. ROUILLER. 2007. Anti-Nogo-A antibody treatment enhances sprouting of corticospinal axons rostral to a unilateral cervical spinal cord lesion in adult macaque monkey. *J Comp Neurol,* **502**(4), pp.644-59.

FREUND, P., N. WEISKOPF, J. ASHBURNER, K. WOLF, R. SUTTER, D. R. ALTMANN, K. FRISTON, A. THOMPSON and A. CURT. 2013. MRI investigation of the sensorimotor cortex and the corticospinal tract after acute spinal cord injury: a prospective longitudinal study. *The Lancet. Neurology,* **12**(9), pp.873-881.

FREUND, P., N. WEISKOPF, N. S. WARD, C. HUTTON, A. GALL, O. CICCARELLI, M. CRAGGS, K. FRISTON and A. J. THOMPSON. 2011. Disability, atrophy and cortical reorganization following spinal cord injury. *Brain : a journal of neurology,* **134**(Pt 6), pp.1610-1622.

FRIESE, A., J. A. KALTSCHMIDT, D. R. LADLE, M. SIGRIST, T. M. JESSELL and S. ARBER. 2009. Gamma and alpha motor neurons distinguished by expression of transcription factor Err3. *Proceedings of the National Academy of Sciences of the United States of America,* **106**(32), pp.13588-13593.

FROST, S. B., C. L. DUNHAM, S. BARBAY, D. KRIZSAN-AGBAS, M. K. WINTER, D. J. GUGGENMOS and R. J. NUDO. 2015. Output Properties of the Cortical Hindlimb Motor Area in Spinal Cord-Injured Rats. *J Neurotrauma,* **32**(21), pp.1666-73.

FRY, E. J., M. J. CHAGNON, R. LÓPEZ-VALES, M. L. TREMBLAY and S. J. G. DAVID. 2010. Corticospinal tract regeneration after spinal cord injury in receptor protein tyrosine phosphatase sigma deficient mice. **58**(4), pp.423-433.

FÜHRMANN, T., P. N. ANANDAKUMARAN, S. L. PAYNE, M. M. PAKULSKA, B. V. VARGA, A. NAGY, C. TATOR and M. S. SHOICHET. 2018. Combined delivery of chondroitinase ABC and human induced pluripotent stem cell-derived neuroepithelial cells promote tissue repair in an animal model of spinal cord injury. *Biomedical Materials,* **13**(2), p024103.

GAGE, G. J., D. R. KIPKE and W. SHAIN. 2012. Whole animal perfusion fixation for rodents. *Journal of visualized experiments : JoVE,* (65).

GALTREY, C. M., R. A. ASHER, F. NOTHIAS and J. W. FAWCETT. 2007. Promoting plasticity in the spinal cord with chondroitinase improves functional recovery after peripheral nerve repair. *Brain : a journal of neurology,* **130**(Pt 4), pp.926-939.

GALTREY, C. M., J. C. KWOK, D. CARULLI, K. E. RHODES and J. W. FAWCETT. 2008. Distribution and synthesis of extracellular matrix proteoglycans, hyaluronan, link proteins and tenascin-R in the rat spinal cord. *The European journal of neuroscience,* **27**(6), pp.1373-1390.

GAMA, C. I., S. E. TULLY, N. SOTOGAKU, P. M. CLARK, M. RAWAT, N. VAIDEHI, W. A. GODDARD, A. NISHI and L. C. HSIEH-WILSON. 2006. Sulfation patterns of

glycosaminoglycans encode molecular recognition and activity. *Nature chemical biology,* **2**(9), pp.467-473.

GARCÍA-ALÍAS, G., S. BARKHUYSEN, M. BUCKLE and J. W. FAWCETT. 2009. Chondroitinase ABC treatment opens a window of opportunity for task-specific rehabilitation. *Nature neuroscience,* **12**(9), pp.1145-1151.

GARCÍA-ALÍAS, G., K. TRUONG, P. K. SHAH, R. R. ROY and V. R. EDGERTON. 2015. Plasticity of subcortical pathways promote recovery of skilled hand function in rats after corticospinal and rubrospinal tract injuries. *Experimental Neurology,* **266**, pp.112-119.

GENDELMAN, H. E. 2002. Neural immunity: Friend or foe? *Journal of NeuroVirology,* **8**(6), pp.474-479.

GENOVESE, T., E. ESPOSITO, E. MAZZON, R. DI PAOLA, R. CAMINITI, P. BRAMANTI, A. CAPPELANI and S. CUZZOCREA. 2009. Absence of endogenous interleukin-10 enhances secondary inflammatory process after spinal cord compression injury in mice. *J Neurochem,* **108**(6), pp.1360-72.

GEOFFROY, C. G., B. J. HILTON, W. TETZLAFF and B. ZHENG. 2016. Evidence for an Age-Dependent Decline in Axon Regeneration in the Adult Mammalian Central Nervous System. *Cell Rep,* **15**(2), pp.238-46.

GEOFFROY, C. G., A. O. LORENZANA, J. P. KWAN, K. LIN, O. GHASSEMI, A. MA, N. XU, D. CREGER, K. LIU, Z. HE and B. ZHENG. 2015. Effects of PTEN and Nogo Codeletion on Corticospinal Axon Sprouting and Regeneration in Mice. **35**(16), pp.6413-6428.

GHERARDINI, L., M. GENNARO and T. PIZZORUSSO. 2013. Perilesional Treatment with Chondroitinase ABC and Motor Training Promote Functional Recovery After Stroke in Rats. *Cerebral Cortex,* **25**(1), pp.202-212.

GHOSH, A., F. HAISS, E. SYDEKUM, R. SCHNEIDER, M. GULLO, M. T. WYSS, T. MUEGGLER, C. BALTES, M. RUDIN, B. WEBER and M. E. SCHWAB. 2009a. Rewiring of hindlimb corticospinal neurons after spinal cord injury. *Nature Neuroscience,* **13**, p97.

GHOSH, A., S. PEDUZZI, M. SNYDER, R. SCHNEIDER, M. STARKEY and M. E. SCHWAB. 2012. Heterogeneous spine loss in layer 5 cortical neurons after spinal cord injury. *Cereb Cortex,* **22**(6), pp.1309-17.

GHOSH, A., E. SYDEKUM, F. HAISS, S. PEDUZZI, B. ZÖRNER, R. SCHNEIDER, C. BALTES, M. RUDIN, B. WEBER and M. E. SCHWAB. 2009b. Functional and anatomical reorganization of the sensory-motor cortex after incomplete spinal cord injury in adult rats. *The Journal of neuroscience : the official journal of the Society for Neuroscience,* **29**(39), pp.12210-12219.

GIAMANCO, K. A. and R. T. MATTHEWS. 2012. Deconstructing the perineuronal net: cellular contributions and molecular composition of the neuronal extracellular matrix. *Neuroscience,* **218**, pp.367-384.

GIAMANCO, K. A., M. MORAWSKI and R. T. MATTHEWS. 2010. Perineuronal net formation and structure in aggrecan knockout mice. *Neuroscience,* **170**(4), pp.1314-1327.

GILBERT, R. J., R. J. MCKEON, A. DARR, A. CALABRO, V. C. HASCALL and R. V. BELLAMKONDA. 2005. CS-4,6 is differentially upregulated in glial scar and is a potent inhibitor of neurite extension. *Mol Cell Neurosci,* **29**(4), pp.545-58.

GIRGIS, J., D. MERRETT, S. KIRKLAND, G. A. S. METZ, V. VERGE and K. FOUAD. 2007. Reaching training in rats with spinal cord injury promotes plasticity and task specific recovery. *Brain,* **130**(11), pp.2993-3003.

GOLDBERG, J. L., M. E. VARGAS, J. T. WANG, W. MANDEMAKERS, S. F. OSTER, D. W. SRETAVAN and B. A. BARRES. 2004. An oligodendrocyte lineage-specific semaphorin, Sema5A, inhibits axon growth by retinal ganglion cells. *The Journal of neuroscience : the official journal of the Society for Neuroscience,* **24**(21), pp.4989-4999.

GRAZIANO, M. S. A. 2016. Ethological Action Maps: A Paradigm Shift for the Motor Cortex. *Trends Cogn Sci,* **20**(2), pp.121-132.

GUNTINAS-LICHIUS, O., D. N. ANGELOV, F. MORELLINI, M. LENZEN, E. SKOURAS, M. SCHACHNER and A. IRINTCHEV. 2005. Opposite impacts of tenascin-C and tenascin-R deficiency in mice on the functional outcome of facial nerve repair. *Eur J Neurosci,* **22**(9), pp.2171-9.

GUTH, L., E. X. ALBUQUERQUE, S. S. DESHPANDE, C. P. BARRETT, E. J. DONATI and J. E. WARNICK. 1980. Ineffectiveness of enzyme therapy on regeneration in the transected spinal cord of the rat. *Journal of neurosurgery,* **52**(1), pp.73-86.

HABUCHI, O. 2000. Diversity and functions of glycosaminoglycan sulfotransferases. *Biochimica et Biophysica Acta (BBA) - General Subjects,* **1474**(2), pp.115-127.

HACHEM, L. D., C. S. AHUJA and M. G. FEHLINGS. 2017. Assessment and management of acute spinal cord injury: From point of injury to rehabilitation. *J Spinal Cord Med,* **40**(6), pp.665-675.

HALL, K. M., M. E. COHEN, J. WRIGHT, M. CALL and P. WERNER. 1999. Characteristics of the Functional Independence Measure in traumatic spinal cord injury. *Arch Phys Med Rehabil,* **80**(11), pp.1471-6.

HANSEN, C. N., L. C. FISHER, R. J. DEIBERT, L. B. JAKEMAN, H. ZHANG, L. NOBLE-HAEUSSLEIN, S. WHITE and D. M. BASSO. 2013. Elevated MMP-9 in the lumbar cord early after thoracic spinal cord injury impedes motor relearning in mice. *The Journal of neuroscience : the official journal of the Society for Neuroscience,* **33**(32), pp.13101-13111.

HARRIS, N. G., Y. A. MIRONOVA, D. A. HOVDA and R. L. SUTTON. 2010. Chondroitinase ABC enhances pericontusion axonal sprouting but does not confer robust improvements in behavioral recovery. *J Neurotrauma,* **27**(11), pp.1971-82.

HARRIS, N. G., M. S. M. NOGUEIRA, D. R. VERLEY and R. L. SUTTON. 2013. Chondroitinase Enhances Cortical Map Plasticity and Increases Functionally Active Sprouting Axons after Brain Injury. *Journal of Neurotrauma,* **30**(14), pp.1257-1269.

HÄRTIG, W., K. BRAUER and G. BRÜCKNER. 1992. Wisteria floribunda agglutinin-labelled nets surround parvalbumin-containing neurons. *Neuroreport,* **3**(10), pp.869-872.

HARTIG, W., A. DEROUICHE, K. WELT, K. BRAUER, J. GROSCHE, M. MADER, A. REICHENBACH and G. BRUCKNER. 1999. Cortical neurons immunoreactive for the potassium channel Kv3.1b subunit are predominantly surrounded by perineuronal nets presumed as a buffering system for cations. *Brain Res,* **842**(1), pp.15-29.

HAUNSØ, A., M. R. CELIO, R. K. MARGOLIS and P.-A. MENOUD. 1999. Phosphacan immunoreactivity is associated with perineuronal nets around parvalbumin-expressing neurones. *Brain Research,* **834**(1-2), pp.219-222.

HAYES, K. C., T. C. HULL, G. A. DELANEY, P. J. POTTER, K. A. SEQUEIRA, K. CAMPBELL and P. G. POPOVICH. 2002. Elevated serum titers of proinflammatory cytokines and CNS autoantibodies in patients with chronic spinal cord injury. *J Neurotrauma,* **19**(6), pp.753-61.

HENG, C. and R. D. DE LEON. 2009. Treadmill training enhances the recovery of normal stepping patterns in spinal cord contused rats. *Experimental neurology,* **216**(1), pp.139-147.

HERNDON, M. E. and A. D. LANDER. 1990. A diverse set of developmentally regulated proteoglycans is expressed in the rat central nervous system. *Neuron,* **4**(6), pp.949-61.

HERRMANN, J. E., T. IMURA, B. SONG, J. QI, Y. AO, T. K. NGUYEN, R. A. KORSAK, K. TAKEDA, S. AKIRA and M. V. SOFRONIEW. 2008. STAT3 is a critical regulator of astrogliosis and scar formation after spinal cord injury. *J Neurosci,* **28**(28), pp.7231-43.

HERZOG, E., M. LANDRY, E. BUHLER, R. BOUALI-BENAZZOUZ, C. LEGAY, C. E. HENDERSON, F. NAGY, P. DREYFUS, B. GIROS and S. EL MESTIKAWY. 2004. Expression of vesicular glutamate transporters, VGLUT1 and VGLUT2, in cholinergic spinal motoneurons. **20**(7), pp.1752-1760.

HSU, J.-Y. C., R. MCKEON, S. GOUSSEV, Z. WERB, J.-U. LEE, A. TRIVEDI and L. J. NOBLE-HAEUSSLEIN. 2006. Matrix metalloproteinase-2 facilitates wound healing events that promote functional recovery after spinal cord injury. *The Journal of neuroscience : the official journal of the Society for Neuroscience,* **26**(39), pp.9841-9850.

HU, H. Z., N. GRANGER, S. B. PAI, R. V. BELLAMKONDA and N. D. JEFFERY. 2018. Therapeutic efficacy of microtube-embedded chondroitinase ABC in a canine clinical model of spinal cord injury. *Brain,* **141**(4), pp.1017-1027.

HU, R., J. ZHOU, C. LUO, J. LIN, X. WANG, X. LI, X. BIAN, Y. LI, Q. WAN, Y. YU and H. FENG. 2010. Glial scar and neuroregeneration: histological, functional, and

magnetic resonance imaging analysis in chronic spinal cord injury. *J Neurosurg Spine,* **13**(2), pp.169-80.

HUANG, L., Z. B. WU, Q. ZHUGE, W. ZHENG, B. SHAO, B. WANG, F. SUN and K. JIN. 2014. Glial scar formation occurs in the human brain after ischemic stroke. *Int J Med Sci,* **11**(4), pp.344-8.

HUANG, W. C., W. C. KUO, S. H. HSU, C. H. CHENG, J. C. LIU and H. CHENG. 2010. Gait analysis of spinal cord injured rats after delivery of chondroitinase ABC and adult olfactory mucosa progenitor cell transplantation. *Neurosci Lett,* **472**(2), pp.79-84.

HULSEBOSCH, C. E. 2002. Recent advances in pathophysiology and treatment of spinal cord injury. *Adv Physiol Educ,* **26**(1-4), pp.238-55.

HYLIN, M. J., S. A. ORSI, A. N. MOORE and P. K. DASH. 2013. Disruption of the perineuronal net in the hippocampus or medial prefrontal cortex impairs fear conditioning. *Learning & memory (Cold Spring Harbor, N.Y.),* **20**(5), pp.267-273.

ICHIYAMA, R. M., J. BROMAN, R. R. ROY, H. ZHONG, V. R. EDGERTON and L. A. HAVTON. 2011. Locomotor Training Maintains Normal Inhibitory Influence on Both Alpha- and Gamma-Motoneurons after Neonatal Spinal Cord Transection. **31**(1), pp.26-33.

ICHIYAMA, R. M., G. COURTINE, Y. P. GERASIMENKO, G. J. YANG, R. VAN DEN BRAND, I. A. LAVROV, H. ZHONG, R. R. ROY and V. R. EDGERTON. 2008. Step training reinforces specific spinal locomotor circuitry in adult spinal rats. *Journal of Neuroscience,* **28**(29), pp.7370-7375.

IRVINE, S. F. and J. C. F. KWOK. 2018. Perineuronal Nets in Spinal Motoneurones: Chondroitin Sulphate Proteoglycan around Alpha Motoneurones. *Int J Mol Sci,* **19**(4).

ISEDA, T., T. OKUDA, N. KANE-GOLDSMITH, M. MATHEW, S. AHMED, Y. W. CHANG, W. YOUNG and M. GRUMET. 2008. Single, high-dose intraspinal injection of chondroitinase reduces glycosaminoglycans in injured spinal cord and promotes corticospinal axonal regrowth after hemisection but not contusion. *J Neurotrauma,* **25**(4), pp.334-49.

JACKSON, C. A., J. MESSINGER, J. D. PEDUZZI, D. C. ANSARDI and C. D. MORROW. 2005. Enhanced functional recovery from spinal cord injury following

intrathecal or intramuscular administration of poliovirus replicons encoding IL-10. *Virology,* **336**(2), pp.173-83.

JÄGER, C., D. LENDVAI, G. SEEGER, G. BRÜCKNER, R. T. MATTHEWS, T. ARENDT, A. ALPÁR and M. MORAWSKI. 2013. Perineuronal and perisynaptic extracellular matrix in the human spinal cord. *Neuroscience,* **238**, pp.168-184.

JAIN, N., K. C. CATANIA and J. H. KAAS. 1997. Deactivation and reactivation of somatosensory cortex after dorsal spinal cord injury. *Nature,* **386**(6624), pp.495-8.

JAIN, N., S. L. FLORENCE, H. X. QI and J. H. KAAS. 2000. Growth of new brainstem connections in adult monkeys with massive sensory loss. *Proc Natl Acad Sci U S A,* **97**(10), pp.5546-50.

JAMES, N. D., K. BARTUS, J. GRIST, D. L. H. BENNETT, S. B. MCMAHON and E. J. BRADBURY. 2011. Conduction failure following spinal cord injury: functional and anatomical changes from acute to chronic stages. *The Journal of neuroscience : the official journal of the Society for Neuroscience,* **31**(50), pp.18543-18555.

JAMES, N. D., J. SHEA, E. M. MUIR, J. VERHAAGEN, B. L. SCHNEIDER and E. J. BRADBURY. 2015. Chondroitinase gene therapy improves upper limb function following cervical contusion injury. *Experimental neurology,* **271**, pp.131-135.

JIN, D., Y. LIU, F. SUN, X. WANG, X. LIU and Z. HE. 2015. Restoration of skilled locomotion by sprouting corticospinal axons induced by co-deletion of PTEN and SOCS3. *Nature Communications,* **6**, p8074.

JONES, L. L., R. U. MARGOLIS and M. H. TUSZYNSKI. 2003. The chondroitin sulfate proteoglycans neurocan, brevican, phosphacan, and versican are differentially regulated following spinal cord injury. *Experimental neurology,* **182**(2), pp.399-411.

JOSET, A., D. A. DODD, S. HALEGOUA and M. E. SCHWAB. 2010. Pincher-generated Nogo-A endosomes mediate growth cone collapse and retrograde signaling. *J Cell Biol,* **188**(2), pp.271-85.

JURE, I. and F. LABOMBARDA. 2017. Spinal cord injury drives chronic brain changes. *Neural regeneration research,* **12**(7), pp.1044-1047.

JURKIEWICZ, M. T., D. J. MIKULIS, W. E. MCILROY, M. G. FEHLINGS and M. C. VERRIER. 2007. Sensorimotor cortical plasticity during recovery following spinal cord injury: a longitudinal fMRI study. *Neurorehabil Neural Repair,* **21**(6), pp.527-38.

KALB, R. G. and S. HOCKFIELD. 1988. Molecular evidence for early activity-dependent development of hamster motor neurons. *J Neurosci,* **8**(7), pp.2350-60.

KANEIWA, T., S. MIZUMOTO, K. SUGAHARA and S. YAMADA. 2010. Identification of human hyaluronidase-4 as a novel chondroitin sulfate hydrolase that preferentially cleaves the galactosaminidic linkage in the trisulfated tetrasaccharide sequence. *Glycobiology,* **20**(3), pp.300-9.

KANEKO, S., A. IWANAMI, M. NAKAMURA, A. KISHINO, K. KIKUCHI, S. SHIBATA, H. J. OKANO, T. IKEGAMI, A. MORIYA, O. KONISHI, C. NAKAYAMA, K. KUMAGAI, T. KIMURA, Y. SATO, Y. GOSHIMA, M. TANIGUCHI, M. ITO, Z. HE, Y. TOYAMA and H. OKANO. 2006. A selective Sema3A inhibitor enhances regenerative responses and functional recovery of the injured spinal cord. *Nat Med,* **12**(12), pp.1380-9.

KANNO, H., Y. PRESSMAN, A. MOODY, R. BERG, E. M. MUIR, J. H. ROGERS, H. OZAWA, E. ITOI, D. D. PEARSE and M. B. BUNGE. 2014. Combination of engineered Schwann cell grafts to secrete neurotrophin and chondroitinase promotes axonal regeneration and locomotion after spinal cord injury. *The Journal of neuroscience : the official journal of the Society for Neuroscience,* **34**(5), pp.1838-1855.

KAO, T., J. S. SHUMSKY, E. B. KNUDSEN, M. MURRAY and K. A. MOXON. 2011. Functional role of exercise-induced cortical organization of sensorimotor cortex after spinal transection. *Journal of Neurophysiology,* **106**(5), pp.2662-2674.

KAO, T., J. S. SHUMSKY, M. MURRAY and K. A. MOXON. 2009. Exercise induces cortical plasticity after neonatal spinal cord injury in the rat. *The Journal of Neuroscience,* **29**(23), pp.7549-7557.

KAPLAN, A., S. ONG TONE and A. E. FOURNIER. 2015. Extrinsic and intrinsic regulation of axon regeneration at a crossroads. *Frontiers in molecular neuroscience,* **8**, p27.

KARIMI-ABDOLREZAEE, S., E. EFTEKHARPOUR, J. WANG, D. SCHUT and M. G. FEHLINGS. 2010. Synergistic effects of transplanted adult neural stem/progenitor

cells, chondroitinase, and growth factors promote functional repair and plasticity of the chronically injured spinal cord. *The Journal of neuroscience : the official journal of the Society for Neuroscience,* **30**(5), pp.1657-1676.

KHAING, Z. Z., L. N. CATES, D. M. DEWEES, A. HANNAH, P. MOURAD, M. BRUCE and C. P. HOFSTETTER. 2018. Contrast-enhanced ultrasound to visualize hemodynamic changes after rodent spinal cord injury. *J Neurosurg Spine,* **29**(3), pp.306-313.

KHAING, Z. Z., B. D. MILMAN, J. E. VANSCOY, S. K. SEIDLITS, R. J. GRILL and C. E. SCHMIDT. 2011. High molecular weight hyaluronic acid limits astrocyte activation and scar formation after spinal cord injury. *Journal of neural engineering,* **8**(4), p46033.

KIGERL, K. A., J. C. GENSEL, D. P. ANKENY, J. K. ALEXANDER, D. J. DONNELLY and P. G. POPOVICH. 2009. Identification of two distinct macrophage subsets with divergent effects causing either neurotoxicity or regeneration in the injured mouse spinal cord. *The Journal of neuroscience : the official journal of the Society for Neuroscience,* **29**(43), pp.13435-13444.

KIM, K. K., R. S. ADELSTEIN and S. KAWAMOTO. 2009. Identification of neuronal nuclei (NeuN) as Fox-3, a new member of the Fox-1 gene family of splicing factors. *The Journal of biological chemistry,* **284**(45), pp.31052-31061.

KIRSHBLUM, S. C., S. P. BURNS, F. BIERING-SORENSEN, W. DONOVAN, D. E. GRAVES, A. JHA, M. JOHANSEN, L. JONES, A. KRASSIOUKOV, M. J. MULCAHEY, M. SCHMIDT-READ and W. WARING. 2011. International standards for neurological classification of spinal cord injury (revised 2011). *The journal of spinal cord medicine,* **34**(6), pp.535-546.

KITAGAWA, H. 2014. Using sugar remodeling to study chondroitin sulfate function. *Biological & pharmaceutical bulletin,* **37**(11), pp.1705-1712.

KITAGAWA, H., K. TSUTSUMI, Y. TONE and K. SUGAHARA. 1997. Developmental regulation of the sulfation profile of chondroitin sulfate chains in the chicken embryo brain. *The Journal of biological chemistry,* **272**(50), pp.31377-31381.

KLEIM, J. A., S. BARBAY, N. R. COOPER, T. M. HOGG, C. N. REIDEL, M. S. REMPLE and R. J. NUDO. 2002. Motor Learning-Dependent Synaptogenesis Is

Localized to Functionally Reorganized Motor Cortex. *Neurobiology of Learning and Memory,* **77**(1), pp.63-77.

KLEIM, J. A., S. BARBAY and R. J. NUDO. 1998. Functional reorganization of the rat motor cortex following motor skill learning. *Journal of neurophysiology,* **80**(6), pp.3321-3325.

KLEIM, J. A., T. M. HOGG, P. M. VANDENBERG, N. R. COOPER, R. BRUNEAU and M. REMPLE. 2004. Cortical synaptogenesis and motor map reorganization occur during late, but not early, phase of motor skill learning. *J Neurosci,* **24**(3), pp.628-33.

KLUSMAN, I. and M. E. SCHWAB. 1997. Effects of pro-inflammatory cytokines in experimental spinal cord injury. *Brain Res,* **762**(1-2), pp.173-84.

KOPPE, G., G. BRUCKNER, W. HARTIG, B. DELPECH and V. BIGL. 1997. Characterization of proteoglycan-containing perineuronal nets by enzymatic treatments of rat brain sections. *The Histochemical Journal,* **29**(1), pp.11-20.

KOPRIVICA, V., K.-S. CHO, J. B. PARK, G. YIU, J. ATWAL, B. GORE, J. A. KIM, E. LIN, M. TESSIER-LAVIGNE, D. F. CHEN and Z. HE. 2005. EGFR Activation Mediates Inhibition of Axon Regeneration by Myelin and Chondroitin Sulfate Proteoglycans. *Science,* **310**(5745), pp.106-110.

KRAJACIC, A., M. GHOSH, R. PUENTES, D. D. PEARSE and K. FOUAD. 2009. Advantages of delaying the onset of rehabilitative reaching training in rats with incomplete spinal cord injury. *European Journal of Neuroscience,* **29**(3), pp.641-651.

KRUEGER, H., V. K. NOONAN, L. M. TRENAMAN, P. JOSHI and C. S. RIVERS. 2013. The economic burden of traumatic spinal cord injury in Canada. *Chronic Dis Inj Can,* **33**(3), pp.113-22.

KUCHER, K., D. JOHNS, D. MAIER, R. ABEL, A. BADKE, H. BARON, R. THIETJE, S. CASHA, R. MEINDL, B. GOMEZ-MANCILLA, C. PFISTER, R. RUPP, N. WEIDNER, A. MIR, M. E. SCHWAB and A. CURT. 2018. First-in-Man Intrathecal Application of Neurite Growth-Promoting Anti-Nogo-A Antibodies in Acute Spinal Cord Injury. *Neurorehabil Neural Repair,* **32**(6-7), pp.578-589.

KUERZI, J., E. H. BROWN, A. SHUM-SIU, A. SIU, D. BURKE, J. MOREHOUSE, R. R. SMITH and D. S. K. MAGNUSON. 2010. Task-specificity vs. ceiling effect: step-

training in shallow water after spinal cord injury. *Experimental neurology,* **224**(1), pp.178-187.

KULLANDER, K., S. J. B. BUTT, J. M. LEBRET, L. LUNDFALD, C. E. RESTREPO, A. RYDSTRÖM, R. KLEIN and O. KIEHN. 2003. Role of EphA4 and EphrinB3 in Local Neuronal Circuits That Control Walking. **299**(5614), pp.1889-1892.

KUMAR, R., J. LIM, R. A. MEKARY, A. RATTANI, M. C. DEWAN, S. Y. SHARIF, E. OSORIO-FONSECA and K. B. PARK. 2018. Traumatic Spinal Injury: Global Epidemiology and Worldwide Volume. *World Neurosurgery,* **113**, pp.e345-e363.

KWOK, J. C., D. CARULLI and J. W. FAWCETT. 2010. In vitro modeling of perineuronal nets: hyaluronan synthase and link protein are necessary for their formation and integrity. *J Neurochem,* **114**(5), pp.1447-59.

KWOK, J. C., G. DICK, D. WANG and J. W. FAWCETT. 2011. Extracellular matrix and perineuronal nets in CNS repair. *Developmental neurobiology,* **71**(11), pp.1073-1089.

LAMPRIANOU, S., E. CHATZOPOULOU, J.-L. THOMAS, S. BOUYAIN and S. HARROCH. 2011. A complex between contactin-1 and the protein tyrosine phosphatase PTPRZ controls the development of oligodendrocyte precursor cells. *Proceedings of the National Academy of Sciences,* **108**(42), pp.17498-17503.

LANDRY, M., R. BOUALI-BENAZZOUZ, S. EL MESTIKAWY, P. RAVASSARD and F. NAGY. 2004. Expression of vesicular glutamate transporters in rat lumbar spinal cord, with a note on dorsal root ganglia. **468**(3), pp.380-394.

LANG, B. T., J. M. CREGG, M. A. DEPAUL, A. P. TRAN, K. XU, S. M. DYCK, K. M. MADALENA, B. P. BROWN, Y.-L. WENG, S. LI, S. KARIMI-ABDOLREZAEE, S. A. BUSCH, Y. SHEN and J. SILVER. 2015. Modulation of the proteoglycan receptor PTPσ promotes recovery after spinal cord injury. *Nature,* **518**(7539), p404.

LEE, B. B., R. A. CRIPPS, M. FITZHARRIS and P. C. WING. 2014. The global map for traumatic spinal cord injury epidemiology: update 2011, global incidence rate. *Spinal Cord,* **52**(2), pp.110-6.

LEE, H., R. J. MCKEON and R. V. BELLAMKONDA. 2010. Sustained delivery of thermostabilized chABC enhances axonal sprouting and functional recovery after spinal cord injury. *Proc Natl Acad Sci U S A,* **107**(8), pp.3340-5.

LEMON, R., S. N BAKER, J. A. DAVIS, P. KIRKWOOD, M. A. MAIER and H. S YANG. 1998. The Importance of the Cortico-Motoneuronal System for Control of Grasp. **218**, pp.202-15; discussion 215.

LEMON, R. N. 2008. Descending Pathways in Motor Control. **31**(1), pp.195-218.

LEMONS, M. L., D. R. HOWLAND and D. K. ANDERSON. 1999. Chondroitin sulfate proteoglycan immunoreactivity increases following spinal cord injury and transplantation. *Exp Neurol,* **160**(1), pp.51-65.

LENDVAI, D., M. MORAWSKI, L. NÉGYESSY, G. GÁTI, C. JÄGER, G. BAKSA, T. GLASZ, J. ATTEMS, H. TANILA, T. ARENDT, T. HARKANY and A. ALPÁR. 2013. Neurochemical mapping of the human hippocampus reveals perisynaptic matrix around functional synapses in Alzheimer's disease. *Acta Neuropathologica,* **125**(2), pp.215-229.

LENSJO, K. K., M. E. LEPPEROD, G. DICK, T. HAFTING and M. FYHN. 2017. Removal of Perineuronal Nets Unlocks Juvenile Plasticity Through Network Mechanisms of Decreased Inhibition and Increased Gamma Activity. *J Neurosci,* **37**(5), pp.1269-1283.

LIEBSCHER, T., L. SCHNELL, D. SCHNELL, J. SCHOLL, R. SCHNEIDER, M. GULLO, K. FOUAD, A. MIR, M. RAUSCH, D. KINDLER, F. P. HAMERS and M. E. SCHWAB. 2005. Nogo-A antibody improves regeneration and locomotion of spinal cord-injured rats. *Ann Neurol,* **58**(5), pp.706-19.

LIN, R., J. C. KWOK, D. CRESPO and J. W. FAWCETT. 2008. Chondroitinase ABC has a long-lasting effect on chondroitin sulphate glycosaminoglycan content in the injured rat brain. *J Neurochem,* **104**(2), pp.400-8.

LIU, K., Y. LU, J. K. LEE, R. SAMARA, R. WILLENBERG, I. SEARS-KRAXBERGER, A. TEDESCHI, K. K. PARK, D. JIN, B. CAI, B. G. XU, L. CONNOLLY, O. STEWARD, B. H. ZHENG and Z. G. HE. 2010. PTEN deletion enhances the regenerative ability of adult corticospinal neurons. *Nature Neuroscience,* **13**(9), pp.1075-U64.

LIU, M., P. BOSE, G. A. WALTER, F. J. THOMPSON and K. VANDENBORNE. 2008. A longitudinal study of skeletal muscle following spinal cord injury and locomotor training. *Spinal Cord,* **46**, p488.

LONGBRAKE, E. E., W. LAI, D. P. ANKENY and P. G. POPOVICH. 2007. Characterization and modeling of monocyte-derived macrophages after spinal cord injury. *J Neurochem,* **102**(4), pp.1083-94.

LUO, Y., D. RAIBLE and J. A. RAPER. 1993. Collapsin: a protein in brain that induces the collapse and paralysis of neuronal growth cones. *Cell,* **75**(2), pp.217-27.

LYNSKEY, J. V., A. BELANGER and R. JUNG. 2008. Activity-dependent plasticity in spinal cord injury. *Journal of rehabilitation research and development,* **45**(2), pp.229-240.

MACKIE, M., D. I. HUGHES, D. J. MAXWELL, N. J. TILLAKARATNE and A. J. TODD. 2003. Distribution and colocalisation of glutamate decarboxylase isoforms in the rat spinal cord. *Neuroscience,* **119**(2), pp.461-72.

MADINIER, A., M. J. QUATTROMANI, C. SJÖLUND, K. RUSCHER and T. WIELOCH. 2014. Enriched Housing Enhances Recovery of Limb Placement Ability and Reduces Aggrecan-Containing Perineuronal Nets in the Rat Somatosensory Cortex after Experimental Stroke. *PLOS ONE,* **9**(3), pe93121.

MAGNESS, A. P., 2ND, K. L. BARNES, C. M. FERRARIO, W. COX and D. F. DOHN. 1980. Effect of hyaluronidase on acute spinal cord injury. *Surg Neurol,* **13**(2), pp.157-9.

MAIER, I. C., R. M. ICHIYAMA, G. COURTINE, L. SCHNELL, I. LAVROV, V. R. EDGERTON and M. E. SCHWAB. 2009. Differential effects of anti-Nogo-A antibody treatment and treadmill training in rats with incomplete spinal cord injury. *Brain : a journal of neurology,* **132**(Pt 6), pp.1426-1440.

MAIKOS, J. T. and D. I. SHREIBER. 2007. Immediate damage to the blood-spinal cord barrier due to mechanical trauma. *J Neurotrauma,* **24**(3), pp.492-507.

MANUEL, M. and D. ZYTNICKI. 2011. Alpha, beta and gamma motoneurons: functional diversity in the motor system's final pathway. *J Integr Neurosci,* **10**(3), pp.243-76.

MARSH, B. C., S. L. ASTILL, A. UTLEY and R. M. ICHIYAMA. 2011. Movement rehabilitation after spinal cord injuries: emerging concepts and future directions. *Brain research bulletin,* **84**(4-5), pp.327-336.

MASSEY, J. M., J. AMPS, M. S. VIAPIANO, R. T. MATTHEWS, M. R. WAGONER, C. M. WHITAKER, W. ALILAIN, A. L. YONKOF, A. KHALYFA, N. G. F. COOPER, J. SILVER and S. M. ONIFER. 2008. Increased chondroitin sulfate proteoglycan expression in denervated brainstem targets following spinal cord injury creates a barrier to axonal regeneration overcome by chondroitinase ABC and neurotrophin-3. *Experimental Neurology,* **209**(2), pp.426-445.

MASSEY, J. M., C. H. HUBSCHER, M. R. WAGONER, J. A. DECKER, J. AMPS, J. SILVER and S. M. ONIFER. 2006. Chondroitinase ABC Digestion of the Perineuronal Net Promotes Functional Collateral Sprouting in the Cuneate Nucleus after Cervical Spinal Cord Injury. *The Journal of Neuroscience,* **26**(16), pp.4406-4414.

MATSUYAMA, Y., K. CHIBA, H. IWATA, T. SEO and Y. TOYAMA. 2018. A multicenter, randomized, double-blind, dose-finding study of condoliase in patients with lumbar disc herniation. **28**(5), p499.

MATTHEWS, R. T., G. M. KELLY, C. A. ZERILLO, G. GRAY, M. TIEMEYER and S. HOCKFIELD. 2002. Aggrecan glycoforms contribute to the molecular heterogeneity of perineuronal nets. *J Neurosci,* **22**(17), pp.7536-47.

MATUTE, C., E. ALBERDI, G. IBARRETXE and M. V. SANCHEZ-GOMEZ. 2002. Excitotoxicity in glial cells. *Eur J Pharmacol,* **447**(2-3), pp.239-46.

MAUREL, P., U. RAUCH, M. FLAD, R. K. MARGOLIS and R. U. MARGOLIS. 1994. Phosphacan, a chondroitin sulfate proteoglycan of brain that interacts with neurons and neural cell-adhesion molecules, is an extracellular variant of a receptor-type protein tyrosine phosphatase. *Proceedings of the National Academy of Sciences,* **91**(7), pp.2512-2516.

MAYNARD, F. M., JR., M. B. BRACKEN, G. CREASEY, J. F. DITUNNO, JR., W. H. DONOVAN, T. B. DUCKER, S. L. GARBER, R. J. MARINO, S. L. STOVER, C. H. TATOR, R. L. WATERS, J. E. WILBERGER and W. YOUNG. 1997. International Standards for Neurological and Functional Classification of Spinal Cord Injury. American Spinal Injury Association. *Spinal Cord,* **35**(5), pp.266-74.

MCRAE, P. A. and B. E. PORTER. 2012. The perineuronal net component of the extracellular matrix in plasticity and epilepsy. *Neurochem Int,* **61**(7), pp.963-72.

MCRAE, P. A., M. M. ROCCO, G. KELLY, J. C. BRUMBERG and R. T. MATTHEWS. 2007. Sensory deprivation alters aggrecan and perineuronal net expression in the mouse barrel cortex. *J Neurosci,* **27**(20), pp.5405-13.

MCTIGUE, D. M., P. G. POPOVICH, T. E. MORGAN and B. T. STOKES. 2000. Localization of transforming growth factor-beta1 and receptor mRNA after experimental spinal cord injury. *Exp Neurol,* **163**(1), pp.220-30.

MECOLLARI, V., B. NIEUWENHUIS and J. VERHAAGEN. 2014. A perspective on the role of class III semaphorin signaling in central nervous system trauma. *Frontiers in cellular neuroscience,* **8**, pp.328-328.

METZ, G. A., A. CURT, H. VAN DE MEENT, I. KLUSMAN, M. E. SCHWAB and V. DIETZ. 2000. Validation of the weight-drop contusion model in rats: a comparative study of human spinal cord injury. *J Neurotrauma,* **17**(1), pp.1-17.

METZ, G. A. and I. Q. WHISHAW. 2009. The ladder rung walking task: a scoring system and its practical application. *J Vis Exp,* (28).

MIDDLETON, J. W., A. DAYTON, J. WALSH, S. B. RUTKOWSKI, G. LEONG and S. DUONG. 2012. Life expectancy after spinal cord injury: a 50-year study. *Spinal Cord,* **50**(11), pp.803-11.

MIKAMI, T., D. YASUNAGA and H. KITAGAWA. 2009. Contactin-1 is a functional receptor for neuroregulatory chondroitin sulfate-E. *J Biol Chem,* **284**(7), pp.4494-9.

MILBRETA, U., Y. VON BOXBERG, P. MAILLY, F. NOTHIAS and S. SOARES. 2014. Astrocytic and vascular remodeling in the injured adult rat spinal cord after chondroitinase ABC treatment. *Journal of neurotrauma,* **31**(9), pp.803-818.

MILLER, G. M. and L. C. HSIEH-WILSON. 2015. Sugar-dependent modulation of neuronal development, regeneration, and plasticity by chondroitin sulfate proteoglycans. *Experimental neurology,* **274**(Pt B), pp.115-125.

MIRE, E., N. THOMASSET, L. B. JAKEMAN and G. ROUGON. 2008. Modulating Sema3A signal with a L1 mimetic peptide is not sufficient to promote motor recovery and axon regeneration after spinal cord injury. *Mol Cell Neurosci,* **37**(2), pp.222-35.

MISAWA, H., M. HARA, S. TANABE, M. NIIKURA, Y. MORIWAKI and T. OKUDA. 2012. Osteopontin is an alpha motor neuron marker in the mouse spinal cord. *J Neurosci Res,* **90**(4), pp.732-42.

MIYATA, S. and H. KITAGAWA. 2016. Chondroitin 6-Sulfation Regulates Perineuronal Net Formation by Controlling the Stability of Aggrecan. *Neural Plast,* **2016**, p1305801.

MIYATA, S., Y. KOMATSU, Y. YOSHIMURA, C. TAYA and H. KITAGAWA. 2012. Persistent cortical plasticity by upregulation of chondroitin 6-sulfation. *Nature neuroscience,* **15**(3), p414.

MONFILS, M. H., E. J. PLAUTZ and J. A. KLEIM. 2005. In Search of the Motor Engram: Motor Map Plasticity as a Mechanism for Encoding Motor Experience. *The Neuroscientist,* **11**(5), pp.471-483.

MONNIER, P. P., A. SIERRA, J. M. SCHWAB, S. HENKE-FAHLE and B. K. MUELLER. 2003. The Rho/ROCK pathway mediates neurite growth-inhibitory activity associated with the chondroitin sulfate proteoglycans of the CNS glial scar. *Mol Cell Neurosci,* **22**(3), pp.319-30.

MONTANI, L., B. GERRITS, P. GEHRIG, A. KEMPF, L. DIMOU, B. WOLLSCHEID and M. E. J. J. O. B. C. SCHWAB. 2009. Neuronal Nogo-A modulates growth cone motility via Rho-GTP/LIMK1/cofilin in the unlesioned adult nervous system. **284**(16), pp.10793-10807.

MOON, L. D. F., R. A. ASHER and J. W. FAWCETT. 2003. Limited growth of severed CNS axons after treatment of adult rat brain with hyaluronidase. *Journal of Neuroscience Research,* **71**(1), pp.23-37.

MOON, L. D. F., R. A. ASHER, K. E. RHODES and J. W. FAWCETT. 2001. Regeneration of CNS axons back to their target following treatment of adult rat brain with chondroitinase ABC. *Nature Neuroscience,* **4**(5), pp.465-466.

MOORE, N. J., G. S. BHUMBRA, J. D. FOSTER and M. BEATO. 2015. Synaptic Connectivity between Renshaw Cells and Motoneurons in the Recurrent Inhibitory Circuit of the Spinal Cord. *J Neurosci,* **35**(40), pp.13673-86.

MORAWSKI, M., G. BRÜCKNER, T. ARENDT and R. T. MATTHEWS. 2012. Aggrecan: Beyond cartilage and into the brain. *The International Journal of Biochemistry & Cell Biology,* **44**(5), pp.690-693.

MORAWSKI, M., M. K. BRUCKNER, P. RIEDERER, G. BRUCKNER and T. ARENDT. 2004. Perineuronal nets potentially protect against oxidative stress. *Exp Neurol,* **188**(2), pp.309-15.

MORAWSKI, M., A. DITYATEV, M. HARTLAGE-RUBSAMEN, M. BLOSA, M. HOLZER, K. FLACH, S. PAVLICA, G. DITYATEVA, J. GROSCHE, G. BRUCKNER and M. SCHACHNER. 2014. Tenascin-R promotes assembly of the extracellular matrix of perineuronal nets via clustering of aggrecan. *Philos Trans R Soc Lond B Biol Sci,* **369**(1654), p20140046.

MORAWSKI, M., T. REINERT, W. MEYER-KLAUCKE, F. E. WAGNER, W. TROGER, A. REINERT, C. JAGER, G. BRUCKNER and T. ARENDT. 2015. Ion exchanger in the brain: Quantitative analysis of perineuronally fixed anionic binding sites suggests diffusion barriers with ion sorting properties. *Sci Rep,* **5**, p16471.

MOREAU-FAUVARQUE, C., A. KUMANOGOH, E. CAMAND, C. JAILLARD, G. BARBIN, I. BOQUET, C. LOVE, E. Y. JONES, H. KIKUTANI, C. LUBETZKI, I. DUSART and A. CHEDOTAL. 2003. The transmembrane semaphorin Sema4D/CD100, an inhibitor of axonal growth, is expressed on oligodendrocytes and upregulated after CNS lesion. *J Neurosci,* **23**(27), pp.9229-39.

MOUNTNEY, A., M. R. ZAHNER, E. R. STURGILL, C. J. RILEY, J. W. ASTON, M. OUDEGA, L. P. SCHRAMM, A. HURTADO and R. L. SCHNAAR. 2013. Sialidase, chondroitinase ABC, and combination therapy after spinal cord contusion injury. *Journal of neurotrauma,* **30**(3), pp.181-190.

MUELLER, A. L., A. DAVIS, S. SOVICH, S. S. CARLSON and F. R. ROBINSON. 2016. Distribution of N-Acetylgalactosamine-Positive Perineuronal Nets in the Macaque Brain: Anatomy and Implications. *Neural Plasticity,* **2016**.

MUIR, E. M., I. FYFE, S. GARDINER, L. LI, P. WARREN, J. W. FAWCETT, R. J. KEYNES and J. H. ROGERS. 2010. Modification of N-glycosylation sites allows secretion of bacterial chondroitinase ABC from mammalian cells. *J Biotechnol,* **145**(2), pp.103-10.

MULLEN, R. J., C. R. BUCK and A. M. SMITH. 1992. NeuN, a neuronal specific nuclear protein in vertebrates. *Development,* **116**(1), pp.201-211.

MULLNER, A., R. R. GONZENBACH, O. WEINMANN, L. SCHNELL, T. LIEBSCHER and M. E. SCHWAB. 2008. Lamina-specific restoration of serotonergic projections after Nogo-A antibody treatment of spinal cord injury in rats. *Eur J Neurosci,* **27**(2), pp.326-33.

NEAFSEY, E. J., E. L. BOLD, G. HAAS, K. M. HURLEY-GIUS, G. QUIRK, C. F. SIEVERT and R. R. TERREBERRY. 1986. The organization of the rat motor cortex: a microstimulation mapping study. *Brain research,* **396**(1), pp.77-96.

NESIC, O., G. Y. XU, D. MCADOO, K. W. HIGH, C. HULSEBOSCH and R. PEREZ-POL. 2001. IL-1 receptor antagonist prevents apoptosis and caspase-3 activation after spinal cord injury. *J Neurotrauma,* **18**(9), pp.947-56.

NEUMANN, S. and C. J. WOOLF. 1999. Regeneration of dorsal column fibers into and beyond the lesion site following adult spinal cord injury. *Neuron,* **23**(1), pp.83-91.

NIEDERÖST, B., T. OERTLE, J. FRITSCHE, R. A. MCKINNEY and C. E. J. J. O. N. BANDTLOW. 2002. Nogo-A and myelin-associated glycoprotein mediate neurite growth inhibition by antagonistic regulation of RhoA and Rac1. **22**(23), pp.10368-10376.

NISHIBE, M., E. T. R. URBAN, 3RD, S. BARBAY and R. J. NUDO. 2015. Rehabilitative training promotes rapid motor recovery but delayed motor map reorganization in a rat cortical ischemic infarct model. *Neurorehabilitation and neural repair,* **29**(5), pp.472-482.

NOBLE, L. J., F. DONOVAN, T. IGARASHI, S. GOUSSEV and Z. WERB. 2002. Matrix metalloproteinases limit functional recovery after spinal cord injury by modulation of early vascular events. *The Journal of neuroscience : the official journal of the Society for Neuroscience,* **22**(17), pp.7526-7535.

NUDO, R. J., W. M. JENKINS and M. M. MERZENICH. 1990. Repetitive microstimulation alters the cortical representation of movements in adult rats. *Somatosensory & motor research,* **7**(4), pp.463-483.

NUDO, R. J. and R. B. MASTERTON. 1990. Descending pathways to the spinal cord, III: Sites of origin of the corticospinal tract. *Journal of Comparative Neurology,* **296**(4), pp.559-583.

NUDO, R. J. and G. W. MILLIKEN. 1996. Reorganization of movement representations in primary motor cortex following focal ischemic infarcts in adult squirrel monkeys. *J Neurophysiol,* **75**(5), pp.2144-9.

O'REGAN, M. H. 1989. Xylazine-evoked depression of rat cerebral cortical neurons: a pharmacological study. *Gen Pharmacol,* **20**(4), pp.469-74.

OHTAKE, Y., D. WONG, P. M. ABDUL-MUNEER, M. E. SELZER and S. LI. 2016. Two PTP receptors mediate CSPG inhibition by convergent and divergent signaling pathways in neurons. *Scientific reports,* **6**, pp.37152-37152.

OKAMOTO, M., S. MORI and H. ENDO. 1994. A protective action of chondroitin sulfate proteoglycans against neuronal cell death induced by glutamate. *Brain Res,* **637**(1-2), pp.57-67.

OLIVEIRA, A. L. R., F. HYDLING, E. OLSSON, T. SHI, R. H. EDWARDS, F. FUJIYAMA, T. KANEKO, T. HÖKFELT, S. CULLHEIM and B. MEISTER. 2003. Cellular localization of three vesicular glutamate transporter mRNAs and proteins in rat spinal cord and dorsal root ganglia. *Synapse,* **50**(2), pp.117-129.

OOHASHI, T., S. HIRAKAWA, Y. BEKKU, U. RAUCH, D. R. ZIMMERMANN, W.-D. SU, A. OHTSUKA, T. MURAKAMI and Y. NINOMIYA. 2002. Bral1, a Brain-Specific Link Protein, Colocalizing with the Versican V2 Isoform at the Nodes of Ranvier in Developing and Adult Mouse Central Nervous Systems. *Molecular and Cellular Neuroscience,* **19**(1), pp.43-57.

OOHIRA, A., F. MATSUI, E. WATANABE, Y. KUSHIMA and N. MAEDA. 1994. Developmentally regulated expression of a brain specific species of chondroitin sulfate proteoglycan, neurocan, identified with a monoclonal antibody 1G2 in the rat cerebrum. *Neuroscience,* **60**(1), pp.145-157.

ORLANDO, C. and O. RAINETEAU. 2015. Integrity of cortical perineuronal nets influences corticospinal tract plasticity after spinal cord injury. *Brain structure & function,* **220**(2), pp.1077-1091.

OYINBO, C. A. 2011. Secondary injury mechanisms in traumatic spinal cord injury: a nugget of this multiply cascade. *Acta Neurobiol Exp (Wars),* **71**(2), pp.281-99.

PANTAZOPOULOS, H. and S. BERRETTA. 2016. In Sickness and in Health: Perineuronal Nets and Synaptic Plasticity in Psychiatric Disorders. *Neural plasticity,* **2016**, p9847696.

PARK, K., Y. LEE, S. PARK, S. LEE, Y. HONG, S. KIL LEE and Y. HONG. 2010. Synergistic effect of melatonin on exercise-induced neuronal reconstruction and functional recovery in a spinal cord injury animal model. *J Pineal Res,* **48**(3), pp.270-81.

PARK, K. K., K. LIU, Y. HU, P. D. SMITH, C. WANG, B. CAI, B. G. XU, L. CONNOLLY, I. KRAMVIS, M. SAHIN and Z. G. HE. 2008. Promoting Axon Regeneration in the Adult CNS by Modulation of the PTEN/mTOR Pathway. *Science,* **322**(5903), pp.963-966.

PASCUAL-LEONE, A. and F. TORRES. 1993. Plasticity of the sensorimotor cortex representation of the reading finger in Braille readers. *Brain,* **116**(1), pp.39-52.

PASTERKAMP, R. J., R. J. GIGER, M. J. RUITENBERG, A. J. HOLTMAAT, J. DE WIT, F. DE WINTER and J. VERHAAGEN. 1999. Expression of the gene encoding the chemorepellent semaphorin III is induced in the fibroblast component of neural scar tissue formed following injuries of adult but not neonatal CNS. *Mol Cell Neurosci,* **13**(2), pp.143-66.

PAXINOS, G. and C. WATSON. 2006. *The rat brain in stereotaxic coordinates: hard cover edition.* Elsevier.

PEARSON, C. S., C. P. MENCIO, A. C. BARBER, K. R. MARTIN and H. M. GELLER. 2018. Identification of a critical sulfation in chondroitin that inhibits axonal regeneration. *eLife,* **7**, pe37139.

PENDLETON, J. C., M. J. SHAMBLOTT, D. S. GARY, V. BELEGU, A. HURTADO, M. L. MALONE and J. W. MCDONALD. 2013. Chondroitin sulfate proteoglycans inhibit oligodendrocyte myelination through PTPσ. *Experimental neurology,* **247**, pp.113-121.

PENFIELD, W. and E. BOLDREY. 1937. Somatic motor and sensory representation in the cernebral cortex of man as studied by electrical stimualtion. *Brain,* **60**(4), pp.389-443.

PERSSON, S., J. L. BOULLAND, M. ASPLING, M. LARSSON, R. T. FREMEAU, R. H. EDWARDS, J. STORM-MATHISEN, F. A. CHAUDHRY and J. J. J. O. C. N. BROMAN. 2006. Distribution of vesicular glutamate transporters 1 and 2 in the rat spinal cord, with a note on the spinocervical tract. **497**(5), pp.683-701.

PHELPS, P. E., R. P. BARBER, C. R. HOUSER, G. D. CRAWFORD, P. M. SALVATERRA and J. E. VAUGHN. 1984. Postnatal development of neurons containing choline acetyltransferase in rat spinal cord: an immunocytochemical study. *The Journal of comparative neurology,* **229**(3), pp.347-361.

PIZZI, M. A. and M. J. CROWE. 2007. Matrix metalloproteinases and proteoglycans in axonal regeneration. *Experimental Neurology,* **204**(2), pp.496-511.

PIZZORUSSO, T., P. MEDINI, N. BERARDI, S. CHIERZI, J. W. FAWCETT and L. MAFFEI. 2002. Reactivation of ocular dominance plasticity in the adult visual cortex. *Science (New York, N.Y.),* **298**(5596), pp.1248-1251.

PLAUTZ, E. J., G. W. MILLIKEN and R. J. NUDO. 2000. Effects of repetitive motor training on movement representations in adult squirrel monkeys: role of use versus learning. *Neurobiol Learn Mem,* **74**(1), pp.27-55.

PRABHAKAR, V., R. RAMAN, I. CAPILA, C. J. BOSQUES, K. POJASEK and R. SASISEKHARAN. 2005. Biochemical characterization of the chondroitinase ABC I active site. *The Biochemical journal,* **390**(Pt 2), pp.395-405.

PROPERZI, F., D. CARULLI, R. A. ASHER, E. MUIR, L. M. CAMARGO, T. H. VAN KUPPEVELT, G. B. TEN DAM, Y. FURUKAWA, T. MIKAMI, K. SUGAHARA, T. TOIDA, H. M. GELLER and J. W. FAWCETT. 2005. Chondroitin 6-sulphate synthesis is up-regulated in injured CNS, induced by injury-related cytokines and enhanced in axon-growth inhibitory glia. *The European journal of neuroscience,* **21**(2), pp.378-390.

PRUSS, H., M. A. KOPP, B. BROMMER, N. GATZEMEIER, I. LAGINHA, U. DIRNAGL and J. M. SCHWAB. 2011. Non-resolving aspects of acute inflammation after spinal cord injury (SCI): indices and resolution plateau. *Brain Pathol,* **21**(6), pp.652-60.

QUATTROMANI, M. J., M. PRUVOST, C. GUERREIRO, F. BACKLUND, E. ENGLUND, A. ASPBERG, T. JAWORSKI, J. HAKON, K. RUSCHER, L. KACZMAREK, D. VIVIEN and T. WIELOCH. 2018. Extracellular Matrix Modulation Is Driven by Experience-Dependent Plasticity During Stroke Recovery. *Molecular Neurobiology,* **55**(3), pp.2196-2213.

RENIER, N., Z. WU, D. J. SIMON, J. YANG, P. ARIEL and M. TESSIER-LAVIGNE. 2014. iDISCO: a simple, rapid method to immunolabel large tissue samples for volume imaging. *Cell,* **159**(4), pp.896-910.

RICHARDSON, P. M., U. M. MCGUINNESS and A. J. AGUAYO. 1980. Axons from CNS neurons regenerate into PNS grafts. *Nature,* **284**(5753), pp.264-5.

RIPELLINO, J. A., M. M. KLINGER, R. U. MARGOLIS and R. K. MARGOLIS. 1985. The hyaluronic acid binding region as a specific probe for the localization of hyaluronic acid in tissue sections. Application to chick embryo and rat brain. *J Histochem Cytochem,* **33**(10), pp.1060-6.

ROBERTS, E. 1975. GABA in nervous system function - An overview. *The Nervous System, the Basic Neurosciences,* **1**.

ROCK, K. L. and H. KONO. 2008. The inflammatory response to cell death. *Annual review of pathology,* **3**, pp.99-126.

ROGERS, C. J., P. M. CLARK, S. E. TULLY, R. ABROL, K. C. GARCIA, W. A. GODDARD and L. C. HSIEH-WILSON. 2011. Elucidating glycosaminoglycan-protein-protein interactions using carbohydrate microarray and computational approaches. *Proceedings of the National Academy of Sciences of the United States of America,* **108**(24), pp.9747-9752.

ROMBERG, C., S. YANG, R. MELANI, M. R. ANDREWS, A. E. HORNER, M. G. SPILLANTINI, T. J. BUSSEY, J. W. FAWCETT, T. PIZZORUSSO and L. M. SAKSIDA. 2013. Depletion of perineuronal nets enhances recognition memory and long-term depression in the perirhinal cortex. *J Neurosci,* **33**(16), pp.7057-65.

ROSENZWEIG, E. S., E. A. SALEGIO, J. J. LIANG, J. L. WEBER, C. A. WEINHOLTZ, J. H. BROCK, R. MOSEANKO, S. HAWBECKER, R. PENDER and C. L. CRUZEN. 2019. Chondroitinase improves anatomical and functional outcomes after primate spinal cord injury. *Nature Neuroscience*, p1.

ROWLANDS, D., K. K. LENSJØ, T. DINH, S. YANG, M. R. ANDREWS, T. HAFTING, M. FYHN, J. W. FAWCETT and G. DICK. 2018. Aggrecan Directs Extracellular Matrix-Mediated Neuronal Plasticity. *The Journal of Neuroscience,* **38**(47), pp.10102-10113.

SANES, J. N., S. SUNER and J. P. DONOGHUE. 1990. Dynamic organization of primary motor cortex output to target muscles in adult rats. I. Long-term patterns of reorganization following motor or mixed peripheral nerve lesions. *Exp Brain Res,* **79**(3), pp.479-91.

SCHEFF, S. and K. N. ROBERTS. 2009. Infinite Horizon Spinal Cord Contusion Model. *In:* J. CHEN, Z. C. XU, X.-M. XU and J. H. ZHANG, eds. *Animal Models of Acute Neurological Injuries.* Totowa, NJ: Humana Press, pp.423-432.

SCHEFF, S. W., A. G. RABCHEVSKY, I. FUGACCIA, J. A. MAIN and J. E. LUMPP. 2003. Experimental modeling of spinal cord injury: characterization of a force-defined injury device. *Journal of neurotrauma,* **20**(2), pp.179-193.

SCHEFF, S. W., D. A. SAUCIER and M. E. CAIN. 2002. A statistical method for analyzing rating scale data: the BBB locomotor score. *J Neurotrauma,* **19**(10), pp.1251-60.

SCHINDELIN, J., I. ARGANDA-CARRERAS, E. FRISE, V. KAYNIG, M. LONGAIR, T. PIETZSCH, S. PREIBISCH, C. RUEDEN, S. SAALFELD, B. SCHMID, J.-Y. TINEVEZ, D. J. WHITE, V. HARTENSTEIN, K. ELICEIRI, P. TOMANCAK and A. CARDONA. 2012. Fiji: an open-source platform for biological-image analysis. *Nat Meth,* **9**(7), pp.676-682.

SCHMIDT, R. D. and V. MARKOVCHICK. 1992. Nontraumatic spinal cord compression. *J Emerg Med,* **10**(2), pp.189-99.

SCHWAB, M. E. 2010. Functions of Nogo proteins and their receptors in the nervous system. *Nat Rev Neurosci,* **11**(12), pp.799-811.

SCIVOLETTO, G., B. MORGANTI and M. MOLINARI. 2004. Neurologic recovery of spinal cord injury patients in Italy. *Archives of Physical Medicine and Rehabilitation,* **85**(3), pp.485-489.

SHAH, P. K., G. GARCIA-ALIAS, J. CHOE, P. GAD, Y. GERASIMENKO, N. TILLAKARATNE, H. ZHONG, R. R. ROY and V. R. EDGERTON. 2013. Use of

quadrupedal step training to re-engage spinal interneuronal networks and improve locomotor function after spinal cord injury. *Brain : a journal of neurology,* **136**(Pt 11), pp.3362-3377.

SHEFNER, J. M., S. A. BERMAN, M. SARKARATI and R. R. YOUNG. 1992. Recurrent inhibition is increased in patients with spinal cord injury. *Neurology,* **42**(11), pp.2162-8.

SHEN, Y., A. P. TENNEY, S. A. BUSCH, K. P. HORN, F. X. CUASCUT, K. LIU, Z. HE, J. SILVER and J. G. FLANAGAN. 2009. PTPsigma is a receptor for chondroitin sulfate proteoglycan, an inhibitor of neural regeneration. *Science (New York, N.Y.),* **326**(5952), pp.592-596.

SHINOZAKI, M., A. IWANAMI, K. FUJIYOSHI, S. TASHIRO, K. KITAMURA, S. SHIBATA, H. FUJITA, M. NAKAMURA and H. OKANO. 2016. Combined treatment with chondroitinase ABC and treadmill rehabilitation for chronic severe spinal cord injury in adult rats. *Neuroscience research,* **113**, pp.37-47.

SHNEIDER, N. A., M. N. BROWN, C. A. SMITH, J. PICKEL and F. J. ALVAREZ. 2009. Gamma motor neurons express distinct genetic markers at birth and require muscle spindle-derived GDNF for postnatal survival. *Neural development,* **4**(1), p1.

SIEBERT, J. R. and D. J. OSTERHOUT. 2011. The inhibitory effects of chondroitin sulfate proteoglycans on oligodendrocytes. *Journal of neurochemistry,* **119**(1), pp.176-188.

SIEGEL, C. S., K. L. FINK, S. M. STRITTMATTER and W. B. CAFFERTY. 2015. Plasticity of intact rubral projections mediates spontaneous recovery of function after corticospinal tract injury. *The Journal of neuroscience : the official journal of the Society for Neuroscience,* **35**(4), pp.1443-1457.

SILVER, J. and J. H. MILLER. 2004. Regeneration beyond the glial scar. *Nature reviews. Neuroscience,* **5**(2), pp.146-156.

SINGH, A., L. TETREAULT, S. KALSI-RYAN, A. NOURI and M. G. FEHLINGS. 2014. Global prevalence and incidence of traumatic spinal cord injury. *Clinical epidemiology,* **6**, pp.309-331.

SIVASANKARAN, R., J. PEI, K. C. WANG, Y. P. ZHANG, C. B. SHIELDS, X. M. XU and Z. HE. 2004. PKC mediates inhibitory effects of myelin and chondroitin sulfate proteoglycans on axonal regeneration. *Nat Neurosci,* **7**(3), pp.261-8.

SMITH, C. C., R. MAURICIO, L. NOBRE, B. MARSH, R. C. WÜST, H. B. ROSSITER and R. M. ICHIYAMA. 2015. Differential regulation of perineuronal nets in the brain and spinal cord with exercise training. *Brain research bulletin,* **111**, pp.20-26.

SODERBLOM, C., X. LUO, E. BLUMENTHAL, E. BRAY, K. LYAPICHEV, J. RAMOS, V. KRISHNAN, C. LAI-HSU, K. K. PARK, P. TSOULFAS and J. K. LEE. 2013. Perivascular fibroblasts form the fibrotic scar after contusive spinal cord injury. *J Neurosci,* **33**(34), pp.13882-7.

SOLEMAN, S., P. K. YIP, D. A. DURICKI and L. D. MOON. 2012. Delayed treatment with chondroitinase ABC promotes sensorimotor recovery and plasticity after stroke in aged rats. *Brain,* **135**(Pt 4), pp.1210-23.

ŠOLTÉS, L., R. MENDICHI, G. KOGAN, J. SCHILLER, M. STANKOVSKA and J. ARNHOLD. 2006. Degradative action of reactive oxygen species on hyaluronan. *Biomacromolecules,* **7**(3), pp.659-668.

SPICER, A. P., A. JOO and R. A. BOWLING, JR. 2003. A hyaluronan binding link protein gene family whose members are physically linked adjacent to chondroitin sulfate proteoglycan core protein genes: the missing links. *J Biol Chem,* **278**(23), pp.21083-91.

SPRINGER, J. E., R. D. AZBILL and P. E. KNAPP. 1999. Activation of the caspase-3 apoptotic cascade in traumatic spinal cord injury. *Nat Med,* **5**(8), pp.943-6.

STAMMERS, A. T., J. LIU and B. K. KWON. 2012. Expression of inflammatory cytokines following acute spinal cord injury in a rodent model. *J Neurosci Res,* **90**(4), pp.782-90.

STARKEY, M. L., K. BARTUS, A. W. BARRITT and E. J. BRADBURY. 2012. Chondroitinase ABC promotes compensatory sprouting of the intact corticospinal tract and recovery of forelimb function following unilateral pyramidotomy in adult mice. *Eur J Neurosci,* **36**(12), pp.3665-78.

STRUVE, J., P. C. MAHER, Y. Q. LI, S. KINNEY, M. G. FEHLINGS, C. T. KUNTZ and L. S. SHERMAN. 2005. Disruption of the hyaluronan-based extracellular matrix in spinal cord promotes astrocyte proliferation. *Glia,* **52**(1), pp.16-24.

SUGIYAMA, S., A. A. DI NARDO, S. AIZAWA, I. MATSUO, M. VOLOVITCH, A. PROCHIANTZ and T. K. HENSCH. 2008. Experience-dependent transfer of Otx2 homeoprotein into the visual cortex activates postnatal plasticity. *Cell,* **134**(3), pp.508-520.

SUN, F., K. K. PARK, S. BELIN, D. WANG, T. LU, G. CHEN, K. ZHANG, C. YEUNG, G. FENG, B. A. YANKNER and Z. HE. 2011. Sustained axon regeneration induced by co-deletion of PTEN and SOCS3. *Nature,* **480**, p372.

SUTTKUS, A., S. ROHN, S. WEIGEL, P. GLÖCKNER, T. ARENDT and M. MORAWSKI. 2014a. Aggrecan, link protein and tenascin-R are essential components of the perineuronal net to protect neurons against iron-induced oxidative stress. *Cell death & disease,* **5**.

SUTTKUS, A., S. ROHN, S. WEIGEL, P. GLÖCKNER, T. ARENDT and M. MORAWSKI. 2014b. Aggrecan, link protein and tenascin-R are essential components of the perineuronal net to protect neurons against iron-induced oxidative stress. *Cell Death & Disease,* **5**(3), pcddis201425.

SYDEKUM, E., C. BALTES, A. GHOSH, T. MUEGGLER, M. E. SCHWAB and M. RUDIN. 2009. Functional reorganization in rat somatosensory cortex assessed by fMRI: elastic image registration based on structural landmarks in fMRI images and application to spinal cord injured rats. *Neuroimage,* **44**(4), pp.1345-54.

SYDEKUM, E., A. GHOSH, M. GULLO, C. BALTES, M. SCHWAB and M. RUDIN. 2014. Rapid functional reorganization of the forelimb cortical representation after thoracic spinal cord injury in adult rats. *NeuroImage,* **87**, pp.72-79.

SZYDLOWSKA, K. and M. TYMIANSKI. 2010. Calcium, ischemia and excitotoxicity. *Cell Calcium,* **47**(2), pp.122-9.

TACHI, Y., T. OKUDA, N. KAWAHARA, N. KATO, Y. ISHIGAKI and T. MATSUMOTO. 2015. Expression of hyaluronidase-4 in a rat spinal cord hemisection model. *Asian Spine J,* **9**(1), pp.7-13.

TAKAHASHI-IWANAGA, H., T. MURAKAMI and K. ABE. 1998. Three-dimensional microanatomy of perineuronal proteoglycan nets enveloping motor neurons in the rat spinal cord. *Journal of Neurocytology,* **27**(11), pp.817-827.

TAKAMORI, S., J. S. RHEE, C. ROSENMUND and R. JAHN. 2001. Identification of differentiation-associated brain-specific phosphate transporter as a second vesicular glutamate transporter (VGLUT2). *J Neurosci,* **21**(22), pRc182.

TANDON, S., N. KAMBI, L. LAZAR, H. MOHAMMED and N. JAIN. 2009. Large-scale expansion of the face representation in somatosensory areas of the lateral sulcus after spinal cord injuries in monkeys. *The Journal of neuroscience : the official journal of the Society for Neuroscience,* **29**(38), pp.12009-12019.

TANG, X., J. E. DAVIES and S. J. A. DAVIES. 2003. Changes in distribution, cell associations, and protein expression levels of NG2, neurocan, phosphacan, brevican, versican V2, and tenascin-C during acute to chronic maturation of spinal cord scar tissue. *Journal of Neuroscience Research,* **71**(3), pp.427-444.

TANTRAL, L., K. MALATHI, S. KOHYAMA, M. SILANE, A. BERENSTEIN and T. JAYARAMAN. 2004. Intracellular calcium release is required for caspase-3 and -9 activation. *Cell Biochem Funct,* **22**(1), pp.35-40.

TATOR, C. H. and M. G. FEHLINGS. 1991. Review of the secondary injury theory of acute spinal cord trauma with emphasis on vascular mechanisms. *J Neurosurg,* **75**(1), pp.15-26.

TAUCHI, R., S. IMAGAMA, T. NATORI, T. OHGOMORI, A. MURAMOTO, R. SHINJO, Y. MATSUYAMA, N. ISHIGURO and K. KADOMATSU. 2012. The endogenous proteoglycan-degrading enzyme ADAMTS-4 promotes functional recovery after spinal cord injury. *Journal of Neuroinflammation,* **9**(1), p53.

TENGBLAD, A. 1981. A comparative study of the binding of cartilage link protein and the hyaluronate-binding region of the cartilage proteoglycan to hyaluronate-substituted Sepharose gel. *The Biochemical journal,* **199**(2), pp.297-305.

TESTER, N. J. and D. R. HOWLAND. 2008. Chondroitinase ABC improves basic and skilled locomotion in spinal cord injured cats. *Exp Neurol,* **209**(2), pp.483-96.

TESTER, N. J., A. H. PLAAS and D. R. HOWLAND. 2007. Effect of body temperature on chondroitinase ABC's ability to cleave chondroitin sulfate glycosaminoglycans. *J Neurosci Res,* **85**(5), pp.1110-8.

THOMPSON, K. M., N. UETANI, C. MANITT, M. ELCHEBLY, M. L. TREMBLAY and T. E. KENNEDY. 2003. Receptor protein tyrosine phosphatase sigma inhibits axonal regeneration and the rate of axon extension. *Molecular and Cellular Neuroscience,* **23**(4), pp.681-692.

TILLAKARATNE, N. J. K., R. D. DE LEON, T. X. HOANG, R. R. ROY, V. R. EDGERTON and A. J. TOBIN. 2002. Use-Dependent Modulation of Inhibitory Capacity in the Feline Lumbar Spinal Cord. *The Journal of Neuroscience,* **22**(8), pp.3130-3143.

TODD, A. J., D. I. HUGHES, E. POLGÁR, G. G. NAGY, M. MACKIE, O. P. OTTERSEN and D. J. MAXWELL. 2003. The expression of vesicular glutamate transporters VGLUT1 and VGLUT2 in neurochemically defined axonal populations in the rat spinal cord with emphasis on the dorsal horn. *European Journal of Neuroscience,* **17**(1), pp.13-27.

TOM, V. J., R. KADAKIA, L. SANTI and J. D. HOULÉ. 2009. Administration of Chondroitinase ABC Rostral or Caudal to a Spinal Cord Injury Site Promotes Anatomical but Not Functional Plasticity. *Journal of Neurotrauma,* **26**(12), pp.2323-2333.

TONA, A. and A. BIGNAMI. 1993. Effect of hyaluronidase on brain extracellular matrix in vivo and optic nerve regeneration. *J Neurosci Res,* **36**(2), pp.191-9.

TOOLE, B. P. 2004. Hyaluronan: from extracellular glue to pericellular cue. *Nature Reviews Cancer,* **4**(7), p528.

TRAN, A. P., S. SUNDAR, M. YU, B. T. LANG and J. SILVER. 2018. Modulation of Receptor Protein Tyrosine Phosphatase Sigma Increases Chondroitin Sulfate Proteoglycan Degradation through Cathepsin B Secretion to Enhance Axon Outgrowth. *J Neurosci,* **38**(23), pp.5399-5414.

TSIEN, R. Y. 2013. Very long-term memories may be stored in the pattern of holes in the perineuronal net. *Proceedings of the National Academy of Sciences of the United States of America,* **110**(30), pp.12456-12461.

UENO, H., S. SUEMITSU, S. MURAKAMI, N. KITAMURA, K. WANI, Y. MATSUMOTO, M. OKAMOTO and T. ISHIHARA. 2019. Layer-specific expression of extracellular matrix molecules in the mouse somatosensory and piriform cortices. *IBRO Reports,* **6**, pp.1-17.

UENO, H., S. SUEMITSU, M. OKAMOTO, Y. MATSUMOTO and T. ISHIHARA. 2017. Sensory experience-dependent formation of perineuronal nets and expression of Cat-315 immunoreactive components in the mouse somatosensory cortex. *Neuroscience,* **355**, pp.161-174.

URBAN, M. W., B. GHOSH, C. G. BLOCK, B. A. CHARSAR, G. M. SMITH, M. C. WRIGHT, S. LI and A. C. LEPORE. 2019a. PTPsigma inhibitory peptide promotes recovery of diaphragm function and sprouting of bulbospinal respiratory axons following cervical spinal cord injury. *J Neurotrauma*.

URBAN, M. W., B. GHOSH, C. G. BLOCK, L. R. STROJNY, B. A. CHARSAR, M. GOULÃO, S. S. KOMARAVOLU, G. M. SMITH, M. C. WRIGHT, S. LI and A. C. LEPORE. 2019b. Long-distance axon regeneration promotes recovery of diaphragmatic respiratory function after spinal cord injury. *eneuro*, pp.ENEURO.0096-19.2019.

VANDENBERG, P. M., T. M. HOGG, J. A. KLEIM and I. Q. WHISHAW. 2002. Long-Evans rats have a larger cortical topographic representation of movement than Fischer-344 rats: a microstimulation study of motor cortex in naive and skilled reaching-trained rats. *Brain Res Bull,* **59**(3), pp.197-203.

VAROQUI, H., M. K.-H. SCHÄFER, H. ZHU, E. WEIHE and J. D. ERICKSON. 2002. Identification of the Differentiation-Associated Na⁺/P_I Transporter as a Novel Vesicular Glutamate Transporter Expressed in a Distinct Set of Glutamatergic Synapses. **22**(1), pp.142-155.

VEILLEUX-LEMIEUX, D., F. BEAUDRY, P. HÉLIE and P. VACHON. 2012. Effects of endotoxemia on the pharmacodynamics and pharmacokinetics of ketamine and xylazine anesthesia in Sprague-Dawley rats. *Veterinary medicine (Auckland, N.Z.)* [online]. **3**, [Accessed 2012], pp.99-109. Available from: http://europepmc.org/abstract/MED/30101090

http://europepmc.org/articles/PMC6067630?pdf=render

http://europepmc.org/articles/PMC6067630

https://doi.org/10.2147/VMRR.S35666.

VITELLARO-ZUCCARELLO, L., P. BOSISIO, S. MAZZETTI, C. MONTI and S. DE BIASI. 2007. Differential expression of several molecules of the extracellular matrix in functionally and developmentally distinct regions of rat spinal cord. *Cell and tissue research,* **327**(3), pp.433-447.

VO, T., D. CARULLI, E. M. EHLERT, J. C. KWOK, G. DICK, V. MECOLLARI, E. B. MOLONEY, G. NEUFELD, F. DE WINTER, J. W. FAWCETT and J. VERHAAGEN. 2013. The chemorepulsive axon guidance protein semaphorin3A is a constituent of perineuronal nets in the adult rodent brain. *Mol Cell Neurosci,* **56**, pp.186-200.

WAKAO, N., S. IMAGAMA, H. ZHANG, R. TAUCHI, A. MURAMOTO, T. NATORI, S. TAKESHITA, N. ISHIGURO, Y. MATSUYAMA and K. KADOMATSU. 2011. Hyaluronan oligosaccharides promote functional recovery after spinal cord injury in rats. *Neuroscience letters,* **488**(3), pp.299-304.

WANG, D. and J. FAWCETT. 2012. The perineuronal net and the control of CNS plasticity. *Cell and tissue research,* **349**(1), pp.147-160.

WANG, D., R. M. ICHIYAMA, R. ZHAO, M. R. ANDREWS and J. W. FAWCETT. 2011a. Chondroitinase combined with rehabilitation promotes recovery of forelimb function in rats with chronic spinal cord injury. *The Journal of neuroscience : the official journal of the Society for Neuroscience,* **31**(25), pp.9332-9344.

WANG, H., Y. KATAGIRI, T. E. MCCANN, E. UNSWORTH, P. GOLDSMITH, Z.-X. YU, F. TAN, L. SANTIAGO, E. M. MILLS, Y. WANG, A. J. SYMES and H. M. GELLER. 2008. Chondroitin-4-sulfation negatively regulates axonal guidance and growth. *J Cell Sci,* **121**(18), pp.3083-3091.

WANG, J.-W., J.-F. YANG, Y. MA, Z. HUA, Y. GUO, X.-L. GU and Y.-F. ZHANG. 2015a. Nogo-A expression dynamically varies after spinal cord injury. *Neural regeneration research,* **10**(2), pp.225-229.

WANG, J., W. RONG, X. HU, X. LIU, L. JIANG, Y. MA, G. DANG, Z. LIU and F. WEI. 2012. Hyaluronan tetrasaccharide in the cerebrospinal fluid is associated with self-repair of rats after chronic spinal cord compression. *Neuroscience,* **210**, pp.467-80.

WANG, J., X. WANG, J. WEI and M. WANG. 2015b. Hyaluronan tetrasaccharide exerts neuroprotective effect and promotes functional recovery after acute spinal cord injury in rats. *Neurochem Res,* **40**(1), pp.98-108.

WANG, K. C., J. A. KIM, R. SIVASANKARAN, R. SEGAL and Z. HE. 2002. P75 interacts with the Nogo receptor as a co-receptor for Nogo, MAG and OMgp. *Nature,* **420**(6911), pp.74-8.

WANG, M. Y., D. J. HOH, S. P. LEARY, P. GRIFFITH and G. J. MCCOMB. 2004. High Rates of Neurological Improvement Following Severe Traumatic Pediatric Spinal Cord Injury. *Spine,* **29**(13), p1493.

WANG, X., S. BUDEL, K. BAUGHMAN, G. GOULD, K. H. SONG and S. M. STRITTMATTER. 2009. Ibuprofen enhances recovery from spinal cord injury by limiting tissue loss and stimulating axonal growth. *J Neurotrauma,* **26**(1), pp.81-95.

WANG, X., K. CAO, X. SUN, Y. CHEN, Z. DUAN, L. SUN, L. GUO, P. BAI, D. SUN, J. FAN, X. HE, W. YOUNG and Y. REN. 2015c. Macrophages in spinal cord injury: phenotypic and functional change from exposure to myelin debris. *Glia,* **63**(4), pp.635-651.

WANG, X., P. DUFFY, A. W. MCGEE, O. HASAN, G. GOULD, N. TU, N. Y. HAREL, Y. HUANG, R. E. CARSON, D. WEINZIMMER, J. ROPCHAN, L. I. BENOWITZ, W. B. J. CAFFERTY and S. M. STRITTMATTER. 2011b. Recovery from chronic spinal cord contusion after Nogo receptor intervention. *Annals of neurology,* **70**(5), pp.805-821.

WANG, X., K. YIGITKANLI, C.-Y. KIM, T. SEKINE-KOMO, D. WIRAK, E. FRIEDEN, A. BHARGAVA, G. MAYNARD, W. B. J. CAFFERTY and S. M. STRITTMATTER. 2014. Human NgR-Fc decoy protein via lumbar intrathecal bolus administration enhances recovery from rat spinal cord contusion. *Journal of neurotrauma,* **31**(24), pp.1955-1966.

WANNER, I. B., M. A. ANDERSON, B. SONG, J. LEVINE, A. FERNANDEZ, Z. GRAY-THOMPSON, Y. AO and M. V. SOFRONIEW. 2013. Glial scar borders are formed by newly proliferated, elongated astrocytes that interact to corral inflammatory and fibrotic cells via STAT3-dependent mechanisms after spinal cord injury. *J Neurosci,* **33**(31), pp.12870-86.

WARREN, P. M. and W. J. ALILAIN. 2019. Plasticity induced recovery of breathing occurs at chronic stages after cervical contusion. *Journal of neurotrauma,* **36**(12), pp.1985-1999.

WARREN, P. M., S. C. STEIGER, T. E. DICK, P. M. MACFARLANE, W. J. ALILAIN and J. SILVER. 2018. Rapid and robust restoration of breathing long after spinal cord injury. *Nat Commun,* **9**(1), p4843.

WATERS, R. L., R. H. ADKINS and J. S. YAKURA. 1991. Definition of complete spinal cord injury. *Paraplegia,* **29**(9), pp.573-81.

WEI, W. J., Z. Y. YU, H. J. YANG, M. J. XIE, W. WANG and X. LUO. 2014. Cellular expression profile of RhoA in rats with spinal cord injury. *J Huazhong Univ Sci Technolog Med Sci,* **34**(5), pp.657-662.

WEIDNER, N., A. NER, N. SALIMI and M. H. TUSZYNSKI. 2001. Spontaneous corticospinal axonal plasticity and functional recovery after adult central nervous system injury. *Proceedings of the National Academy of Sciences of the United States of America,* **98**(6), pp.3513-3518.

WHISHAW, I. Q., S. M. PELLIS, B. GORNY, B. KOLB and W. TETZLAFF. 1993. Proximal and distal impairments in rat forelimb use in reaching follow unilateral pyramidal tract lesions. *Behavioural brain research,* **56**(1), pp.59-76.

WU, C. W. and J. H. KAAS. 1999. Reorganization in primary motor cortex of primates with long-standing therapeutic amputations. *J Neurosci,* **19**(17), pp.7679-97.

WU, J., Z. ZHAO, B. SABIRZHANOV, B. A. STOICA, A. KUMAR, T. LUO, J. SKOVIRA and A. I. FADEN. 2014. Spinal Cord Injury Causes Brain Inflammation Associated with Cognitive and Affective Changes: Role of Cell Cycle Pathways. **34**(33), pp.10989-11006.

XU, B., D. PARK, Y. OHTAKE, H. LI, U. HAYAT, J. LIU, M. E. SELZER, F. M. LONGO and S. LI. 2015. Role of CSPG receptor LAR phosphatase in restricting axon regeneration after CNS injury. *Neurobiology of Disease,* **73**, pp.36-48.

XU, W., L. CHI, R. XU, Y. KE, C. LUO, J. CAI, M. QIU, D. GOZAL and R. LIU. 2005. Increased production of reactive oxygen species contributes to motor neuron death in a compression mouse model of spinal cord injury. *Spinal Cord,* **43**(4), pp.204-13.

Y CAJAL, S. R. 1991. *Cajal's degeneration and regeneration of the nervous system.* History of Neuroscience.

YAGÜE, J. G., D. HUMANES-VALERA, J. AGUILAR and G. FOFFANI. 2014. Functional reorganization of the forepaw cortical representation immediately after thoracic spinal cord hemisection in rats. *Experimental Neurology,* **257**, pp.19-24.

YAMADA, H., K. WATANABE, M. SHIMONAKA and Y. YAMAGUCHI. 1994. Molecular cloning of brevican, a novel brain proteoglycan of the aggrecan/versican family. *Journal of Biological Chemistry,* **269**(13), pp.10119-10126.

YAMADA, J. and S. JINNO. 2017. Molecular heterogeneity of aggrecan-based perineuronal nets around five subclasses of parvalbumin-expressing neurons in the mouse hippocampus. *Journal of Comparative Neurology,* **525**(5), pp.1234-1249.

YAMADA, J., T. OHGOMORI and S. JINNO. 2015. Perineuronal nets affect parvalbumin expression in GABAergic neurons of the mouse hippocampus. *The European journal of neuroscience,* **41**(3), pp.368-378.

YAMAGUCHI, Y. 2000. Lecticans: organizers of the brain extracellular matrix. *Cellular and molecular life sciences : CMLS,* **57**(2), pp.276-289.

YANG, S., M. CACQUEVEL, L. M. SAKSIDA, T. J. BUSSEY, B. L. SCHNEIDER, P. AEBISCHER, R. MELANI, T. PIZZORUSSO, J. W. FAWCETT and M. G. SPILLANTINI. 2015. Perineuronal net digestion with chondroitinase restores memory in mice with tau pathology. *Exp Neurol,* **265**, pp.48-58.

YI, J.-H., Y. KATAGIRI, P. YU, J. LOURIE, N. J. BANGAYAN, A. J. SYMES and H. M. GELLER. 2014. Receptor protein tyrosine phosphatase σ binds to neurons in the adult mouse brain. *Experimental neurology,* **255**, pp.12-18.

YI, J.-H. H., Y. KATAGIRI, B. SUSARLA, D. FIGGE, A. J. SYMES and H. M. GELLER. 2012. Alterations in sulfated chondroitin glycosaminoglycans following controlled cortical impact injury in mice. *The Journal of comparative neurology,* **520**(15), pp.3295-3313.

YOO, M., M. KHALED, K. M. GIBBS, J. KIM, B. KOWALEWSKI, T. DIERKS and M. SCHACHNER. 2013. Arylsulfatase B improves locomotor function after mouse spinal cord injury. *PloS one,* **8**(3), pp.e57415-e57415.

YOON, Y. W., H. DONG, J. J. A. ARENDS and M. F. JACQUIN. 2004. Mechanical and cold allodynia in a rat spinal cord contusion model. *Somatosensory & Motor Research,* **21**(1), pp.25-31.

ZHANG, J. S., J. HONKANIEMI, T. YANG, T. T. YEO and F. M. LONGO. 1998. LAR tyrosine phosphatase receptor: a developmental isoform is present in neurites and growth cones and its expression is regional- and cell-specific. *Mol Cell Neurosci,* **10**(5-6), pp.271-86.

ZHAO, R.-R. R., M. R. ANDREWS, D. WANG, P. WARREN, M. GULLO, L. SCHNELL, M. E. SCHWAB and J. W. FAWCETT. 2013. Combination treatment with anti-Nogo-A and chondroitinase ABC is more effective than single treatments at enhancing functional recovery after spinal cord injury. *The European journal of neuroscience,* **38**(6), pp.2946-2961.

ZHAO, R. R., E. M. MUIR, J. N. ALVES, H. RICKMAN, A. Y. ALLAN, J. C. KWOK, K. C. ROET, J. VERHAAGEN, B. L. SCHNEIDER, J. C. BENSADOUN, S. G. AHMED, R. J. YANEZ-MUNOZ, R. J. KEYNES, J. W. FAWCETT and J. H. ROGERS. 2011. Lentiviral vectors express chondroitinase ABC in cortical projections and promote sprouting of injured corticospinal axons. *J Neurosci Methods,* **201**(1), pp.228-38.

ZHOU, X., X. HE and Y. REN. 2014. Function of microglia and macrophages in secondary damage after spinal cord injury. *Neural regeneration research,* **9**(20), pp.1787-1795.

ZORNER, B. and M. E. SCHWAB. 2010. Anti-Nogo on the go: from animal models to a clinical trial. *Ann N Y Acad Sci,* **1198 Suppl 1**, pp.E22-34.